AFASES 2019

ISSN, ISSN-L: 2247-3173
DOI:10.19062/2247-3173.2019.21

Publishing House of “Henri Coanda” Air Force Academy Str. Mihai Viteazu 160, Brasov 500183, ROMANIA Phone: +40 268 423 421, Fax: +40 268 422 004 Webpage: www.afahc.ro/ro/editura/editura.html
E-mail: editura@afahc.ro

INTERNATIONAL SCIENTIFIC COMMITTEE

Andreas MATZARAKIS, PhD
"Albert Ludwigs" University, Freiburg, Germany/ German Meteorological Service, Freiburg, Germany
Vasile NĂSTĂSESCU, PhD
Military Technical Academy, Bucharest, Romania
Dragoș Marian POPESCU, PhD
University of Medicine and Pharmacy, Craiova, Romania/ head of the Medical Department, MoD, Bucharest, Romania
Daniela ROȘCA, PhD
University of Craiova, Romania
Alexandra SARCINSCHI, PhD
"Carol I"National Defense University, Bucharest, Romania
Michael TODOROV, PhD
Technical University, Sofia, Bulgaria
Michal ŽÁK, PhD
Charles University, Prague, Czech Republic

ORGANIZING COMMITTEE

Chair:

Prof habil. **Adrian LESENCIUC**, PhD
Vice Rector for Science, 'Henri Coandă' Air Force Academy , Brasov, Romania

Members:

Prof Eng. **Constantin ROTARU**, PhD
Prof **Sorin CHEVAL**, PhD
Assoc Prof Eng. **Laurian GHERMAN**, PhD
Assoc Prof **Cătălin CIOACĂ**, PhD
Assist Prof Eng **Vasile PRISACARIU**, PhD
MD **Alexandru KERESZTES**
Col. **Sorin BĂLĂSESCU**, PhD
Psich. **Mihaela OANCEA**

Secretariat:

Maj **Adrian FĂGĂRAȘ**
WO **Serjiu OBREJA**
Eng **Mariana GHINDĂOANU**
Eng **Daniela OBREJA**
Inf **Adrian ROTARU**
Inf **Adina DOBRIȚOIU**

LOGISTICS:

Col **Simion PETRIC**
LtC **Ionel FEROIU**
LtC **Daniel ŞTEFĂNESCU**
LtC **Cătălin PASCAL**
Maj **Marius PAVEN**
Lt **Bogdan CĂBĂL**
OR **Mihăiţă POPA**
WO **Marian MIHALACHE**
WO **Marius TĂNASE**
WO **Călin DOBREAN**
WO **Marius CODREANU**
OR **Alexandru PAŞCA**
OR **Adrian BUTOI**
Std **Mihail VASILACHE**
Std **Oana NICOLAE**
Std **Roxana SAVIN**
Std **Andreea BEGA**
Std **Sonia DELIMAN**
Std **Oana MAXIM**
Std **Narcisa PINTELEI**
Std **Vasilică FLOARE**
Std **Andreea VLACH**
Std **Andrei COSMA**
Std **Denisa MĂLUȚAN**
Std **Alexandru SPINOSU**
Std **Ionuţ ALDULEA**
Std **Eduard BOTAS**
Std **Rebeca DOBRIN**
Std **Andrei DRĂGAN**
Std **Ciprian IONEL**
Std **Răzvan LEAŞ**
Std **Andreea MOISA**
Std **Vlad OPREA**
Std **Marian DRĂCEA**
Std **Vlăduţ PREUT**

CONTENTS

FUNDAMENTAL SCIENCES & ENGINEERING

METHODS OF RESEARCH AND ORGANIZATIONAL DEVELOPMENT OF MILITARY STRUCTURES

Adrian Valentin CÎȚĂ

„Nicolae Bălcescu” Land Forces Academy, Sibiu (adivalentin_steaua28@yahoo.com)

DOI: 10.19062/2247-3173.2019.21.1

Abstract: *The purpose of this research topic is to establish the main organizational research and development methods used by military organizations, their effectiveness and the way in which members of the organization accept or oppose organizational development.*

The main objectives of the theme are represented by:

• identifying the main methods of organizational research and development;

• integrating them into military organizations.

The achievement of the objective will be achieved through the two chapters "GENERAL PRINCIPLES AND OBJECTIVES OF ORGANIZATIONAL RESEARCH", in which are presented the directions of development of the organizational research and its underlying principles and "ORGANIZATIONAL DEVELOPMENT", in which are presented the most used the definitions of the development organization and its characteristics.

The conclusion will take the form of conciliations formulated on the basis of the contents of the paper and proposals to solve and improve some of the R & D issues in military organizations.

Keywords: *methods, research, development.*

1. GENERAL PRINCIPLES AND OBJECTIVES OF ORGANIZATIONAL RESEARCH

Research involves scientific and inductive thinking, promoting the development of logical thinking habits and organizing it. The role of research has grown considerably in modern times, so we can say that today we have a leading role in most areas of social life, such as the economic, political, medical, academic and military.

Organizational research aims at identifying and quantifying key factors that describe the climate and culture of any organization. This is done on a closed and limited environment as the number of respondents, and the impact of the research on the organization is direct and very strong.

We can define organizational research as a systematic, controlled, empirical and critical investigation into assumptions about alleged relationships between certain phenomena, the effort to acquire new knowledge and to find answers to questions.

The objectives of organizational research are the way to distinguish the culture of an organization, to determine the possibilities for further development of this culture, to identify the possible changes that need and can be achieved at the managerial level within the investigated organizations. The determination of the objectives must be very specific and it is necessary to outline all the activities that will be carried out as a result of this research.

Organizational research appears as a kind of interface between theory and practice.

It is based on good theory, inspiring, borrowing and using concepts, rules, procedures or tools to better know reality, to find and find solutions, answers or explanations on theoretical or applied problems. The results obtained in the research use for the improvement, construction or reconstruction of the theory, the enrichment of the knowledge of the realm and the reality. Theory is the support and beneficiary of the research, and the practice plays the role of beneficiary of the research results, but also a provider of many of the problems that it is called upon to solve.

Since organizations have different needs, over time research has undergone numerous changes, which has led to its development in three main directions, namely:

- Fundamental (theoretical) and experimental research represents the search, processing and promotion of scientific knowledge and fundamental scientific knowledge.
- It is also known as "pure" research, as it develops theoretical concepts through the formulation of abstract ideas and explanatory models.
- applied scientific research is the incorporation of fundamental scientific knowledge and a empirical knowledge in a finished priode, process or service that can in principle have value market;
- technological development is the bringing of the finished product, the process, the service obtained by applied research, either directly or through technology transfer, at entry level into production, to become a product, process or market value service, respectively.

Regardless of the object and typology of research studies, in order to be effective, they must follow the following principles:

- the purpose of the research is clearly defined;
- use common concepts;
- the research procedure is described in detail;
- achieve the most objective results, the research project must be carefully planned;
- conscientiously report the shortcomings in the project and correctly estimate their effects on the results;
- the data analysis must be sufficiently appropriate for its significance to be highlighted;
- the methods of analysis used should be those suitable for research;
- the validity / reliability of the data is carefully checked;
- conclusions should be limited to what is justified by research data;
- conclusions should be limited to data that provide an adequate basis;
- the researcher should have experience, be reputable in the field of scientific research and be an integral person.

2. ORGANIZATIONAL DEVELOPMENT

One of the basic concepts for organizational change is "organizational development". This notion has appeared relatively recently in the field of organizational terminology (the '70s) and, as any term of social science, has known and knows a whole series of definitions.

One of the most representative definitions of organizational development is that which considers organizational “development a response to change, a complex educational strategy that intends to modify the organization's norms, values, attitudes and structure so that it can better adapt to new technologies”[1], the new challenges of the market and the dizzying rate of contemporary change.

Another important definition is that organizational development is a set of theories, values, strategies and techniques based on social sciences and behavior that want to implement a planned change in the organizational activity framework in order to improve individual development and increase organizational performance by altering the behavior of the organization's members at work.

In short, organizational development can be defined as a planned and sustained effort to apply behavioral sciences to improve the system, using reflexive self-analytical methods.

The defining characteristics of organizational development are as follows:

- Organizational development focuses on culture and organizational processes;
- Organizational development encourages collaboration between leaders and members of the organization in the process of structuring the culture and processes;
- Groups (teams) of any kind are particularly important for the performance of tasks and are targets of organizational development;
- „Organizational development focuses on the social and human side of the organization and, throughout this process, also intervenes in the social and structural dimensions";[2]
- Participating and involving all organizational levels in problem solving and decision-making is specific and characteristic for organizational development;
- Organizational development focuses on the total change of the system and perceives the organization as a complex social system;
- Those who implement organizational development are facilitators, mediators, collaborators, and colleagues in the learning process with the client system;
- The ultimate goal of organizational development is to empower the client system to be able to solve problems by itself by transmitting the skills and knowledge necessary for the learning process. Organizational development views the organization's progress as a continuous process in the context of an ever-changing environment;
- Organizational development adopts a position on the progress of the organization that emphasizes both individual development and the organization as a whole. Organizational development programs always try to create "win-win" situation.

For employees, leaders and managers, organizational development involves, in the first instance, the choice of tools followed by measurements and finally feedback. It facilitates the processes of awareness, acceptance and action to identify practical strategies and actions that will help the person to improve their personal effectiveness in implementing actions that can lead to changes in personal styles of behavior, management approach and leadership strategies. After a period of time, the evaluation is repeated to check the evolution and identify improvements to development strategies and actions.

For organizations, organizational development means collaborating members of the organization to identify group, interpersonal, or both issues in order to eliminate them in order to meet the objectives and improve the group's performance.

At organizational level, the idea of organizational development is based on establishing a plan for evaluating the entire organization. This plan includes choice of questionnaire, methodology, feedback, strategy / action development, and post-test. It is important from the beginning to understand that in organizational development, a study is an action-research approach. Simply making the study and communicating results to senior management that will then decide what to do, will only increase the gap between management and other members of the organization.

Action-research studies use the data collected to involve everyone in the organization in understanding their meaning and then building practical actions through awareness, acceptance and action processes.

Participants determine what they can implement at department level and what strategies / actions of change they want to recommend to senior management.

The study is then re-administered after a period of time to assess the progress and results of implementing change strategies.

CONCLUSIONS AND SUGGESTIONS

Concluding the aforementioned, we can state that organizational research is about identifying and quantitating key factors that describe the climate and culture of any organization that is applicable to a closed and limited environment as the number of respondents, and the „impact of research on the organization is direct and very strong.

The objectives of organizational research are the way to distinguish the culture of an organization, to determine the possibilities for further development of this culture, to identify the possible changes that need and can be achieved at the managerial level within the investigated organizations."[3] The determination of objectives must be very specific, and it is necessary to outline all the activities that will be carried out as a result of this research.

"Organizational development consists in improving individual, group and organizational performance to advance the organization's ability to respond effectively to changes in the external environment"[4] on the one hand and helps increase internal capabilities by ensuring that organization structures, human resources, posts, communication systems, and leadership / management processes make full use of people's motivation and help them work to their full potential. Properly, this improvement can cause changes in how people, groups, or even the organization work.

A critical aspect in organizational research is the realization from the beginning of the management's promise to correct the problems identified in this research, whatever they may be. The absence of systematic and rapid activities following research will lead to employee dissatisfaction. As long as management is not ready to make improvements in the organization, it is not advisable to start the organizational research project.

REFERENCES

[1] http://shodhganga.inflibnet.ac.in/bitstream/10603/185036/15/11_chapter 2.pdf;

[2] https://www.coursehero.com/file/p6qd5vkd/3-Employee-Development-Organizational-development-focuses-on-increased/;

[3] https://smallbusiness.chron.com/internal-external-factors-affect-organization-16641.html;

[4] https://articles.extension.org/sites/default/files/Organizational Climate and Culture Review.pdf.

FUNDAMENTAL TREATIES BETWEEN THE RUSSIAN FEDERATION AND THE USA IN THE NUCLEAR MISSILE SPHERE

Alexandru-Marius FUGARETU

”Nicolae Balcescu” Land Forces Academy, Sibiu, Romania (fughy_xts@yahoo.com)

DOI: 10.19062/2247-3173.2019.21.2

Abstract: *The most significant role in advancing the process of nuclear disarmament was played by bilateral agreements between the Russian Federation (USSR) and the USA in the nuclear missile sphere. In particular, among the key achievements in this area are the Treaty between the USSR and the United States on the Elimination of Intermediate-Range and Shorter-Range Missiles (the INF Treaty), as well as the Treaty between the Russian Federation and the United States of America on Measures for the Further Reduction and Restriction of Strategic Offensive Arms START Treaty).*

Keywords: *nuclear missile sphere, nuclear disarmament, bilateral agreements.*

1. INTRODUCTION

Issues of arms control and non-proliferation regimes are the most important in the system of international relations. Treaties and agreements in this area remain the most effective mechanism for strengthening international security and stability, as well as confidence between states. Due to this, starting from the second half of the 20th century, chemical, biological and geophysical weapons were practically derived from the means of warfare. Significantly reduced nuclear and conventional weapons. Significantly reduced the threat of the outbreak of another world war.

Nevertheless, the problem of maintaining effective control over nuclear weapons (NW) is still relevant and occupies a key position in ensuring international security.

The main tools aimed at accomplishing this task include: agreements on the limitation and prohibition of nuclear tests, the limitation and reduction of nuclear weapons, agreements on zones free of nuclear weapons, as well as various initiatives to combat the proliferation of these weapons, acts nuclear terrorism and others.

2. BILATERAL AGREEMENTS BETWEEN THE RUSSIAN FEDERATION (USSR) AND THE USA IN THE NUCLEAR MISSILE SPHERE

The most significant role in advancing the process of nuclear disarmament was played by bilateral agreements between the Russian Federation (USSR) and the USA in the nuclear missile sphere. In particular, among the key achievements in this area are the Treaty between the USSR and the United States on the Elimination of Intermediate-Range and Shorter-Range Missiles (the INF Treaty), as well as the Treaty between the Russian Federation and the United States of America on Measures for the Further Reduction and Restriction of Strategic Offensive Arms (the New START Treaty).

2.1. The treaty between the USSR and the United States on the elimination of intermediate-range and shorter-range missiles (the INF Treaty)

The INF Treaty was signed in Washington on December 8, 1987, entered into force on June 1, 1988 and is indefinite.

However, art. XV provides for the right to withdraw from the Treaty if any of the parties considers that its further compliance threatens its highest national interests. After the collapse of the USSR, the participants in this document are Russia, the USA, Belarus, Kazakhstan and Ukraine.

In accordance with this agreement, the parties pledged to eliminate all medium-range (in the range from 1000 to 5 500 km) and shorter (500-1000 km) range and not to have them in the future.

Soviet medium-range ballistic missiles (SSB) SS-20 Pioneer, SS-4, SS-5 and ground-based cruise missiles (CRNB) S-X-4, as well as operational tactical missiles (OTP) SS-12 were to be eliminated and SS-23 (types of missiles according to NATO classification).

The United States was supposed to eliminate the Pershing-2 medium range missiles, the BGM-109G KRNB (land-based Tomahawk KR), as well as the short-range missiles - the Pershing-1A OTP.

According to the Treaty, the deadline for the elimination of medium-range missiles is three years, a shorter range is one and a half.

Proposed methods for the destruction of rockets by exploding or burning their steps. In the first six months after the entry into force of the agreement, liquidation of up to 100 RSD was allowed using the launch method. The warheads of the nuclear-free missiles were destroyed by deforming their hulls.

Monitoring compliance with the Treaty was carried out by on-site inspections in the territory of both the USSR and the USA, and the countries of deployment of Soviet and American missiles (GDR, Czechoslovakia, West Germany, Great Britain, Italy, Belgium and the Netherlands, respectively). In addition, it was provided for continuous monitoring of the lack of production of missiles at manufacturing plants (for 13 years): for the USSR - Botkinsky Machine-Building Plant (Udmurt ASSR), for the USA - Plant No. 1 Hercules (Magna, Utah).

In order to resolve issues related to the implementation of the Treaty, a Special Control Commission was established. The exchange of notices stipulated by the agreement is carried out by the parties using the National Centers for Reducing Nuclear Hazard, which were established in accordance with a special Agreement between the USSR and the USA, signed in September 1987.

Over the three years of the implementation of the INF Treaty - from June 1988 to June 1991 - 1,846 missiles, 825 launchers (launchers), 812 warheads, and about 6,000 units were eliminated in eight locations in Russia and a number of former Soviet republics. other elements of missile systems (containers, installers, vehicles, stationary shelters, etc.).

The United States destroyed 846 missiles, 289 launchers, 442 warheads and more than 2,500 other elements in four locations.

As a result, ballistic and cruise ground-based missiles in the range of 500 to 5,500 km were completely withdrawn from the arsenals of the two nuclear powers.

The inspection activities provided for in the Treaty ended on May 31, 2001 (Belarus, Kazakhstan and Ukraine joined after the collapse of the USSR).

At the same time, at the present stage, a situation has arisen when, in conditions of continued missile proliferation in the world, only the USA, Russia and the three former USSR republics (Belarus, Kazakhstan and Ukraine) were bound by the possession of a wide range of medium and short range missiles.

Other countries, including such countries as Iran, India, Israel, North Korea, China, Pakistan, are successfully developing similar land-based systems.

In 2008, Russia took the initiative to make the INF Treaty global. The United States agreed with the Russian initiative, calling the current situation unfair. Washington said that "a general rejection of ballistic and cruise missiles of land-based with a range of 500-5500 km and the termination of related programs will contribute to curtailing the international regime of nuclear missile non-proliferation."

However, at the UN General Assembly, the United States limited itself to adopting a joint statement with the Russian Federation, but did not support the idea of starting a multilateral negotiation process on changing the status of the said Treaty. They refused to promote this proposal also in the Organization for Security and Cooperation in Europe, citing the fact that this initiative supposedly should be oriented not to the North Atlantic space, but to the Middle East and Asian regions. In their opinion, "such problematic states as the DPRK, Iran, Syria and Pakistan should be pulled up to the Treaty first of all."

The situation around the Treaty and in relation to its implementation in recent years has become seriously complicated. This was primarily due to the position of the United States itself, for which the provisions of the INF Treaty created problems almost from the very beginning of their implementation of plans to deploy a global missile defense system (PRO) and to equip unmanned aerial vehicles with a combat payload.

At the same time, the corresponding US activities in these areas led them to the following violations of this Document.

1. In the interests of testing missile defense elements in the United States, a family of various target missiles (Hera, Super Hera, LRALT, and others) is used with a range limited by the INF. Tests of each such missile without active fire impact on it by means of antimissile defense do not differ from tests of high-grade combat missiles of medium-range ground-based, which is prohibited by Art. VI Treaty.

In addition, the Americans are engaged in the development of new universal missile accelerator facilities, which, depending on the configuration of their mounted warheads, can be used as combat ballistic missiles, which is prohibited by the INF Treaty.

2. Unmanned aerial vehicles with combat payloads (combat UAVs) with a range of 500-5 500 km strictly fall under the definition of the term "cruise missile" in accordance with paragraph 2 of Art. II of the Treaty ("unmanned, equipped with its own propulsion system means, the flight of which on most of its trajectory is provided by the use of aerodynamic force" and "which is a means of delivering weapons") and, therefore, are prohibited.

At present, there are hundreds of similar devices in the US military (in particular, the MQ-1B Predator and MQ-9A Ri-per), with a limited range of action that can strike ground targets.

3. The deployment of Aegis Ashor anti-missile systems in Europe with the same launch equipment (Mk 41) with Tomahawk cruise missiles with a range of up to 2,400 km (in this case, they acquire ground-based status) directly contradicts provisions of the INF.

However, the United States categorically refuses to eliminate these violations.

In the interests of "rectifying the situation," when the United States finds itself in the role of violator of the INF Treaty, they put forward "counter" claims against the Russian Federation for its implementation of this Treaty.

At the same time, Washington refuses to provide any results of objective monitoring of this activity or other specific factual evidence of the claims being made.

In order to increase the corresponding pressure on the Russian Federation, on the initiative of the United States, for the first time after a 13-year hiatus, in October 2016, a session of the Special Control Commission with the participation of Russia, the USA, Belarus, Kazakhstan and Ukraine was convened, where the US side indicated its claim in a five-sided format without providing any substantiated evidence.

Then the United States voiced the accusation against the Russian Federation and within NATO. The subsequent meeting in the format of the JCC, held in December 2017, did not bring any progress in the process of resolving the problem around the INF. Both Russia and the United States categorically reject any claims brought against each other.

Instead of facts, Washington deliberately continues to discredit the Russian Federation by creating a negative information background around Moscow’s alleged non-fulfilment of its obligations, which is used to build up anti-Russian propaganda, strengthen its influence in Europe and rally NATO allies against the "new Russian threat." The factor of the declared “violation of the Russian Federation of the Treaty” is fully used by them as a guarantee of the necessary public and political support for the course being implemented for strategic deterrence of Russia and the corresponding adaptation of the coalition nuclear policy.

As a result, the US took advantage of the prevailing situation around the INF Treaty to justify its actions contrary to the provisions of the Treaty, including military ones. In particular, the American Congress is considering the possibility of starting the development of medium-range missiles, deploying air and sea-based cruise missiles near the Russian borders, and expanding the missile defense program.

Thus, as of June 2018, the confrontation around the DDRMD has increased significantly, the problem is politicized and finding positive solutions to its implementation is becoming increasingly problematic.

It is possible that this treaty to come to an end on 2019 due to the fact that on February 1st, Secretary of State Mike Pompeo announced that the United States was suspending its obligations under the Intermediate-Range Nuclear Forces (INF) Treaty, and notified Russia and the other treaty parties that the United States would be withdrawing from the treaty in six months, pursuant to Article XV of the treaty. In response, on February 2nd, the russian president Vladimir Putin stated that Russia was also suspending its obligations under the treaty.

2.2. The treaty between the Russian Federation and the United States of America on measures for the further reduction and restriction of strategic offensive arms (the new start treaty)

The treaty between the Russian Federation and the United States of America on measures to further reduce and limit strategic offensive arms was signed by the presidents of the two countries on April 8, 2010 in Prague (Czech Republic) and entered into force after ratification by both parties on February 5, 2011.

In accordance with the provisions of the Treaty, each of the parties reduces and limits its ICBMs and SLBMs, their launchers, heavy bombers (TB), warheads on deployed ICBMs and SLBMs so that seven years after the entry into force of this agreement (until February 5, 2018) and further, the total quantities did not exceed:

- 700 units for deployed ICBMs, SLBMs and TB;
- 1,550 units for warheads on deployed ICBMs and SLBMs, as well as nuclear warheads counted for deployed heavy bombers and;
- 800 units for deployed and non-deployed launchers of ICBMs and SLBMs, deployed and non-deployed heavy bombers.

Moreover, each of the parties has the right to independently determine the composition and structure of its strategic offensive arms.

A similar regime is applied to all means of strategic offensive arms, excluding special measures of control over these or other systems.

Structurally, the new Treaty is a package of documents consisting directly of the text of the Treaty itself, its Protocol and annexes, which are an integral part of it.

The text of the agreement includes a preamble and 16 articles. The Protocol specifies the provisions of the Treaty and prescribes the procedure for their implementation. It contains definitions of terms, data categories with regard to funds subject to the Treaty, the nomenclature of notifications, defines the main parameters of the parties to refit and liquidate funds, regulates the inspection regime, the exchange of telemetry information, the work of the Bilateral Consultative Commission, the temporary application of the Treaty. The Protocol also includes the agreed statements of the parties on certain issues related to the implementation of the Agreement.

The contract is valid for 10 years (until 2021). By mutual agreement of the parties, it may be extended for a period of not more than five years, if not replaced before this period by a subsequent agreement on the reduction and limitation of strategic offensive arms.

The Treaty stipulates a ban on the basing of strategic offensive arms outside the national territory. However, these obligations do not affect the rights of the parties in accordance with the generally recognized principles and norms of international law regarding the passage of submarines, aircraft flights, and submarine calls at ports of third countries.

The parties, in the exercise of their state sovereignty, have the right to withdraw from the Treaty if they decide that the exceptional circumstances related to its content have put their highest interests at risk.

The restrictions imposed by this agreement on the nuclear potentials of both states provide an acceptable level of strategic deterrence and allow them to remain at parity level on strategic offensive arms.

In preparing the Treaty, the existing significant gap between the number of parties' strategic offensive arms was taken into account and steps were taken not only to reduce it, but also to reduce the capacity to build up the so-called return capacity. In particular, the limit set in the agreement is 800 units for the total number of deployed and non-deployed launchers of ICBMs and BRIL, as well as deployed and non-deployed TB, limits the return potential of the parties, preventing the possibility of increasing the number of deployed START carriers by transferring part of the carriers from the category of undeployed.

Of particular importance is the fact that the Treaty establishes the relationship of strategic offensive and strategic defensive weapons, with an emphasis on its growing importance in the process of reducing strategic offensive arms. The Russian Federation, in a separate statement within the framework of its signing, stipulated the possibility of withdrawing from the START treaty in the event of a qualitative and quantitative increase in the US missile defense system.

The United States has undertaken legal obligations not to re-equip and not use launchers of ICBMs and SLBMs to deploy missiles in them and, conversely, not to alter missile launchers to accommodate ICBMs and SLBMs. In addition, under the control mechanism of the Treaty, all the anti-missile defense missiles of the second US missile defense position area at Vandenberg (California) were hit.

The agreement spelled out provisions for the control of PU launchers of sea-based cruise missiles on strategic carriers - SSGN, converted from nuclear submarines of the "Ohio" type.

During the term of the Treaty (until 2021), all converted SLBM and ICBM launchers, as well as heavy bombers (both nuclear and equipped for non-nuclear weapons) will be checked for their reconversion.

Inspection activities under the Treaty began on April 6, 2011. Verification of the fulfilment of US commitments on the limits of deployed strategic carriers and warheads is carried out during inspections at all ICBM, SLBM and TB bases. Verification of the fulfilment of US commitments on the limits of undeveloped strategic carriers is provided during inspections at all strategic offensive weapons sites.

To ensure the reliability of control during these inspections, specific means of strategic offensive arms are selected randomly from all those located at the inspected facility.

In the course of the inspection activities, the parties confirm the data and characteristics of strategic offensive weapons on a specific ICBM base, submarines or air base.

During the year, all existing facilities of the sides of the parties can be subjected to such selective control several times, and each party determines the list of inspected objects on the basis of its priorities.

In the interest of increasing the effectiveness of verification activities, part of the tasks of monitoring compliance by the parties with their obligations on strategic offensive arms levels are additionally assigned to national technical means of control (NTSC).

An analysis of the practical implementation by the United States of its obligations under the Treaty showed that they, experiencing certain difficulties with entering START levels specified by this agreement, were forced not only to intensively reduce these weapons, but also to take additional steps to remove as much as possible from the contractual limitations strategic offensive means.

By February 5, 2018, the US State Department announced that it had fulfilled its obligations to reduce strategic offensive arms and reach the total amounts established by the Treaty (652 deployed ICBMs, SLBMs and TB; 1,350 warheads on deployed ICBMs, SLBMs and counted for deployed TB; 800 deployed and non-deployed PU ICBM, SLBM and TB).

At the same time, the declared achievement of the indicators established by the agreement was achieved by the United States not only as a result of real arms reductions, but also due to re-equipment that was uncoordinated with the Russian side into the non-nuclear version of the TB B-52N part and the Trident-2 missile launchers unsuitable for use. The Russian inspectors are unable to confirm the bringing of these strategic offensive weapons into a state unsuitable for the use of nuclear weapons, as provided for by the Protocol to the Treaty.

In addition, the United States also unreasonably withdrew from the counting "ICBM mine launchers intended for training", due to their arbitrary retraining in the category "training mines" unprovided by the Treaty.

Thus, the United States unlawfully independently excluded part of its strategic offensive arms from the restrictive format of the Treaty, effectively exceeding its limits.

In this regard, the Russian Federation stated that as long as there is no relevant joint agreement on the harmonization of procedures for converting TB and SSBMs and redeploying the silos of ICBMs, Russia does not consider the designated START funds as "converted", does not recognize their exclusion from and urges the United States to continue a constructive search for mutually acceptable solutions to this problem.

3. CONCLUSIONS

In general, despite the disagreements between the Russian Federation and the United States regarding compliance with these treaties, it is impossible not to emphasize their generally recognized historical significance in promoting nuclear disarmament, strengthening strategic stability and international security. In addition, the fact of reaching such agreements can serve as an example of successful Russian-American cooperation in areas where the mutual interests of the two countries coincide.

The INF Treaty is historic both in its goal - the complete destruction of two classes of nuclear missile weapons, and the novelty and scale of the control measures provided for it, which became the starting point for developing verification mechanisms in subsequent agreements on nuclear weapons.

4. REFERENCES

[1] Arms Control Association, *The Intermediate-Range Nuclear Forces (INF) Treaty at a Glance*. Available at www.armscontrol.org, accessed on 10 May 2019;
[2] A. E. Kramer, *The I.N.F. Treaty, Explained*. Available at www.armscontrol.org, accessed on 09 May 2019.
[3] USA Secretary of State Mike Pompeo, *Remarks to the Press*. Available at www.state.gov, accessed on 11 May 2019.
[4] Arms Control Association, *New START at a Glance*. Available at www.armscontrol.org, accessed on 10 May 2019;
[5] F. A. Rose, *The end of an era? The INF Treaty, New START, and the future of strategic stability*. Available at www.brookings.edu, accessed on 11 May 2019;
[6] The Organization for Security and Co-operation in Europe, *The New START Treaty*. Available at www.osce.org, accessed on 10 May 2019.

GLIDER FLIGHT TRAINING APPLICATION IN TURKISH AIR FORCE

Goksel KESKIN*, Hasim KAFALI, Seyhun DURMUS***, Selim GURGEN*, Melih Cemal KUSHAN***

*Eskişehir Osmangazi University, Turkey (gokselkeskin@outlook.com, sgurgen@ogu.edu.tr, erzesk@gmail.com)
**Mugla Sıtkı Koçman University, Dalaman School of Civil Aviation, Muğla, Turkey (hasimkafali@mu.edu.tr)
***Balıkesir University, Edremit School of Civil Aviation, Balıkesir, Turkey (drmsyhn@gmail.com)

DOI: 10.19062/2247-3173.2019.21.3

Abstract: *Using gliders in training both popular and cheap in civil and military aviation. Although it is cheap, all of the flight's phases include aerobatic training can be learned by glider. For this reason, most countries use gliders in their Air Forces. Turkish Air Force also has gliders for training. In this work, quality of training and intensity of glider usage? has been assessed. Also, differences in training and size of the fleet have been compared with other countries' air forces. As a result, gliding training in Turkish Air Force isn't as noteworthy and sufficient as in other countries. Points that need to be improved were disclosed and discussed.*

Keywords: *Gliding, Soaring, Sailplane, Flight Training, Glider, Turkey*

1. INTRODUCTION

Gliding is popular in both popular civil and military aviation thanks to its low operational cost for training. There are too many benefits of glider training before going on powered airplanes. For this reason, some of the armies use gliders as a basis for flight training. This kind of training is cheap and beneficial for air forces because they can determine the ability of the cadets' skills in this way. However, gliding is not popular in Turkey and the Turkish Air Force only has 4 training gliders for cadets. In this study, glider training will be evaluated and compared with the air force of other countries.

2. BENEFITS OF GLIDING

These days pilots are trained as a computer operator by limited flight systems which reduce the importance of the pilot's skills in civil aviation. However, military aviation requires significant piloting skills. First of all, gliders' cockpit generally divided into two parts, front and rear like most of the advance military trainers (KT-1T, Super Tucano, T-38, etc.) but aircraft are used for the basics of flight (T-41, Cessna 172-182, etc) are designed side-by-side. According to this specification, glider cockpits are more likely to military cockpits. The dual command system is another important part of the training. Besides, glider flight ensures coordinated control which means using ailerons and rudder in balance. Moreover, cadets can experience how aircraft behave in the stall, spin, and other abnormal situations and learn how to manage it. Two-seater glider's ''G limits'' also higher than single engine basic aircraft which provide better aerobatic performance. Although higher G limits of the glider, cadets learn every phase of aerobatic maneuvers at lower G and speed than military jets or ~~turbine~~ piston props. Aerobatic maneuvers and complete gliding flight teach pilots energy management. In addition, cadets learn energy management by using thermals and other meteorological occurrences and can test the force of the air. Finally, flight planning should be perfect in glider flight because there is only one landing. For this reason, altitude control by using spoiler, following flight path and checkpoints are enormously important. This important factor can prepare cadets emergency landings engineless like Sully (Chesley Sullenberger) who was a famous former military pilot and commercial airline pilot [1-3].

3. GLIDING IN TURKEY

Gliding isn’t popular in Turkey there is only one glider flight school under Turkish Aeronautical Association. This school has been in Eskişehir İnönü since 1935 and has 6 active two-seater SZD-50-3 Puchacz. In addition, 2 Puchacz, 2 Ventus, 2 Discus, 3 Jantar 48 Std, 3 Jantar 42-2 Open Class, 3 IS-29 D2, 3 motoglider, and 3 PZL-104 Wilga tow planes have been grounded due to lack of maintenance since 2013. Also, one Grob 103 two-seater has just had airworthiness under İstanbul Glider Club. Therefore, there is only training flight for beginners and some intermediate students. Cross-country flights and glider races aren’t organized in Turkey and the only İnönü airfield is open for civil flights. Training is divided into 2 parts beginner gliding course which includes dual command training by the instructor and license course include gliding badge A, B, C, and glider pilot license (GPL) with many solos [3-5].

FIG. 1. Turkish Air Force’s SZD-50 Puchacz glider in Yalova Airfield.

4. GLIDER TRAINING IN TURKISH AIR FORCE

Students at the 2nd grade of Air War College, National Defence University takes a glider training course in summer. This course consists of beginner gliding course and gliding badge A course. So, candidates are trained in 23-25 sorties flight training in Yalova airfield. These flights are made with Air Force’s own Puchacz gliders. Turkish Air Force has 4 gliders for these training but there is no glider flight instructor in the army. For this reason, Turkish Aeronautical Association sends civil instructors for these flights.

In Yalova, it's impossible to use thermals or slope liftings due to geographical conditions thus flight time is limited.

All flights are made by winch launching which is another criteria limits flight time. Consequently, all lessons are conducted from releasing winch cable until the landing. The only advantage of the airfield is being at the sea level which does increase the performance of the glider. In addition, until the 2015 military high school students had a beginner glider course in Bursa [6-9].

5. GLIDER TRAINING IN OTHER COUNTRIES' AIR FORCES

Glider flight is much popular in the rest of Europe, Australia, New Zealand, and America. Whence, some of these countries use glider for training under the cadet program. For example, Canadian Air Cadet which is supported by the Canadian Air Force conducts an average of 50000 glider flights (Familiarization, training, competitions) annually and 350 cadets are trained in these courses. These flights are made with Schweizer 2-33 and 2-33A low-performance gliders [10-11].

Another example is the Royal Air Force Gliding Soaring Association (RAFGSA) which has 1 center and 7 clubs in the United Kingdom. That association was founded to provide glider flight opportunity for RAF servicemen and women. With its large fleet (Self Launch Gliders, Motogliders, Gliders, Tow planes), RAFGSA offers flight courses for all level student pilots and pilots and some of them can be free. Moreover, RAFGSA organizes competitions in the United Kingdom [12-14].

FIG. 2. Royal Air Force's Grob T1 Viking (Military version of Grob 103) Two-Seater Training Glider in RAF RIAT Air show (https://hiveminer.com/Tags/glider%2Cmilitary, Micheal Hibbins)

Australian Air Force Cadets also gives importance to the glider training. In these flights, brand new ASK-21 MI (Self-launched) and DG-1001 gliders are used for. These courses are supported by the Australian Air Force's scholarships [15-18].

Gliding training has an important place in the United States Air Force (USAF). The extremely large fleet is in service for cadets training. In this fleet, TG-10B (Military version of L-23 Super Blanik) is used for basic of training (Airmanship 251).

In this program, the 3rd grade of cadets reaches almost 300 solo flight every year in over 7000 sorties. Later, 40 cadets are selected to become a soaring flight instructor (Airmanship 461). These instructors teach the basics of glider flight. To keep them motivated, the USAF Academy has 2 competition team. One of them joins aerobatic championships with TG-10B. Other one joins cross-country flights and competition with TG-15A (Military version of Schempp-Hirth Duo Discus) and TG-15B (Military version of Schempp-Hirth Discus-2). This team try to break national records and compete against other civil clubs in the USA. In addition, the USAF Academy has been renewing fleet by DG-1001 (TG-16) high-performance two-seater gliders and that academy has reached over 200000 sorties yearly [19-21].

FIG. 3. TG-16A is prepared for flight by cadets and instructor (https://www.usafa.af.mil/News/Photos/igphoto/2000933786/).

CONCLUSIONS

Glider flight training is common worldwide but the level of development depends on gliding culture. Countries with well gliding opportunities also have good support from their armies. In these armies, glider flight has an important role to introduce aviation to air cadets. For this reason, undeveloped gliding in Turkey may cause a low level of glider training in Turkish Air Force. With 4 gliders and instructor, cadets can only have gliding badge A in the summer season. In 2017, only 73 air cadets got gliding badge in Turkish Air Force [22]. If the fleet made wider, cadets would experience soaring better. Also, glider training would be part of the academic year with credit lessons like the USAF Academy. On the other hand, it’s legal to fly students who are 16-year-old in Turkey. So, it is possible to give military high school students, just can have a beginner course, gliding badge A or more. With that cheap training, the military can keep cadets motivated for years. In addition, the Turkish Air Force can train own glider flight instructors in the military. With that way, cadets’ interest would increase for gliding.

Flying with different types of aircraft brings experience to the pilot. Positive factors of gliding cannot be ignored. A famous example of aviation history, Captain Sullenberger who was a former fighter pilot had glider flight training in USAF Academy, didn’t hesitate to land on the Hudson River without both engines of a huge airliner. In addition to his experience and knowledge, he also was guided by his knowledge of gliding. So, the engineless flight must be experienced for emergencies and abnormal situations.

REFERENCES

[1] Stewart, K., The glider pilot's manual, Airlife, 2001;
[2] FAA., Gliding Handbook, 2013;
[3] Keskin, S., Türk Hava Kurumu Genel Başkanlığı Planör Uçuş Okulu Başlangıç Eğitim El Kitabı, Ankara, 1988;
[4] Kushan M.C., Gurgen S., A to Z World Airplanes, Helicopters and Unmanned Aerial Vehicles (in Turkish), Nisan Publishing, Eskisehir, Turkey, 2016;
[5] https://www.thk.org.tr/ ;
[6] https://www.msu.edu.tr/eng/sayfadetail?SayfaId=49&ParentMenuId=43;
[7] http://www.hho.edu.tr/Documents/TanitimKitapcigi/08_Askeri.pdf;
[8] http://www.hho.edu.tr/EN/Military/UcusEgitimi.aspx;
[9]https://www.hvkk.tsk.tr/trtr/T%C3%BCrk_Hava_Kuvvetleri/%C4%B0nsan_Kaynaklar%C4%B1/E%C4%9Fitim_ve_%C3%96%C4%9Fretim/Hava_Harp_Okulu_Komutanl%C4%B1%C4%9F%C4%B1;
[10] http://www.cadets.ca/en/summer-opportunities/training-centres-eastern-gliding-about.page;
[11] http://www.cadets.ca/en/summer-opportunities/training-courses.page;
[12] https://web.archive.org/web/20110405171920/http://www.raf.mod.uk/rafgliding/;
[13] https://www.rafsportsfederation.uk/sports/;
[14] http://www.rafgsa.org/;
[15] http://www.aviation.3wg.aafc.org.au/about/fleet;
[16] http://www.aafc.org.au/wp-content/uploads/AAFC-Gliding.pdf;
[17] http://www.aafc.org.au/what-we-do/gliding/;
[18]https://australianaviation.com.au/2015/03/australian-air-force-cadets-presented-with-newest-glider-at-avalon/;
[19] https://www.aetc.af.mil/About-Us/Fact-Sheets/Display/Article/261039/soaring-programs-at-usafa/;
[20] https://www.academyadmissions.com/the-experience/military/airmanship/;
[21]https://www.dg-flugzeugbau.de/en/wp-content/uploads/sites/2/2016/12/US-Air-Force-DG-1001-segelfliegen-INTERNATIONAL.pdf;
[22] Türk Hava Kurumu Faaliyet raporu, 2018, Ankara, Turkey.

DISCIPLINARY LIABILITY OF THE MILITARY PERSONNEL

Mihai-Alin MECLEA, Dumitru TOADER

”Henri Coandă” Air Force Academy, Braşov, Romania

DOI: 10.19062/2247-3173.2019.21.4

Abstract: *Liability "occurs on the grounds of an already done evil”, that is after committing an offense. Specific violations committed by public officials, including those with special status, is the fact that they can intervene while performing their function, either in connection with this performance or simply by the deviation from certain rules which have no direct connection, with the function, but which may question the prestige of the public employee. The disciplinary liability is a form of the administrative liability, together with the contraventional and asset liabilities.*

Keywords: *discipline**,** disciplinary deviation, legal liability, discipline responsibility, the military, disciplinary sanctions*

1. INTRODUCTION

Liability as a fundamental institution of law has, for the military, some special connotations resulted from their special responsibility, but not at such extent that this profession avoid the general principles of liability. As for civil employees, generally speaking, also for the military, liability occurs when executing their function or in connection with its execution, they deviate from the legal norms of their profession. Thus, the soldiers are passive subjects of the following forms of liability: disciplinary, contravention, material and criminal.

The disciplinary liability is a form of the administrative liability, together with the contraventional and asset liabilities. All three forms of liability occur as a result of committing administrative violations, the difference being that in the first two cases it is a sanctionary legal liability and in case of asset liability, we speak about a reparatory liability.

The term "discipline" comes from Latin, where the meaning was, on the one hand, system, rule, moral principles, good standing, and on the other hand, training, school, education, science, skill, meanings that we find today, respectively the assembly of the rules of conduct, of order, imposed on members of a group members for a proper functioning of its social organization and, of a particular domain of knowledge or branch of a science, field of instruction or area of learning curricula [1].

The discipline supposes the leadership right to formulate obligations and prohibitions, the authority to make them be observed and the power to apply sanctions if necessary. Mandatory in all areas of social life, discipline is essential to the military organization, being one of the determinant factors of the fighting capacity of the army, based both on the conscious acceptance of the established rules of conduct and the granted rewards and sanctions enforcement [2].

2. THE LEGAL NATURE OF MILITARY DISCIPLINE

The legal nature of military discipline is the law regarding the statute [3] which establishes among other duties of the military, to respect the military oath and the provisions of normative acts in force, the exact execution of the commanders' and chiefs' orders, the military being responsible for the way they fulfill the tasks entrusted to them.

The commander is the one responsible for the application of the military discipline norms within the structure he commands and the delegation of competence does not exclude entirely his liability. As a result, the legal nature of the military discipline is not related to the working right, it does not stems from a contract of employment but from a stipulated by law, that is why all the characteristic of an institution of administrative law meet. The importance of military discipline is that in many armies, the disciplinary norms should be grouped into a real "disciplinary law" as distinct institution, specifically recognized as military law and regulations exist to this effect.

The disciplinary deviation is a form of illicit behavior that manifests itself in a breach of the obligations by the military, obligations that result from laws, orders and regulations which, altogether, constitute the functional tasks of the military but also the military discipline content. Thus, the only legal basis for the disciplinary sanction is disciplinary deviation and where the military's act was noticed as well as a crime, the disciplinary proceedings shall be suspended until the non-initiation of the criminal prosecution or by the date on which the court dispose the trial discharging or cessation.

Disciplinary violation involves two minimum conditions of military, that is the quality of military duties and breach of a statutory duty. This means that the subject of the disciplinary offense stipulated by the military discipline rules can be only military and the disciplinary violations scope is limited to acts of conduct by which the military honor and dignity are compromised, the duties of service are violated by failing or faulty performance of functional tasks and mission accomplishment.

3. DISCIPLINARY RESPONSIBILITY OF THE MILITARY

Disciplinary responsibility of the military has the following features: it is based on the breach by a military of a report of administrative law; the active subject is always a military commander or a public authority, subordinated in the violated judicial report; it is based on the passive subject's guilt who has the capacity of administrative law within the violated juridical report; the sanctions have a systemic configuration.

The disciplinary sanctions are coercive means, stipulated by law, whose purpose is to defend the disciplinary order, to develop the spirit of responsibility and accountability for the accomplishing the work duties, the rules of conduct as well as the prevention of acts of indiscipline. They are expressly and limiting stipulated by law, having both an educational character but also preventive.

Establishing disciplinary responsibility for soldiers who have committed disciplinary violations is done by sending them, as appropriate, in front of the Honour Board, trial council or prior research commission where they always have the right to the audience, defence and petition. Nevertheless, those who consider themselves mistreated by the applied sentence can address by written report to the direct superior of the person who issued the sanction decision and who is obliged to name a research commission. The decision proposed by the new research committee may maintain or cancel the disciplinary sanction or may apply another sanction. In its turn, it may be appealed in a court of law by administrative contentious in charge, in accordance with the administrative contentious Law in force.

The legality control of the act of punishment exercised by the administrative contentious is both a formal inspection and background control.

The formal control consists in verifying the legal procedure for application of the legal procedure sanction, that is the military hearing before the Honour Board or the court, as appropriate, the prior research, the document issued by the competent organ, etc.

Upon completion of the formal control, it will be determined whether the penalty is legal under procedural circumstances and if not, the sanction document will be sanctioned, so that the background control is unnecessary.

The background control aims at the checking the existence of military's fault, which can be done based on documents that have been the basis for issuing the notice of penalty, of his guilt, the consequences of the crime committed and the causal link between the act committed and the consequences produced.

As a result of the background check, it will be determined whether the conditions of applying the disciplinary sanction and whether the individualization of the penalty was correct.

If these conditions are not met, a notice of cancellation penalties will be provided, and if the penalty was not correctly individualised, the act of punishing shall be amended in order to apply a lighter penalty.

From our point of view, setting another disciplinary sanction, a lighter one, is possible only if such a penalty has been requested by the plaintiff military, because in this way the court gives what was not required and it will violate a general principle of procedural law, namely the principle of availability.

Also, in our opinion, changing the actual act of punishment, for the purposes of applying another disciplinary sanction, an easier one, must be also done by the defendant, military authority, according to the limits laid down in the final and irrevocable judicial decision of administrative court, whereas military authority is by law the sole disciplinary power over his subordinates [4].

The status of military personnel is governed by the constitutional provisions contained in Article 118 paragraph (2) of the Constitution, according to which the structure of the national defence system, the preparation of population, economy and territory for defence, as well as the status of military personnel are established by organic law, constitutional provisions under which the legislator adopted Law no. 80/1995 with regard to the status of military personnel. Enlisted and professional soldiers are subject to the Status of Enlisted and Professional Soldiers, approved by law (Law No. 384/2006 on the Status of Professional Soldiers and Enlisted, published in the Official Gazette of Romania, Part I, No. 868 of 24 October 2006).

By Decision no. 71 of 29 January 2019, the Constitutional Court of Romania declared that the provisions of Article 34, Article 35 paragraph (3) of the Law no. 80/1995 on the status of military personnel are non-constitutional. From the assessment made, the Court held that military personnel are the subject of a service relationship, and in the exercise of their duties under the law and the provisions of the military regulations, officers, warrant officers and non-commissioned officers are invested with the exercise of public authority, enjoying protection, according to the criminal law (Article 6 of Law 80/1995). This service report is initiated, executed and terminated under special conditions. As a consequence, the essential elements regarding the initiation, execution and termination of service relations inherently refer to the status of military personnel, a status to be regulated by organic law. At the same time, the Court notes that the evaluation of the activity and conduct of the military staff refers to the manner in which the service relationship is executed and, through the effects produced, may have the effect of modifying or even terminating it, namely the postponement of the next rank promotion for 1or 2 years (Article 33 of Law No. 80/1995), or the changeover from active-duty to reserves, as a sanction (Article 51, Letter e) of the Military Discipline Regulations] or promotion to the next rank (Article 32, Letter k) of the Regulation of the military discipline], the granting of defence and security weapons with engraved names, according to the law [Article 29 paragraph (3) Letter g) of the Military Discipline Regulation].

As a consequence, given that by the provisions of Article 34 and Article 35 paragraph (3) of the Law no. 80/1995 on the status of military personnel, the Minister is assigned to regulate some aspects regarding rewards, deviations from the military discipline, disciplinary sanctions, the organization and functioning of the councils of honour, the conditions for setting up councils of honour, the functioning of councils of honour, the appeals of the decisions of the councils, the organization and functioning of the appeal councils, respectively the evaluation of the activity and the conduct of the military personnel as part of some essential matters related to the service relationship and their status, and which are regulated by infra-legal acts, respectively by regulations that are approved by orders of the Minister of National Defence, the Court finds that all these elements must be regulated, according to Article 118 paragraph (2) of the Constitution, by organic law.

In particular, to comply with the provisions of Article 118 paragraph (2) of the Constitution, the Court points out that the above-mentioned essential aspects relating to the assessment of military personnel's activity and conduct as part of essential aspects of the service relationship and their status, the initial disciplinary procedure, the enforcement of disciplinary sanctions or the work of the discipline council activity and that of councils of honor and trial, including the arms regime (the granting of defence and security weapons with engraved names), must be regulated by organic law and the rules specific to the evaluation procedure must be explained and detailed by order of the minister of defence.

Normative orders are issued only on the basis of and in compliance with the law, and must be strictly limited to the framework established by the documents on the basis and in the execution of which they have been issued and cannot contain solutions that are contrary to its provisions. However, the provisions of Articles 34 and 35 paragraph (3) of Law no. 80/1995, before being amended by Law no. 101 of May 8, 2019 (published in the Official Gazette No. 371 of May 13, 2019), did not regulate the essential aspects related to the career of military personnel, but they delegated the regulation of these matters to the Minister of Defence. Thus, the Minister of National Defence was empowered to adopt military orders and military regulations that did not circumscribe to the constitutional requirements, as they allowed the adoption of legislative acts of an infra-legal rank that could modify the status of military personnel. Thus, there may have appeared some situations when some essential aspects concerning the execution and / or termination of military service relationships to be regulated by an administrative act that contained elements beyond the legal framework, even to be later on added to the law.

CONCLUSIONS

In conclusion, the administration put, as fundament of its entire activity, the application and observance of law, the principle of legality being one of the basic works of administration activity, including the military. Liability in any of its forms is determined by the committing of illegal acts, by the violation of the value system established by the city and recognized by law norms. In legal literature we find the thesis according to which in any branch of law we place ourselves, the liability has two purposes: to restore the violated legal order, causing a return to legality status; to express a negative reaction to the author of the illicit act, with the aim of determining him realize the significance of his deed, to regret and, in the future, not to repeat it again. To talk about responsibility, it necessarily requires its relationship approach with responsibility. Responsibility precedes responsibility and can remove it. It involves observance by the individual of the value system established by the city, at a global or micro social level. If this value system is respected, man lives in harmony with himself and with others, with his society, as a whole. When the value system is denied, the man ceases to be responsible; he becomes liable for its unlawful behavior1. The career military personnel must take responsibility as a priority in their behaviour. For them, there is no other value, more important than accomplishing his tasks; a belief emerged from rational understanding of phenomena. They must carry out their tasks, not because they are required to, but because they are convinced that it is their professional role.

REFERENCES

[1] *Dicționarul enciclopedic*, vol. 2, Editura Enciclopedică București, 1996, p.107.
[2] *Art. 2 din Regulamentul disciplinei militare, publicat în M.Of.*, Partea I, nr. 399 din 03.07.2013.
[3] Legea nr. 80/1995 privind statutul cadrelor militare cu completările și modificările ulterioare și Legea nr. 384/2006 privind statutul soldaților și gradaților voluntari
[4] *Art. 4 din Legea nr. 188/1999 privind statutul funcționarilor publici*, publicată în M.Of., Partea I, nr. 365 din 29.05.2007.

POLIHEURISITC APPROACH OF CYBERWARFARE BASED ON CYBER POWER INDEX

Horațiu MOGA*, Andrei LUCHIAN, Razvan BOBOC****

*”CNIF-MFP, Braşov, Romania (horatiu.moga@gmail.com)
**Transilvania University, Brașov, Romania (riesigen@gmail.com, razvan_13_13@yahoo.com)

DOI: 10.19062/2247-3173.2019.21.5

Abstract: *This research paper presents a merging way for study the cyberwarfare based on two theoretical approaches. The first one poliheuristic approach proposed by Alex Mintz in study of foreign policy, and the second way is the concept of cyber power index created by Intelligence Unit division of the british journal „The Economist”. The cyberwarfare poliheuristic study approach uses the EUI's cyber-power index questionnaire for a qualitative approach based on the evaluation of the decision matrix rates and weights. The presented method aims to become a standard in the field of cyberwarfare and an alternative to the purely rationalist approaches that are currently being invoked in this research field.*

Keywords: *decision matrix, foreign policy management style, decision rules*

1. INTRODUCTION

The poliheuristic paradigm of foreign policy aims to study the foreign policy motivations and behaviors of a state. For the motivation study, the poliheuristic decision matrix together with the decision-making mechanisms based on “cognitive short-cuts” were used. For the research of behavior are adopted various typologies. In this research, we adopt Clausewitz's idea [1]: cyberwarfare is a behavior by which a state actor continues its foreign policy with cyber offensive means that have the support its main critical cyber infrastructure. (the definition can also be adapted to non-state actors involved in cyber activities, even if they have no foreign policy). Through the concept of national critical cyber infrastructure, we consider the collection of computer-servers, computer-clients and physical information systems (cables, fiber optics, radio antennas) connected in a systemic ensemble [2]. These components of critical cyber infrastructure provide the modern way to a knowledge-based society but can also constitute the projection elements of the power of a state or non-state actor in the international relations arena. To measure this cyber power of a state, the Intelligence Unit division of the british journal „The Economist” (EUI) [3] proposed a cyber power rating questionnaire found in the appendix of this article. The cyber power, defined in EUI as the way to manifest the foreign policy of an actor in the online space, has five dimensions: Legal and Regulatory Framework, Economic and Social Context, Technology Infrastructure, Industry Application, Background Indicators. These dimensions of critical cyber power are the elements that are either mathematical evaluations or psychological projections based on ”cognitive short-cuts” defining the motivation of an actor. For the manifestation of cyber power as a behavior, we will use the typology proposed by Craig B. Greathouse [1]:

1. Action of Cyber Espionage and Cyber Crime - is the way in which state or non-state actors use organized crime methods with the collection of any type of information about a critical infrastructure as target; 2. Action of Denial of Service - these are the attacks on critical cyber infrastructure that perform the "denial of service" effect between computer-servers and computer-clients; 3. Action of Focused Cyber Attack - these are the types of attacks to critical cyber infrastructure that allow it to recover quickly through some mechanisms such as data recovery; 4. Action of Massive Cyber Assault - refers to attacks to critical cyber infrastructure that generate great damage and its inability to recover shortly and data recovery is not allowed. Because all cyberwarfare specific elements are dealt with in the field of poliheuristic paradigm of foreign policy, we will further detail the elements of this paradigm.

The paternity of the poliheuristic paradigm belongs to Israeli political scientist Alex Mintz [4]. The central concept of this paradigm is that the foreign policy decision of a leader, decision-maker or decision-making group - depending on the state management mode in foreign policy - is carried out in two stages (two-stage decision process). As a result of the first stage of the decision, the author proposed the use of cognitive decision paradigms in psychology, and in the second stage of the decision the paradigm of rational choice is used [4]. We can certainly say that the poliheuristic paradigm is a new generational synthesis paradigm, such as the new approach in Operational Code Analysis [5] or economical theories based on bounded rationality. For the first cognitive decision-making stage of the decision-maker (leader, decision-making group or decision-making groups), the author believes that making a judgment is based on bias. This bias is a result of cognitive mechanisms of "cognitive short-cuts" heuristics at the base of the human brain [4]. Alex Mintz proposed in his paper the following biases mechanisms based on "heuristics cognitive short-cuts" [4]: 1. "Focusing on short-term benefits rather than longer-term problems"; 2. "Preference over preference"; 3. "Locking on one alternative"; 4. "Wishful thinking"; 5. "Post-hoc rationalization"; 6. "Relying on the past"; 7. "Focusing on a narrow range of policy options rather than on a wide range of options"; 8. "Groupthink"; 9. "Overconfidence; over-estimating one's capabilities and underestimating rival's capabilities "; 10. "Ignoring critical information; denial and avoidance "; 11. "Focusing on only part of the decision problem"; 12. "Turf battles leading to suboptimal decisions"; 13. "Lack of tracking and auditing of prior decisions and plans"; 14. "Poliheuristic bias"; 15. "Shooting from the hip"; 16. "lthink"; 17. "Group polarization effect".

The paradigm is called poliheuristic because in the analysis of a certain foreign policy decision, there are several models of "cognitive short-cuts heuristics" in combination. After identifying the bias patterns used by the political decision-maker, it will be taken into the first stage of the decision to construct its decision matrix by establishing the types of actions to be followed, namely the dimensions of the objectives-results, which it aims to touch them.

In the second step of the decision-making process, the rational choice paradigm will be used to decide a sequence of actions based on constraints or other preferences of the decision-maker related to gains or losses.

In their research on Danish intervention in the Libyan crisis in 2011, Dennis Hansen, Spetim Ibisi, Ramne Pranaityte concluded that the poliheuristic paradigm is characterized by [6]:

1. Decision-makers based on poliheuristic biases that use rapid decisions focusing on critical dimensions of results and rejecting actions that provide unacceptable results.

2. For the evaluation of the remaining actions the analysis for the critical dimensions will focus on the rational choice paradigm that aims at maximizing profits, minimizing losses and risks.

That is why the poliheuristic paradigm has a bounded rationality that cannot encompass the whole spectrum of options of the decision maker. Several variants of specific prejudices for certain actions of the decision matrix can lead to different rational options such as maximizing profits vs minimizing risk or minimizing losses versus minimizing risk.

All three Danish authors consider their research based on the poliheuristic paradigm has the following features [6]: “The compromise of the two schools of thought provides a reliable tool for the analysis, and has empirically provided the field of FPA (foreign policy analysis) with new insights into the decision making process. The first step focuses on identifying when the decision makers have utilized cognitive shortcuts to make the decision process simpler and more comprehensible. The second step relies on a rational choice on how much Denmark is *capable* of engaging in the international contribution to the humanitarian intervention in Libya”.

In addition to the paradigm of synthesis of a new generation in which the political actor decides not to focus only on the outcome as in the case of the rational paradigm, Alex Mintz believes that in his proposed theory the decision is influenced by the domestic political process [4]. The same author points out that the following features of the decision-making process: “Political leaders virtually always take into account (explicitly or implicitly) domestic political factors and consequences while making decisions. The noncompensatory principle of poliheuristic theory suggests that in a choice situation, if a certain alternative is unacceptable politically” [4]. *By the non-compensatory principle, the author suggested that it is important to establish a hierarchy between the dimensions of the objective-result so that the decision maker aims to simplify the decision-making process*. One of the most important dimensions of the decision matrix is the decision-maker's internal political system, which is considered by a number of authors to be the supreme constraint in the poliheuristic approach [4]. Here's how to construct the poliheuristic decision matrix that characterizes the process in two steps.

2. METHODOLOGY

Poliheuristic decision matrix - operation with this analytical tool is characterized by two stages. The first stage determines the composition of the decision matrix and in the second stage the decision making rules are established.

2.1. The first element is to establish the model of management in foreign policy. There is a multitude of political psychology studies such as those focused only on the leader [7], leader-group-decision-making groups [8]. Once the type of decision-maker and his / her management in foreign policy has been established, the process of building the decision-maker matrix of the decisional actor based on his / her experience will be pursued. With the help of the poliheuristic matrix of decision-making, Alex Mintz believes that we can reverse the way how the decision-maker has cognitively implemented information processing from his past political experiences [4]. Thus, the structure of a decision-making matrix is presented in Figure 1, consisting of lines explicitly expressed on the critical dimensions of the objectives-results $o_1, \dots, o_m$,, respectively on the actions that make up the columns $a_1, \dots, a_n$.

	a_1	$\ldots$	a_n	w
o_1	r_{11}	$\ldots$	r_{1n}	w_1
$\ldots$	$\ldots$	$\ldots$	$\ldots$	$\ldots$
o_m	r_{m1}	$\ldots$	r_{mn}	w_m
Final Choice				

FIG.1. Poliheuristic decision matrix to a state decision-maker.

From the analysis of the foreign policy management process to identifying foreign policy actions, a decision criterion is needed. From our bibliographic analysis, the most appropriate criterion for the cyber warfare poliheuristic study is the typology of Craig B. Greathouse, to which we add the action of non-involvement or neutrality "do nothing". *Actions* – the actions of decision matrix are the following: Do nothing, Action of Cyber Espionage and Cyber Crime, Action of Denial of Service, Action of Focused Cyber Attack, Action of Massive Cyber Assault.

Dimensions - to the management criterion, another important element is the identification of the critical dimensions of the objectives and the results. In this research, we consider the five dimensions of the cyber power index in the Appendix: Legal and Regulatory Framework, Economic and Social Context, Technology Infrastructure, Industry Application, Background Indicators.

Implications - are explanations of the consequences an alternative may have on one or more critical dimensions (e.g.: may be explanations of synthesis summaries of items in Appendix).

Ratings - are numerical values attributed to the particular action (mean) for a specific dimension (scope); the implications that explain the goal-mean relationship that can be evaluated from -10 (very bad) to +10 (very good); critical dimensions' goal having positive rates.

Weights - are part of the management criterion in foreign policy and indicate to the analyst the level of importance that the decision maker gives to a dimension of the objectives or results of the poliheuristic decisional matrix. It has values of 0 and 10.

2.2. Determining the decision rules - if in the first stage the negative rates were associated with the dimensions of the decision matrix and a first evaluation of the implications was made in this way, we can establish the critical dimensions for the decider after the positive value of the rates. After excluding the uncritical dimensions in the decision matrix we move from the cognitive to the rational stage in which we determine the decision rules following the models below [9] for apposition of *the non-compensatory principle*:

1.Weak dominance – is an order relation noted as $a_k \geq a_{k+i}$ if and only if

$$r_{kj} \geq r_{(k+i)j}, \forall k, i = \overline{1,n}; \forall j = \overline{1,m}. \tag{1}$$

2.Strong dominance – is an order relation noted as $a_k > a_{k+i}$ if and only if for some k

$r_{kj} \geq r_{(k+i)j}$ and for the remaining k $r_{kj} > r_{(k+i)j}, k, i = \overline{1,n}; \forall j = \overline{1,m}$ (2)

3.Maximin - is an order relation noted as $a_k \geq a_{k+i}$ is and only if

$$\min(r_{kj}) \geq min(r_{(k+i)j}), \forall k, i = \overline{1,n}; \forall j = \overline{1,m}. \tag{3}$$

4.Leximin - is an order relation noted as $a_k > a_{k+i}$ if and only if

$\min\left(r_{k(j+p)}\right) > min\left(r_{(k+i)(j+p)}\right), \forall k, i = \overline{1,n}; j+p \leq m, \forall j, p = \overline{1,m}$ and for the remaining k, $\min(r_{kl}) = min\left(r_{(k+i)l}\right), \forall k, i = \overline{1,n}; \forall l, p = \overline{1,m}, l < p.$ (4)

5.Maximax and the optimism–pessimism rule – Naturally, α is assumed to be fixed throughout the evaluation of all alternatives a_i. Is an order relation noted as $a_k > a_{k+i}$, if and only if the following relation is satisfied:

$$\alpha \cdot max\left(r_{kj}\right) + (1-\alpha) \cdot min\left(r_{kj}\right) > \alpha \cdot max\left(r_{(k+i)j}\right) + (1-\alpha) \cdot min\left(r_{(k+i)j}\right), \forall k, i = \overline{1,n}; \forall j = \overline{1,m}. \quad (5)$$

6.$\alpha \cdot max\left(r_{kj}\right) + (1-\alpha) \cdot min\left(r_{kj}\right) >$ $\alpha \cdot max\left(r_{(k+i)j}\right) + (1-\alpha) \cdot min\left(r_{(k+i)j}\right), \forall k, i = \overline{1,n}; \forall j = \overline{1,m}$.Minimax regret - is an order relation noted as $a_k > a_{k+i}$ if and only if the following relation is satisfied:

$$\max\{(r_{kj} - \max(r_{kj}))\} > \max\{(r_{(k+i)j} - \max(r_{(k+i)j}))\}, \forall k, i = \overline{1,n}; \forall j, p = \overline{1,m} \quad (6)$$

7.$max\left\{\left(r_{kj} - max\left(r_{kj}\right)\right)\right\} > max\left\{\left(r_{(k+i)j} - max\left(r_{(k+i)j}\right)\right)\right\}, \forall k, i = \overline{1,n}; \forall j = \overline{1,m}$The principle of insufficient reason – is an order relation noted as $a_k > a_{k+i}$, if and only if the following relations are satisfied:

$w_j = \frac{1}{n}\sum_{i=1}^{n} r_{ij}$, and $w_j > w_{j+p}, \forall k, i = \overline{1,n}; j+p \leq m, \forall j, p = \overline{1,m}$ (7)

3. RESULTS

A number of case studies will be undertaken to build the decision-making matrix of a state actor that will analyze the types of behavior that it can adopt. Possible cyberwarfare behaviors are: Do not, Action of Cyber Crime, Action of Denial of Service, Action of Focused Cyber Attack, Action of Massive Cyber Assault. For each action, we analyze how to conduct leadership, group leadership, or groups. Then we identify the critical dimensions of the decision matrix. We suppose that in this study all five dimensions of the cyber power index are critical. For each case study, the cyber power index post-event questionnaire will be applied, because the consequences of past events are based on a "cognitive short-cuts" decision. For multiple items in the questionnaire, a five-step scale is used from 0 to 4. For items that do not have defined scales, similar scales will be built. For each rate in the table from Fig. 2, an average rate will be calculated as follows (8):

$$r_{ij} = \left[\frac{\sum_{i=1}^{N_j}(1+s_{ij})}{N_j}.2\right] \quad (8)$$

Where N_j is the number of items of each dimension in the cyber power index questionnaire, and s_{ij} is the score of an item i of the size j and has values from 0 to 4, which are found in the case study. Operator [] represents the integer of the average value multiplied by two to obtain integer values between 0 and 10.

Once we have established the values of rates and weights based on expression (8), the rules of Weak dominance (1), Strong dominance (2), Maximin (3), Leximin (4), Maximax and the optimism-pessimism rule (5), Minimax regret (6), the principle of insufficient reason (7) will determine the order of the actions from the most preferred to the less preferred by calculating the final choice based on relationships that defines decision rules.

	Do nothing	Action of Cyber Espionage and Cyber Crime	Action of Denial of Service	Action of Focused Cyber Attack	Action of Massive Cyber Assault	
Legal and Regulatory Framework	r_{11}	r_{12}	r_{13}	r_{14}	r_{15}	w_1
Economic and Social Context	r_{21}	r_{22}	r_{23}	r_{24}	r_{25}	w_2
Technology Infrastructure	r_{31}	r_{32}	r_{33}	r_{34}	r_{35}	w_3
Industry Application	r_{41}	r_{42}	r_{43}	r_{44}	r_{45}	w_4
Background Indicators	r_{51}	r_{52}	r_{53}	r_{54}	r_{55}	w_5
Final Choice						

FIG.2. Poliheuristic decision matrix for cyberwarfare actions.

4. CONCLUSIONS AND FUTURE WORKS

This research paper proofed a merging way for study the cyberwarfare based on two theoretical approaches. The first one poliheuristic approach proposed by Alex Mintz in study of foreign policy, and the second way is the concept of cyber power index created by Intelligence Unit division of the british journal „The Economist”.

The cyberwarfare poliheuristic study approach uses the EUI's cyber-power index questionnaire for a qualitative approach based on the evaluation of the decision matrix rates and weights. The presented method aims to become a standard in the field of cyberwarfare and an alternative to the purely rationalist approaches that are currently being invoked in this research field. Also in the future researches this method will be integrated with image indicators based on verbs into the context system with quantitative methods such as game theory, agent-based modeling, and qualitative predictive methods such as Lockwood Analytical Method for Prediction and will become a standard for cyber and cyberwarfare intelligence studies.

There is a procedure for implementing bounded rationality decision, which will endeavor to enrich itself in the future with research based on cognitive consistency. The presented model does not address the analysis of the cognitive consistency specific to the poliheuristic paradigm that will be dealt with in a future research as well as the introduction of the concept of learning in the cyberwarfare process.

APPENDIX: CYBER POWER INDEX QUESTIONNAIRE AFTER EUI [3]

1.Legal and Regulatory Framework

1.01. “National cyber plan - This indicator measures whether there is a national cyber plan with targets and deadlines. The scoring for this indicator is as follows: 0 = No; 1 = No, but plan is being developed; 2 = Yes, but plan is vague or is poorly enforced; 3 = Yes, but plan is not comprehensive or has a few shortcomings in implementation; 4 = Yes, plan is comprehensive and has specific targets and deadlines. (Source: Economist Intelligence Unit, Year = 2011) "

1.02. "Public/private partnerships - This indicator measures whether the government engages in public/private partnerships (PPPs). The scoring for this indicator is as follows: 0 = Cyber-related PPPs do not exist; 1 = Government makes limited efforts to partner with private sector; 2 = Active, but uneven efforts; 3 = Above-average efforts; 4 = Strong efforts. (Source: Economist Intelligence Unit, Year = 2011)"

1.03. "Cyber enforcement authority - This indicator measures whether there is a central cyber enforcement authority. The scoring for this indicator is as follows: 0 = No central enforcement authority or collaboration across agencies; 1 = No central enforcement exists, but there is minimal collaboration across agencies; 2 = No central enforcement exists, but there is moderate collaboration across agencies; 3 = Central agency exists with shortcomings in enforcement; 4 = Central enforcement agency exists with evidence of strong enforcement. (Source: Economist Intelligence Unit, Year = 2011)"

1.04. "Cybersecurity laws - This indicator measures whether the country passed national cybersecurity laws, such as data privacy and computer-misuse laws. The scoring for this indicator is as follows: 0 = No cybersecurity laws exist; 1= A few laws exist, but are not enforced; 2 = A few laws exist, with moderate enforcement; 3 = Several laws exist and are adequately enforced; 4 = Laws cover all main areas of cybersecurity and are strictly enforced. (Source: Economist Intelligence Unit, Year = 2011)"

1.05. "Cyber crime response - This indicator measures whether the country has a CERT security response team in place and actively responds to cyber crime. The scoring for this indicator is as follows: 0 = No; 1 = Minimal or limited response; 2 = Uneven response; 3 = Above-average response; 4 = Strong response. (Source: Economist Intelligence Unit, Year = 2011)"

1.6. "International cybersecurity commitments - This indicator measures whether a country is a signatory to an international commitment on cybersecurity, with particular consideration to the Convention on Cybercrime, also known as the Budapest Convention on Cybercrime. The scoring for this indicator is as follows: 0 = No; 1 = Acceding; 2 = Signatory; 3 = Ratified; 4 = In force. (Source: Economist Intelligence Unit, Year = 2011)"

1.07. "Cybersecurity plan - This indicator measures whether the country has a cybersecurity plan with explicit targets. The scoring for this indicator is as follows: 0 = No; 1 = No, but plan is being developed; 2 = Yes, but plan is vague; 3 = Yes, but plan is not comprehensive; 4 = Yes, plan is comprehensive and has specific targets and deadlines. (Source: Economist Intelligence Unit, Year = 2011)"

1.08. "Cyber censorship - The scoring for this indicator is as follows: 2 = Free (0–11 points); 1 = Partly free (12–23 points); 0 = Not free (24–35 points). (Source: Freedom House, Freedom on the Net 2011, Year = 2011)"

1.09. "Political efficacy - A composite score measured on a scale of 0–100, which measures effectiveness of policy formulation; quality of bureaucracy; excessive bureaucracy/red tape; vested interests/cronyism; corruption; accountability of public officials; and human rights. (Source: Economist Intelligence Unit Risk Briefing, Year = 2010)"

1.10. "Intellectual property protection - A measure of the strength of intellectual property protection measured on a scale of 0–4, where 0=best. (Source: Economist Intelligence Unit Risk Briefing, Year = 2010)"

2.Economic and Social Context

2.01. "Tertiary student enrollment as a percentage of total enrollment - The percentage of the 18–22 age group, who are enrolled full-time in tertiary education. (Source: UN Educational, Scientific and Cultural Organization, Year = Latest year available, between 2006 and 2010, unless otherwise indicated in the model)"

2.02. "Expected years of education - The total number of years of schooling (primary to tertiary) that a child of a certain age can expect to receive in the future, assuming that the probability of his or her being enrolled in school at any particular age is equal to the current enrollment ratio for that age. (Source: UN Educational, Scientific and Cultural Organization, Year = Between 2008 and 2009, unless otherwise indicated in the model)"

2.03. “Labor productivity growth - Efficiency of labor, measured in terms of output per worker (real GDP per person employed). This indicator is measured as the percentage change between 2009 and 2010. (Source: Economist Intelligence Unit, Year = 2010)”

2.04. “Researchers in research and development per million people - Researchers in R&D are professionals engaged in the conception or creation of new knowledge, products, processes, methods, or systems, and in the management of the projects concerned. Postgraduate doctoral students (ISCED97 level 6) engaged in R&D are included. (Sources: UN Educational, Scientific and Cultural Organization, Year = Latest year available, between 2006 and 2008, unless otherwise indicated in the model)”

2.05. “Science and Engineering degrees as a percentage of total degrees awarded - The OECD definition of science degrees includes: life sciences; physical sciences; mathematics and statistics; and computing. The OECD definition of engineering degrees includes: engineering and engineering trades; manufacturing and processing; and architecture and building. (Source: Organization for Economic Co-operation and Development; UN Educational, Scientific and Cultural Organization; National Science Foundation; Economist Intelligence Unit, Year = Latest year available, between 2006 and 2010)”

2.06. “English literacy - The scoring for this indicator is as follows: 0 = Very low proficiency; 1 = Low proficiency; 2 = Moderate proficiency; 3 = High proficiency; 4 = Very high proficiency. (Source: Education First; Economist Intelligence Unit, Year = 2011)”

2.07. ”Information and communication technology exports as a percentage of total exports - ICT exports include telecommunication, audio and video, computer-related equipment, and electronic components, among other ICT goods. Software is excluded. (Source: UN Comtrade, Year = 2009)”

2.08. “Information and communication technology imports as a percentage of total imports - ICT imports include telecommunication; audio and video; computer-related equipment; and electronic components, among other ICT goods. Software is excluded. (Source: UN Comtrade, Year = 2009)”

2.09. “Openness to trade - This indicator is measured on a scale of 0–5, where 5=best, and represents for trade as a percentage of GDP. (Source: Economist Intelligence Unit Business Environment Rankings, Year = 2010)”

2.10. “Research and development expenditure as a percentage of gross domestic product - R&D expenditure includes current and capital expenditure on creative, systematic activity that increases the country’s stock of knowledge. (Source: UN Educational, Scientific and Cultural Organization, Year = Latest year available, between 2006 and 2008, unless otherwise indicated in the model)”

2.11. “Domestic patent filings per million people - A patent filing is defined as the procedure for requesting IP protection at an IP office. The resident filing refers to an application filed with the Office of, or acting for, the State, in which the first-named applicant in the application concerned has residence. (Source: World Intellectual Property Organization, Year = 2009, unless otherwise indicated in the model)”

2.12. “Private equity and venture capital as a percentage of gross domestic product - Private equity is defined as securities that are not listed on a public exchange and is taken as a percentage of gross domestic capital.

Venture capital is considered a sub-set of private equity. (Source: Organization for Economic Co-operation and Development; National Venture Capital Associations; Economist Intelligence Unit, Year = 2010, unless otherwise indicated in the model)”

3.Technology Infrastructure

3.01. “Internet penetration - This indicator measures Internet users per 100people. It also includes subscribers who pay for Internet access (dial-up, leased line, and fixed broadband) and people with access to the worldwide computer network without paying directly, either as the member of a household, or from work or school. (Source: International Telecommunications Union; Economist Intelligence Unit, Year = 2008)”

3.02. “Mobile cellular penetration - This indicator measures mobile cellular subscriptions per 100 people. It also includes the number of subscriptions to a public mobile telephone service using cellular technology, which provides access to the Public Switched Telephone Network.

Post-paid and prepaid subscriptions are included. (Source: Economist Intelligence Unit Technology Indicators, Year = 2008)"

3.03. "Wi-Fi hotspots per million people - This indicator measures the penetration of wireless hotspots, derived from JiWire's database of 636,927 free and paid Wi-Fi locations in 142 countries. (Sources: JiWire, Year = 2011)"

3.04. "Social media penetration - This indicator measures social media users as a percentage of Internet users. (Source: comScore; Economist Intelligence Unit, Year = 2010)"

3.05. "Fixed broadband subscriber lines per 100 inhabitants - Subscriber lines with a transmission speed greater than 128 Kbps per 100 people. Subscriber lines include primary rate interface (PRI) ISDN connections; xDSL connections; cable modem and cable telephony connections; and high-speed fixed wireless connections. (Sources: Economist Intelligence Unit Technology Indicators, Year = 2010 data, unless otherwise indicated in the Global Dynamism Index)"

3.06. "International Internet bandwidth - This indicator is defined as the capacity of backbone operators to carry Internet traffic. (Source: International Telecommunication Union and TeleGeography, Year = 2009)"

3.07. "Information technology spending as a percentage of gross domestic product - This indicator measures total IT spending on packaged software, hardware, and IT services as a percentage of gross domestic product. (Source: Economist Intelligence Unit Technology Indicators, Year = 2010)"

3.08. "Mobile phone tariffs - This indicator measures average per-minute cost of various mobile cellular calls, and is used as a measure of ICT affordability. Tariffs are expressed in international dollars, adjusted for purchasing power parity. (Source: , World Economic Forum; International Telecommunications Union, Year = 2008)"

3.09. "Broadband Internet tariffs - This indicator measures the residential monthly fee of fixed broadband tariffs and is used as a measure of ICT affordability. Tariffs are expressed in international dollars, adjusted for purchasing power parity. (Source: World Economic Forum; International Telecommunications Union, Year = 2008)"

3.10. "Secure servers - This indicator measures the number of servers using encryption technology for Internet transactions. (Source: Netcraft, Year = Latest available year, 2009 or 2010)"

4.Industry Application

4.01. "Smart grids - The scoring for this indicator is as follows: 0 = Smart grids do not exist within the country; 1 = Plans for grid modernization are underway; 2 = Smart grids are moderately, but unevenly, developed; 3 = Smart grids are well-developed; 4 = Smart grids are highly advanced and are widely deployed geographically. (Source: Economist Intelligence Unit, Year = 2011)"

4.02. "E-Health - E-Health initiatives include the development of electronic medical records, tele-medicine provision, and mobile health delivery. The scoring for this indicator is as follows: 0 = E-Health technology does not exist within the country;
1 = Minimal e-Health infrastructure exists; 2 = Moderately deployed, yet unevenly integrated across common avenues; 3 = Deployed across most common avenues; 4 = Well-developed and integrated across all common avenues. (Source: Economist Intelligence Unit , Year = 2011)"

4.03. "Businesses placing orders via the Internet - This indicator is measured as the percentage of business Internet users. The scoring for this indicator is as follows: 0 = 0–9%; 1 = 10–24%; 2 = 25–39%; 3 = 40–54%; 4 = 55%+. (Source: UN Conference on Trade and Development; Organization for Economic Co-operation and Development; Economic Intelligence Unit, Year = Latest year available, between 2006 and 2010)"

4.04. "Individuals placing orders via the Internet - This indicator is measured as the percentage of Internet users. The scoring for this indicator is as follows: 0 = 0–19%; 1 = 20–39%; 2 = 40–59%; 3 = 60–79%; 4 = 80%+. (Source: UN Conference on Trade and Development; Organization for Economic Co-operation and Development; Economic Intelligence Unit, Year = Latest year available, between 2007 and 2010)"

4.05. “Individual use of Internet banking - This indicator is measured as the percentage of Internet users. The scoring for this indicator is as follows: 0 = 0–19%; 1 = 20–39%; 2 = 40–59%; 3 = 60–79%; 4 = 80%+. (Source: UN Conference on Trade and Development; Organization for Economic Co-operation and Development; Economic Intelligence Unit, Year = Latest year available, between 2007 and 2010)”

4.06. “Intelligent transportation – Intelligent transportation systems include arrange of measures, from simple GPS systems to advanced sensor technology, leading to inventions such as electronic tolls; variable speed limits; dynamic traffic lights; and advanced notification and tracking systems. The scoring for this indicator is as follows: 0 = Intelligent transportation systems do not exist within the country;1 = Plans are underway or minimal intelligent transportation systems exist; 2 = Moderately deployed, yet unevenly integrated across common avenues; 3 = Deployed across most common avenues; 4=Well-developed, and integrated across all common avenues. (Source: Economist Intelligence Unit, Year = 2011)”

4.07. “E-Government - This indicator measures the quality, scope, and utility of online services. It is measured on a scale of 0–1, where 0=low provision of online services and 1=high provision of online services. (Source: UN Online Services Index, Year = 2010)”

5.Background Indicators

5.01. “Real gross domestic product, US$atPPP - This indicator measures real gross domestic product at purchasing power parity, divided by the population. (Source: Economist Intelligence Unit Country data, Year = 2010)”

5.02. “Real gross domestic product growth - Percentage change of gross domestic product over 3 years, from 2007 to 2010. The underlying gross domestic product data are calculated at constant market prices, rebased to 2005 constant prices and translated into US$ using the LCU: $ exchange rate in 2005. (Source: Economist Intelligence Unit Country data, Year = 2010)”

5.03. “Human development index - UN composite index that measures development progress by combining indicators of life expectancy, educational attainment and income. This indicator is measured on a scale of 0 to 1, where 0=low human development and 1=very high human development. (Source: UN, Year = 2010)”

5.04. “Gini coefficient - This indicator assesses the level of inequality and is measured on a scale of 0 to 100, where 100=perfect equality. (Source: World Bank, Year = Latest year available, 2007 or 2008)”

REFERENCES

[1] Craig B. Greathouse, *Cyber War and Strategic Thought: Do the Classic Theorists Still Matter?*, in Cyberspace and International Relations Theory, Prospects and Challenges, Jan-Frederik Kremer and Benedikt Müller (Eds.), Springer; 2014;

[2] Horatiu Moga, Mircea Boscoianu, Delia Ungureanu, R. Lile, Nurettin Erginoz, Massive Cyber-attacks Patterns Implemented with BDI Agents, *Applied Mechanics and Materials, OPTIROB 2015,* Vol. 811, pp. 383-389, 2015;

[3] *** EIU - Cyber Power Index Findings and Methodology, Iun 2014, Available at https://www.sbs.ox.ac.uk/cybersecurity-capacity/system/files/EIU%20-% 20Cyber%20Power%20 Index%20Findings%20and%20Methodology.pdf;

[4] Alex Mintz and Karl DeRouen Jr, *Understanding Foreign Policy Decision Making,* Cambridge University Press, 2010;

[5] M. Schafer and S. Walker, *Beliefs and Leadership in World Politics: Methods and Applications of Operational Code Analysis*, Palgrave Macmillan, 2006;

[6] Dennis Hansen, Spetim Ibisi, Ramune Pranaityte, *Foreign Policy Analysis: The Danish Decision to Intervene in Libya,* Roskilde University, Dept. of Society & Globalisation, 2011;

[7] Margaret G. Hermann: *Assessing Leadership Style: a Trait Analysis,* 1999, Available at https://socialscience.net / docs/LTA.pdf;

[8] Martha L. Cottam, Elena Mastors, Thomas Preston, Beth Dietz, Beth Dietz-Uhler, *Introduction to Political Psychology,* Psychology Publisher, 2009;

[9] Martin Peterson, *An Introduction to Decision Theory,* Cambridge University Press, 2009.

SWOT ANALYSIS OF "BALTICA 07" MISSION FROM CIVIL-MILITARY COOPERATION PERPECTIVE

Cosmina-Oana ROMAN

"Henri Coandă" Air Force Academy, Braşov, Romania
(roman.cosmina@afahc.ro)

DOI: 10.19062/2247-3173.2019.21.6

Abstract: *The Romanian Army has not always had concerns to train specialized forces in the field of CIMIC. The relations between Romanian militaries and civilians in the operational areas were based on the formers' responsible commitment, as well as on the ability to inspire confidence, good will, respect, appreciation and consideration. With Romania joining NATO structures, the experience of the Alliance in the field of relations between soldiers and civilians made possible the embrace of the CIMIC concept and the establishment of the first specialized structures in this field. I do consider that the process is still in the beginnings. The perception by various categories of army forces of the role and importance of CIMIC in fulfilling their missions, especially in terms of their participation in missions outside the national territory, is not yet at the expected level within this research. The answers given by interviewees to the research questions were often conventional, with little depth of observation. Practically, all respondents agreed, at the maximum acceptance level, to my views, which was why a statistical processing of the answers was not necessary. However, I have used the observations of those who have been involved, with detailed responses with maximum receptivity. I do believe that this perception will improve, as challenges arise and awareness of the existence of specialists responding to these challenges. This research is intended to be a contribution to this awareness process.*

Keywords: *CIMIC, air policing mission, operations area*

1. INTRODUCTION

At the time of the "Baltica 07" mission was developing, the experience of Romania in the field was still limited. The Romanian legislation did not allow funding such activities, which, as one of the participants noted, was carried out "*often by collecting personal funds*". Neither from symbolic value perspective, these actions did obviously and professionally involve the national symbols, values that are specific to Romanians. For such missions where the military conflict is absent and, therefore, the cultural component of the missions can be maximized, the detachment must be available from the stage of preparation of the promotional material mission specific to the Romanian culture and civilization, simple objects printed with national flags (flags, scarves, pens, toys, figurines, etc.), and for visits to schools and orphanages, or for protocols, packages of non-perishable goods, or symbolic gifts. Definitely, there should also be special financial resources available to the detachment for such activities, which can be managed by the public relations officer and the mission commander. Given that the frequency and importance of the Romanian Armed Forces missions outside the national territory are increasing year after year, and that the international military cooperation actions in NATO, or non-NATO exercises, applications and training are becoming more frequent, the Ministry of National Defense should prepare within specialized structures, through orders and acquisitions, or through their own forces, a wide range of promotional materials, both for the promotion of Romania as a nation and for the promotion of various categories of army forces. At the same time, for the immediate preparation of specific missions, traditional materials should be made, as well as, in case of charitable actions, certain professional packages, inscribed with national symbols. Under any circumstance, when missions outside the national territory require *CIMIC*-type actions, the status of the Romanian military force must be that of national dignity, of confirmation of the Romanian Armed Forces as a distinct entity, solid values and principles undoubtedly anchored in the cultural and spiritual patrimony of the Romanian people. Under no circumstances should the Romanian Army and, in particular, the Romanian Air Force leave the impression of the Alliance's "poor relative". The indisputable professionalism of Romanian soldiers participating in missions outside the national territory must be favored with the dignity, honor and prestige of the country of which they are citizens.

2. IMPORTANT DATA ABOUT "BALTICA 07"

"Baltica 07" mission consisted in "*defending the integrity of the Baltic Sea Airspace in peacetime for 24 hours a day with aircraft capable of taking off and acting in the event of an aircraft being violated by mistake or intentionally, the flight regime in the airspace of the Baltic States*" [1]. The mission lasted for 3 months, between 31st of July – 31st of October, 2007. The mission was attended by 4 Mig-21 LanceR "C" aircraft and a detachment of 67 militaries from "General Emanoil Ionescu" Air Base 71 from Câmpia Turzii. The mission took place within NATO, „*under the command and tactical control of the Combined Air Operations Center– CAOC) from UEDEM, Germany*" and „*in collaboration with Lithuanian commanders Siauliai and Karmelava bases*." [1]

One of the major concerns of the Baltic States, after independence, was the development of military forces to ensure its preservation and defense. Rapid joining NATO structures and massive participation in the Alliance's military activities is one of the core factors of this concern.

Of the three Baltic countries, only Latvia has a professional army. The Latvian defense concept is based on a Swedish-Finnish model, which involves the establishment of a Rapid Reaction Force and a mobilization center to build this force.

Lithuania abolished mandatory military service in 2008, but it reintroduced it in 2015, keeping under its arms a staff of 15,000 active soldiers.

Estonia has never proposed the abolition of compulsory military service, which has a variable duration of 8-11 months, depending on specialization, but it also prepares a Paramilitary National Guard (League of Defense).

Since joining NATO, the armies of the Baltic States participated and still participate with significant forces and means at international peace missions in theaters of operations in different parts of the world, having a great deal of experience in this field. They have an important contribution to the development and dissemination of experience in various fields, participating in the work of centers of excellence and even hosting some of them. It is of interest for the study the participation of Latvia at the NATO Center of Excellence in the field of civilian-military cooperation from the Low Lands.

3. SWOT ANALYSIS OF "BALTICA 07" MISSION

Therefore, the SWOT analysis of "Baltica 07" mission from *CIMIC* perspective, is as follows:

Crt.	Details	Content
1	Strong points	• Very good military and specialized training of all military personnel participating in the mission. • The benefits of *CIMIC* training provided to the mission as a whole by NATO. • *CIMIC* experience shared by national detachments present during previous rotations. • The existence of communication, cooperation and logistics channels fully developed in previous rotation. • *CIMIC* training of the mission commander, of Public Relations Officer and of mission personnel. • The existence of a "Soldier's Handbook", for all military participants. • Knowledge, by all possible staff involved in *CIMIC*-related cooperation, of English, universal language of communication within NATO and, in particular, in the air force. • Exceptional availability of dialogue between the two cooperating parties, Romania and Lithuania.
2	Weak points	• The complete novelty of the mission and the lack of experience in carrying out such missions. • Too general *CIMIC* training and poorly adapted to the mission and deployment area of the detachment. Absence of a *CIMIC* specialist in the mission. • The absence of a Russian-language translator, given that the Lithuanian population over 20 is 80% Russian-speaking. • The low availability of certain specific resources for social and cultural integration activities (financial resources, promotional materials, etc.). Lack of legal regulations in this area. • The still low level of implementation, in the Lithuanian Air Force, of the NATO air base equipping standards and assimilation of procedures. • The non-existent interest of the Romanian Consulate in Vilnius towards the mission of the Romanian detachment.
3	Threats	• Decrease in the confidence of cooperation partners in their air defense potential, as MIG-21 LanceRs are at the resource limit, being the oldest aircraft among those present in the Air Police Mission in the Baltic States, and together with the MIG-29 aircraft of Poland, the only ones of Russian manufacture.
4	Opportunities	• The development of an international system of training exercises and applications within NATO on *CIMIC* creates the circumstances for increasing the degree of interoperability of the air force in solving *CIMIC* issues in missions outside the national territory. • The participation of the Romanian Air Force in "Baltica 07" mission has created the premises for a better understanding of the specificity of such missions, with equal benefits of Romanian and Lithuanian troops, as well as mutual knowledge between the two armies and the cohesion increase within NATO.

4. CONCLUSIONS OF THE SWOT ANALYSIS

Until the start of "Baltica 07" mission, the Romanian Air Force did not have the opportunity to carry out missions outside the national territory since the Second World War.

Moreover, this mission was the most important of the Romanian Air Force within NATO. The choice of this mission for the present case study, to compete with the air traffic management mission at Kabul Airport in Afghanistan, was driven by more thorough research, as in the case of "Baltica 07", combat aircraft actually took part, unlike the case of Kabul, where only specialists and security officers and aeronautical managers participated. Of course, in the case of Kabul, we were in a full conflict area with infinitely greater challenges in terms of mission security and difficulty, but "Baltica 07" allowed the test of the air force capability to carry out joint missions, using the whole complex airspace management required by the activities under the air policing concept. From civil-military cooperation perspective, the case of Kabul may have been more spectacular and more challenging, but in the case of "Baltica 07" these requests were easier to identify and more readily available.

The wins of this case study are obvious. They consist, firstly, in assessing the degree of involvement of *CIMIC* specialists in the preparation and deployment of a Romanian Air Force mission outside the national territory, as well as in evaluating the effectiveness of this involvement. The conclusions of the case study are, as follows:

- *CIMIC* specialists involved themselves in mission preparation, staff training, and provided a behavior guide, as the *CIMIC* manual calls the "Soldier's Manual".
- Participants opinion was that the training was general, less applied to the specifics of the mission, and the "manual" contained few particular aspects of the area.
- The *CIMIC* component of the Romanian Armed Forces did not consider it necessary to attach a *CIMIC* specialist to the mission, with possibly knowledge of Russian language or of the Northern culture and civilization.
- It is probably necessary for similar missions to make a much more *CIMIC* training, specific to the deployment area, and possibly to assign a *CIMIC* specialist, even a temporary employee.

A second conclusion is related to the legal framework for the execution of such missions. The Romanian state should be more interested in the presence of Romanian detachments in missions outside the national territory and to use these opportunities with more rigor and professionalism to promote the image of Romania. Legislation needs to be enacted, existing consular resources should be put in place and, in particular, material and financial resources must be provided for this purpose. It is unacceptable for a three-month presence of a Romanian detachment in a state with several million inhabitants not to be taken into account by the consular office attached to it.

A third conclusion is related to the lessons learned. A mission of such importance must be treated in all its complexity, without avoiding any of the aspects that can ensure success. Among these, civil-military cooperation is one that leaves deep traces in the consciousness of the population and of civil institutions in the host country. The military aspects are of utmost interest in national and regional security structures. For the common man, the cultural and socio-emotional impression left by foreign soldiers is the one that remains. According to this trace, a peoples, a nation, a country is characterized by.

CONCLUSIONS

As a conclusion, the participation of the Romanian Air Force in missions outside the national territory is not only a working hypothesis for applications and trainings. Local and regional instability in different parts of the globe, driven by ethnic, political or religious rivalries, by actions against human rights, by terrorist, separatist, dissolving states actions, has already led to the engagement of the international community through its representative bodies, but also through the North Atlantic Alliance under international mandate to protect populations and legitimate authorities. The obligations arising for Romania as an active member of the international bodies to which it belongs, the Romanian Army's NATO membership, as well as the commitments assumed within this alliance, made it possible and necessary to participate, with significant effects, in numerous missions outside the national territory, Romania being considered a significant contributor to peace efforts in various conflict areas in the Balkans, Iraq or Afghanistan. To this, a significant number of international observers requested to Romania to supervise and validate peace efforts in various hot zones of the globe is added. It can be said that Romania is an actor involved in peace efforts, its pacifist vocation generating trust and hope worldwide. Given these conditions, the Romanians, whether civilian or military, have inspired feelings of safety, mutual acceptance, cooperation and open cooperation through their behavior in relation to civilian actors and the people in the areas of responsibility.

REFERENCES

[1] M. Barac, S. Săftoiu, *Baltica 07 – O misiune militară, culturală şi socială, Cer senin,* Review of Romanian Air Force, No. 5(95), 2007;

[2] Marshall McLuhan, *Understanding Media: The Extensions of Man*, Cambridge, MA: MIT Press, 1994, cap. 1, p. 1, available at http://web.mit.edu/allanmc/www/mcluhan.mediummessage.pdf, (accessed on 3rd January, 2018);

[3] Nielsen, Don M.Snider (eds), *American Civil-military Relations: The Soldier and the State in a New Era*, Suzanne C., Baltimore, 2009, p. 189;

[4]***. *Action Plan on Strategic Communication*, European Council, Bruxelles, Ref. Ares (2015) 2608242 – 22 June, 2015, p. 1;

[5]***. Joint Doctrine Note 1/12 (JDN 1/12), *Strategic Communication: The Defence Contribution*, U.K. Ministry of Defence, January 2012, available at https://www.gov.uk/government/uploads/ system/uploads/attachment_data/file/33710/20120126jdn112_Strategic_CommsU.pdf , accessed on 20th February, 2018;

[6] ***. *Joint Doctrine Note 1/12 – Strategic Communication: The Defence Contribution*, DCDC/MoD, January, 2012, p.1-1;

[7]***. *Strategic Communiucation Joint Integrating Concept*, (JROCM 166-09), Version 1.0, 7 October, 2009, p. ii, available at http://www.jcs.mil/Portals/36/ Documents/Doctrine/concepts/ jic_strategiccommunications.pdf?ver=2017-12-28-162005-353 (accessed on 20 February, 2018);

[8]***. Norberto R. Menendez, *Theory as Foundation for Strategic Communication Doctrine*, 4 May, 2009, pp.15-16 (article in Faculty of Naval War College), available at https://www.researchgate.net/ publication/235153510_Theory_as_Foundation_for_StrategicCommunication_Doctrine (accessed on 24th February, 2018);

[9]***. *(AD) 95-2*/2012, p.3-1 (b);

[10]***. *Strasbourg – Kehl NATO Summit Declaration*, 4 April 2009, pct. 16;

[11]***. *MC 0628 – NATO Military Policy on Strategic Communications*, North-Atlantic Council, 19 July 2017, p. 4;

[12]***. *Department of Defense Dictionary of Military and Associated Terms*, US Ministry of Defense, March 2017, p. 223;

[13]***. *Allied Joint Doctrine, AJP-01*, February, 2017.

THE EUROPEAN UNION CITIZENSHIP

Dumitru TOADER

„Henri Coandă" Air Force Academy, Braşov, România

DOI: 10.19062/2247-3173.2019.21.7

Abstract: *The Treaty of Maastricht, introduced the European citizenship to strengthen the existing relationship between the EU and the Member State citizens, but did not define the term. In fact, the Treaties of Maastricht and Amsterdam, although based on the two concepts of the Europe of the citizens and the European Union citizenship, establish a set of rights that are closer to the concept of citizenship in the traditional sense than to the one of the Europe of citizens. The citizenship of the European Union under the Maastricht Treaty is closely linked to the nationality of a Member State and is regarded as a first outline of a common European identity and cannot be compared with the citizenship of a state since it does establish a relationship between the citizen and the European Union regarding rights and obligations. The European citizenship is fundamentally distinct from the national one, which, by the wording of the Treaty of Amsterdam, "is completed but not replaced by the former".*

Keywords*: citizen, citizenship, European citizen, European citizenship, national citizenship, Europe of the citizens, Treaty of Maastricht, Treaty of Amsterdam, Treaty of Lisbon*

The entry into force, on 1 January 1993, of the Maastricht Treaty was also thought to be, in a more or less justified manner, the change of the elitist, technocratic and economic Europe into one in which the citizen formally became the protagonist of the European political system, an European citizen who "participates in the affairs of the city "in accordance with the principle of Aristotle.

The report on the European Union prepared by LéoTindemans, the Belgian Prime Minister, in 1975, has the merit of having summarized the various ambitious stages of the construction of the status of "citizen" at European level: be it about the year 1974, when the principle of direct elections for the European Parliament was introduced or about the period 1990 – 1991 that preceded the Treaty of Maastricht in which the term "citizen" was formally defined. Additionally, this report emphasizes the need of closer relationships between the European institutions and the citizens, but also the foundation of some "European solidarity" thus proposing an active European citizenship. It also presented several tools: encouraging the collaboration among national television and radio, the equivalence of diplomas and study programs, as well as more exchanges between universities. All these target the interaction among European people, thus the citizens being able to know each other and to build relationships.

Even if the content of the Treaty of Maastricht mentions through Article 20 that "each citizen having the citizenship of any member state is also a citizen of the Union" and that "European Union citizenship adds to and doesn't replace the national citizenship", soon after the formalization of the status of European citizen there was confusion over the national and European citizenship. Therefore, immediately after the entry into force of the Treaty of Maastricht, the European Commission received some letters from the people of the member states in which, on the one hand, they thanked for the intention of giving them the “European citizenship” and, on the other hand, they refused the proposition as they rejected giving up their own national citizenship.

Subsequently, the aim of the *Treaty of Amsterdam* was, among others, to specify more clearly the rights and obligations of a European, national citizenship being only a sine qua non condition. Furthermore, the *Treaty of Lisbon* brought forward two new facets of the European citizenship, namely the right of the citizens to legislative initiative and the enhancement of the power awarded to the European Parliament, therefore stronger ties among institutions and citizens.

In positive law, citizenship continues to designate the legal status that allows a person to play an active part in the life of the state, enjoying civil and political rights such as the right of residence, the right to elect and be elected, the right to apply for public positions, the right to diplomatic and consular protection, etc… and being, as well, subject to certain obligations, such as the military service. The structure of the European Union therefore includes the exercise of rights at both EU and member state levels.

European citizenship does not suppress any of the rights inherent in national citizenship. It simply gives additional rights that are exercised either at EU level (for example the right to vote and be elected in the European Parliament) or at Member State level (for example the right to elect and be elected in the municipal elections). Some elements of the European citizenship can sometimes be likely to weaken the national citizenship to the extent that a national of a Member State is recognized rights that used to be reserved only to the citizens of that state. European citizenship can thus be seen as threatening or competing national citizenship. This is particularly obvious in what regards the right of residence or the right to elect or be elected, not only in the European Parliament but also in municipal elections; hence the reluctance of many states in developing European citizenship. Thus, Denmark has sought to declare that EU citizenship does not grant, by any means, the right to acquire Danish nationality.

In conclusion, the status of European citizen is subsequent to the possession or acquisition of the nationality on a member state and the national law of each EU member state must determine whether a person has his/her nationality or not. This solution was expressly confirmed by the declaration on the nationality of a Member State appended to the Maastricht Treaty and according to which “each time the Treaty establishing the European Community refers to the citizens of the member states, the issue whether a distinct person owns the citizenship of one or another member state is to be cleared only by the national law of the state in question. Difficulties may arise if the EU states have different laws and practices concerning granting and withdrawal of citizenship (a conflict between *jus soli (the right of the soil)* and *jus sanguinus (the right of blood)* conflict, different practices in the naturalization of foreign laborers). The States that restrict the acquisition of citizenship reluctantly accept opening their territory, the labor market, and the political rights for citizens from other Member States that are more liberal in this area. Thus, the European citizenship demands the member states to harmonize their national legislation in this area, although, it has to be admitted, there still are political sensitivities.

In 1984, The European Council of Fontainebleau developed the concept of *the Europe of the citizens*. The basic idea was that the citizen must be placed in the heart of the European construction, to develop in him a sense of belonging to the European Union. Among the specific rights recognized in the perspective of a *Europe of the citizens’* there are, undoubtedly, special rights inherent in the European citizenship and which establish a genuine political citizenship. But we find also some rights deriving from the economic integration, such as the free access to employment in a chosen country and other rights that consecrate the widening of the integration field, such as the right to culture and environmental protection.

But this conception takes away a large part of concept's specificity as the rights of citizens are no longer distinguishable from the rights of every human being.

In 1992, The Treaty of Maastricht, introduced the European citizenship to strengthen the existing relationship between the EU and the Member State citizens, but did not define the term. In fact, the Treaties of Maastricht and Amsterdam, although based on the two concepts of *the Europe of the citizens* and *the European Union citizenship*, establish a set of rights that are closer to the concept of citizenship in the traditional sense than to the one of *the Europe of citizens*. *The citizenship of the European Union* under the Maastricht Treaty is closely linked to the nationality of a Member State and is regarded as a first outline of a common European identity and cannot be compared with the citizenship of a state since it does establish a relationship between the citizen and the European Union regarding rights and obligations. The literature has described this judicial institution as a civic political dimension added to the state membership of the citizens of the Common Market. The European citizenship is fundamentally distinct from the national one, which, by the wording of the Treaty of Amsterdam, "*is completed but not replaced by the former*".

The dispositions included in the second part of the CE Treaty under the title "the citizenship of the European Union" constitute a study guide of the status of the European citizen and they proclaim, in a logical manner, that the citizens of the European Union not only have rights but are also subject to obligations. However, there is limited reference to "the obligations provided by the present treaty", the content of which is not mentioned. As far as the rights are concerned, on the one hand the Treaty reaffirms the already recognized right of free travelling and of residence, and, on the other hand, it consecrates new political rights (the right to vote and to be elected in European and municipal elections) and protection rights (diplomatic and consular protection, the right of petition, the complaint addressed to the mediator, the right of communication with the community institutions and organs).

The freedom of travelling and of residence is one of the fundamentals of the European Community and its ties to the European citizenship are critical, mainly from a symbolic point of view. It is currently a "branch" that separates from the citizenship due to the part it has played in the development of the community integration. Regarding the other rights, they derive from the two concepts of *European citizenship* and of *the Europe of the citizens*, but neither of them is entirely respected. Traditionally, the citizenship regards a status that is essentially political. That is why the access to public position shows affinities with political rights, such as the participation in the elections for the European Parliament and in the municipal elections. The protection rights provided by the Treaty refer to a Europe of the citizens that is not, however, limited to the citizens of the Member States. These guarantees have strong with the jurisdictional protection and the access to documents. In fact, the treaties enshrine these complementarities.

The confusion between the two perspectives, *the European citizenship* and *the Europe of citizens*, is very common. Thus, in its Resolution of 17 May 1995 on the functioning of the European Union Treaty, the European Parliament demanded that European citizenship should be strengthened especially by the European Union's accession to the European Convention on the Human Rights, the prohibition of the death penalty, the protection of minorities, the equality between men and women, and by strengthening the political citizenship. Clearly, these rights, although recognized in the European Union law, are human rights in general, so they are neither for the citizens of the Member States, nor reserved rights inherent in European citizenship.

The inclusion of articles 17-22 about *the European Union citizenship* in the EC Treaty and not in the EU Treaty, as it would have been natural, is explained by the fact that these articles are subjective rights of the citizens of the European Union whose legal protection can be better achieved by Community courts. The question whether the legal institution of the European Union citizenship incorporates rights provided in column two (CFSP, Common Foreign Security Policy) and three (CPJ - Police and Judicial Cooperation in Criminal Matters) of European integration (the European Union), has a negative answer as CFSP and CPJ are forms of interstate cooperation, and the acts of this framework force only Member States only, not their citizens.

Currently, the Treaty of Lisbon has the rank of primary Community law and modifies the constituent treaties (the Treaty regarding the European Union - the Maastricht Treaty and the European Community Treaty - the Treaty of Rome), the EU Treaty being called the Treaty on the European Union (TEU) and the EC Treaty - the Treaty on the Functioning of the European Union (TFEU) **[1]**, and the provisions on the EU citizenship take on a new stand-alone title called “Non-discrimination and the citizenship of the European Union”. A novelty is the introduction of the right of legislative initiative of the EU citizens. At the initiative of at least two million citizens of the Union, who are nationals of a significant number of Member States, the European Commission may be invited to submit, within the limits of its attributions, an appropriate proposal on matters that these citizens consider necessary to be subject to legal acts of the Union in order to implement the treaties **[2].**

The euro-barometer survey published in June 2009 outlines a few lines of cleavage between citizens of different Member States in terms of understanding the benefits of EU membership, the trust in institutions, the voice of the country within the EU, the knowledge about Brussels institutions. For Romanians, the European citizenship translates into the freedom to travel, study and work on the territory of any Member State. For understanding this, there is no need for polls - many of them not coping with the phenomenon - and no need for official reports. Just look at social changes: over a million Romanians working or studying in other EU countries, the political parties have been campaigning in Italy and Spain and routes as Suceava-Madrid or Bacău-Turin, etc. In other words, they live the European citizenship in the Romanian style.

However, the 2009 European elections results reveal a decrease in the rate of participation of European citizens to vote. This is felt not only in Romania and Bulgaria, countries that are still in the process of adjustment, but also in countries like Spain or Italy. In this case, is European citizenship rather formal than functional? Possibly, but certainly there are three dimensions that are key variables in explaining this phenomenon: the understanding of the process of functioning of the European Union, the capacity of information transmission from institutions to citizens and the discourse of the political leaders at national level.

REFERENCES

[1] Consolidated versions of the Treaty on the European Union and the Treaty on the Functioning of the European Union, the Official Journal of the European Union. C 115/2008, p. 1-361.

[2] Article 11 of the Treaty on the European Union.

RESEARCH ON APPLICATIONS OF MINI-TURBOJET AND TURBOJET ENGINED MILITARY UAVS

Mehmet TURKAY*, Selim GURGEN*, Göksel KESKIN*, Seyhun DURMUS
Melih Cemal KUSHAN***

*Eskisehir Osmangazi University, Turkey (turkaymhmt@gmail.com, sgurgen@ogu.edu.tr, gokselkeskin@outlook.com, erzesk@gmail.com)
**Balıkesir University, Turkey (drmsyhn@gmail.com)

DOI: 10.19062/2247-3173.2019.21.8

Abstract: *This study examines the diversity of unmanned aerial vehicles (UAVs) in recent years and the developments in these areas. The use of these aircraft in different areas, especially in military areas, has evolved rapidly. Due to this development, additional requirements emerged. At this point, the increase in these properties increased the weights of the UAVs and led to the search of high-thrusting engines. The aim of this study is to investigate the integration of mini-turbojet and turbojet engines from the class of gas turbines with high propulsion power into the UAV systems. Within the scope of our aim, the working principles of gas turbines, their types and turbines which on development stages are briefly introduced. The types of engines used in UAVs are tried to be explained with some vehicles. Examples of mini-turbojet air vehicles used in the past are given and current works of private companies are mentioned. As a result of the researches, it was concluded that there was no examples of fleet level of UAVs with turbojet engines and the development studies are continued today.*

Keywords: *Gas Turbines, Mini-Turbojets, Turbojet, Unmanned Aerial Vehicle (UAV)*

1. INTRODUCTION

In recent years, popularity on UAV has become very prominent, and it will continue to increase of popularity on UAVs [1]. If it should support this argument, in Europe, number of UAV was 181 in 2012, this number increased to 1032 in 2016 [2]. Especially UAV is used for military and civil application domains extensively. Also in civil markets for people who are professions and curious mini UAVs became easy to reach. Users used in different domains related to this easy accessibility. Users began using them for their scientific data and some exploration business [3]. Some examples of this saving rare creatures in places that has less accessibility. In addition to these examples they were used in some actions as illegal hunting, destruction of forests. While new areas are added in the civilian and military domains new capabilities are expected from the UAVs due to the increase of in these technologies. Some of these capabilities can be listed as follows; day and night high-resolution imaging, early warning system, low noise level, precision guided munitions, tactical strike and defense system, effective maneuverability and low visibility on radar are some of them. As integration of these capabilities that was added to UAVs was useful increases of the weight. Depending on its weight, it needs propulsion power which ought to be enough to fly toward the weight. With the increase in automation and digitization developments in aviation area [4], the work of unmanned aerial vehicles has gained more importance.

In addition to these examples increasing number of UAVs on military domains caused and accelerated on the new generation of high speed fighter UAVs that could destroy these unmanned aerial vehicles. In these researches a problem occurs in high speed propulsion power that was a similar problem in 1950's as ramjets and turbojets engined UAVs. That researches described as ancestor of UAVs at this point, this article inspects from 1950's to recent examples of models of turbojet engined UAVs and development of turbojet engined UAVs.

2. GAS TURBINES

Gas turbine engines are engines designed to convert the chemical energy that is generated by the combustion of the fuel, into another useful power, such as shaft power or high-speed thrust [5, 6].

Mini-turbojet and turbojet engines are gas turbine engines used for propulsion in UAVs. In generally gas turbine is located in the vehicles tail section and there are many important tasks [7]. These engines are particularly suitable in target and reconnaissance platforms, especially in military domains [8, 9]. There is no difference between in the working principles of mini-turbojet and turbojet engines [10].

3. TURBOJET ENGINES USED IN UAVS

The most common types of air craft engines used in aviation are gas turbine engines and piston engines. The piston engine types are simple-designed, fuel-efficient motors and are often used in small aircraft. In general, these engines lose their performances at high altitudes and if piston engine gets boosted its weight becomes heavier as engine size. Increasing the weight is a problem in aircraft design. Gas turbine engines are the engines that can fly at every altitude and produce high-speed, torque and bleed air [11, 12].

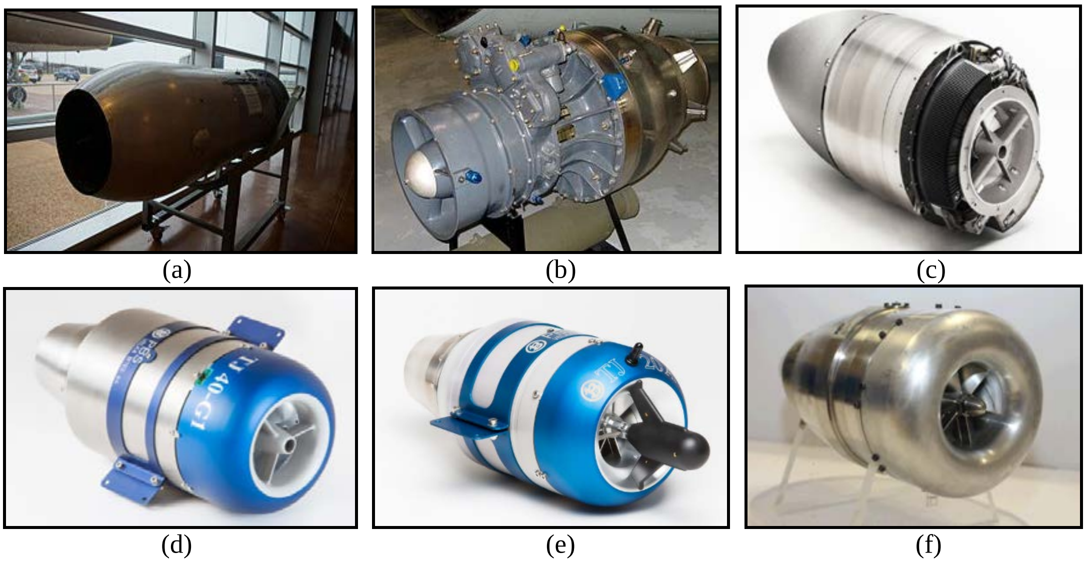

FIG. 1. Turbojet engines used in UAVs, (a) Fairchild J44 Small Turbojet Engine [13], (b) Teledyne CAE J69 Small Turbojet Engine [14], (c) PBS Aerospace TJ100 Turbojet [15], (d) PBS Aerospace TJ40 Mini-Turbojet [15], (e) PBS Aerospace TJ40 Micro-Turbojet [15], (f) TEI TJ90 Turbojet Engine [16]

Characteristic factors of the motors used in unmanned aerial vehicles differ on size, fields of use, etc. The engine used for a UAV for the purpose of reconnaissance may not provide the required efficiency when it is integrated into the UAV that will be used in another field.

As in aviation applications, the increase in the size of the aircraft due to the increase in aircraft size also applies to UAVs.

The turbojet engine was developed in 1940 by the Fairchild engine division. In 1944, Fairchild J44 (see Fig. 1.a) was used in target aircraft, missiles and as jet support into some aircraft [17].

Teledyne CAE J69 (see Fig. 1.b), an example of a small turbojet engine, was developed under the license of CAE Continental Aviation and Engineering. In the US, some airplanes were used as propulsion power to missiles and small UAVs. The Teledyne CAE J69 was developed to work at higher altitudes, and the J100, the top model, is out [18, 19, 20].

PBS Aerospace TJ100 (see Fig. 1.c) is a 4th generation turbojet engine and especially suitable for unmanned aerial vehicles. They can be used in military domains such as rescue and reconnaissance and also in other tasks for military domains. These engines are also ideal for glider experimental aircraft. The TJ 100 engine has a compact design and has low fuel consumption and excellent power rating for the output category. This engine is also suitable for landing into the water [15].

PBS Aerospace TJ40 Mini-Turbojet (see Fig. 1.d), has been developed to confuse enemy air defense systems and small reconnaissance aircraft. It is a turbojet engine used in UAV systems such as target aircraft and feed aircraft. It has a weight of only 3.25 kg, a thrust of 395 N and an advantage of 98,000 rpm max [15].

PBS Aerospace TJ40 Micro-Turbojet (see Fig. 1.e), is a turbojet engine designed for UAV systems, such as target drones and decoy drones, in order to confuse enemy air defenses and small reconnaissance drones. TJ40 mini-turbojet is used in UAVs systems such as target aircraft and feed aircraft. It only has a 1.98 kg weight and 210 N thrust power and a max revolution of 115000 rpm. It has a fuel pump and an electric spark plug located in the casing of the combustion chamber. Ideal for UAV systems [15].

In 2011, TEI TJ90 Turbojet Engine (see Fig. 1.f), has been started to provide a higher thrust than TJ35 turbojet engine development work in TEI plant in Turkey [16].

4. TURBOJET ENGINE APPLICATIONS IN MILITARY UAVS

Military aircraft are required to fly in all environmental conditions worldwide. They have to achieve success in the various and critical maneuvers they use in their operations [21]. Mini-turbojet and turbojet engines are gas turbine engines used to thrust unmanned aerial vehicles.

Radioplane Q-1 (see Fig. 2.a) was born from the need of a high-speed target aircraft of the US air force in 1950 and was manufactured as an advanced turbojet-powered aircraft. Radioplane Q-1 was launched by carrier planes and without the landing gear, landing operation carried out by the help of parachutes. The Continental YJ-69 turbojet engine was used in The Radioplane Q-1, the air required for the jet engine supplies from the space in its nose. Newly developed Ryan Q-2 aircraft ended its production. Radioplane Q-1 played a pioneer role in the development of air defense missiles [28, 29].

The Ryan Firebee (see Fig. 2.b) was developed in 1951 and is the most widely used target aircraft ever. The Ryan Firebee plane was launched with the aid of a carrier or with the aid of the rocket-assisted take-off RATO on the launch pad. Fairchild J44-R and Continental J69-T turbojet engines were used in Ryan Firebee [30]. In the developed models, various control systems have been installed to provide fighter maneuverability. They are also equipped with wingtip thermal flares, which aims to target wing fins rather than engine exhaust that will protect them from heat-oriented missiles. Developed radar devices that allow imitating aircraft [31].

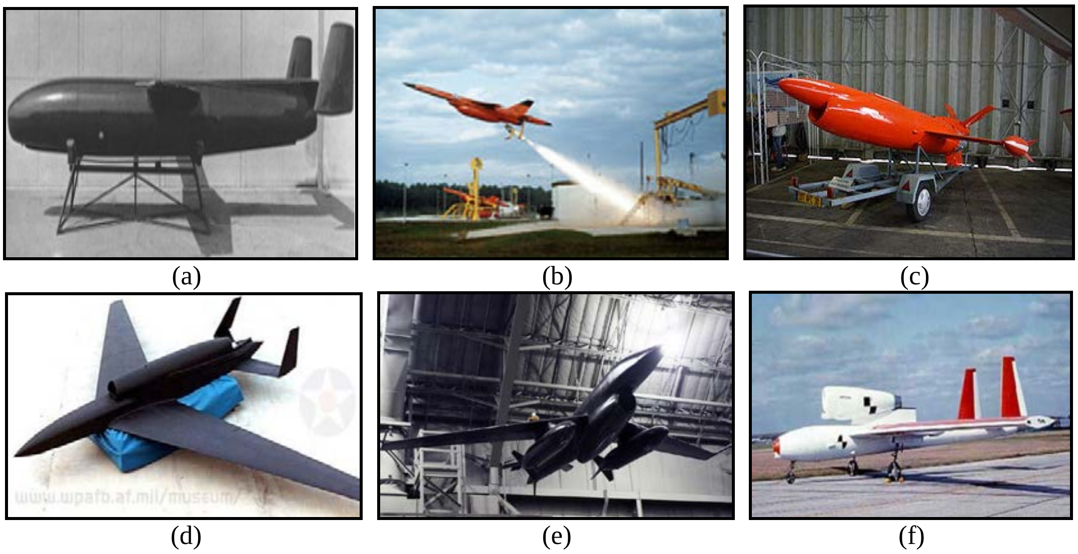

FIG. 2. Turbojet engine applications in UAVs , (a) Radioplane Q-1 [22], (b) Ryan Firebee [23], (c) Nord Aviation CT20 [24], (d) Teledyne Ryan AQM-91 Firefly [25], (e) Ryan Model 147 Lightning Bug [26], (f) Boeing YQM 94A Compass Cope [27]

Nord Aviation CT.20 (see Fig. 2.c) was evolved in 1957 by developing from the SFECMAST5.510, a remote controlled target aircraft with a French turbojet engine. After the start of the turbojet, the target aircraft is placed on a ramp and launched using two rockets. During the flight, the aircraft is controlled by radio signals from the ground. Because of its lightweight material, it can float and be recovered if it is forced into water [32].

In 1966, Teledyne Ryan Firefly (see Fig. 2.d) developed on the basis of long-range high-altitude, photographic exploration and made its first flight in 1968. Teledyne Ryan AQM-91 Firefly is a subsonic UAV operating with General Electric J97 turbojet engine. It can climb to a height of 23700 m after launching from the carrier aircraft. Since there is no landing gear, it’s landing operation carried out by parachute. A microwave command routing system has been used and stage of the flight was controlled by the Doppler/Inertial navigation system, which had a precision of about 0.5% of the distance. The primary task equipment is the Itek KA-80A panoramic camera. It is also equipped with IR (instrument flight authorization) sensors and ELINT (electronic intelligence equipment).

Teledyne Ryan Firefly is specifically designed for low observability, it has a sharped nose, a round fuselage, and an inwardly folded tail. The engine mounted on the top of the fuselage and the signature of the IR are minimized. Non-metallic structural elements and critical fields were made of radar absorbent material to further reduce radar reflection. Teledyne Ryan Firefly has been removed due to changes in the requirements of conditions [33, 34, 35].

The Ryan Model 147 Lightning Bug (see Fig. 2.e) series is produced as a target aircraft operating with the Teledyne J69 turbojet engine. Ryan Model 147s are manufactured without landing gear to save weight and they are able to perform in the aid of their parachute. Served in different positions in the US Army from 1962 to 1975, each of the UAVs became stronger, and more equipped than previous model. The tasks of the Ryan Model 147 series include high and low altitude photography, electronic antenna discoveries, reconnaissance, electronic warfare, pointing memory and psychological warfare. In addition, a simple warning system called AN/APR-26 is integrated into the Ryan Model 147E.

The next model, Ryan Model 147 F, also carries the system AN/ALQ-51, which manipulates radar signals, confusing that the target is in another position from the actual position. They are painted in black with high visibility at low altitude. Another feature of these unmanned aircraft is that they are radio controlled by the crew on the carrier aircraft instead of using an automatic guidance system. It has an advanced camera system and can display a 96-kilometer landmark. The forward model of this series, Ryan Model 147SRE, uses an almost unrecognizable infrared flash and infrared film from the ground that provides night exploration. BGM-34 model has precision-guided ammunition to carry out various ground strikes and defense missions on these aircraft. It is also powered by the Teledyne CAE J69-T-41A (8.5 kN thrust) engine. This model has not been used in any task. A pre-programmable digital flight control system was added to increase the maneuverability of the Model 147 series and test flights up to 10G were performed.

Although they were produced for exploration and espionage in 1972, they were replaced by F-4 Phantom planes and used leaflet bombs. Furthermore, the top models of the Ryan Model 147 Lightning Bug were fitted the Teledyne J100 turbine engines. In the aid of these engines, they would perform at 23000 m and 1260 kg thrust power. Because of all of these features, Ryan Model 147 Lightning Bug will be the ancestor of the new generation jet UAVs that will be produced in the future [34, 36].

The Boeing YQM 94A Compass Cope (see Fig. 2.f) was created in the military and intelligence department for higher-performance, high-altitude long-life UAV requirements. In addition to these requirements, it was necessary to take a traditional air runway alone and takes up to 24 hours of service. Moreover, it should be able to perform operational tasks under the conditions of day and night and in all weather conditions, and should also be able to obtain battlefield exploration, signal intelligence, photographic exploration, ocean reconnaissance and atmospheric sampling [37].

CONCLUSIONS

In recent years, with the increase of varieties in unmanned aerial vehicles a transaction from the reconnaissance to air defense and attack function has been observed. This function change resulted some problem, such as useful load, high altitude and speed have initiated the search for new propulsion power. Although turbojet engines are the power, turbojet engines have still no permanent solution for high sound and high fuel combustion. These two limiting factors reduce the efficiency expected from the UAVs. In addition to this, due to the fact that UAVs are independent of human physiology, it is thought that they will replace manned warplanes later on. Therefore, this and other similar studies are very important. At present, it is deduced that there is no examples of UAVs which possess turbojet engine yet at the level of fleet, and it is a continuing process of searching and developing.

REFERENCES

[1] M. Toscano, Unmanned aircraft systems roadmap to the future, *in 7th North Dakota Research Corridor UAS Summit*, pp. 569–572, 2013;

[2] M. C. Kushan, The relationship between the European states air force and their geopolitical positions, International *Conference of Scientific Paper AFASES 2013*, 23-25 May 2013;

[3] H. Shakhatreh, A. Sawalmeh, A. Al-Fuqaha, Z. Dou, E. Almaita, I. Khalil, N. S. Othman, A. Khreishah, and M. Guizani, Unmanned Aerial Vehicles: A Survey on Civil Applications and Key Research Challenges, pp.6 April 2018;

[4] M. Kushan, *Aircraft Technology*, Intechopen, pp.209-226, London, 2018;

[5] J. D. Mattingly, *Elements of Gas Turbine Propulsion*, McGraw-Hill, Mechanical Engineering Series, 1996;

[6] W. W. Bathie, *Fundamentals of Gas Turbines*, John Wiley & Sons, Inc., Newyork, 1996;

[7] M. C. Kushan, Z. Peng, and Shuzhi Peng, A new system of failure warning and monitoring control system for gas turbine compressor (GTC)/ auxiliary power unit (APU) of aircrafts and a sample study,*Advanced Materials Research*, vols.503-504, pp.1633-1638, 2012;

[8] C. Rodgers, Turbofan design options for mini UAV's, *37th AIAA/ASME/SAE/ASEE Joint Propulsion Conference and Exhibit*, 2001;

[9] N. Muller, and P. Akbari, Performance ınvestigation of small gas turbine engines topped with wave rotors, *39th AIAA/ASME/SAE/ASEE Joint Propulsion Conference and Exhibit*, 2003;

[10] R. Ö. İÇKE, and O. TUNÇER, Investigation of a micro turbojet engine via reverse engineering, *Dokuz Eylul University Faculty Of Engineering Journal Of Science And Engineering*, vol.18, no.3, pp.562-579, 2016;

[11] Turkish Airlines, Jet Aircraft Maintenance Fundamentals Education Materials;

[12] I. Yazar, *Mathematical model and controller design of a turbojet engine*, Thesis, Anadolu University, Eskisehir, 2015;

[13] Frontiers of Flight Museum December 2015 077. Available at www.wikidata.org, accessed on May 2019;

[14] G. Goebe, Teledyne-Continental J69 turbojet, Warner-Robbins Air Museum, Georgia, 2008. Available at www.flickr.com, accessed on May 2019;

[15] PBS Aerospace TJ100 turbojet engine, PBS Aerospace TJ40 mini-turbojet engine, PBS Aerospace TJ40 micro-turbojet engine. Available at www.pbsaerospace.com accessed on January 2019;

[16] TEI, *TJ90 Turbojet Development Project*, Available at www.tei.com.tr, accessed on May 2019;

[17] P. H. Wilkinson, *Aircraft Engine of the World*, 11th ed., Sir Isaac Pitman&Sons Ltd., pp. 46, London, 1953;

[18] P. H. Wilkinson, *Aircraft Engine of the World*, 15th ed., Sir Isaac Pitman&Sons Ltd., pp. 74-75, London, 1957;

[19] B. Gunston, *World Encyclopedia of Aero Engines*, 5th ed., Sutton Publishing Institution, pp.79, England, 2006;

[20] R. A Leyes II and W. A. Fleming, *The History of North American Small Gas Turbine Aircraft Engines*, Smithsonian Institution, Washington, 1999;

[21] I. Moir, and A. Seabridge, *Aircraft Systems: Mechanical, Electrical, and Avionics Subsystems Integration*, J.Wiley&Sons, 3rd ed., 2011;

[22] Image of Radioplane Q-1 target drone, November 2011. Available at www.wikidata.org, accessed on May 2019;

[23] Bukvoed, Teledyne Ryan Firebee UAV at Muzeyon Heyl ha-Avir, Hatzerim Airbase, Israel 2006. Available at www.wikipedia.org, accessed on May 2019;

[24] French target drone Nord Aviation CT20 belonging to the Musee des Anciennes, Toulouse, France, July 2008. Available at www.wikidata.org, accessed on May 2019;

[25] Teledyne Ryan AQM-91A Compass Arrow, USAF Museum, October 2006. Available at www.wikidata.org, accessed on May 2019;

[26]Teledyne-Ryan AQM-34Q Combat Dawn Firebee, February 2011. Available at www.nationalmuseum.af.mil, accessed on May 2019;

[27] Boing YQM-94A Compass Cope B, USAF Museum, 2006. Available at www.wikidata.org, accessed on May 2019;

[28] L. R. Newcome, *Unmanned Aviation: A Brief History of Unmanned Aerial Vehicles*, American Institute of Aeronautics and Astronautics, pp.72 Inc, Reston, Virginia, 2004;

[29] B. Yenne, *Attack of the Drones: A History of Unmanned Aerial Combat*, MBI Publishing Company, 2004;

[30] M. C. Kushan, and S. Gurgen, *A'dan Z'ye Dunya Ucaklari, Helikopterleri ve Insansiz Hava Araclari*, Nisan Kitabevi, Eskisehir, 2016;

[31] J. W. Taylor, *Jane's All the Word's Aircraft 1982-1983*, Jane's Yearbooks, London, 1982;

[32] CT-20 target drone main characteristics, *Aviation Week & Space Technolog*, vol.73, no.27, pp.118, 1960;

[33] W. Wagner, and W. P. Sloan, *Fireflies and Other UAVs(Unmanned Aerial Vehicles)*, Midland Publishing Limited, 1992;

[34] K. Munson, *World Unmanned Aircraft*, 1st ed., Janes Information Group, 1988;

[35] B. Miller, USAF widens unmanned aircraft effort, *Aviation Week & Space Technology* vol.9, pp.46, November 1970;

[36] T. P. Ehrhard, *Air Force UAV's: the Secret History*, A Mitchell Institute Press, July 2010;

[37] J. W. Taylor, *Jane's All the World's Aircraft 1973-74,* Jane's Yearbooks, pp.159, London, 1973.

THE DETERMINATION METHOD OF THE COMBAT POSSIBILITIES OF MILITARY UNIT

Azer ALIEV, Azad BAYRAMOV

Armed Forces War College of the Azerbaijan Republic,
Baku, Azerbaijan Republic

DOI: 10.19062/2247-3173.2019.21.29

Abstract: *in the paper, by using of the known factor of military unit combat power the problem of its combat possibilities calculation has been considered. By using of these estimations the method of tactical operation calculation of the task implementation possibility, the factor of battle parties losses and the attack movement rate has been offered.*

Keywords: combat power, task implementation probability, losses, attack rate, interpolation.

1. INTRODUCTION

The assessment methods of combat possibilities have especial position among the support systems of the process of military decision-making (Smith: 2011). The correct decision-making of combat activities and the impartially assessment of combat possibilities of the battle both sides for define of combat tasks have much significance. For lack of reliable methods in this area the commanders are reluctant to make intuitive decision based only on the own practical experience.

The assessment of combat possibilities is not new problem (Aliev & Bayramov: 2018) and in this area many investigations are carried out (Bobrikov: 2009; Buravlev & Rusanov: 2009). However, for practical calculation of combat possibilities in the various offered methods the fire, blow and maneuver possibilities are defined on the basis of various methods, and the quantity describing the common combat possibility of unit is not calculated. It complicates to implement of tactical operational calculations on its basis.

In the paper, on the basis of dynamic power of the military unit (Demenkov: 1993) described its combat possibilities the tactical operational calculations implementation method has been offered.

2. CALCULATION OF ELATIVELY COMBAT POWER AND PROBABILITY OF TASKS IMPLEMENTATION

For the purpose of assessment of expected battle victory we can calculate a combat power ratio of battle both sides (both for attack and defence sides) (Demenkov: 1993):

$$GN_h = \frac{G_D^h}{G_D^m}\,;\; GN_m = \frac{G_D^m}{G_D^h} \qquad (1)$$

Here: GN_h – is a combat power ratio for the attack side, G_D^h – is a combat dynamic power for the attack side, GN_m – is a combat power ratio for the defence side, G_D^m – is a combat dynamic power for the defence side.

If GN_h >1 then it is means that a attack side will has a reliable victory and the propability of its success P_T is directly proportional to value of GN_h (Demenkov: 1993).

During attack some of time after beginning, the content of attacking troop for utter defeat of the enemy is defined by the level of possible losses of the sides. The dependence between the combat power ratio of sides (*GN*) and the possible losses is determined by below formula (Demenkov: 1993):

$$\dot{I}_h = 1 - \sqrt{1 - GN_m^2 \times \dot{I}_m \times (2 - \dot{I}_m)} \quad (2)$$

$$\dot{I}_m = 1 - \sqrt{1 - GN_h^2 \times \dot{I}_h \times (2 - \dot{I}_h)} \quad (3)$$

Here: $\dot{I}_h$ – is a losses factor of attacking side, $\dot{I}_m$ – is a losses factor of defending. Its quantities change between (0÷1) range.

The wars' expirience has shown if an attacking side has 30-50% losess ($\dot{I}_h = 0{,}3 \div 0{,}5$) then it gives up the attack or it must organize a new attack. If an attacking side has more 50% losess, in this case the continuation of attack is not possible. If a defending side has 50-70% losess then its combat possibilities decrease much, and it must organize a defence over again. If a defending side has more 70% losess, in this case it cannot defend itself at all (Demenkov: 1993).

If the losesses for an attacking side are 30-50% and for a defending side are 50-70% the these losesses are called critical. From this we can calculate a combat critical power ration for battle both sides. If $GN_h = GN_{h.critic}$ and $GN_m = GN_{m.critic}$, then after battle beginning, at the same time, both sides losess are begun critical, and in this case the combat tasks implementation possiilities for both sides are equal. If, $GN_h < GN_{h.critic}$ and $GN_m > GN_{m.critic}$, then a defending side will obtain rather critical losess and for an attacking side the combat tasks implementation possiilities will more much. Below formulas can be used for calculation of both sides critical ratio (Demenkov: 1993):

$$GN_{h,critic} = \sqrt{\frac{(2 \times \dot{I}_m - \dot{I}_m^2)}{(2 \times \dot{I}_h - \dot{I}_h^2)}} \quad (4)$$

$$GN_{m,critic} = \sqrt{\frac{(2 \times \dot{I}_h - \dot{I}_h^2)}{(2 \times \dot{I}_m - \dot{I}_m^2)}} \quad (5)$$

There have been shown below in table 1 the calculated values of critical ratio of the combat power for both attacking ($GN_{h.critic}$ in denominator) and defending sides ($GN_{m.critic}$ in denominator).

Table 1. The critical ratio of the combat power for both sides (GN).

		Losess of attacking side				
		30%	35%	40%	45%	50%
The losess of defending side	50%	$\frac{1.213}{0.821}$	$\frac{1.140}{0.878}$	$\frac{1.083}{0.924}$	$\frac{1.037}{0.964}$	$\frac{1.000}{1.000}$
	55%	$\frac{1.251}{0.800}$	$\frac{1.175}{0.851}$	$\frac{1.116}{0.900}$	$\frac{1.069}{0.935}$	$\frac{1.031}{0.970}$
	60%	$\frac{1.283}{0.779}$	$\frac{1.206}{0.829}$	$\frac{1.146}{0.873}$	$\frac{1.097}{0.913}$	$\frac{1.058}{0.945}$
	65%	$\frac{1.312}{0.762}$	$\frac{1.233}{0.811}$	$\frac{1.171}{0.854}$	$\frac{1.122}{0.892}$	$\frac{1.082}{0.925}$
	70%	$\frac{1.336}{0.749}$	$\frac{1.255}{0.797}$	$\frac{1.192}{0.839}$	$\frac{1.142}{0.876}$	$\frac{1.102}{0.908}$

For the pupose of break open and exploit an attack deep in the enemy defense for the retention of combat possibilities the attacking side losess must be less 30% ($\dot{I}_h \leq 0.3$). In this case, the defending side will has the minimum 70% losess ($\dot{I}_m \geq 0.7$) and will crushed. For such losess the appropriate relative combat power of attaking side is called full one (a full superiority) (Demenkov: 1993). By using formula (4) let us calculate its value:

$$GN_{h.full} = \sqrt{\frac{2 \times 0.7 - 0.7^2}{2 \times 0.3 - 0.3^2}} = 1.34$$

Therefore, if $GN_h \geq GN_{h.full}$ then the attacking side has much probability to implement combat task. By analogy, the defending side losess must be less 50% ($\dot{I}_m \leq 0.5$) that to provide defence capability. In this case the attacking side must to has more 50% losess ($\dot{I}_h \geq 0.5$). For such losess the appropriate relative combat power of defending side is called full one (a full superiority). By using formula (5) let us calculate its value:

$$GN_{m.full} = \sqrt{\frac{2 \times 0.5 - 0.5^2}{2 \times 0.5 - 0.5^2}} = 1$$

Therefore, if $GN_m \geq GN_{m.full}$ then the defending side has much probability to implement combat task.

In (Trosenko: 2008) the dependence of combat task implementation probability on some values of relatively combat power and the method of probability calculation have been presented. However, thre are the inverse tasks in many practical problems: for given probability of task implementaton the necessary relatively combat power should be determine. For this porpuse let us determine $P_T = F_P(GN_h)$ and $GN_h = F_G(P_T)$ functions by using of coefficients given in table 2.

Table 2. The probability of task implementaton and the dependence of relatively combat power.

Given $F_P(GN_h)$	GN_h	2.18	1.81	1.59	1.44	1.34	1.26	1
	P_T	0.71	0.65	0.6	0.56	0.54	0.51	0.5
Calculated by interpolation $F_P(GN_h)$	P_T	0.71	0.65	0.60	0.56	0.54	0.52	0.50
	Error	0.00	0.00	0.00	0.00	0.00	0.01	0.00
Calculated by interpolation $F_G(P_T)$	GN_h	2.18	1.76	1.59	1.45	1.34	1.10	1.00
	Error	0.00	0.05	0.00	0.01	0.00	0.16	0.00

For determination these functions let us use Newton's interpolation formula:

$$P_n(x) = a_0 + a_1 \times (x - x_0) + a_2 \times (x - x_0) \times (x - x_1) + \cdots + a_n \times (x - x_0) \times (x - x_1) \times \ldots \times (x - x_n) = a_0 + \sum_{i=1,n} a_i \times \prod_{j=0,i-1} (x - x_i) \quad (6)$$

a_0 is obtained from $P_n(x_i) = y_i$. If *i=0*, $a_0 = y_0$; *i=1* then $a_0 + a_1 \times (x_1 - x_0) = y_0$, From here $a_1 = (y_1 - y_0)/(x_1 - x_0)$.

By analogy, the another factors can be calculated.

For interpolation by using data from table 2 (1, 3, 5, 7 columns) below factors have been obtained:

–for $F_P(GN_h)$ function: $a_0 = 1.15;\ a_1 = -1.53;\ a_2 = 1.11;\ a_3 = -0.23$

–for $F_G(P_T)$ function: $a_0 = 53.81, a_1 = 268.02;\ a_2 = -436{,}73;\ a_3 = 239.88$

From interpolation formula obtained $F_P(GN_h)$ and $F_G(P_T)$ values are given in table 1. The low errors allow to assert that factors are quite adequate. Let us write these dependences as:

$$P_T = 1.15 - 1.53 \times GN_h + 1.11 \times GN_h^2 - 0.23 \times GN_h^3 \quad (7)$$
$$GN_h = -53.81 + 268.02 \times P_T - 436{,}73 \times P_T^2 + 239.88 \times P_T^3 \quad (8)$$

During headquarter activities the operation-tactic target setting with necessary calculations can be various. However, there are three main parts for each tasks: the content of attacking side and its dynamic power G_D^h; the content of defending side and its dynamic power G_D^m; combat task and its implementation probability P_T. From this point of view there is a below classification of tasks:

I-st type task - G_D^h and G_D^m are given, P_T is found;

II-nd type task - G_D^h and P_T are given, G_D^m is found;

III-rd type task - G_D^m and P_T are given, G_D^h is found.

In I-st type task (7) formula can be applied for determination of probability of task implementation for both attacking and defending sides:

$$P_T^h = 1.1498 - 1.1498 \times \frac{G_D^h}{G_D^m} + 1.1104 \times (\frac{G_D^h}{G_D^m})^2 - 0.2298 \times (\frac{G_D^h}{G_D^m})^3 \quad (9)$$
$$P_T^m = 1.1498 - 1.1498 \times \frac{G_D^m}{G_D^h} + 1.1104 \times (\frac{G_D^m}{G_D^h})^2 - 0.2298 \times (\frac{G_D^m}{G_D^h})^3 \quad (10)$$

II-nd and III-rd type tasks have been solved usually combat task setting during atack (defence) planning. In this time if the unit's content and task implementation probability are known then (8) formula can be applied:

$$G_D^m = G_D^h / (-53.81 + 268.02 \times P_T^h - 436{,}73 \times (P_T^h)^2 + 239.88 \times (P_T^h)^3)$$
(11)
$$G_D^h = G_D^m \times (-53.81 + 268.02 \times P_T^m - 436{,}73 \times (P_T^m)^2 + 239.88 \times (P_T^m)^3)$$
(12)

3. CALCULATION OF LOSSES

For the purpose of losses calculation by using (1) and (2) equations the losses of one side must been known. However, in some time the both sides' losses must been known. For this purpose to combat power ratio of both attacking and defending sides appropriate the values based on the practical losses expirience can used (K.K.K.: YY-8: 1986). Let us determine a functional relationship between losses and relatively combat power by using of Newton's interpolation formula. For interpolation below factors have been obtained:

– in attack: a_0 = 2.4179; a_1 = -1.8032;
  a_2 = 0.5395; a_3 = -0.0524
– in defence: a_0 = 0.3086; a_1 = 0.0884;
  a_2 = 0.0417; a_3 = 0.0016.

Functional relationships between losses and relatively combat power for unit during 1 hour battle have been expressed as:

$$\dot{I}_h = 2.4179 - 1.8032 \times GN_h + 0.5395 \times GN_h^2 - 0.0524 \times GN_h^3 \quad (13)$$
$$\dot{I}_m = 0.3086 + 0.0884 \times GN_h + 0.0417 \times GN_h^2 + 0.0016 \times GN_h^3 \quad (14)$$

Calculated by interpolation equation and shown in figures 1 and 2 the dependnces between losses and relatively combat power allow to conclude that the results of interpolation are quite adequate.

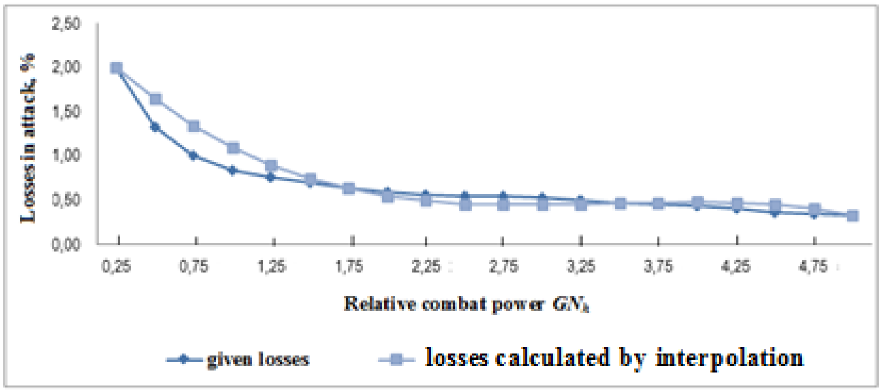

FIG. 1 The dependence of losses on relatively combat power in attack.

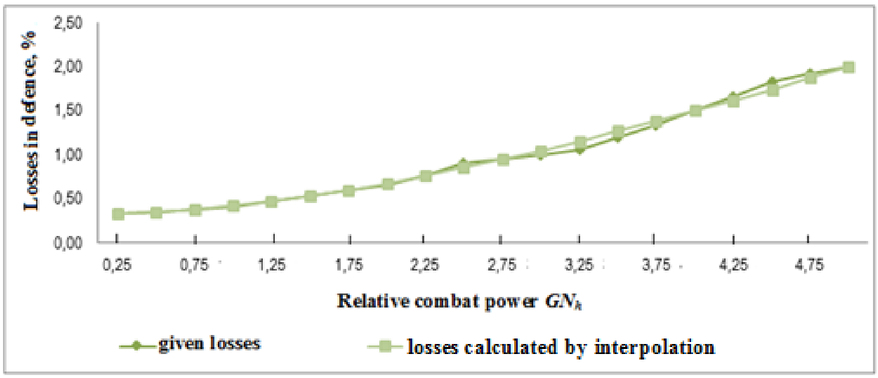

FIG. 2 The dependence of losses on relatively combat power in defence.

When the unit's losses have been determined then its should be divided on the categories of personal, weapons and military technics. İn this case the losses for various categories will different. It is conditioned by application properties on the battle area. The personal, weapons and military technics losses's factors given in (K.K.K.: YY-8: 1986). The losses of unit's weapons and military technics can calculated by below equation:

$$\dot{I}SH_j = \dot{I} \times N_j \times K_j, \quad j = I, II, \ldots IX \tag{15}$$

Here: $\dot{I}SH_j$ is a number of j weapon category losses, $\dot{I}$ is the factor of unit's common losses, N_j is a number of weapons of j category, K_j is a losses factor of j weapon category. For calculation of unit's personal losses balow equation is used:

$$\dot{I}ŞH = \sum_{j=I,\ldots,IX} \dot{I}SH_j \times Ş_j \tag{16}$$

Here: $\dot{I}SH_j$ is losses for each weapon's category; $Ş_j$ is a factor of personal losses for the same weapon's category.

4. CALCULATION OF ATTACK RATE

The unit's attack rate is depended on many factors: the type of unit, the conditions of terrain and weather, the disposition of defence and the engineering fortifications. The units of measurement of the attack rate are km/hour for (squad ÷ brigade) and km/day for (army's corps ÷ army). Here, km/day cannot displace to km/hour, because attack rate are not same in day and night, it is taken as average quantity.

First of all, let us consider attack rate during 1 hour. The war and military trainings expirience have shown that in dependence on the ratio of both sides combat power the attacking side rate is given in (K.K.K.: YY-8: 1986). For the pupose of determination of the functional dependence between ratio of combat power and attack rate let us use Newton's interpolation formula (6) and determine a_i factors. Taking into account of directly proportional smooth dependence between unit's attack rate and relatively combat power let us take this dependence as non-linear one of third degree. For interpolation below factors have been obtained: a_o = -1.0631; a_1 = 1.4952; a_2 = -0.4900; a_3=0.0579. The dependence of unit's progress common rate (km/hour) in attack on relatively combat power can calculated by below equation:

$$CHT_{hour} = -1.0631 + 1.4952 \times GN_h - 0.4900 \times GN_h^2 + 0.0579 \times GN_h^3 \qquad (17)$$

The dependence of progres rate in km/hour on combat power (Fig.3) shows that interpolation results are adequate.

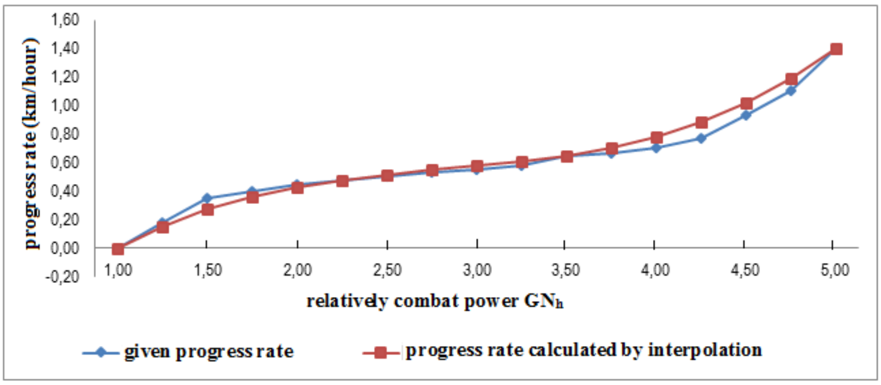

FIG. 3 The dependence of progress common rate in attack on relatively combat power.

Now, let us consider a progress rate during 1 day for brigade and bigger military formations in attack operations. Taking into account that in attacking operations during all day long the progress rate are different then 24x$CHT_{hour} \neq CHT_{day}$. The losses data during both 1 hour and 1 day have been taken from different sources (K.K.K.: YY-8: 1986; KKYY-190-7(A): 2001). Let us determine the functional dependence between relatively combat power and losses. By using of Newton's interpolation formula below interpolation factors have been obtained: a_0=1.4711; a_1=1.6067; a_2=0.8575; a_3 = -0.0895. In attack the dependence of unit's progress common rate (in km/day) on relatively combat power can expressed below equation:

$$CHT_{day} = 1.4711 + 1.6067 \times GN_h + 0.8575 \times GN_h^2 - 0.0895 \times GN_h^3 \qquad (18)$$

The result of interpolation of the attacking progress rate in km/day are shown in Fig. 4.

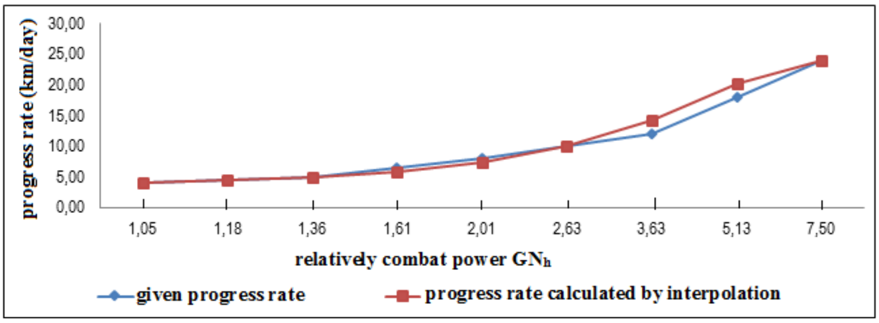

FIG. 4. The dependence of attacking progress rate on relatively combat power.

In attack the unit's really progress rate is depended on the type of unit, terrain and weather conditions, time of day (if rate is measered in km/hour) and the type of fortifications. These factors must be considered for calculation of attacking progress rate. These factors are given in (K.K.K.: YY-8: 1986; KKYY-190-7(A): 2001). Taking into account of these factors unit's attacking progress rate is expresses by next equation:

$$HT_{day} = CHT_{day} \times WC \times TC \times BT \times MS \times SV \tag{19}$$

$$HT_{day} = CHT_{day} \times WC \times TC \times BT \times MS \tag{20}$$

Here: *HT* is an attacking progress rate; *CHT* is a attacking progress common rate (9, 10); *WC* is weather influence factor; *TC* is terrain influence factor; *BT* is unit's type influence factor; *MS* is fortifications' density influence factor; *SV* is time of day influence factor.

During planning of military operations (tactic activities) the inverse problem can be often considered: the Staff determines an attacking progress rate and the unit's commander must determine necessary power ratio. Thereto, let us determine the dependence of combat power ratio on attacking rate. By using of Newton's interpolation formula below functional dependence's factors have been obtained: a_0 = -0.3424; a_1=0.3940; a_2 = -0.0131; a_3=0.0003.

By using of these factors the below functional dependence of attacking side's combat power ratio on the given attacking rate:

$$GN_h = -0.3424 + 0{,}3940 \times CHT_{day} - 0.0131 \times CHT_{day}^2 + 0.0003 \times CHT_{day}^3 \tag{21}$$

Taking into account of (21) equation the next formula is obtained:

$$GN_h = -0.3424 + 0{,}3940 \times \frac{HT_{day}}{WC \times TC \times BT \times MS} - 0.0131 \times \left(\frac{HT_{day}}{WC \times TC \times BT \times MS}\right)^2 + 0.0003 \times \left(\frac{HT_{day}}{WC \times TC \times BT \times MS}\right)^3$$

CONCLUSION

Therefore, the method of tactical operation calculation of the task implementation possibility has been developed and offered. On the basis of the unit's dynamic combat power the some factors defined combat capability are determined. There are relatively combat power, including critical and full, combat task implementation probability, both sides losses and attacking progress rate among these factors. The equations for calculation these factors have been obtainned.

REFERENCES

[1] Aliev A.A., Bayramov A.A. (2018) The problem of combat capability determination. *Proc. of "Azerbaijan Armed Forces and Military Sciences" Conference. Armed Forces War College*. Baku, 28 June. pp. 13-14.
[2] Bobrikov A.A. (2009) The method of assessment of combat capability of troops for the purpose of construction and application of Armed Forces tasks justification. *Voennaya Misl*, №12, Moscow. pp. 14-22.
[3] Buravlev A.I., Rusanov I.P. (2009) The assessment model of effectiveness of combat systems. *Voennaya Misl*. №5, Moscow, pp. 24-32
[4] Demenkov M.T. (1993) *The tactics of troops' units and parts. Division (regiment) in attack*. Moscow: Voennoye Izdatelstvo. 448 p.
[5] K.K.K.: YY-8. (1986) *Birlik ağırlıklı değeri kullanma broşürü*. Ankara. :K.K.K. Basımevi və Basılı Evrak Depo Müdürlüğü. 87 p.
[6] KKYY-190-7(A). (2001) *Birlik etkinliklerinin değerlendirilmesinde harekat etkinliği metodu*. K.K. Basımevi və Basılı Evrak Depo Müdürlüğü, Ankara. 101 p.
[7] Smith C. (2011) *Design and Planning of Campaigns and Operations in the Twenty-First Century.* Land Warfare Studies Centre, Canberra. 38 p.
[8] Trosenko K.A. (2008) About realization of combat capabilities of tactical troop's groups. *Voennaya Misl*, №6, Moscow. pp.70-75.

COMPUTING OF PERFECT BAYESIAN EQUILIBRIUM INVOLVED IN RADIO-JAMMING WARFARE BASED ON INCOMPLETE INFORMATION DYNAMIC GAMES WITH KNOWN CHANCE *p*

Andrei LUCHIAN*, Horațiu MOGA, Razvan BOBOC***

*Transilvania University, Brașov, Romania (riesigen@gmail.com, razvan_13_13@yahoo.com)
**CNIF-MFP, Braşov, Romania (horatiu.moga@gmail.com)

DOI: 10.19062/2247-3173.2019.21.9

Abstract: *The actual research paper proposes a model of radio-jamming warfare based on incomplete information dynamic games with known chance, with two actors and competing jamming and anti-jamming strategies. Our model based on the computing of perfect Bayesian equilibrium proof that anti-jamming solutions are more efficient than the classic ones.*

Keywords: *radio-jamming warfare, incomplete information dynamic games, known chance p*

1. INTRODUCTION

The current scientific and technological revolution has led to the rapid computerization of modern society. In this respect, the development of contemporary science and technology has enabled the world's armies to acquire electronic equipment and systems for research, command and control, communications, warning and protection, among which: modern electronic control systems, electronically controlled electronic systems integrated (as elements that condition the conduct of modern military actions), electronic sensors, performing computers capable of complex operations, satellite communications systems.

On these latest acquisitions, modern armies base their mobility, reaction speed and destruction capacity.

Electronic systems ensure and condition the holding and processing, as well as the transmission of a great deal of information, the optimization of troop leadership and the directing of the weapon at the real time scale, amplifying the power of the means of fire with precision, opportunity and efficiency. The operation of these systems is based on the use of electromagnetic energy, with the armies of the world becoming extremely dependent on the use of the electromagnetic space in their own interest.

As the share of electronic equipment in military equipment increased, the general aspect of combat action has changed, along with the energy component of the war, which defines the destructive character, and the information-decision component is also stated. With the introduction of these electronic systems a distinct form of the information warfare and a component of the command-control war appeared, namely RADIO-JAMMING WARFARE [1, 2, 3].

Electronic warfare is the main element of confrontation for achieving superiority in the use of electromagnetic space and plays an important role in achieving security, functioning of electronic systems, ensuring the social, political, economic and military activities of a country. We can say about the battlefield configuration that it has been heavily affected by the performance of all the technical and weapon categories provided by the defense industries under the impact of the technical-scientific revolution.

The actual research paper proposes a model of radio-jamming warfare based on incomplete information dynamic games with known chance [4, 5], with two actors and competing jamming and anti-jamming strategies [6, 7].

2. METHDOLOGY

The first step in this research is to define the jamming and anti-jamming strategies. The next approach are the next jamming strategies: Partial Dwell Jamming of FHSS Systems, Noise Jamming, Swept Jamming, Pulse Jamming, Follower Jamming. Follow the exposure of the anti-jamming strategies like: Direct Sequence Spread Spectrum, Fast Frequency Hopping Systems, Slow Frequency Hopping Systems, Ultra wideband Systems, Hybrid Spread Spectrum Systems. After define all the strategies propose a mathematical model of radio-jamming warfare between two actors using incomplete information dynamic games with known chance [6].

2.1.For radio-jamming strategies present below:

2.1.1.Partial Dwell Jamming of FHSS Systems - Frequency Spread-Spectrum (FHSS) systems are extensively used in military communications to neutralize the effects of various types of intentional blocking, including jamming and anti-jamming. FH communication can be locked effectively by blocking the successor [1, 2, 3, 6].

2.1.2.Noise Jamming - One way to prevent the proper functioning of a radar receiver (or any other receiver) is to saturate it with noise. The noise is a continuous signal and is different from the radar signal. Radar signal or echo is a periodic pulse sequence [1, 2, 3, 6].

2.1.3.Swept Jamming - Major techniques of noise interference. In the general blocking class, there are three different techniques for generating the night signal to be used. In the case of spot blocking, all the output power of the jamming antenna is concentrated in a very narrow bandwidth, ideally identical to that of the radar. The propagation barrier and jam propagate their energy over a bandwidth much higher than that of the radar signal [1, 2, 3, 6].

2.1.4.Pulse Jamming - The impulse requires the operator to know the rotation of a fixed enemy radar installation. At a prescribed point in the rotation of that radar, the jammer activates, thus negating the radar view of a particular sector. This sector does not have to align with the location of jamming, which makes it difficult for the enemy to locate the source of the jamming [1, 2, 3, 6].

2.1.5.Follower Jamming - Loop blocking is a jamming signal blocking means that can track the frequency of hopping, the instantaneous frequency of the jitter signal being narrower, but the frequency of each frequency may overlap. Tracker lock is a correlation of the blocking of a certain condition that the jamming power must reach the VHF receiver before moving to a new set of frequency channels [1, 2, 3, 6].

2.1.6. Conclusion 1: The most efficient jamming technique necessary to annihilate and comprehend the enemy's might over the battlefield is Follower Jamming followed by Partial Dwell Jamming. Thus using these types of jamming one does not reveal their position while executing vast maneuvers to annihilating the enemy's systems.

2.2.For anti-jamming strategies follow the next ones:

2.2.1.Direct Sequence Spread Spectrum - DSSS is a spread spectrum modulation technique used to transmit digital air wave signals.

It was originally developed for military use and used hard-to-detect broadband signals to resist jamming attempts. It is also developed for commercial purposes in local and wireless networks [1, 2, 3, 6].

2.2.2.Fast Frequency Hopping Systems - In the scattered spectrum with fast propagation frequency, the signal is a large cost on a random frequency spectrum from Frequency to Frequency, speaking a receiver unreliably. A reception between the frequency in synchronization with the transmitter, the part of the message signal reaches the "lock". It is a method of transmitting a radio signal by radio that rapidly switches a carrier between several frequency channels, using a pseudo administration sequence known to both the transmitter and the receiver [1, 2, 3, 6].

2.2.3.Slow Frequency Hopping Systems - Low Frequency Load is a process of changing the radio frequencies of a communication on a regular basis (model). The single frequency transmission is usually much longer than the time it takes to send multiple bits of digital information. Slow frequency synchronization is used to reduce the effects of fading radio signals and to minimize the effects of interference from radio channels operating on the same frequency [1, 2, 3, 6].

2.2.4.Ultra wideband Systems - Ultra-lateral communication systems (UWB) can be broadly classified as any communications system whose instantaneous bandwidth is often higher than the minimum needed to provide specific information. This excessive bandwidth is the defining feature of the UWB [1, 2, 3, 6].

2.2.5.Hybrid Spread Spectrum Systems - In recent years, there has been a great deal of interest in the use of HSS for commercial applications, especially within the Intelligent Network, in addition to their inherent uses in military communications. This is because HSS can accommodate high data rates with high integrity of links, even in the presence of significant multipath effects and interference signals [1, 2, 3, 6].

2.2.6. Conclusion 2: The best method to protect one's team would be to use the Ultra Wideband System followed by the Fast Frequency Hopping System. Using wideband one can extend its security measure thus assuring the enemy to use full force and expose itself while doing so and using fast frequency hopping system in the same time with wideband to intensify its protection.

Following conclusion 1 and 2 may we constructed table 1 with efficiency of anti-jamming versus jamming strategies. The meaning of the tables numbers are the following: 1 – the lowest efficiency; 2 - the low efficiency; 3 - the average efficiency; 4 - the high efficiency; 5 – the highest efficiency.

Table 1. Table established a ranking between anti-jamming and jamming methods

Jamming / Anti-Jamming	Partial Dwell Jamming of FHSS Systems	Noise jamming	Sweep jamming	Pulse jamming	Follower jamming
Direct Sequence Spread Spectrum	1	3	3	2	2
Fast Frequency Hopping Systems	5	2	3	2	4
Slow Frequency Hopping Systems	1	4	3	3	2
Ultra wideband Systems	5	2	3	3	4
Hybrid Spread Spectrum Systems	3	5	4	3	2

2.3. Scenario of using radio jamming strategies and radio electronic jamming - in our research we consider two W and V actors using radio-electronic / anti-jamming strategies in their radio-electronic confrontation.

The model of confrontation between W and V assumes that actor W maintains the average 3 radio-electronic and anti-jamming strategies. Actor V with a known p probability will improve his resilience and overwhelming capabilities from his original strategy of 1 or 2 jamming versus anti-jamming strategies efficiency to 4 or 5 final efficiency.

In our research for the behavior of the two actors W and V are modeled by the incomplete information dynamic game theory in which the nature of the actor V changes with a probability p. The significance of the utility functions for W and V players is the following calculated on the Cartesian product among the sterile ones two pre-modification and post-modification actors of the nature of V. For player W, the utility function grid indices in the game matrix have the meaning: matrix line 1 for the pure use of Noise Jamming jitter strategies; lines 2 and 3 for the concurrent use of Noise Jamming and Anti-Noise Jamming strategies; line 4 of the array is specific to using only Anti-Noise Jamming strategies. For actor V, the significance of the indices assigned to the utility functions in the game matrix are the following: column 1 of the game matrix for conjugate Swept Jamming and Follower Jamming; column 2 of the game matrix for conjugate Swept Jamming and Anti-Follower Jamming; column 3 of the game matrix for Follower Jamming and Anti-Swept Jamming conjugate use; column 4 of the game matrix for using Follower Jamming and Swept Jamming conjugate. For this dynamic game with incomplete information and with exogenous probability p will compute the perfect Bayesian equilibrium with Lagrange multiplier method in results section [4, 5].

Based on the above function definitions, we will define the incomplete information game equations that characterize the interaction between W and V [4, 5]. Where p_1, p_2, p_3 are the probabilities by which W opts for one of the four strategies obtained by the Cartesian product and mentioned above up. The probabilities q_1, q_2, q_3 represent the options V has for the same four strategies composed by Cartesian product [7].

$$\begin{cases} U^W = (p_1, p_2, p_3, 1-p_1-p_2-p_3) \cdot \begin{bmatrix} U_{11}^W & U_{12}^W & U_{13}^W & U_{14}^W \\ U_{21}^W & U_{22}^W & U_{23}^W & U_{24}^W \\ U_{31}^W & U_{32}^W & U_{33}^W & U_{34}^W \\ U_{41}^W & U_{42}^W & U_{43}^W & U_{44}^W \end{bmatrix} \cdot \begin{pmatrix} q_1 \\ q_2 \\ q_3 \\ 1-q_1-q_2-q_3 \end{pmatrix} \\ U^V = (p_1, p_2, p_3, 1-p_1-p_2-p_3) \cdot \begin{bmatrix} U_{11}^V & U_{12}^V & U_{13}^V & U_{14}^V \\ U_{21}^V & U_{22}^V & U_{23}^V & U_{24}^V \\ U_{31}^V & U_{32}^V & U_{33}^V & U_{34}^V \\ U_{41}^V & U_{42}^V & U_{43}^V & U_{44}^V \end{bmatrix} \cdot \begin{pmatrix} q_1 \\ q_2 \\ q_3 \\ 1-q_1-q_2-q_3 \end{pmatrix} \end{cases} \tag{1}$$

3. RESULTS

Applying the Lagrange multiplier method for relations (1), we get next six expressions in (2) [8, 9]:

$$\begin{cases} \dfrac{\partial U^W}{\partial p_1} = 0 \quad \dfrac{\partial U^W}{\partial p_2} = 0 \quad \dfrac{\partial U^W}{\partial p_3} = 0 \\ \dfrac{\partial U^V}{\partial q_1} = 0 \quad \dfrac{\partial U^V}{\partial q_2} = 0 \quad \dfrac{\partial U^V}{\partial q_3} = 0 \end{cases} \tag{2}$$

Development of first partial derivative in expressions (3), (4), (5) with substitutions of (6), (7), (8) drive to system of equations (16).

$$\frac{\partial U^W}{\partial p_1} = (1,0,0,-1)\cdot\begin{bmatrix} U_{11}^W & U_{12}^W & U_{13}^W & U_{14}^W \\ U_{21}^W & U_{22}^W & U_{23}^W & U_{24}^W \\ U_{31}^W & U_{32}^W & U_{33}^W & U_{34}^W \\ U_{41}^W & U_{42}^W & U_{43}^W & U_{44}^W \end{bmatrix}\cdot\begin{pmatrix} q_1 \\ q_2 \\ q_3 \\ 1-q_1-q_2-q_3 \end{pmatrix} = 0 \tag{3}$$

$$\frac{\partial U^W}{\partial p_2} = (0,1,0,-1)\cdot\begin{bmatrix} U_{11}^W & U_{12}^W & U_{13}^W & U_{14}^W \\ U_{21}^W & U_{22}^W & U_{23}^W & U_{24}^W \\ U_{31}^W & U_{32}^W & U_{33}^W & U_{34}^W \\ U_{41}^W & U_{42}^W & U_{43}^W & U_{44}^W \end{bmatrix}\cdot\begin{pmatrix} q_1 \\ q_2 \\ q_3 \\ 1-q_1-q_2-q_3 \end{pmatrix} = 0 \tag{4}$$

$$\frac{\partial U^W}{\partial p_3} = (0,0,1,-1)\cdot\begin{bmatrix} U_{11}^W & U_{12}^W & U_{13}^W & U_{14}^W \\ U_{21}^W & U_{22}^W & U_{23}^W & U_{24}^W \\ U_{31}^W & U_{32}^W & U_{33}^W & U_{34}^W \\ U_{41}^W & U_{42}^W & U_{43}^W & U_{44}^W \end{bmatrix}\cdot\begin{pmatrix} q_1 \\ q_2 \\ q_3 \\ 1-q_1-q_2-q_3 \end{pmatrix} = 0 \tag{5}$$

$$\begin{aligned} a_{11} &\stackrel{\text{def}}{=} (U_{11}^W - U_{41}^W) - (U_{14}^W - U_{44}^W) \quad & a_{12} &\stackrel{\text{def}}{=} (U_{12}^W - U_{42}^W) - (U_{14}^W - U_{44}^W) \\ a_{13} &\stackrel{\text{def}}{=} (U_{13}^W - U_{43}^W) - (U_{14}^W - U_{44}^W) \quad & b_1 &\stackrel{\text{def}}{=} U_{44}^W - U_{14}^W \end{aligned} \tag{6}$$

$$\begin{aligned} a_{21} &\stackrel{\text{def}}{=} (U_{21}^W - U_{41}^W) - (U_{24}^W - U_{44}^W) \quad & a_{22} &\stackrel{\text{def}}{=} (U_{22}^W - U_{42}^W) - (U_{24}^W - U_{44}^W) \\ a_{23} &\stackrel{\text{def}}{=} (U_{23}^W - U_{43}^W) - (U_{24}^W - U_{44}^W) \quad & b_2 &\stackrel{\text{def}}{=} U_{44}^W - U_{24}^W \end{aligned} \tag{7}$$

$$\begin{aligned} a_{31} &\stackrel{\text{def}}{=} (U_{31}^W - U_{41}^W) - (U_{34}^W - U_{44}^W) \quad & a_{32} &\stackrel{\text{def}}{=} (U_{32}^W - U_{42}^W) - (U_{34}^W - U_{44}^W) \\ a_{33} &\stackrel{\text{def}}{=} (U_{33}^W - U_{43}^W) - (U_{34}^W - U_{44}^W) \quad & b_3 &\stackrel{\text{def}}{=} U_{44}^W - U_{34}^W \end{aligned} \tag{8}$$

Development of first partial derivative in expressions (10), (11), (12) with substitutions of (13), (4), (15) drive to system of equations (17).

$$\frac{\partial U^V}{\partial q_1} = (p_1, p_2, p_3, 1-p_1-p_2-p_3)\cdot\begin{bmatrix} U_{11}^V & U_{12}^V & U_{13}^V & U_{14}^V \\ U_{21}^V & U_{22}^V & U_{23}^V & U_{24}^V \\ U_{31}^V & U_{32}^V & U_{33}^V & U_{34}^V \\ U_{41}^V & U_{42}^V & U_{43}^V & U_{44}^V \end{bmatrix}\cdot\begin{pmatrix} 1 \\ 0 \\ 0 \\ -1 \end{pmatrix} = 0 \tag{10}$$

$$\frac{\partial U^V}{\partial q_2} = (p_1, p_2, p_3, 1-p_1-p_2-p_3)\cdot\begin{bmatrix} U_{11}^V & U_{12}^V & U_{13}^V & U_{14}^V \\ U_{21}^V & U_{22}^V & U_{23}^V & U_{24}^V \\ U_{31}^V & U_{32}^V & U_{33}^V & U_{34}^V \\ U_{41}^V & U_{42}^V & U_{43}^V & U_{44}^V \end{bmatrix}\cdot\begin{pmatrix} 0 \\ 1 \\ 0 \\ -1 \end{pmatrix} = 0 \tag{11}$$

$$\frac{\partial U^V}{\partial q_3} = (p_1, p_2, p_3, 1-p_1-p_2-p_3)\cdot\begin{bmatrix} U_{11}^V & U_{12}^V & U_{13}^V & U_{14}^V \\ U_{21}^V & U_{22}^V & U_{23}^V & U_{24}^V \\ U_{31}^V & U_{32}^V & U_{33}^V & U_{34}^V \\ U_{41}^V & U_{42}^V & U_{43}^V & U_{44}^V \end{bmatrix}\cdot\begin{pmatrix} 0 \\ 0 \\ 1 \\ -1 \end{pmatrix} = 0 \tag{12}$$

$$\begin{aligned} c_{11} &\stackrel{\text{def}}{=} (U_{11}^V - U_{14}^V) - (U_{41}^V - U_{44}^V) \quad & c_{12} &\stackrel{\text{def}}{=} (U_{21}^V - U_{24}^V) - (U_{41}^V - U_{44}^V) \\ c_{13} &\stackrel{\text{def}}{=} (U_{31}^V - U_{34}^V) - (U_{41}^V - U_{44}^V) \quad & d_1 &\stackrel{\text{def}}{=} U_{44}^V - U_{41}^V \end{aligned} \tag{13}$$

$$\begin{aligned} c_{21} &\stackrel{\text{def}}{=} (U_{12}^V - U_{14}^V) - (U_{42}^V - U_{44}^V) \quad & c_{22} &\stackrel{\text{def}}{=} (U_{22}^V - U_{24}^V) - (U_{42}^V - U_{44}^V) \\ c_{23} &\stackrel{\text{def}}{=} (U_{32}^V - U_{34}^V) - (U_{42}^V - U_{44}^V) \quad & d_2 &\stackrel{\text{def}}{=} U_{44}^V - U_{42}^V \end{aligned} \tag{14}$$

$$c_{31} \stackrel{\text{def}}{=} (U_{13}^{V} - U_{14}^{V}) - (U_{43}^{V} - U_{44}^{V}) \quad c_{32} \stackrel{\text{def}}{=} (U_{23}^{V} - U_{24}^{V}) - (U_{43}^{V} - U_{44}^{V})$$
$$c_{33} \stackrel{\text{def}}{=} (U_{33}^{V} - U_{34}^{V}) - (U_{43}^{V} - U_{44}^{V}) \qquad d_{3} \stackrel{\text{def}}{=} U_{44}^{V} - U_{43}^{V} \tag{15}$$

Following the above substitutions, we obtain solutions for the perfect Bayesian equilibrium of the dynamic game with incomplete information based on determinants [4, 5]:

$$\begin{cases} \dfrac{\partial U^{W}}{\partial p_1} = a_{11} \cdot q_1 + a_{12} \cdot q_2 + a_{13} \cdot q_3 = b_1 \\ \dfrac{\partial U^{W}}{\partial p_2} = a_{21} \cdot q_1 + a_{22} \cdot q_2 + a_{23} \cdot q_3 = b_2 \\ \dfrac{\partial U^{W}}{\partial p_3} = a_{31} \cdot q_1 + a_{32} \cdot q_2 + a_{33} \cdot q_3 = b_3 \end{cases} \tag{16}$$

$$\Delta_q = \begin{vmatrix} a_{11} & a_{12} & a_{13} \\ a_{12} & a_{22} & a_{23} \\ a_{31} & a_{32} & a_{33} \end{vmatrix} \quad \Delta_{q1} = \begin{vmatrix} b_1 & a_{12} & a_{13} \\ b_2 & a_{22} & a_{23} \\ b_3 & a_{32} & a_{33} \end{vmatrix}$$
$$\Delta_{q2} = \begin{vmatrix} a_{11} & b_1 & a_{13} \\ a_{12} & b_2 & a_{23} \\ a_{31} & b_3 & a_{33} \end{vmatrix} \quad \Delta_{q3} = \begin{vmatrix} a_{11} & a_{12} & b_1 \\ a_{12} & a_{22} & b_2 \\ a_{31} & a_{32} & b_3 \end{vmatrix}$$

$$\begin{cases} \dfrac{\partial U^{V}}{\partial q_1} = c_{11} \cdot p_1 + c_{12} \cdot p_2 + c_{13} \cdot p_3 = d_1 \\ \dfrac{\partial U^{V}}{\partial q_2} = c_{21} \cdot p_1 + c_{22} \cdot p_2 + c_{23} \cdot p_3 = d_2 \\ \dfrac{\partial U^{V}}{\partial q_3} = c_{31} \cdot p_1 + c_{32} \cdot p_2 + c_{33} \cdot p_3 = d_3 \end{cases} \tag{17}$$

$$\Delta_p = \begin{vmatrix} c_{11} & c_{12} & c_{13} \\ c_{12} & c_{22} & c_{23} \\ c_{31} & c_{32} & c_{33} \end{vmatrix} \quad \Delta_{p1} = \begin{vmatrix} d_1 & c_{12} & c_{13} \\ d_2 & c_{22} & c_{23} \\ d_3 & c_{32} & c_{33} \end{vmatrix}$$
$$\Delta_{p2} = \begin{vmatrix} c_{11} & d_1 & c_{13} \\ c_{12} & d_2 & c_{23} \\ c_{31} & d_3 & c_{33} \end{vmatrix} \quad \Delta_{p3} = \begin{vmatrix} c_{11} & c_{12} & d_1 \\ c_{12} & c_{22} & d_2 \\ c_{31} & c_{32} & d_3 \end{vmatrix}$$

Computing the probabilities (18) and (19) will get the perfect Bayesian equilibrium solution for the transition of strategies followed by actor V with expression (20) and (21) [4, 5].

$$\begin{cases} q_{01} = \dfrac{\Delta_{q1}}{\Delta_q} \\ q_{02} = \dfrac{\Delta_{q2}}{\Delta_q}, \Delta_q \neq 0 \\ q_{03} = \dfrac{\Delta_{q3}}{\Delta_q} \end{cases} \tag{18}$$

$$\begin{cases} p_{01} = \dfrac{\Delta_{p1}}{\Delta_p} \\ p_{02} = \dfrac{\Delta_{p2}}{\Delta_p}, \Delta_p \neq 0 \\ p_{03} = \dfrac{\Delta_{p3}}{\Delta_p} \end{cases} \tag{19}$$

$$U_0^{W} = (p_{01}, p_{02}, p_{03}, 1 - p_{01} - p_{02} - p_{03}) \cdot \begin{bmatrix} U_{11}^{W} & U_{12}^{W} & U_{13}^{W} & U_{14}^{W} \\ U_{21}^{W} & U_{22}^{W} & U_{23}^{W} & U_{24}^{W} \\ U_{31}^{W} & U_{32}^{W} & U_{33}^{W} & U_{34}^{W} \\ U_{41}^{W} & U_{42}^{W} & U_{43}^{W} & U_{44}^{W} \end{bmatrix} \cdot \begin{pmatrix} q_{01} \\ q_{02} \\ q_{03} \\ 1 - q_{01} - q_{02} - q_{03} \end{pmatrix} \tag{20}$$

$$U_0^{V} = (p_{01}, p_{02}, p_{03}, 1 - p_{01} - p_{02} - p_{03}) \cdot \begin{bmatrix} U_{11}^{V} & U_{12}^{V} & U_{13}^{V} & U_{14}^{V} \\ U_{21}^{V} & U_{22}^{V} & U_{23}^{V} & U_{24}^{V} \\ U_{31}^{V} & U_{32}^{V} & U_{33}^{V} & U_{34}^{V} \\ U_{41}^{V} & U_{42}^{V} & U_{43}^{V} & U_{44}^{V} \end{bmatrix} \cdot \begin{pmatrix} q_{01} \\ q_{02} \\ q_{03} \\ 1 - q_{01} - q_{02} - q_{03} \end{pmatrix} \tag{21}$$

CONCLUSIONS AND FUTURE WORKS

Computing the perfect Bayesian equilibrium in this paper research proves that anti-jamming solutions for the best results in protecting one's team is more efficient nowadays in comparison to the jamming solution offered. While one searches and „jamms", another becomes vulnerable due to the fact that he must expose himself to do so. This research proves that the wideband anti-jamming solution still has an Achilles foot, more exactly the follower jammer and of course a wideband equipment at end of the line that works in the same frequency range as him.

REFERENCES

[1] D. L. Adamy, *EW 101: A first course in electronic warfare*. Artech House, 2001;
[2] D. L. Adamy, *EW 102: A second course in electronic warfare*. Artech House, 2004;
[3] D. L. Adamy, *EW 103: Tactical battlefield communications electronic warfare*. Artech House, 2009;
[4] Felix Munoz-Garcia and Daniel Toro-Gonzalez, *Strategy and Game Theory: Practice Exercises with Answers*, Springer, 2016;
[5] Gisèle Umbhauer, Game Theory and Exercises, Routledge, 2016;
[6] Richard A Poisel, *Modern Communications Jamming: Principles and Techniques*, Artech House, 2nd Edition, 2011;
[7] Richard A Poisel, *Information Warfare and Electronic Warfare Systems*, Artech House, 2011;
[8] E. N. Barron, *Game Theory: An Introduction*, Wiley, 2nd Edition, 2013;
[9] Horațiu Moga, Ana-Maria Bolborici and Elena Valentina Constantinescu, Calculul punctului de echilibru perfect Bayesian bazat pe șansă. Studiu de caz: Strategia nucleară a RPD Coreene, *Revista de Geografie Politică, GeoPolitică, GeoStrategie*, Anul XVI, No. 75, pp. 178-188, 3/2018.

ASPECTS ABOUT INTEGRATE RESPONSIVE WEBSITES FOR CYBER DEFENSE STRATEGIES - BOOTSTRAP VERSUS W3.CSS

Livia SANGEORZAN*, Nicoleta ENACHE-DAVID*, Claudia-Georgeta CARSTEA, Denisa-Iulia CATANA***

*Transilvania University, Braşov, Romania (sangeorzan@unitbv.ro, nicoleta.enache@unitbv.ro, denisa04.c@gmail.com)
"Henri Coanda" Air Force Academy, Brașov, România (claudia.carstea@afahc.ro)

DOI: 10.19062/2247-3173.2019.21.10

Abstract: *This paper presents Bootstrap and W3.CSS and the difference of using them. Bootstrap gives to the web designers the ability to easily create responsive designs, since W3.CSS is a free front-end framework for faster and easier web development. In addition, it is faster and smaller than other CSS frameworks and uses standard CSS, but does not use JavaScript or jQuery. Data security represent a strategic importance in military information systems. For web designers this represent a problem because they have the responsibility to protect personal data and classified information.*

Keywords: *web responsive design, CSS, framework, web development.*

1. INTRODUCTION

Once the web technologies are developing, web designers need to know easier and faster solutions for their work. In this paper we highlight some advantages and disadvantages in using Bootstrap and W3.CSS frameworks for designing responsive websites. The paper is structured as following: in Section 2 we present the definition of responsive design and in Section 3 and Section 4 we present some Bootstrap and W3.CSS basic elements. Finally, in Section 5 we present an application, a slide show realized with the two frameworks.

The pre-emptive principle is very important when we talk about military information systems. Privacy must be integrated into the architecture of the website, data must be secured and protected end-to-end. Web attacks are some of the most frequent ones to occur. The threat of cyber-attacks is rapidly expanding and transforming.

In conclusion, W3.CSS offers much more page customization than Bootstrap, but the two frameworks can be used successfully in web design.

2. RESPONSIVE DESIGN

Responsive design is a method used in web programming that optimizes the content of a web page in order to be displayed on a certain device. For example, the desktop might get a widescreen layout that is optimized for large displays, since a mobile phone gets a smaller layout in which all the elements of the web page is well arranged. Such elements can be used in designing complex informatics systems like the authors mention in [1] and [2].

Bootstrap uses CSS media queries that measure the width of the browser and then use the appropriate style sheet. So, the web pages can be displayed in well conditions on tablets or phones or another device.

In order to add custom CSS based on the media query, one can either include all rules in one CSS file or can use entirely different CSS files. But for larger site, we can divide each media query into a separate CSS file. In the HTML file, we can call them with the <link> tag in the head of the document.

3. BOOTRSTRAP

Bootstrap is a free front-end framework for faster and easier web development. Furthermore, Bootstrap contains HTML and CSS based design templates for forms, buttons, tables, navigation, slide shows and other elements, as well as optional JavaScript plugins. Bootstrap also gives the web programmer the possibility to create responsive designs.

Bootstrap has been launched in August 2011 and it won a big popularity. Basically, Bootstrap can be used for responsive web design and supports a 12-column, 940px-wide grid. On Bootstrap's website one can use the build tool that allows the user to customize the build as he wish, by choosing the CSS and JavaScript features.

Bootstrap is designed to be responsive to mobile devices. To ensure proper rendering and touch zooming, the web designer must add the following **<*meta*>** tag inside the **<*head*>** element:

```
<meta name="viewport" content="width=device-width, initial-scale=1">
```

The width=device-width part sets the width of the page to follow the screen-width of the device. This can be different, depending on the device. The initial-scale=1 part sets the initial zoom level when the page is first loaded by the browser, as it is mentioned in [6].

With Bootstrap, we include the link to the CSS style sheet and the JavaScript:

```
<!DOCTYPE html>
<html><head>
<title>Bootstrap 101 Template</title>
<link href="css/bootstrap.min.css" rel="stylesheet">
</head>
<body>
<script src="js/bootstrap.min.js"></script>
</body></html>
```

Buttons

Using Bootstrap, the user can customize the buttons so they have the same layout on the entire web site. For example, all the elements that use the class of *.btn* will inherit the default look of a gray button with rounded corners. However, the user can change the color of the buttons by adding new classes on the CSS definition.

The classes .btn-large, .btn-small, or .btnmini can be used on buttons in order to make the buttons larger or smaller.

```
<p>
<button class="btn btn-large btn-primary" type="button">Large button</button>
<button class="btn btn-large" type="button">Large button</button></p>
<p>
<button class="btn btn-primary" type="button">Default button</button>
<button class="btn" type="button">Default button</button></p>
<p>
<button class="btn btn-small btn-primary" type="button">Small button</button>
<button class="btn btn-small" type="button">Small button</button></p>
```

To create buttons that display like a block-level element, one simply can add the ***.btnblock*** class. These buttons will be displayed at 100% width.

Images

In Bootstrap, the images can be stylized using three style classes: *img-rounded* adds border-radius of 6px to give the image rounded corners, *.img-circle* makes the entire image round by adding border-radius: 500px, and *.img-polaroid* adds a bit of padding and a gray border.

Bootstrap offers more than 140 icons that can be used with buttons, links, navigation, and form fields. These icons are provided by GLYPHICONS. [5]

In order to use the icons, one must use an <i> tag with the namespaced ***.icon-*** class. For example, for the edit icon, one can add the ***.icon-edit*** class to the <i> tag:

```
<i class="icon-edit"></i>
```

If we want to use the white icon, simply add the ***.icon-white*** class to the tag:

```
<i class="icon-edit icon-white"></i>
```

Bootstrap contains a set of components that can be used in designing web application interfaces. These are plugins available on a separate Java Script file. The following components can be found in Bootstrap library:

- Dropdown Menus
- Buttons with Dropdowns
- Navigation Elements
- Navbar
- Button groups
- Pagination

Being an open source project, Bootstrap is a powerful tool because of the development community that supports it.

- One can download the source, or if wants to easily customize a few of the colors, sizing, or plugins, one can cater the Bootstrap to your needs via the Bootstrap website.
- When one wants to the customize page, may decide what components needs or if he uses or not any JQuery plugin. [5]
- Generally speaking, Bootstrap can fill the needs of any complex web project. Containing extensive JavaScript plugins, and robust interface components and being easy-to-use, Bootstrap is a very complex tool in web programming.

4. W3.CSS

As Bootstrap, W3.CSS is a free front-end framework for faster and easier web development. W3.CSS is web responsive and support modern responsive design. In addition, is faster and smaller than other CSS frameworks and use standard CSS, does not use JavaScript or jQuery.

The usage of this framework is easy, it is necessary to add the following link in the page source:

```
<link rel="stylesheet" href="https://www.w3schools.com/w3css/4/w3.css">
```

Another possibility to use it is to download the framework, has the same option as Bootstrap.

The most important part from W3.CSS are the containers, more exactly the ***w3-container class***. It provides equality like: common margins, common paddings, common vertical/horizontal alignment, common fonts and colors. [4]

The w3-container class is typically used with HTML container elements, like: <div>, <header>, <footer>, <article>.

Images

W3.CSS offers more possibilities for images design. All images created with these new technologies are web responsive. In addition, at all type of images one can add grayscale effect using the w3-grayscale classes, sepia effect using w3-sepia classes and other effects. Using this framework one can create: round, circle, bordered images, etc.

Furthermore, one can find templates for creating photo albums. As Bootstrap, W3.CSS provide also the possibility to make slide show presentation.

Forms

In comparison with Bootstrap, W3.CSS provides more templates and more different types of forms. The framework provides colorful forms and in the same time animated fields. This is the most interesting functionality provide. To crate animated field is needed the w3-animate-input class that transforms the width of an input field to 100% when it gets focus.

Another form template provided by W3.CSS is Icon Labels forms. In order to create this form is needed to combine more classes and styles. The form is looking like the following one:

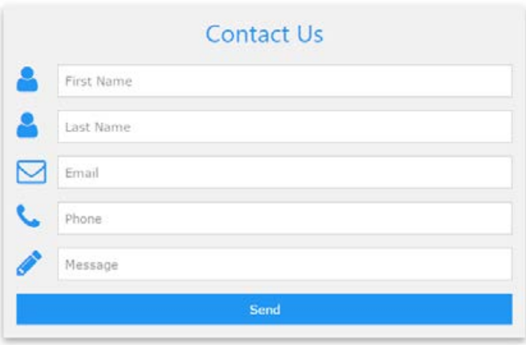

Buttons

W3.CSS provides a big diversity of buttons. One can add in his web site what type of button he wants. The buttons can be added in the source code easily using the class name of the button type wanted. The buttons classes are the following [6]:

- *w3-btn:* A rectangular button with a shadow hover effect. Default color is black
- *w3-button*: A rectangular button with a gray hover effect. Default color is light-gray in W3.CSS version 3. Default color is inherited from parent element in version 4
- *w3-bar*: A horizontal bar that can be used to group buttons together
- *w3-block*: Class that can be used to define a full width (100%) button
- *w3-circle*: Can be used to define a circular button
- *w3-ripple*: Can be used to create a ripple effect.

All buttons can be customizing in the way the user wants. One can add the desired color, size and shape; buttons can have different text effects, or shadow.

4. APPLICATION: SLIDE SHOW

In this section we will present different approaches of using Bootstrap and W3.CSS frameworks creating a slide show with pictures, buttons, and forms.

Slide Show

To create the slide show with HTML it is necessary to write JavaScript and PHP functions so that one can see the photos like a slide show. The functions are used for previous and next photo. We have created one more function so that the photo can be rotated. The CSS is written for each rotation degree (for 0^o, 90^o, 180^o and 270^o).

```
function rotater() {
    object = document.getElementById('rotator' + current);
    if (object.className == "rotate0")
    {
        object.className = "rotate90";
    }
    else if (object.className == "rotate90")
    {
        object.className = "rotate180";
    }
    else if (object.className == "rotate180")
    {
        object.className = "rotate270";+
    {
        object.className = "rotate0";
    }
}
```

FIG. 1 Image rotate function

It is necessary to add buttons so that the pictures can be played. The functions are presented in Fig. 2.

```
<script language="JavaScript" type="text/javascript">

    first=1;
    last=9;
    current=1;
    i=0;
    var ns6 = document.getElementById&&!document.all;

    function imgFilter(id) {
    var imgId = $(id); $("imgId").each(function(i)
        {
            $("this").setAttribute('src', $("this").getAttribute('data-src'));
        });
    };

    function nextPicture() {
        object = document.getElementById('slide' + current);
        object.style.display='none';
        if (current == last) { current=1; }
            else {current++ }
        object = document.getElementById('slide' + current);
        object.style.display = 'block';
    }

    function previousPicture() {
        object = document.getElementById('slide' + current);
        object.style.display='none';
        if (current == first) { current=last;}
            else {current--; }
        object=document.getElementById('slide' + current);
        object.style.display = 'block';
    }
```

FIG.2 Functions for slideshow navigation

Using HTML5 with Bootstrap it is much easier to create the slide show. Bootstrap has a class called Carousel that is designed specially for slide show. The code is included in a <div> element and is presented in Fig. 3.

```
<div class="container">
  <h2>Photo album</h2>
  <div id="myCarousel" class="carousel slide" data-ride="carousel">
    <!-- Indicators -->
    <ol class="carousel-indicators">
      <li data-target="#myCarousel" data-slide-to="0" class="active"></li>
      <li data-target="#myCarousel" data-slide-to="1"></li>
      <li data-target="#myCarousel" data-slide-to="2"></li>
    </ol>

    <!-- Wrapper for slides -->
    <div class="carousel-inner" role="listbox">
      <div class="item active">
        <img class="d-block img-fluid" src="img1.jpg" alt="ski"  class="img-responsive">
      </div>

      <div class="item">
        <img class="d-block img-fluid" src="img2.png" alt="lac" style="width:100%;" class="img-responsive" >
      </div>

      <div class="item">
        <img class="d-block img-fluid" src="img1.jpg"  class="img-responsive">
      </div>
    </div>

    <!-- Left and right controls -->
    <a class="left carousel-control" href="#myCarousel" data-slide="prev">
      <span class="glyphicon glyphicon-chevron-left"></span>
      <span class="sr-only">Previous</span>
    </a>
    <a class="right carousel-control" href="#myCarousel" data-slide="next">
      <span class="glyphicon glyphicon-chevron-right"></span>
      <span class="sr-only">Next</span>
    </a>
  </div>
</div>
```

FIG. 3 Slide show with Bootstrap

Another method for realizing a slide show is using HTML5 with W3.CSS. The only disadvantage using this framework is that is needed to write JavaScript code. JavaScript functions are added to select images. The function showDivs() is used to display the first image and the function plusDivs() is called when the user clicks one of the buttons. The first function hides all elements with the class mySlides and displays the element with the given index. If the index is higher than the number of elements then the variable is set to zero and if the index is less than 1 it is set to number of elements.

It is also necessary to create many elements using the class mySlides. These elements are the images from the slide show. In the end we add two buttons to scroll the images, like in Fig. 4.

```
<h3>3. Slide show</h3>
    <div class="w3-content w3-display-container">
        <img class="mySlides" src="img1.jpg" style="width:100%">
            <div class="w3-display-bottomleft w3-large w3-container w3-padding-16 w3-black"> Lac </div>
        <img class="mySlides" src="img2.png" style="width:100%">
        <img class="mySlides" src="img1.jpg" style="width:100%">

        <button class="w3-button w3-black w3-display-left" onclick="plusDivs(-1)">&#10094;</button>
        <button class="w3-button w3-black w3-display-right" onclick="plusDivs(1)">&#10095;</button>
    </div>
```

FIG.4 Buttons for images scrolling

Using W3.CSS to create the album is very easy and provides more templates for albums gallery. Beside the slide show, this framework comes up with other predefined templates for albums. In Figure 5 one can see two more types of albums using W3.CSS.

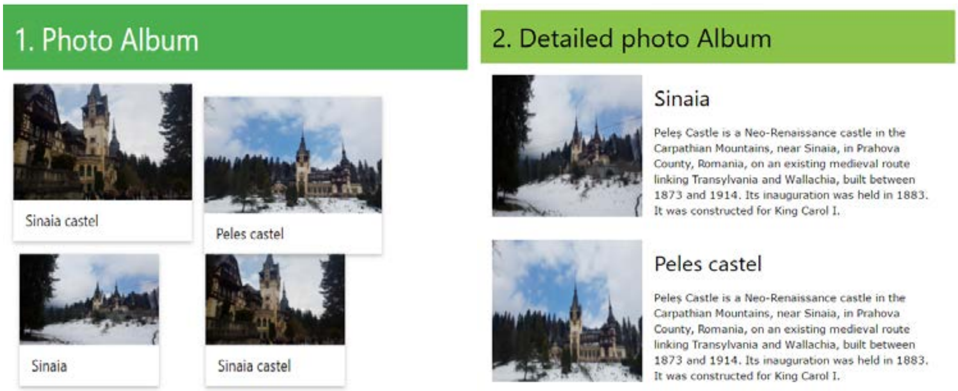

FIG. 5. Types of photo albums with W3.CSS

Images

In Bootstrap and W3.CSS photos can have different shapes. For example, they can have the shape of a circle or they can have border. The classes used for images are almost similar in Bootstrap and W3.CSS, the difference is that W3.CSS class has **w3** followed by the shape name [4]. In Figure 6 one can see the HTML code with Bootstrap and W3.CSS.

```
<!--Bootstrap-->

    <img class="img-rounded" src="img1.jpg" width="350" height="236">
    <img src="img2.png" class="img-circle" width="304" height="236">
    <img src="img1.jpg" class="img-thumbnail" width="304" height="236">

<!--W3.CSS-->

    <img src="img1.jpg" class="w3-round-xlarge" style="width:20%">
    <img src="img2.png" class="w3-circle" style="width:20%">
    <img src="img1.jpg" class="w3-border" style="padding:4px;width:20%">
```

FIG. 6 HTML code for images with Bootrstrap versus W3.CSS

In browser we can see

W3.CSS has classes for different effects like opacity, sepia or hover image. This effect can be added to a photo using inside the <img> tag the desired class. One can set the size of the picture using the property “style”.

```
<img src="img1.jpg" class="w3-opacity-max" style="width:150px">
```

CONCLUSIONS

In conclusion, the most effective way to create more interactive and diversified web pages is to use the W3.CSS framework. It offers much more page customization than Bootstrap, but the two can be used in a similar way and with many elements in common.

In addition, an extra reason for using HTML5 is its feature of being compatible with all Internet browsers. It is compatible with browsers such as Chrome, Internet Explorer, Firefox, Opera or Safari.

Considering the massive explosion of mobile phones, smart phones, tablets and other mobile gadgets, HTML5 is optimized to build applications and mobile sites. HTML5 is used to build responsive sites supported by different types of mobile interfaces.

REFERENCES

[1] C.G. Carstea, Modeling System’s Process for Control Of Complex Information Systems, Proceedings of The 25th International Business Information Management Association Conference (IBIMA), May 7-8, Amsterdam, Netherlands, ISBN: 978-0-9860419-4-5, pg.566, 2015;

[2] C. Carstea, New approach about project management of complex information systems, Ed. LAP LAMBERTAcademic Publishing GmbH & Co., Germany, 2011;

[3] R. Nixon, Learning PHP, MySQL & JavaScript With jQuery, CSS & HTML5 – Fourth Edition, Sebastopol California, Ed. O’Reilly Media, 2014;

[4] L. Sangeorzan, G.A. Stelea, N. Enache-David, Web Development Techniques for Applications and Websites, Ed. Univ. Transilvania din Brasov, 2016;

[5] Spurlock, J., Bootstrap, Sebastopol California, Ed. O’Reilly Media, 2013.

[6] https://www.w3schools.com/w3css/.

COMPARATIVE REVIEW OF THE LEGAL STATUS OF CADETS AND STUDENTS IN BULGARIAN HIGHER EDUCATION INSTITUTIONS

Yosif YOSIFOV, Nikolay ZHECHEV, Alexander KUMANOV

Faculty of Artillery, Air Defense and CIS National Military University „Vasil Levski“, Bulgaria

DOI: 10.19062/2247-3173.2019.21.11

Abstract: *Education in the professional field “Military Science” is related to the protection of the national security of the state. The main functions of the modern state are governing, economical, protective and social, including educational. Ensuring the quality of education in the professional field “Military Science” is a simultaneous realization of the protective and educational functions.*

The fundamental legal framework of the principles of higher education in this professional field is regulated in the Constitution of the Republic of Bulgaria, in the Higher Education Act, in the Law of Defense and Armed Forces of the Republic of Bulgaria, as well as in various decrees, ordinances and instructions.

The foundations of the modern Bulgarian army were laid after the Liberation in 1878 simulateneously with the establishment of the military educational institutions in Bulgaria, when initially the Sofia Military School was located the same year. The first higher military school in Bulgaria - the Military Academy - was established in 1912.

Keywords: *Right of Education, Higher Education, Military Schools, Cadets*

The main functions of the modern state are governing, economical, protective and social, including educational. Ensuring the quality of education in the professional field “Military Science” is a simultaneous realization of the protective and educational functions.

The First Military Higher Education Schools were established in Russia (military engineering schools created in the XVIIIth century by Emperor Peter I) , France (Saint Cyr Military School, founded in 1802 by Napoleon Bonaparte), USA (West Point Military Academy, established on 4 July 1802), United Kingdom (The Royal Military Academy Sandhurst, established in 1947).

Military educational institutions in Bulgaria are created immediately after the Liberation in 1878, when the foundations of the modern Bulgarian army were laid. Initially the Sofia Military School (1878) was opened, and the first higher military school in Bulgaria - the Military Academy - was established in 1912.

The fundamental legal framework of the principles of higher education in this professional field “Military Science” is regulated by the Constitution of the Republic of Bulgaria, in the articles of the Higher Education Act, also in the Law of Defense and Armed Forces of the Republic of Bulgaria, as well as in various decrees, ordinances and instructions.

The Constitution of Republic of Bulgarian provides that the State is obliged to create conditions for the free development of science and education. (art. 23). The right of education is promulgated as fundamental civil right. Under terms established by the law, tuition at public higher schools is free of charge. (art. 53).

The Higher Education Act (HEA) categorizes higher education institutions as universities, research universities, specialized higher education institutions and independent colleges. (art. 17).

A university is a higher school which:

- provides training in a wide range of subjects in professional areas within at least three of the four major branches of science - humanities, natural sciences, social sciences and technical sciences;
- employs full-time faculty required to conduct no less than half of all lecturing and practical sessions under the academic curriculum in each major, whereas the habilitated faculty members deliver no less than seventy percent of all lecturing courses in each major;
- holds adequate facilities to ensure that practical training is also conducted in compliance with the state standard requirements;
- offers bachelor's, master's and doctor's degrees in the respective major branches of science;
- has ample scientific and artistic potential and through its activities contributes to the development of major branches of science and culture;
- provides the faculty, the students and the doctoral candidates with adequate conditions for printing of scientific works, textbooks, monographs, as well as for the achievement of typical creative accomplishments;
- owns a library and other means for information services to instruction and research;
- maintains international contacts both in the provision of academic instruction and in its creative activities;
- has an academic information centre for administrative services to students and doctoral candidates;
- has an intellectual property protection system which includes rules and a structure for the implementation of research results and other objects of intellectual property, as well as for training in the field of intellectual property rights protection.

A specialised higher school conducts scientific research or artistic and creative activities and offers courses of training in one of the major areas of science, arts, physical culture, and military science and meets the university description criteria. Its appellation shall signify the specific area in which it trains specialists.

Students, PhD students and postgraduates are trained in higher education institutions. Student is the one who is trained to acquire the Bachelor's and Master's degrees. (Article 66 of the HEA). Cadets are trained in specialized higher education institutions.

The main differences in the training of cadets and students are in three directions - admission, ensuring their training and the rights and obligations.

The admission of the cadets is done by selecting the candidates for the cadets. The admission of cadets is determined in accordance with Art. 142. Para 1 of the Law on Defense and Armed Forces of the Republic of Bulgaria. The terms and procedures for enlistment to military academies and higher military schools and professional colleges shall be determined with a regulation of the Minister of Defence.

Cadets trained to meet the needs of the Ministry of Defence enter into contracts for military service, and the term of such contracts includes the period of training thereof. For the period of training at higher military schools the cadets have been prepared for doing military service as a profession and must be provided with:

- funds from the budget of the Ministry of Defence, to the extent not provided for otherwise by law:
  - scholarships for rank – under terms, procedure and in amounts specified in an act of the Minister of Defence;
  - food, clothes and gear supply – under terms, procedure and in amounts specified in an act of the Minister of Defence;
  - medical services;
  - compulsory insurance against death and disability as a result of accident during or in relation to the implementation of obligations connected to their training for doing military service as a profession;
  - accommodation at residences of higher military schools;
  - transport and accommodation when implementing tasks related to their training for doing military service, outside the permanent place of training, and when travelling for medical purposes;
- use of recreation and sports facilities of the Ministry – under the terms and procedure laid down by an act of the Minister of Defence;
- leave of 30 calendar days per school year under terms and procedures specified in the regulations on the organisation and operation of the higher military schools;
- opportunities for election to the collective management bodies at the higher military school.

Cadets are promoted in rank pursuant to Article 138, paragraph 3 with an order of the commander of the higher military school under terms and procedures specified in the regulation on its organisation and operation.

Graduating cadets for the needs of the Ministry of Defence are obliged to perform military service for a period of at least ten years.

The rights and obligations of the cadets are determined in the regulations on the organisation and operation of the military academies and the higher military schools and in the military service contract.

Cadets in the higher military schools shall be awarded the following ranks:

1. cadet;
2. cadet - junior sergeant (in the Navy - cadet - petty officer 2nd class);
3. cadet - sergeant (in the Navy - cadet - petty officer 1st class);
4. cadet - senior sergeant (in the Navy - cadet - chief petty officer);
5. cadet - sergeant-major (in the Navy - cadet - midshipman).

According to the art. 70 of HEA students are entitled to:

- select subjects (courses) under such terms as are set forth in the curriculum;
- receive qualified assistance and supervision in their academic and professional development;
- study more than one specialty (major) at a time or take additional courses under terms prescribed by the higher school;
- participate in the higher school's research activities whereas any rights of theirs arising out of the applicable laws on the protection of copyright, intellectual property rights and the neighbouring rights, as well as any remuneration payable to them shall be guaranteed;
- elect and be elected to the higher school's governing bodies;
- use students' hostels, canteens, health-care services, reduced fares for the mass and rapid transit and the intercity transportation and all the higher school's facilities for study,

research, sports and cultural activities, as well as other welfare benefits for normal life and studies under terms set by the state and the respective higher school;

- associate in academic, scientific, cultural and sports fellowships for protection and satisfaction of their interests, as well as to have membership in (of international organisations whose activities are not contradictory to the laws of the Republic of Bulgaria;
- transfer to another higher school, faculty, department, specialty, level or forms of study in accordance with the higher school's Rulebooks;
- discontinue their studies and resume them subsequently under terms and procedures laid down in the higher school's Rulebooks;
- have holidays of minimum thirty days inside of one academic year;
- receive scholarships (stipends);
- use credits for payment of (tuition) fees and /or for maintenance during the course of training.

Special incentives are provided for students who are orphans, persons with sensory disabilities and other disabled people with long-term disability or reduction of the ability to work by 70 percent or more or disabled war veterans, and victims or persons raised at orphanages until they become of age, or mothers of children below the age of six, or depending on direct clinical observation shall be entitled to special privileges and alleviations as set forth in the respective higher school's Rulebooks.

Training in the military field is related to the protection of the national security of the state. That is why the requirements for the cadets are higher than those for the students, while different conditions for their realization after the completion of the higher education are envisaged.

REFERENCES

[1] Dachev L., (2001) State Sciences. Sofia, “Svida”
[2] https:// www.neaa.government.bg/

NUMERICAL MODELING OF ACOUSTIC WAVE PROPAGATION IN UNLIMITED SPACE

Alina-Elena ADETU*, Cătălin ADETU, Vasile NĂSTĂSESCU***

*Military Technical Academy, Bucharest, Romania (adetu.alina@yahoo.com)
** "Politehnica" University of Bucharest, Romania

DOI: 10.19062/2247-3173.2019.21.12

Abstract: *This article refers to the process of numerical modeling of acoustic wave propagation in unlimited space. Existing analytical methods are difficult to apply but present the main difficulty because they lead to some point values so that analysis of entire domain involves a large volume and is difficult to interpret. This paper put in evidence the influence of a sound absorption panel present. Numerical calculation provides post-processing of results a quick image of the distribution of acoustic pressure in the analyzed domain. The numerical analysis was carried out using Ansys program.*

Keywords: *acoustic pressure, acoustic elements, acoustic impedance, FEM.*

1. INTRODUCTION

Worldwide, the overall noise level is alarmingly high, we live in a noisy society mainly due to the technological environment in which we evolved.

The impact of noise on communities which are living in the proximity of airports represents a major importance for the aircraft manufacturers and airline operators for more than four decades. Knowing both aeronautics and acoustics is essential for a clear understanding of any aviation noise issue. Such an understanding is a necessary condition for controlling indoor and outdoor noise.

The main noise source of an aircraft is its propulsion system. Therefore, regarding the noise, airplanes can be classified in terms of their engine types.

Existing analytical methods are difficult to apply in this case and the main problem is that they lead to some point values so that analysis of entire domain involves a large volume and is difficult to interpret.

Numerical calculation provides post-processing results as a quick image of the distribution of acoustic pressure in analyzed domain. The finite element method is a numerical method that can be used for the accurate solution of complex engineering problems. Over the years, the finite element technique has been so well established, that today it is considered one of the best methods for solving a wide variety of practical problems efficiently.

2. MODELING WITH FINITE ACOUSTIC ELEMENTS

2.1. Fundamentals.

Finite Element Method is a general method of roughly solving differential equations with partial derivatives that describe or not a physical phenomenon.

There are two kinds of models: 2D or plane models and 3D or spatial models. For each model type finite elements were created. As the Ansys finite element library is concerned 2D acoustic fluid and 3D acoustic fluid elements exist.

The most used acoustic finite elements are named FLUID29 for 2D modeling and respectively FLUID30 for 3D modeling, in the Ansys finite element library.

Next to these finite elements other kinds of finite elements were designed for infinitely modeling of the acoustic domain; practically, such finite elements are placed on the acoustic domain boundary and they work like a damping at the boundary by simulating the energy dissipation. So, no reflection wave occurs.

FLUID 129 and respectively FLUID130 finite elements are used for endless boundary modeling in the wave propagation direction.

In the case of the interaction between acoustic waves with a structure, like in the case of present of an acoustic absorbing panel, others proper structure finite elements can be used. A detailed description of all these finite elements can be found in Ansys theoretical manual and in main literature about finite element modeling [1], [6], [10] and [11]. Those two finite element types are presented in the Fig. 1.

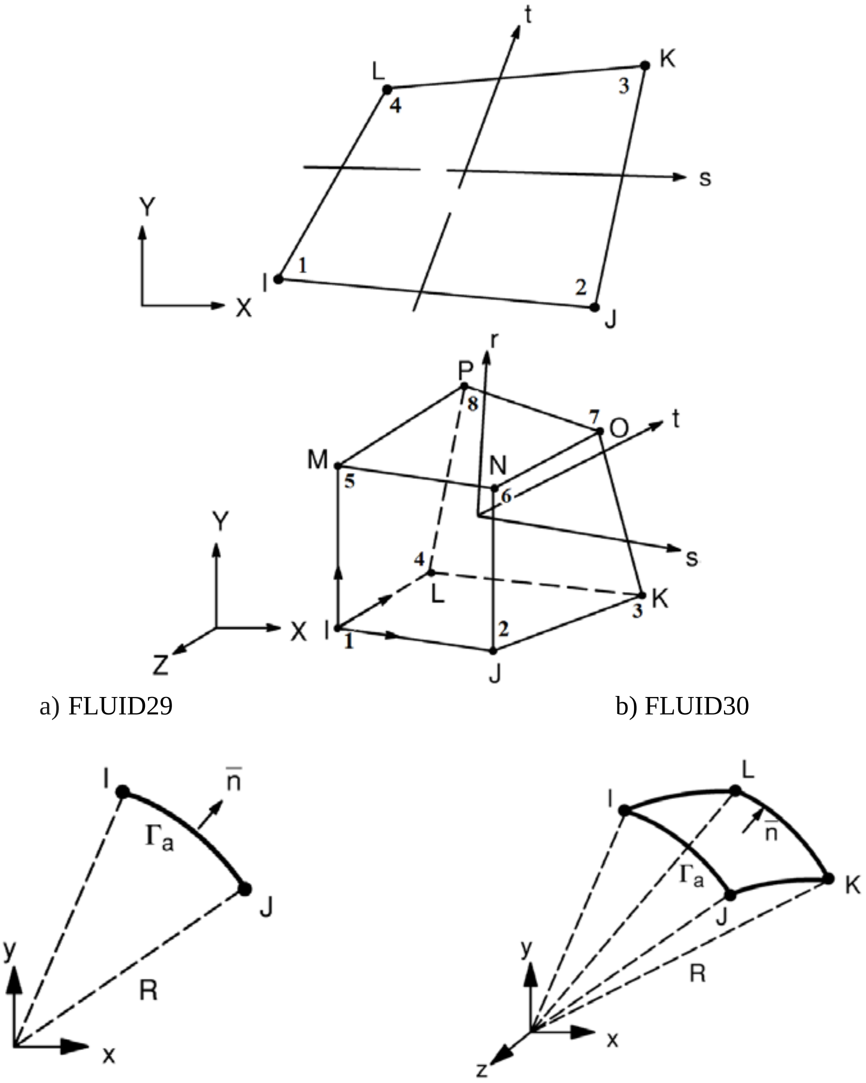

a) FLUID29 b) FLUID30

c) FLUID129 d) FLUID130

FIG.1. Acoustic finite elements

The FLUID29 is a plane finite element, in the xOy plane, having two options: a planar or an axisymmetric finite element. All acoustic finite elements are isoparametric elements. Numerical analysis by FEM is made under following assumptions: the fluid is compressible (density changes due to pressure variations), the fluid is inviscid (no viscous dissipation exists), there is no mean flow of the fluid and the mean density and pressure are uniform throughout the fluid.

The fundamentals of acoustic finite element analysis start from the lossless acoustic wave equation [11],

$$\frac{1}{c^2}\frac{\partial^2 P}{\partial t^2} - \nabla^2 P = 0 \qquad (1)$$

where c is the speed of sound and P is the acoustic pressure.

The field parameters like acoustic pressure P and displacements u, inside the finite element can be calculated:

$$P = \{N\}^T \{P_e\} \qquad (2)$$

$$u = \{N'\}^T \{u_e\} \qquad (3)$$

where $\{N\}$ is the element shape function for pressure, $\{N'\}$ is element shape function for displacements, $\{P_e\}$ is the nodal pressure vector and $\{u_e\} = \{u_{ex}\}, \{u_{ey}\}, \{u_{ez}\}$ are the nodal displacement component vectors.

After some mathematical operations, from relation (1), the acoustic fluid matrices are obtained [11]:

$$\frac{1}{c^2}\int_V \{N\}\{N\}^T dV \{\ddot{P}_e\} + \int_V [B]^T [B] dV \{P_e\} + \rho_0 \int_S \{N\}\{n\}^T \{N'\}^T dS \{\ddot{u}_e\} = \{0\} \qquad (4)$$

or,

$$\left[M_e^P\right]\{\ddot{P}_e\} + \left[K_e^P\right]\{P_e\} + \rho_0 [R_e]^T \{\ddot{u}_e\} = \{0\} \qquad (5)$$

where the acoustic fluid matrices are:

$\left[M_e^P\right] = \frac{1}{c^2}\int_V \{N\}\{N\}^T dV$ is the fluid mass matrix; (6)

$\left[K_e^P\right] = \int_V [B]^T [B] dV$ is the fluid stiffness matrix; (7)

$\rho_0 [R_e] = \rho_0 \int_S \{N\}\{n\}^T \{N'\}^T dS$ is the coupling mass matrix (fluid-structure interface). (8)

$\{B\} = \{L\}\{N\}^T$ is a matrix resulting from applying of the matrix operator $\{L\}$ to element shape functions, and

$$\{L\} = \nabla(\ ) = \begin{bmatrix} \frac{\partial}{\partial x} \\ \frac{\partial}{\partial y} \\ \frac{\partial}{\partial z} \end{bmatrix} \qquad (9)$$

As the shape functions are concerned, these are those known from the general theory of finite element analysis, which can be expressed in local or general coordinates.

The modeling of the acoustic pressure field has some peculiarities dependind on acoustic domain which can be a closed one or an open one. In this case, a 2D model has to be an axisymmetric model; a 3D model can be used in any case, but it can be a complete one or a partial one, depending on the domain characteristics.

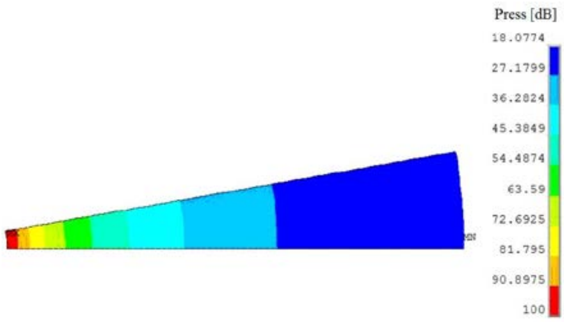

FIG. 2 Acoustic pressure field in 2D analysis

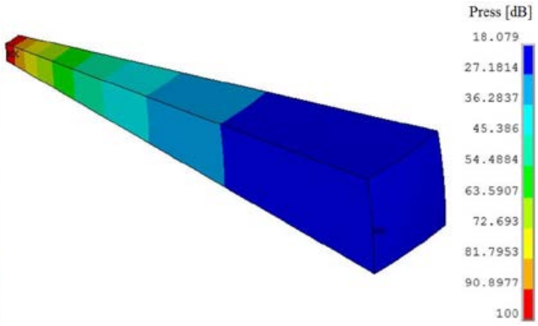

FIG. 3 Acoustic pressure field in 3D analysis

The Figures 2 and 3 present the calculus results for the same problem, but in two cases of modeling, 2D and respectively 3D.

Looking at the Fig. 2 and Fig. 3 we can see that the acoustic pressure values are practically the same no matter the model type 2D or 3D. Of course, a 2D model, when it is appropriate, is more efficient than a 3D model being easier to build and being solved in a shorter computer time.

2.2. Problem Formulation and Modeling.

Because we are interested not only in the acoustic field modeling, but in studding the influence of an acoustic absorbing panel, the problem domain is represented by a piece of acoustic field around the panel. So, the acoustic wave propagation range is defined in cylindrical coordinates with an angular symmetrical opening of 10 degrees and 1 m dimension on the propagation direction, as Fig. 4 shows.

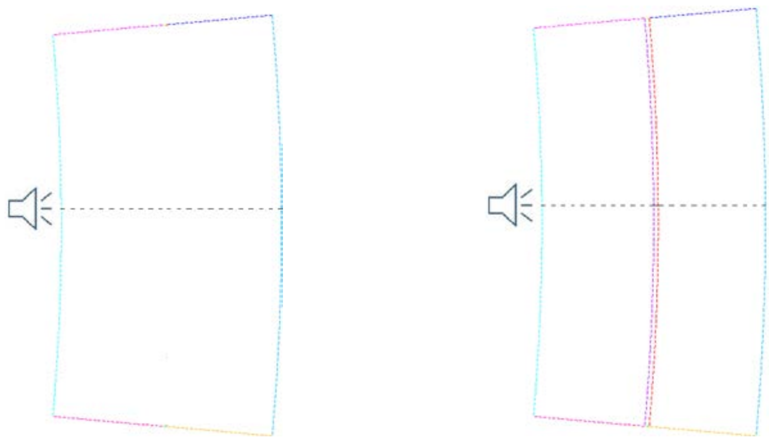

a) Acoustic source and domain   b) Geometrical model with absorbing panel

FIG. 4 Geometrical models

The authors have opted for a 2D axisymmetric model, this being most convenient (easy to build, shorter computer time).

Table 1. The properties of the materials

Details	*Density* (ρ)	*Sonic velocity* (c)	*Impedance* ($c \cdot \rho$)	Young's modulus (E)	Poisson ratio (υ)
	kg/m^3	m/s	$N \cdot s/m^3$	Pa	-
Air	1.225	340	416.50		
Aluminum	2700	5200	14040000	$0.7*10^{11}$	0.33

The Fig. 4 presents those two cases taken into account: without absorbing panel (Fig. 4-a) and with the present of the absorbing panel (Fig.4-b). In the both cases a stationary nodal acoustic source with 100 dB was considered. The absorbing panel is made of aluminum having a thickness of 20 mm.

In the Table 1 the main properties of materials, used for solving the problem, are presented. The mesh used in developing of the acoustic numerical analysis was chosen after a short analysis of three versions (a, b and c) regarding the finite element size. Those three sizes of finite elements were 10 mm, 20 mm and 30 mm, for all those three element types: FLUID29, FLUID129 and PLANE42.

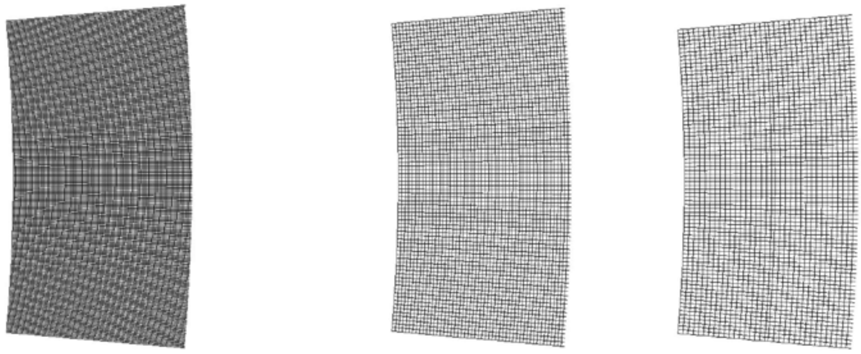

a) FE size = 10 mm   b) FE size = 20 mm   c) FE size = 30 mm

FIG. 5 Finite element models

The acoustic panel (screen) is placed in the middle of the field (Fig. 4-b), across the opening, each element having 4 nodes (the finite element PLANE42). The panel, as a mechanical structure, is clamped at the lower and upper parts. The right hand side of the domain boundary is also meshed with finite elements FLUID129.

For choosing the best mesh, those three mesh versions were used, running the program without any acoustic panel. Fig. 6 shows the acoustic pressure field for those three mesh versions considered.

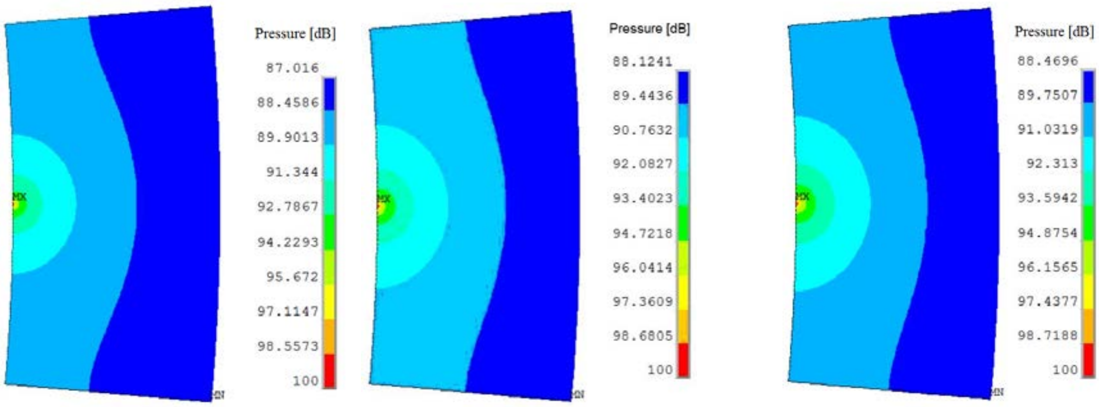

a)   *b)*   *c)*

Fig. 6 The acoustic pressure field for three mesh versions

The Table 2 presents a synthetically analysis of the results obtained those three mesh version.

Table 2. Comparative analysis

F.E. size	Nodes	Elements	Max. value	Min. value	Differences
1 cm	16261	16160	88.4586	87.0160	1.4426
2 cm	4131	4080	89.4436	88.1241	1.3195
3 cm	2835	2800	89.7507	88.4696	1.2811
		Average values:	***89.2176***	***87.8699***	***1.3477***
Errors (%) towards average value:					
1 cm			***-0.85***	***-0.97***	***7.04***
2 cm			***0.25***	***0.29***	***-2.09***
3 cm			***0.60***	***0.68***	***-4.94***

As it results from the analysis of the values presented in the Table 2, the best mesh version is that having the finite element size of 20 mm.

3. RESULTS AND DISCUSSIONS

The results of numerical analysis with finite elements are presented synthetically and suggestively in the figures below, where these were obtained by graphically post-processing.

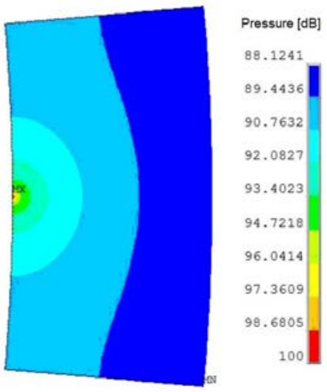

FIG. 7 Acoustic pressure field without panel

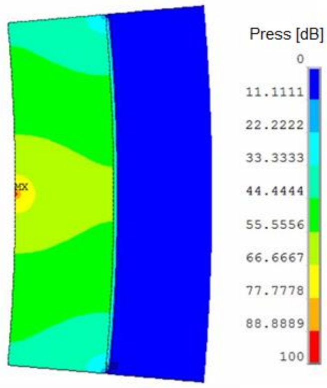

FIG. 8 Acoustic pressure field with panel

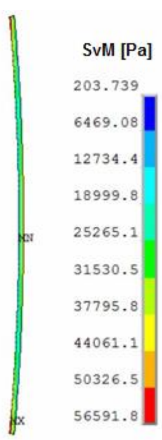

FIG. 9 Equivalent von Mises stress field of the panel

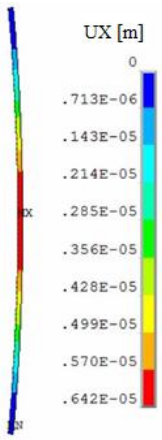

FIG. 10 UX-displacement field of the panel

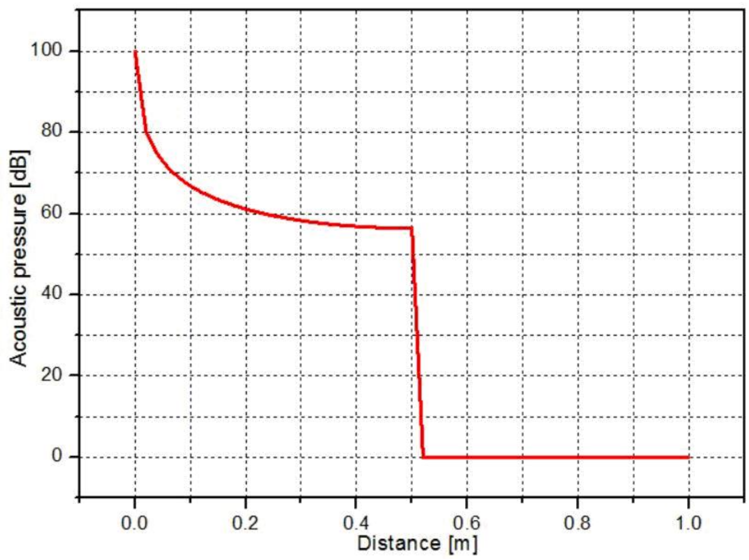

FIG. 11 Pressure-distance curve on median propagation direction

Fig. 7 and Fig. 8 demonstrate the significant effect of the acoustic absorbing panel considered, which causes the sound pressure level behind not to exceed 11.111 dB; the efficiency of the screen is proven by the comparative analysis of the Figures 7 and 8.

It is found that in the absence of the screen, the sound pressure level in the field does not fall below 88.1241 dB, thus remaining very high (the decrease is only 11.876% from the source level).

The acoustic pressure has the effect of an elastic stress loading on the screen, as shown in Figure 9 which shows the von Mises equivalent stress field in the screen, where the maximum value is 0.056592 MPa (low value, which does not raise problems from point in terms of mechanical strength).

Figure 10 shows the field of the nodal displacements of the acoustic absorbing panel in the direction of the acoustic wave propagation. As expected, the maximum displacement occurs at the middle of the screen, reaching the value of 0.00642 mm (this value is a small one, meaning the reduced mechanical load due to the acoustic pressure action).

Fig. 11 contains the variation curve with the distance from the source of the acoustic pressure in the direction of the acoustic wave propagation at the source level, in the conditions of acoustic panel existing.

As it seen in the Figure 11, a significant drop in the sound pressure level is produced by the panel presence. The considered acoustic absorbing panel produces a consistent variation, from 56.4 dB to zero dB.

The acoustic absorbing panel, under the given conditions, without significant mechanical stress, produces significant sound insulation.

A wider and more useful discussion can be done through similar simulations of several types of screens, different in size, material and shape.

4. CONCLUSIONS

Numerical analysis by finite element method allows a quantitative and qualitative evaluation of the effects of soundproof panels (screens). In this paper the methodology is presented first, for a given case, so that the conclusions and the observations are based on quantitative determinations.

The adopted 2D model allows fast calculation, which favors the study of a significant number of variants of the screen within a reasonable time.

The effect of soundproof screens can be studied by numerical simulation, both in the case of acoustic waves in transient mode and taking into account the influence of the frequency of sound waves. These issues are the subject of further studies, including a doctoral thesis.

REFERENCES

[1] BATHE, K-J., *Finite Element Procedures In Engineering Analysis*, Prentice-Hall Inc., 1982

[2] J.P. COYEWE, G. VANDERBORCK, W. STEICHEW, *A coupling procedure for modeling acoustic problems using finite elements and boundary elements*, Journal de Physique IV, Colloque C5, supplement au Journal de Physique III, Volume 4, Mai 1994

[3] HRISTEV ANATOLIE, *Mecanica si Acustica*, Editura Didactica si Pedagogica, Bucuresti, 1984

[4] S. LANGDON, S. N. CHANDLER-WILDE, *Finite element methods for acoustic scattering*, Lecture notes, Department of Mathematics, University of Reading, Berkshire, UK, July 18, 2007

[5] LAWRENCE E. KINSLER, AUSTIN R. FREY, ALAN B. COPPENS, JAMES V. SANDERS, *Fundamentals of Acoustics*, Fourth Edition, John Wiley & Sons, Inc., 2000

[6] NĂSTĂSESCU V., STEFAN A., LUPOIU C., *Analiza neliniară a structurilor mecanice prin metoda elementelor finite*, Editura Academiei Tehnice Militare, Bucuresti, 2002

[7] NĂSTĂSESCU V., BÂRSAN GH., *Metoda particulelor libere în analiza numerică a mediilor continue*, Editura AGIR, Bucuresti, 2015

[8] NĂSTĂSESCU V., BÂRSAN GH., *Metoda elementelor libere Galerkin în analiza structurilor*, Editura Academiei Romane, Bucuresti, 2018

[9] SANDEEP T VARGHESE, NIRMAL CHANDRAN, *Acoustic Structure Interaction with Damping Interface*, International Journal of Engineering Research & Technology (IJERT), Vol. 4 Issue 11, November-2015

[10] ZIENKIEWICZ, O.C., TAYLOR, R.L., ZHU, J.Z., *The Finite Element Method Its Basis and Fundamentals*, 6ed, Elsevier, 2005

[11] * * * *Ansys, Inc. Theory*, Release 5.7, Twelfth Edition, 2001

TRACKING MANEUVERING TARGET WITH KALMAN FILTER AND INTERACTIVE MULTIPLE MODEL

Deyan ATANASOV

”Vasil Levski” National Military University, Artillery, Air Defence and CIS Facutly, Shumen, Bulgaria (daatanasov@nvu.bg)

DOI: 10.19062/2247-3173.2019.21.13

Abstract: *In this work, a study has been conducted on the capabilities of the Kalman and Interactive Multiple Model filters to track the trajectory of a maneuvering target. The results of the experiment clearly show the better performance of the Multiple Model algorithm than Kalman's.*

Keywords: *tracking, Kalman filter, Interactive Multiple Model*

1. INTORDUCTION

The most effective solution that does not require the deployment of new facilities in radar systems to make better Air Traffic Control (ATC) is to improve the algorithms it operates with. The main challenge and difficulty of ATC is to track a maneuvering target in a clutter environment [3]. The present work explores existing algorithms for processing radar information. One is the standard linear Kalman filter widely used in tracking systems, and the other is the Bar-Shalom tracking algorithm called the Interactive Multiple Model (IMM) algorithm [4] that estimates with significant noise suppression and rapid sequence response from target maneuvers. The paper compares the capabilities of the two algorithms with regard to the accuracy in tracking the target trajectory.

2. KALMAN FILTER

It is a repeating mathematical process that uses certain equations and sequential input data to quickly calculate the true values of the object to be measured when the measured values contain unpredictable or random errors.

An important advantage of the Kalman filter is that the obtained theoretical solution directly determines its practical realization and the expressions for assessing the state vector and its covariance have a recurrent form which provides a sequential refinement of the state vector upon receipt of each new measurement. It is assumed that all trajectory information is locked in the last estimate, so it is not necessary to store all previous measurements and process their entire set after receiving the new measurement [5].

Kalman filter - this is a recursive Bayesian algorithm for optimal linear filtration of the vector random process. The algorithm (Fig.1) is the solution of the following equation system [2].

$$
\begin{aligned}
&z_k = H\,x_k + v_k\\
&x_k^- = F\,\hat{x}_{k-1} + w_k\\
&P_k^- = F\,\hat{P}_{k-1}F^T + Q\\
&S_k = H\,P_k^- H^T + R\\
&K_k = P_k^- H^T S_k^{-1}\\
&\hat{x}_k = x_k^- + K_k\left(z_k - H\,x_k^-\right)\\
&\hat{P}_k = \left(I - K_k H\right)P_k^-
\end{aligned}
\tag{1}
$$

The task of Kalman filter is to find an optimal estimation of the *k* stage vector state of its covariate matrix $\hat{P}_k$. Matrices **F**, **H**, **Q** and **R** are considered to be known.

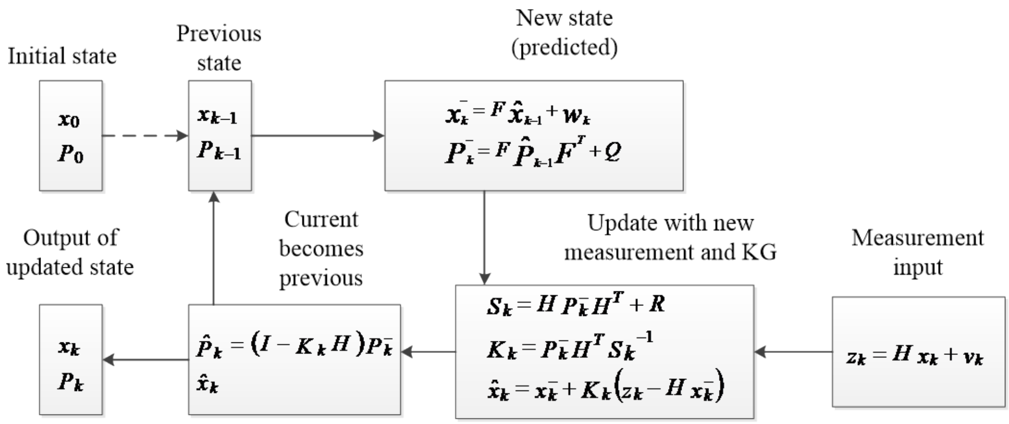

FIG. 1 A complete picture of Kalman filter operations

According to the summarized Bayesian estimating scheme, the Kalman filter consists of two sequentially coupled devices, an extrapolator predicting the state of the object step by step, and a filter specifying the extrapolated meaning based on the new measurement. The extrapolated state vector estimate x_k^- and its covariance P_k^- are based on the previous estimate $\hat{x}_{k-1}$ and its covariance $\hat{P}_{k-1}$.

The matrix elements of Kalman gain **K** reflect the weight of created discrepancy in the resultant state estimation. **K** is in a direct ratio to the covariance of the predicted (current) estimate and in an inverse ratio to the covariance of the discrepancy (measurement). The less accurately the predicted estimate (and greater its covariance), the higher the **K** is, and the larger the weight gives to the measurement. Greater gain means rapid response of the measurement filter (the result is close to measurement), small - slow response (the result is close to the predicted estimate). In a private area, this corresponds to a large and small bandwidth of the filter: the narrower the bandwidth, the better the noise suppress and hence the better the filtration quality, the wider - the chances of tracing the target maneuvers are bigger.

3. INTERACTIVE MULTIPLE MODEL (IMM)

It is a Dynamic MM-algorithm. This type of algorithm gives that the nature of the target movement can change at any moment. Therefore, they choose not one model, true for the entire observation interval, but a sequence of pattern changes from the beginning of observation to the current moment including.

Dynamic MM algorithms appear to be optimal for the system, the real state of which changes uneven into a set identical to the set of models used in them. The law change model is usually applied in Markov or semimarkov processes of the first order, with certain transition probabilities π_{is} [5].

The optimal dynamic MM-algorithm for filtering the mixed random process having its N-model composition to form a result-based estimation of states at that point in time must be computed $l = N^k$ estimations to take into account all possible system implementations over time to *k* including , and also evaluate their probabilities. For this, it is necessary to have N^k operating parallel elementary trajectory filters. Types of first and second order algorithms are usually considered, requiring *N* and N^2 filters respectively. In IMM, each filter is triggered with its value, in which it is taken into account the extent to which the model corresponds to the state in which the system is at a time *k-1*.

Let a system of random structure be described with equations:

$$\begin{aligned} x_k &= F(M_{k-1})x_{k-1} + G(M_{k-1})u_{k-1} + w_k \\ z_k &= H(M_{k-1})x_k + v_k \end{aligned} \tag{2}$$

where u_k - an unknown input vector modeling the target maneuver; w_k - Gaussian process noise; v_k - Gaussian noise of observation; system matrices - **F**, **G**, **H**.

The sequence of states $M_k, M_k \in \{M^s\}_{s=1}^{N}$ used in the system is described by the Markov chain with known transitions probabilities: a system located at time point *k-1* in a state M^i switches to a time point *k* in a state M^s with probability π_{is}. The Markov chain is considered stationary, i.e., the transition probabilities do not depend of the current step *k*.

Let Z_k^{k-1} - a set of ticks from the beginning of observation to the time of *k-1*; z_k - ongoing observation. From the previous step we know the probabilities of finding the system in the *i* state $\mu_{k-1}^i = p\{M_{k-1}^i \mid Z_1^{k-1}\}$, *i = 1, ..., N*, and the estimations $\hat{x}_{k-1}^i$ of the filters with covariance P_{k-1}^i. The task of an IMM algorithm is to calculate the estimate $\hat{x}_k$ and its covariance P_k at time *k*.

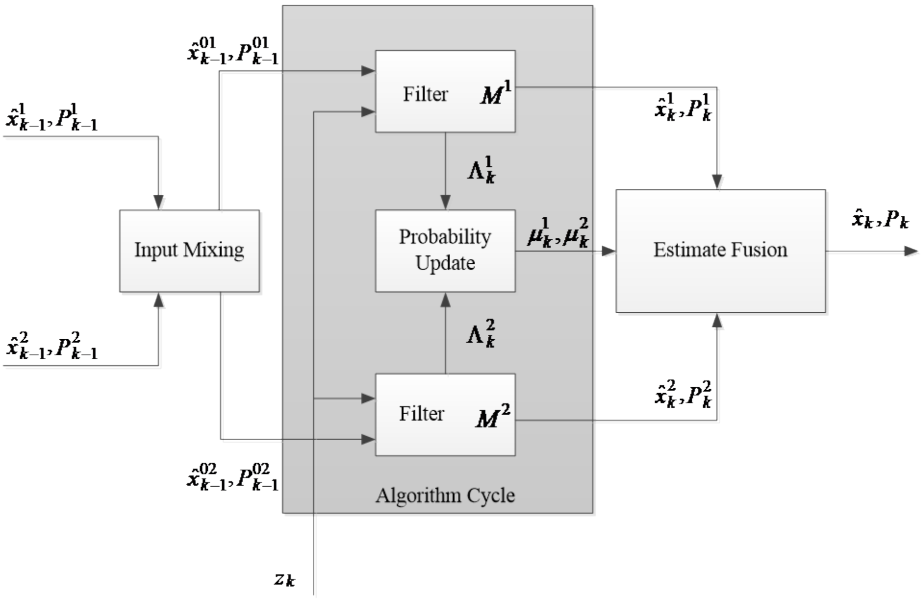

FIG. 2 Flow chart of an IMM algorithm with two models

Fig. 2 shows an IMM structure with two models. An IMM algorithm cycle consists of the following 5 steps [5]:

1) Calculation of the mixing probabilities.
2) Determine the initial conditions of each model filter (mixing estimates).
3) Mode-matched filtering.
4) Mode probability update. Estimation of a posteriori probability for genuineness of the models.
5) Estimate and covariance combination. Calculation of the resultant estimations of the state vector and its covariate matrix.

4. TARGET MOTION MODEL

Constant velocity rectilinear motion

The non-maneuvering motion is a Constant velocity rectilinear motion. The motion equation in this model is the type [5]

$$\mathbf{x}_{k+1} = \mathbf{F}_{CV}\mathbf{x}_k + \mathbf{w}_k \tag{2}$$

where $\mathbf{x} = [x\dot{x}y\dot{y}]^T$ - state vector; $\mathbf{F}_{CV} = \begin{bmatrix} 1 & T_0 & 0 & 0 \\ 0 & 1 & 0 & 0 \\ 0 & 0 & 1 & T_0 \\ 0 & 0 & 0 & 1 \end{bmatrix}$ - prediction matrix (T_0 - the time interval between the measurements $\mathbf{x}_k$ and $\mathbf{x}_{k+1}$); $\mathbf{w}_k$ - random sequence in the form of white Gaussian noise with zero mean and a known covariance matrix $\mathbf{Q} = \begin{bmatrix} \sigma_x^2 & 0 \\ 0 & \sigma_y^2 \end{bmatrix}$, σ_x^2 and σ_x^2 - dispersion of noise at the relevant coordinates, which takes into account the impact of random accelerations due to deviation from the course, wind shifting and other factors.

Since there is some deviation from the straight rectilinear movement in this model, it is sometimes called a motion at almost constant velocity, referred to as CV1.

Maneuvering motion with known constant turn.

The model describes a maneuver in which the target moves at a constant velocity ν to turn at a constant turning velocity ω (CT, Coordinated Turn or Constant Turn). A situation where the target is turning at a constant and known turning velocity occurs when civilian aircrafts are tracked to the areas of the aerodrome where the maneuvers of the aircraft are strictly regulated. The state vector and input matrix of the CT model correspond to the CV model, and the predicted matrix has the type [5]

$$\mathbf{F}_{CT} = \begin{bmatrix} 1 & \frac{\sin \Omega T}{\Omega} & 0 & -\frac{1-\cos \Omega T}{\Omega} \\ 0 & \cos \Omega T & 0 & -\sin \Omega T \\ 0 & \frac{1-\cos \Omega T}{\Omega} & 1 & \frac{\sin \Omega T}{\Omega} \\ 0 & \sin \Omega T & 0 & \cos \Omega T \end{bmatrix}.$$

Dynamic Models of flying Aircraft

Let the target location be counted with a sample period T = 1s.

This target moves in a plane initially at a constant rate and speed to the first k = 50 measurements and then performs a coordinated maneuver in the next 50 sample periods at a constant turning velocity. In the third 50 sample periods, it continues his constant course and in the last 50 samples it carried out a second maneuver at the same constant velocity. Using the constant velocity target motion model given in equation (3), the model with the maneuver in equation (4) and the model of measurement in equation (5) simulates the movement of the target (fig.3, 4) [1,4].

$$\mathrm{x}(\mathrm{k}+1) = \begin{bmatrix} 1 & \mathrm{T} & 0 & 0 \\ 0 & 1 & 0 & 0 \\ 0 & 0 & 1 & \mathrm{T} \\ 0 & 0 & 0 & 1 \end{bmatrix} x(k) + \begin{bmatrix} \frac{1}{2}T^2 & 0 \\ T & 0 \\ 0 & \frac{1}{2}T^2 \\ 0 & T \end{bmatrix} w(k) \tag{3}$$

$$x(k+1) = \begin{bmatrix} 1 & \frac{\sin \Omega T}{\Omega} & 0 & -\frac{1-\cos \Omega T}{\Omega} \\ 0 & \cos \Omega T & 0 & -\sin \Omega T \\ 0 & \frac{1-\cos \Omega T}{\Omega} & 1 & \frac{\sin \Omega T}{\Omega} \\ 0 & \sin \Omega T & 0 & \cos \Omega T \end{bmatrix} x(k) + \begin{bmatrix} \frac{1}{2}T^2 & 0 \\ T & 0 \\ 0 & \frac{1}{2}T^2 \\ 0 & T \end{bmatrix} w(k) \tag{4}$$

$$z(k) = \begin{bmatrix} 1 & 0 & 0 & 0 \\ 0 & 0 & 1 & 0 \end{bmatrix} x(k) + v(k) \tag{5}$$

In equations (3) and (4) $w(k)$ is a zero-mean white Gaussian noise with covariance

$\Sigma_w = \begin{bmatrix} \sigma^2 & 0 \\ 0 & \sigma^2 \end{bmatrix}$ and $\sigma^2 = 10^{-3}$

In equation (5), $v(k)$ is a zero-mean white Gaussian noise with covariance $\Sigma_v = \begin{bmatrix} \sigma_v^2 & 0 \\ 0 & \sigma_v^2 \end{bmatrix}$ with $\sigma_v^2 = 10^{-3}$

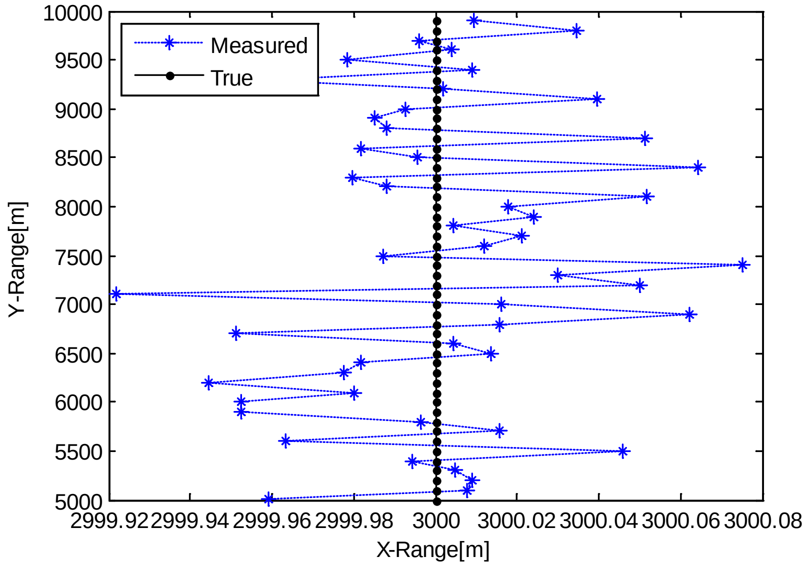

FIG. 3 Target trajectory in the first 50 samples

In Fig. 3 we observe the measured noise of the measurement with blue. Since the target in this section of its trajectory is not shifted to the coordinate x, this noise can be seen how it fluctuates in very small values. In Fig. 4, however, the noise cannot be seen despite its existence, as the entire trajectory of the target is observed, where its x and y coordinate displacements are considerably larger than the noise values.

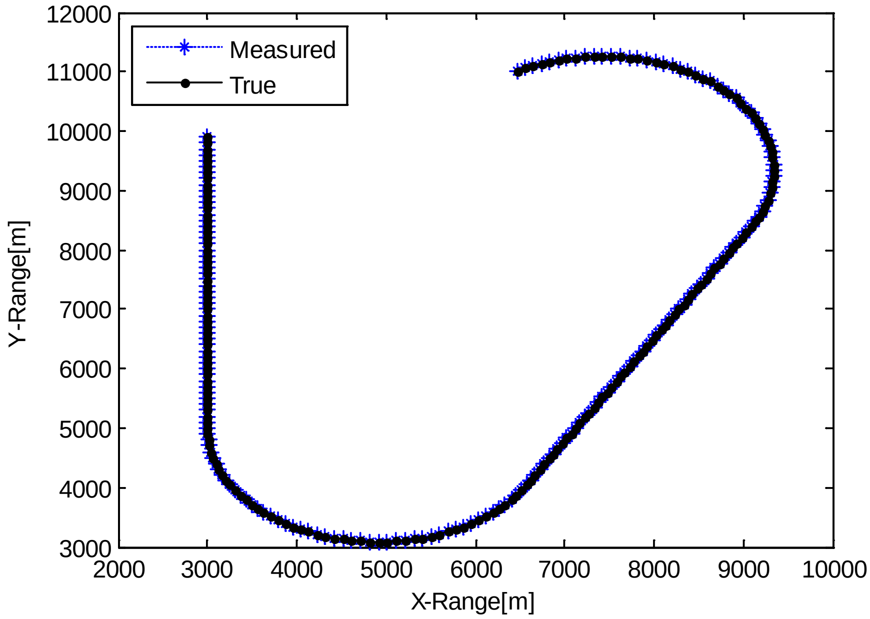

FIG. 4 Target trajectory for the entire 200 sample periods

5. RESULTS OF THE EXPERIMENT.

Kalman filter

Two Kalman filters have been modeled. In one for transition matrix, reflecting the relationship of the previous and last meaning of x, is used $\mathbf{F}_{CV}$, and in the other matrix $\mathbf{F}_{CT}$.

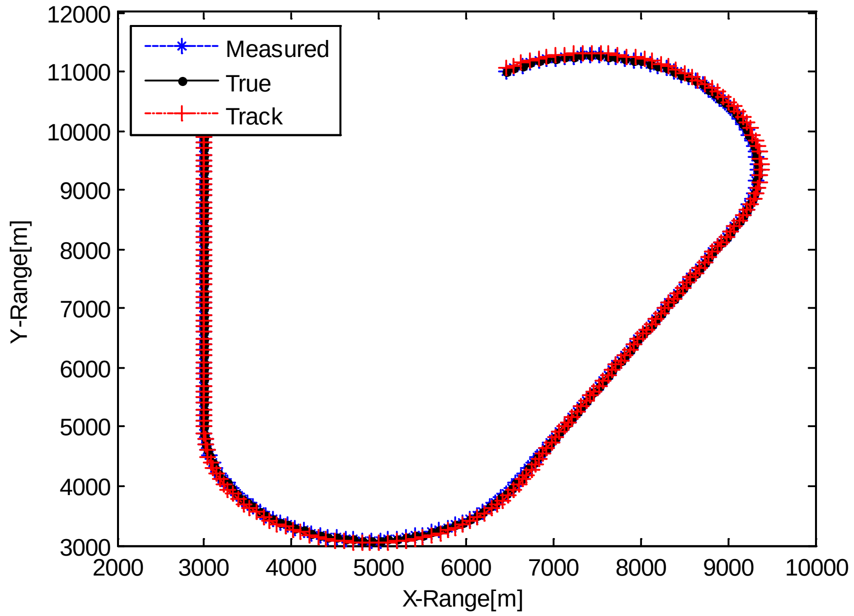

FIG. 5 Tracking with KF in the first model

The first Kalman filter tracks the course at a constant velocity (Fig. 5), the calculated error is insignificant, but when it tracks the maneuver, the calculated error becomes tangible - about 40 meters (Fig. 6).

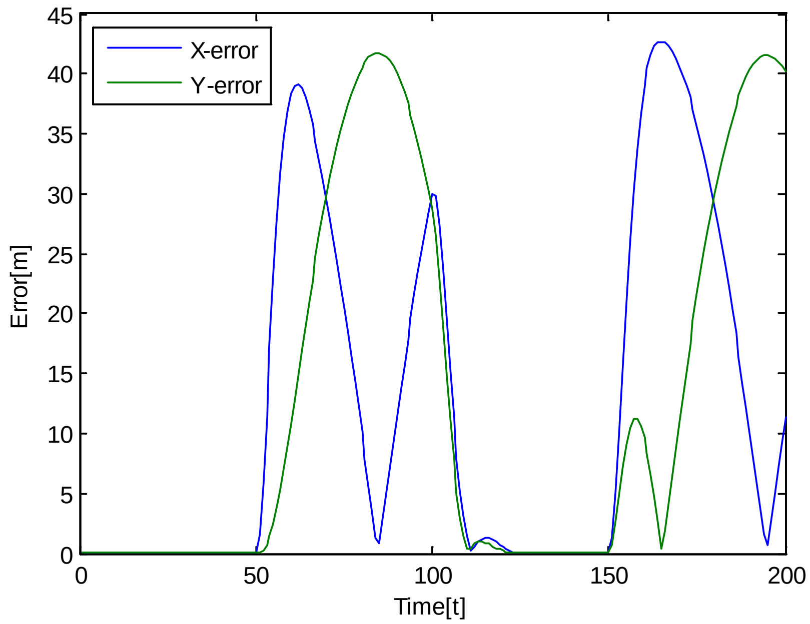

FIG. 6 Estimating of the error in the first model.

On the opposite, the second Kalman filter can accurately track the maneuver (Fig.7), but the estimated error at constant velocity is greater (Fig.8).

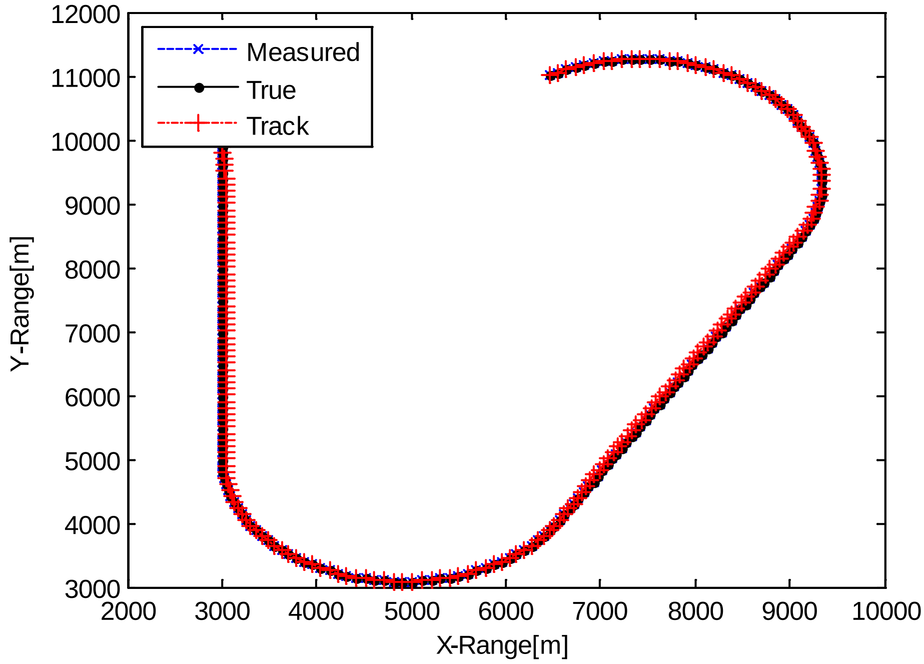

FIG. 7 Tracking with KF in the second model.

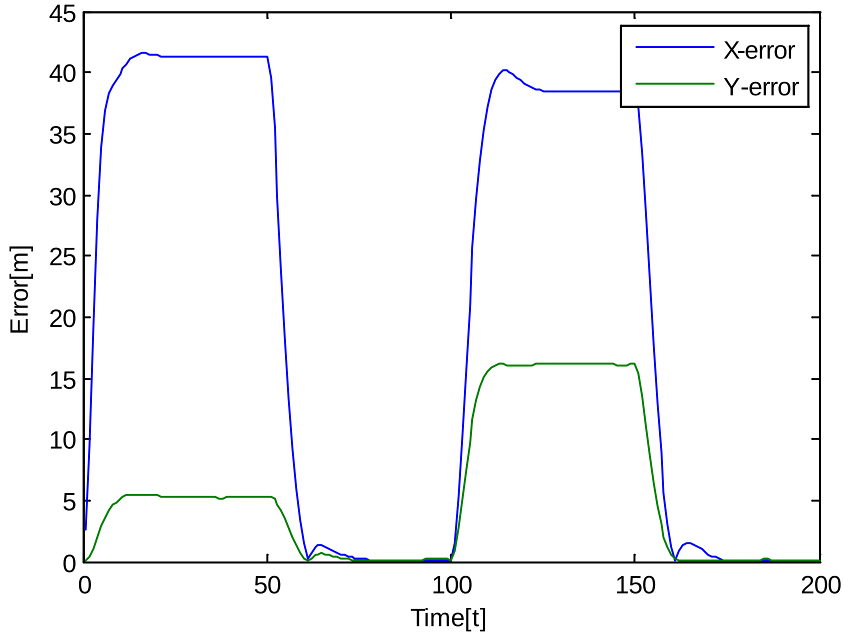

FIG. 8 Estimation of the error in the second model.

Interactive Multiple Model

In this algorithm, there are two models of elemental trajectory filters. The sequence of patterns used in the system is described with a Markov chain with known transition probabilities through the following transition matrix: $\left[\pi_{ij}\right] = \begin{bmatrix} 0.95 & 0.05 \\ 0.05 & 0.95 \end{bmatrix}$ [4]. The tracking results are very accurate to the real target movement (Fig.9).

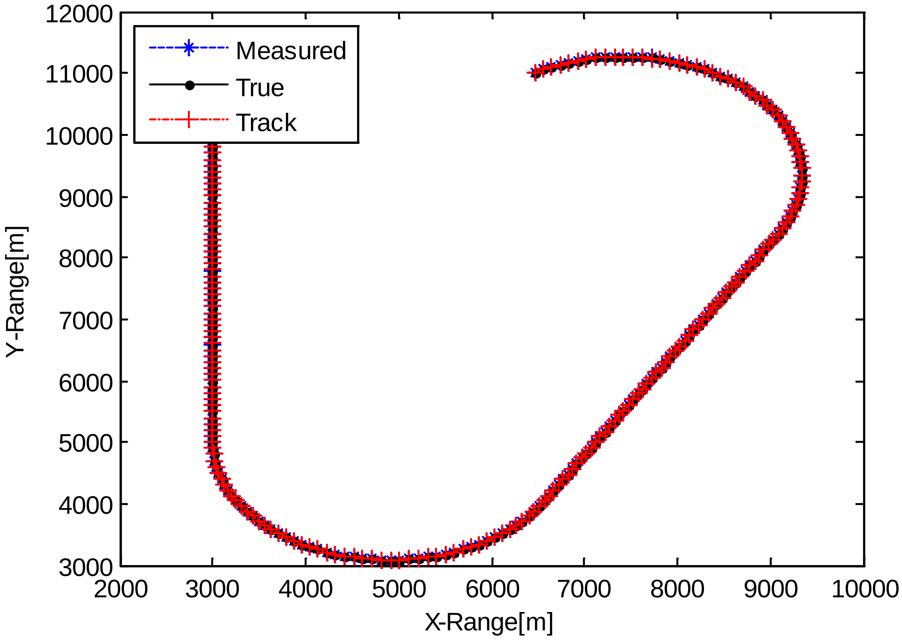

FIG. 9 Tracking with an IMM algorithm

In Fig. 10 shows that the error of the IMM algorithm is less than 0.25 m throughout the entire tracking process.

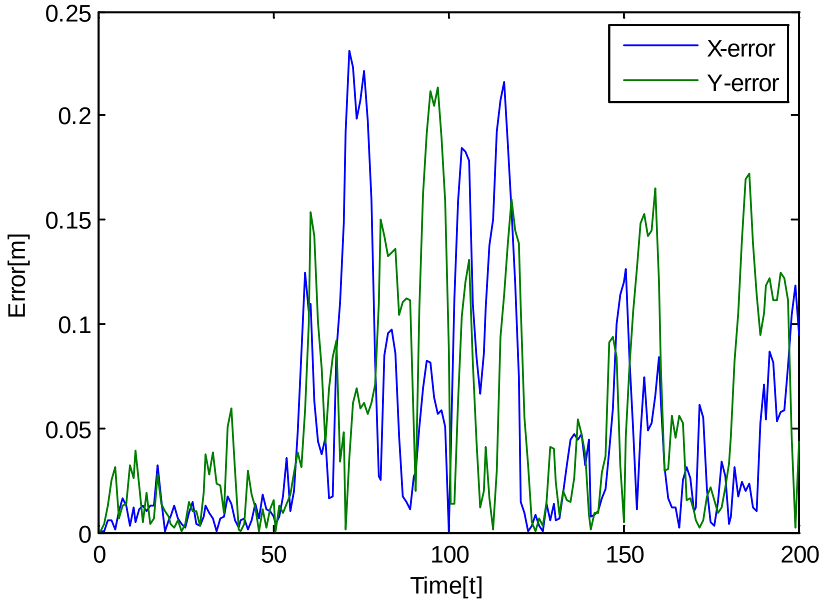

FIG. 10 Estimation of the tracking error with the IMM algorithm.

CONCLUSION

This paper presents two filters through which the target trajectory models are passed. One is a linear Kalman filter, and the other is an Interactive Multiple Model (IMM) algorithm. The results of the experiments show that the performance of the IMM algorithm during target tracking is better than the Kalman filter.

With the simulated input parameters, the Kalman filter tracing errors exceed those of the IMM algorithm up to 40 times. It is precisely the robustness and rapid response to the target maneuver that necessitated the widespread use of the Interactive Multiple Model Estimator.

REFERENCES

[1] D. Dimitrov and M. Kirov, *Using multi-carrier probing signals for detecting non-linear objects*, AFAHC 2016, DOI: 10.19062/2247-3173.2016.18.1.33,
http://www.afahc.ro/ro/afases/2016/ELECTRO/DIMITROV_KIROV.pdf

[2] G. Welch and G. Bishop, *An Introduction to the Kalman Filter*, UNC-Chapel Hill, TR 95-041, July 24, 2006;

[3] S.S. Jan and Y.C. Kao, *Radar Tracking with an Interacting Multiple Model and Probabilistic Data Association Filter for Civil Aviation Applications*, Sensors 2013, vol. 13, pp. 6636-6650, doi:10.3390/s130506636;

[4] Y. Bar-Shalom, X.R. Li and T. Kirubarajan, *Estimation with Applications to Tracking and Navigation*, John Wiley & Sons: New York, NY, USA, 2001; pp. 466–476.

[5] А. А. Коновалов, *Основы Траекторной Обработки Радиолокационной Информации – Част 2,* Издательство СПбГЭТУ „ ЛЭТИ “, Санкт-Петербург, 2014.

REFLECTIONS OF ILLUSTRATED POSTCARDS IN THE PROMOTION OF ROMANIAN MINING ACTIVITIES

Bogdan CIORUȚA[*], Mirela COMAN[**], Alexandru Leonard POP[*]

[*]Technical University of Cluj-Napoca - North University Centre of Baia Mare, Office of Informatics & Communications, Romania (bogdan.cioruta@staff.utcluj.ro, alexandru.pop@staff.utcluj.ro)
[**]Technical University of Cluj-Napoca - North University Centre of Baia Mare, Faculty of Engineering, Romania (comanmirela2000@yahoo.com)

DOI: 10.19062/2247-3173.2019.21.14

Abstract: *The natural heritage is defined and accepted as the set of physico-geographic and biocenotic (floristic, faunistic) components and structures of the natural environment, whose ecological, economic, scientific, biogenic, sanogenic, landscape, recreational and cultural-historic significance and value has a relevant significance for present and future generations. Constantly promoting philatelic themes that address the natural beauties and richness of our country, the post office issuing entity performs a series of postage stamps in whose pictures Romanian sceneries of rarity. In this paper we propose an insight into the history of philately and bring into discussion the significant concerns in promoting Romanian mining activities, by presenting stamps and illustrated postcards, from the beginning of Romanian philatelic time.*

Keywords: *natural heritage, Romanian mining activities, philatelic appearances, postcards.*

1. INTRODUCTION

Philately can be defined as the activity of collecting and studying philatelic products, especially stamps. However, philately signifies more than a concern for beauty; challenge, information, education, friendship and fun are some of the characteristics of one of the most popular hobbies in the world [4].

Today, after over 160 years of philately in Romania [4], our preoccupations for this extremely vast field is to study not only of the postage stamps of various kinds and types, but also other categories of philatelic - postage envelopes (first day covers/envelopes, homage envelopes, postcards, postcards and maximum postcards etc), summarize and focus on everything intimate to mining activities.

By constantly promoting philatelic themes that deal with the natural beauties and richness of our country [3], the administrative entity responsible for issuing philatelic-postal items produces a series of issues in which images of the mining activity are found, especially miners.

Starting from the idea that Romania is, especially from the point of view of the natural heritage, a place blessed with extremely well-rounded biodiversity and geodiversity, of a rare beauty [3], we chose to present a series of philatelic-postal issues that come to refine the individual's need for aesthetics and cultural-educational development. At the same time, during the study we tried to emphasize the cultural importance of philately in society and we try to give the public a part of the forgotten history of mining in Romania, which has been the basis of the national economy for a good time.

2. MATERIAL AND METHODS

The working methodology for this study comes as an accessible concern from all points of view of the current generation. As with the practice of philately, no special, long-term training is required, as in the present study, no innovative methodology, expensive equipment and / or instruments is required, but creativity is needed for the conduct of research, stamp. Objectively speaking, beyond the passion of the authors for philately - as satisfaction for the aesthetic need and as a cultural-educational development [3], the working methodology consisted in identifying, indexing and describing the main philatelic pieces issued in Romania (postal stamps, FDCs, occasional envelopes, maxicards), which in the meantime remain to promote Romanian mining activities.

In our research period both author collections and international open-source philatelic databases have been thoroughly consulted, including Delcampe (*www.delcampe.net*), Colnect (*colnect.com*), StampWorld (*www. stampworld.com*), PicClick (*picclick.com*) and RomaniaStamps (*www.romaniastamps.com*) as well as specialized international philatelic catalogs: Yvert (Yv), Michael (Mi), Gibson (G) and Scott (S) [9].

The above mentioned bibliographic resources added, for the fullness of the study, a series of specialized catalogs on philatelic errors, curiosities and varieties [1, 2] as well as an important series of Romanian specialty papers with general character on Romanian postal stamps, which offer valuable information and authenticity to clarify the following parameters: *date of issue* [1, 2, 5-8], *layout and indexing of the pieces* [1, 2, 5-7], respectively *their description* (name, format, lace etc) [5-10].

At the same time, the open-source philatelic content platforms, especially the discussion forums, have been of great use, where, as a result of the online meetings of philately enthusiasts, valuable information has been found that guarantees the correctness of the data presented in this study.

3. ROMANIAN MINING EXPLOITATIONS REFLECTED IN PHILATELY

Although it may seem slightly exaggerated, the involvement and reflection of philately in promoting the intrinsic values of mining activity in Romania is felt, for the first time, in the period preceding the 1950s, when a series of postage stamps appear to celebrate the "Labor Day" later, "Miner's Day".

In the 1950-1954 period, when the first carto-philatelic and maxifilatelic parts appeared, as a laudation for the exploration and exploitation of minerals [6, 7], we identified a series of issues that were not neglected.

(a)

(b)

FIG. 1. Variations and editions of the "Mining Day", 21.08.1951 (LP #285)
(a) first day envelope, 12.08.1951, București;
(b) ocazional envelope - „Filatelic Exhibition”, 07-17.11.1951, Baia Mare

Thus, the oldest identified piece, which opens the way for philately to promote mining is the "Day of the Miner", which appeared in the form of "first day cover" (FDC) on 12.08.1951, under the Ministry of Postal and Telecommunications - the Philatelic Office in Bucharest (see Fig. 1a) [11, 12]. Some sources, however, mention the date of issue is on August the 21st, 1951 [2, 6-8, 10].

The graphic theme of this envelope was used in the making of a homage envelope on the occasion of the philatelic exhibition from 07-17.11.1951 which took place in Baia Mare. In this sense, the color of the printing ink, as well as the legend accompanying the image (see Fig. 1b), was changed [13].

The second piece on which we stopped is also entitled "Miner's Day", Fig. 2b, appeared on August 11th, 1952, but stamped on August 10th, 1952 and franked by the stamps of the "Mining Day" show of 15.08.1952 (LP #328) [14-17]. The FDC presents itself as a 9×16.5 cm white envelope and a black drawing that reproduces the 20-pound stamp (RO #1570) of the show, which, along with the 55 bani, comes stamped with the "miner badge" and circulated in more than 1,400 pieces [7].

(a) (b) (c)

FIG. 2. Variations and editions of the "Mining Day", 11.08.1952 (LP #328)
(a) maximal postal card - „Filatelic Exhibition”, 06-20.11.1952, Baia Mare;
(b) first day cover (FDC), 10.08.1952, București;
(c) occasional envelope - „Mining Day”, 24.10.1952, Tg. Mureș

The stamps, laced, indexed by Yv #1274...5, Mi #1402...3, G #2258...9 and S #902...3, are 28×33 mm in size. They were painted by N. Popescu, in a very generous circulation (1,000,000 series), in finished sheets of 100 pieces.

The graphic representation of the FDC reproduces the stamp model with a face value of 20 bani [14, 15]. Along with the aforementioned FDC, in our searches we identified a series of movements that were not neglected. Thus, in Fig. 2a we have a maximum postcard made on the occasion of the philatelic exhibition in Baia Mare that took place between 06-20.11.1952. In the illustration of the postal support we can find the miner statue and the building of the Baia Mare Technical School. The circulation of this edition, comprising both the stamps of the show, was 500 copies [18]. In Fig. 2c we present a circulated occasional envelope.

The 1955-1959 period is poor in graphical representations to propagate various mining activities or riches of the Earth. However, in the relatively extended research framework we have identified a circulation that we consider to be interesting (Fig. 3a) [19] and, of course, a series of errors and varieties thereof (Fig. 3b-d) [1, 2, 21-23] for the postage stamp "a miner" (RO #1673) [20] of the usual "Activities" (LP #381) issue dated 29.03.1955.

(a)

(b)

(c)

(d)

FIG. 3. Variations editions of postage stamps for "miner" (RO #1673)
(a) postal service postmark bearing the "miner" (RO #1673), 30.12.1960, Bucharest;
(b) UFO in front of the stamp; (c) white vertical stripe over the nose;
(d) UFO (interruption) at the neck level

In addition to the pieces already presented, for the years 1960-1975 a number of postcards were also identified - see Fig. 4 [24, 25], Fig. 5 [26-30] and Fig. 6 [31-35], about which are little known, although they have facilitated the promotion of Romanian mining.

(a)

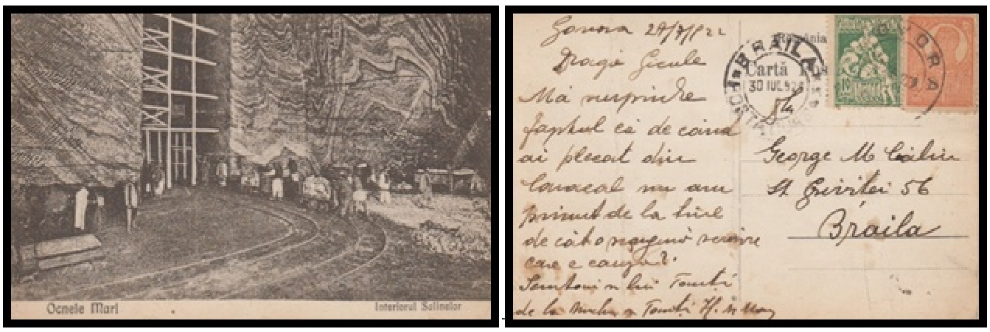

(b)

FIG. 4. Illustrated postcards circulated during the 1960-1975 (I)
(a) "Entry into the mine" Salina Tg. Ocna; (b) "Entry into the mine", Salina Ocnele Mari (Vâlcea).

(a)

(b)

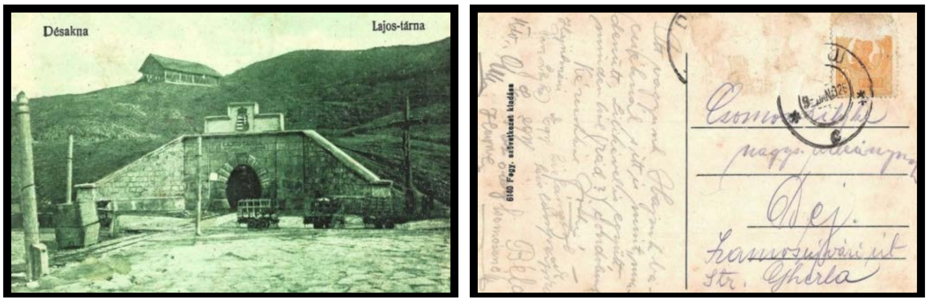

(c)

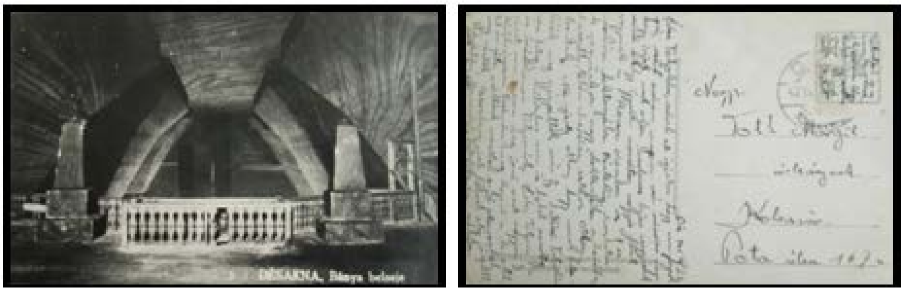

(d)

(e)

FIG. 5. Illustrated postcards circulated during the 1960-1975 (II)
(a) "Entry into the mine" Salina Dej; (b) "Entry into the mine", Baia Mare;
(c)-(e) "Entry into the mine" and "Salt exploitation", Dej

(a) (b) (c) (d) (e)

FIG. 6. Illustrated postcards circulated during the 1960-1975 (III)
(a)-(b) "Salt exploitation", Slănic-Prahova; (c) "View for exploitation", Baia Sprie;
(d) "View for exploitation", Aninoasa; (e) "View for exploitation", Slănic-Prahova

On the opposite side, while retaining the emphasis on promoting Romanian mining by presenting the main exploits of the time, there are the uncirculated postcards that we present synthetically, without verso, in Fig. 7 [36-42].

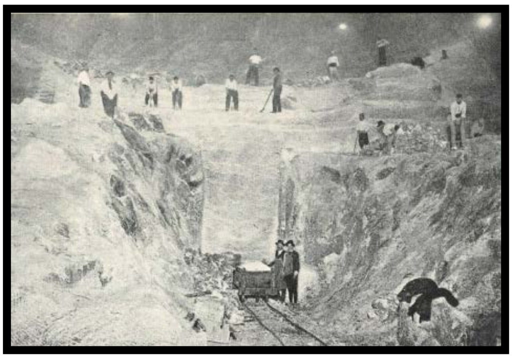

(a)

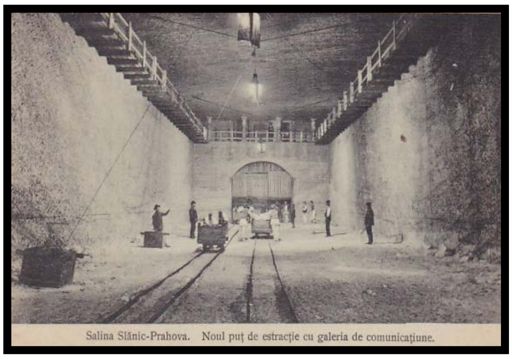

(b)

(c)

(d)

(e)

(f)

(g)

FIG. 7. Illustrated postcards non-circulated from the 1960-1975
(a) "Transport of exploited salt", Ocna Dej; (b) "Transport of exploited salt", Slănic-Prahova;
(c)-(d) "Entry into the mine", Baia Mare; (e) "View to the exploitation facilities", Reșița;
(f) "View towards exploitation", Petroșani; (g) "Miner working", Petroșani

4. CONCLUSIONS

By publishing this study we hope that we will make available to all those interested a useful tool of information, education and philatelic orientation in what was the mining activity in Romania over time. We would like the work to be the first light to guide through the intricate philatelic galleries of Romanian mining.

Also, to somewhat revive the sober style, proper corrections and catalogs, and of course to remove the monotony specific to a purely philatelic study, we sought to present the material in the form of not so analytical, but descriptive notes.

This study is mainly addressed to passionate philatelists, but can also be of interest to other professional categories that can develop similar studies. It can be highlighted once again that philately by its stamps and postcards has a special beauty - is capable of being a true embassy of culture and a post of human mining history passage.

REFERENCES

[1] S. Găbureac, *România - erori filatelice 1903-2006* (catalog specializat ilustrat), Ed. Biblioteca Bucureştilor, Bucureşti, 2008;

[2] S. Găbureac, *România - curiozităţi şi varietăţi filatelice 1903-2006* (catalog specializat semiilustrat), Ed. Biblioteca Bucureştilor, Bucureşti, 2010;

[3] M. Mesaroş, B. Cioruţa, M. Coman, *Protected natural heritage on route from philosophy to environment engineering*, Scientific Bulletin of North University Center of Baia Mare, Series D, Mining, Mineral Processing, Non-ferrous Metallurgy, Geology and Environmental Engineering, Baia Mare, vol. XXXII, no. 1, pg. 63-72, 2018;

[4] A.L. Pop, B. Cioruţa, M. Coman, *Considerations regarding the implications of philately in ecological education*, Scientific Bulletin of North University Center of Baia Mare, Series D, Mining, Mineral Processing, Non-ferrous Metallurgy, Geology and Environmental Engineering, Baia Mare, volume XXXI, no. 1, pg. 57-62, 2017;

[5] C. Scăiceanu, *Catalogul machetatorilor mărcilor poştale româneşti*, Ed. Oscar Print, BucureştiSpineanu C. (1984) *Catalogul mărcilor poştale româneşti 1948-1984*, vol. II, Direcţia Generală a Poştelor şi Telecomunicaţiilor, Bucureşti, 2018;

[6] Gh. Tudor, C. Chiricheş, Gh. Mermeze, *Catalogul mărcilor poştale româneşti 1858-1989 (LP 1-1233),* Editura AXA, Bucureşti, 2017;

[7] ***, *Catalog filatelic oficial al timbrelor R.P. Române*, 1954;

[8] ***, *Catalogul expoziţiei filatelice „Ziua mărcii poştale româneşti”*, 1987, Bucureşti;

[9] ***, *Standard Postage Stamp Catalogue*, Scott Publishing Co., vol. 5, 2008;

[10] ***, *Zumstein Briefmarken-Katalog*, Band 4: Europa-OST, 1984;

[11] ***, www.delcampe.net/.../miners-day-mining-minerals-special-cover-1951.html;

[12] ***, picclick.com/Romania-1951-Miner-DayMineMining/.../Bergarbeiterrare-FDC.html;

[13] ***, picclick.com/1951-MinerMiners-DayMineMining/.../Stamp-Expo-CDS-cover.html;

[14] ***, www.delcampe.net/.../minerals-miners-day-special-cover-1952-romania.html;

[15] ***, picclick.com/1952-Miner-Day/.../RomaniaMi1402FDC.html;

[16] ***, www.stampworld.com/stamps/Romania/Postage-stamps/g1406;

[17] ***, colnect.com/ro/stamps/.../Day_of_Miners/year/1952;

[18] ***, www.delcampe.net/.../miners-commemorative-monument-mine-cachet.html;

[19] ***, www.ebay.co.uk/itm/Romania-Cravata-Rosie-Pioneer-Press-30-12-1960-Registered-Cover-Abroad-to-USSR/352625239160;

[20] ***, colnect.com/ro/stamps/list/country/2668-Romania/theme/126-Mineri/year/1955;

[21] ***, picclick.com/1955-MinerBergmannMineurDefinitivesRomaniaMi1503VFUPrint-variety-Error-192752188876.html;

[22] ***, picclick.com/1955-MinerBergmannMineurMinatoreDefinitivesRomania1503 Variety-Error-2MNH.html;

[23] ***, picclick.com/1955-MinerBergmannMineurDefinitivesRomaniaMi1503variety-ErrorVFU.html;

[24] ***, www.delcampe.net/fr/collections/cartes-postales/roumanie/romania-rumanien-roumanie-bacau-targu-ocna-intrarea-in-tunelul-minei-mining-salt-mines.html;

[25] ***, www.delcampe.net/fr/collections/cartes-postales/roumanie/romania-rumanien-roumanei-valcea-ocnele-mari-salt-mining-428977972.html;

[26] ***, www.delcampe.net/fr/collections/cartes-postales/roumanie/romania-ocna-dejului-salt-mining-380937194.html;
[27] ***, www.delcampe.net/fr/collections/cartes-postales/roumanie/romania-baia-mare-dealul-crucii-gold-mine-230173081.html;
[28] ***, https://picclick.co.uk/Romania-Transylvania-1926-Ocna-Dejului-D%C3%A9saknaSalt-Mineentrance-coaches-302250852498.html;
[29] ***, https://picclick.co.uk/Romania-Ocna-Dejului-Desakna-Cluj-Transylvania-salt-mine-333107817479.html;
[30] ***, https://picclick.co.uk/Romania-Transilvania-Ocna-Dej-Mine-Salt.html;
[31] ***, https://picclick.co.uk/b78612-salina-slanic-prahova-taierea-sarei-salt-mine.html;
[32] ***, https://picclick.co.uk/Romania-SLANIC-Extractia-sarei-din-mine.html;
[33] ***, www.delcampe.net/fr/collections/cartes-postales/roumanie/romania-baia-sprie-gold-mining-industry-jud-maramures-319474200.html;
[34] ***, www.delcampe.net/fr/collections/cartes-postales/roumanie/aninoasa-mining-tools-vedere-view-1960-postcard-romania-326219344.html;
[35] ***, https://picclick.co.uk/b78502-stanci-de-sare-de-la-slanic-prahova.html;
[36] ***, https://picclick.co.uk/Romania-Ocna-Dejului-Desakna-Cluj-Transylvania-salt-mine-333123059995.html;
[37] ***, www.delcampe.net/fr/collections/cartes-postales/roumanie/romania-slanic-prahova-salt-mining-323988341.html;
[38] ***, www.delcampe.net/fr/collections/cartes-postales/roumanie/romania-baia-mare-gold-mining-mina-valea-rosie-369564607.html;
[39] ***, www.delcampe.net/fr/collections/cartes-postales/roumanie/romania-baia-mare-gold-mining-36313483.html;
[40] ***, https://picclick.co.uk/ROMANIA-mining-industry-Resita-1930s-factory-general-view-333107817388.html;
[41] ***, https://picclick.co.uk/Roumanie-Romania-Petrosani-Mines-De-Charbon-Petite-Image-121867657900.html;
[42] ***, www.delcampe.net/fr/collections/cartes-postales/photographie/romania-mining-press-photo-322645197.html.

INFLUENCE OF AUTOMATION OF AIRSPACE ACTIVITIES ON AIR TRAFFIC SAFETY

Ionică CÎRCIU, Vasile PRISACARIU

"Henri Coanda" Air Force Academy, Braşov, Romania
(circiuionica@yahoo.co.uk,aerosavelli73@yahoo.com)

DOI: 10.19062/2247-3173.2019.21.15

Abstract: *The Traffic Avoidance and Collision Alert System is a system that reduces the risk of airplane crashes in the air. The system operates independently of the Air Traffic Service and has the role of informing and recommending maneuvers when approaching another aircraft. It monitors airspace around an aircraft for other aircraft equipped with an active transponder independent of air traffic control, and alerts pilots to the presence of other transponder-equipped aircraft that may present an air collision hazard.*

Keywords: *flight safety, TCAS, UAV, sensors*

Acronyms

TCAS	Traffic Avoidance and Collision Avoidance System	TA	Traffic Advisory
GCS	Ground Control System/Station	RA	Resolution Advisory
ADS-B	Automatic Dependent Surveillance-Broadcast	RPA	Remotely Piloted Aircraft

1.THEORETICAL CONSIDERATIONS

Increasing flight safety is based on the automation of the flight with the modernization of the instrument instruments and their correlation with a secondary radar-based system that allows the determination of the future positions of the aircraft, Fig.1.

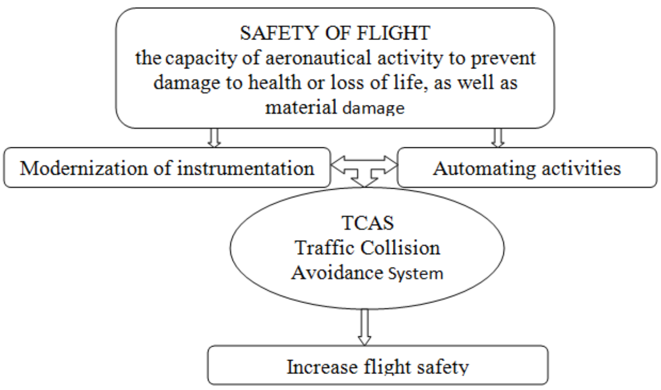

FIG. 1. A flight safety chart

The problem of detecting and avoiding fixed and mobile obstacles involves two distinct approaches: avoiding increased air traffic and avoiding collisions [1].

These aspects involve the use of in-flight technology technologies with acquisition, integration, processing and execution functions. The Traffic Avoidance and Collision Avoidance System (TCAS) is a system that reduces the risk of aircraft crashing in the air [2, 3].

TCAS operates independently from the Air Traffic Service and has the role of informing and recommending crew maneuvers in the event of another airline approaching. It should be noted that the system can not provide any protection against an aircraft that does not have an integrated transponder. After the presented models the TCAS has the components, (Fig.2).

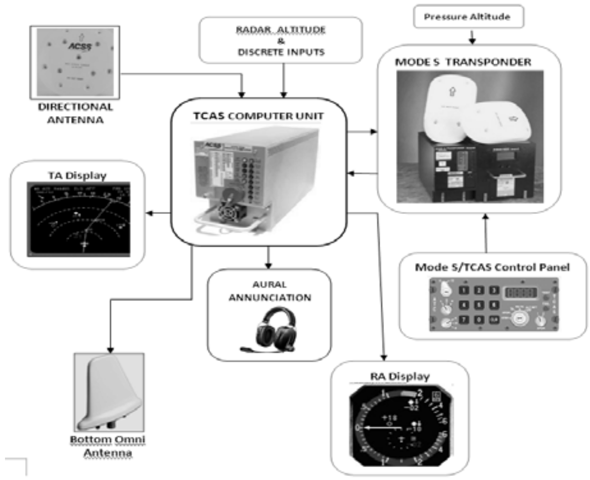

FIG.2. Simplified block scheme of the TCAS system [1].

To determine the distance and altitude, the air vectors identifies itself in a Cartesian coordinate system.

$$(D_n)_t=\left[(D_n)_{x,t};(D_n)_{y,t};(D)_{a,t}\right]^T \tag{1}$$

3D position equation for the airship n and

$$(J_n)_t=\left[(J_n)_{x,t};(J_n)_{y,t};(J_n)_{a,t}\right]^T \tag{2}$$

The 3D express of the speeds, where *x*, *y* represent the horizontal system of the axes and a represents the altitude.

The notion of perpendicularity of two air vectors in the plane.

Two functions α_1 and α_2, defined on an interval (u,v) into r are said to be orthogonal if :

$$\int_u^v \alpha 1(x) \bullet \alpha_2 (x)\, dx = 0,\ \ \alpha_1 \neq \alpha_2 \tag{3}$$

$$\int_u^v \alpha 1(x) \bullet \alpha_2 (x)\, dx \neq 0,\ \ \alpha_1 = \alpha_2 \tag{3'}$$

A set of real, valued functions – $\{\alpha_1(x),\ \alpha_2(x)\ \ldots\ \alpha_n(x)\}$ is said to be orthonormal if:

$$\int_u^v \alpha_m(x) \bullet \alpha_n (x)\, dx = 0,\ \ m \neq n \tag{4}$$

$$\int_u^v \alpha_m(x) \bullet \alpha_n (x)\, dx \neq 0,\ \ m = n \tag{4'}$$

We have two types of alerts:

Traffic Advisory (TA), which is designed to assist the pilot in identifying the intrusive aircraft, and in announcing it to be ready for a potential Resolution Advisory (RA). Resolution Advisory (RA), which are maneuvers recommended to the pilot. When the intruder is also equipped with a warning system, both warning systems coordinate their RAs via the transponder Mode S data link to select complementary solutions, (fig.3), [2, 3, 4].

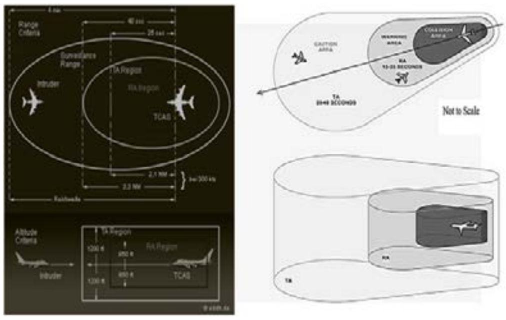

FIG.3. Protection zones between 5,000 and 10,000 feet [3, 4].

We have a fairly rapid growth lately, regarding the use of aerial vectors without flying on board by human factor (UAV). At present, UAVs are equipped with sens and avoid systems for detecting and resolving air traffic conflicts, see figure 4, [4, 5].

FIG.4. UAV with sense and avoid detection system, [6, 7]

For the speed and accuracy of the detection process, these systems are equipped with a series of sensors that can retrieve information from both the proximity of the air vector and the area of interest, such as minimum values for: EO sensors (Opto Electronics) with 5 -8 miles; radar at 5 miles; ADS-B (Air Data System) for air traffic surveillance over a 15-mile radius, see Figure 5, [6].

The conflict resolution procedure includes both maneuvers of command and control from the GCS (Ground Control System) initiated by the human operator (based on maneuvers indicated by the system) and on automatic emergency mode when the direct link has interruptions or delays.

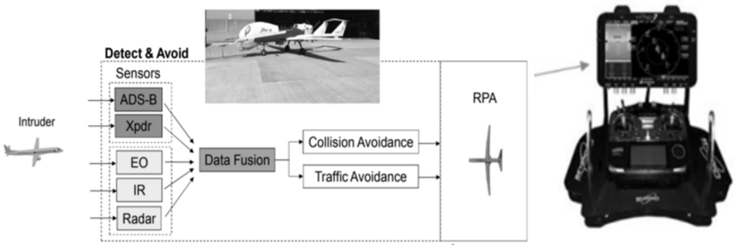

FIG.5. Sense and avoid system operating diagram [7].

2. AVOIDANCE SENSOR SYSTEM

Radar is a sensor used to detect aircraft; it can be a reasonable choice for detecting intruders [10, 11] with the ability to detect all objects. Although new technologies have caused radar size reduction, gauge, mass and power consumption constraints require a number of hardware performance restrictions that lead to significant compromises on antenna precision and field of view available, so this type of detection is suitable for UAS with dimensions similar to those piloted, [12].

Optical sensors (EO) can be used on UASs, they do not require cooperative communication from intruder aircraft, and however the tests have revealed a low detection accuracy (bad weather conditions) that does not provide time for avoidance manoeuvres speed, [13].

IR sensors have the advantage of night-time use but, as with EO sensors, the level of detection is compromised by signal degradation due to weather conditions and LIDAR sensors provide accurate system size data that does not offer the ability to use on small UAVs.

Automatic Dependent Surveillance-Broadcast (ADS-B) is a co-operation sensor that can be an option for small UASs, the information of this system is not affected by weather conditions and the on-directional antennas used have low power requirements. The disadvantage of ADS-B is dependence on the degree of airspace GPS coverage (compromised information in valleys and urban areas), see Figure 6.

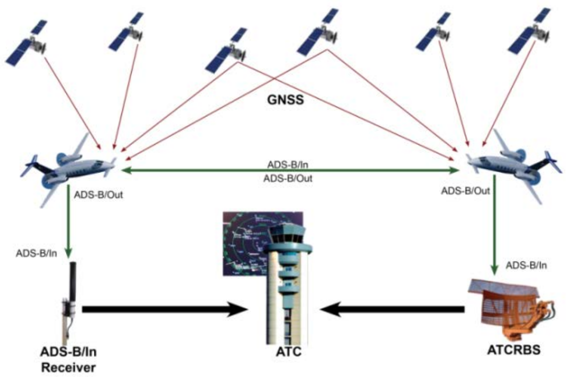

FIG.6. ADS-B transmission, [14]

A series of ADS-B-based collision avoidance studies have demonstrated its capacity to transmit up to 20nm to small-scale, commercial-grade systems [15, 16, 17].

TCAS and ACAS X are aircraft collision avoidance systems based on secondary surveillance radar transponders to provide proximity traffic pilot information and potential conflicts by querying aircraft equipped with transponders (aircraft identification and altitude data).

3.COLLISION AVOIDANCE SYSTEM

Our proposal is that: the air vector equipped with such a system monitors the air traffic within the sensing range of the sensors in order to prevent collisions, so that in order to have time for the avoidance process a threshold of avoidance is defined, the avoidance process contains a series of actions that allow acquisition of surveillance data, estimation of current and future status, detection of possible risks and finding an optimal avoidance maneuver, see Figure 6, [8].

Traffic detection and tracking involves activating detection, tracking, monitoring and fusing functions and verifying data from sensors.

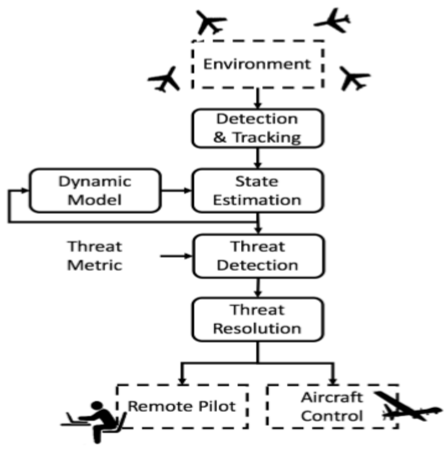

FIG.6. Steps of operation of the collision avoidance system

Current status evaluation consists of a process of estimating a set of variables describing the current situation in terms of the presence of an intruder or group of intruders in their own volume of maneuver. For example, TCAS is based on an estimate of time to the closest approach point and relative altitude up to vector to threat.

Future status evaluation allows estimation of own kinetics and intruder by response patterns that include optimal avoidance trajectories.

The threat assessment may depend on the value of the vector-intrusive distance, the maneuvering speed, the time to the closest approach point, and the time until the collision volume is violated (horizontal or horizontal and vertical values can be considered), so assessing the threat of and TCAS includes a series of actions in time and space under multiple conditions that must be met before an intruder is declared a threat. Threat detection includes assigned processes for each monitored aircraft that reveals a collision risk estimate based on present status, design status, and collision avoidance threshold.

Threat solving is carried out after an intruder has been flagged as a threat to threat resolution. It calculates an optimal avoidance maneuver that can affect your own speed, horizontal direction, and vertical direction. Avoidance can be materialized by a large avoidance maneuver or even a complete trajectory.

CONCLUSIONS

In the UAS field, it is desirable to implement non-transponder traffic detection methods based on a single sensor or sensor network with a series of limitations determined by relative data and varying degrees of accuracy.

The sensor systems contain design elements that compete at the overall performance level, determined by optimal sensor selection or by creating a series of sensors that can cover the control volumes in the vicinity of the aircraft.

The situation of sensor systems involves fusion data from the same type of sensors or from different sensors. Merged data is processed using fusion algorithms that cover detection and undetectability in the presence of single targets or multiple targets.

The use of TCAS warning systems does not alter the responsibilities of pilots, UAV ground operators, air traffic controllers for the safe operation of aircraft.

A technological challenge is the optimal use of sensors according to airframe characteristics and performances, the correct alignment of the sensors is made according to the airplane-related information acquisition resolution so that it has an optimal area of data sampling.

The system's sense and avoid system operation chart, which we propose, eliminates uncertainty areas and offers viable protection solutions.

REFERENCES

[1] I. Cîrciu, A. Luchian *Integrated Avionic System Specific for Air Traffic Safety* (Review of the Air Force Academy, 2014);

[2] *** PANS-OPS, *Procedures for Air Navigation Services - Aircraft Operations* – (Volume I Flight Procedures - ICAO Doc. 8168 OPS/611, Fifth edition – 2006 plus Amendment 3);

[3] *** ICAO Annex 10, vol. IV, *Aeronautical Telecommunications - Surveillance and Collision Avoidance Systems* (Fourth Edition, July 2007 – Definitions);

[4]*** *Airborne Collision Avoidance System (ACAS,) (Manual Doc. 9863)*;

[5] Oliver Ciuică, Eduard Mihai, Carmen Ștefan, *Flight Safety Introduction for student pilots* (Scientific Research and Education in the Air Force-AFASES, Brasov, Romania, 2016);

[6] Xiang Yu,Youmin Zhang, *Sense and avoid technologies with applications to unmanned aircraft systems* **(**Review and prospects, Progress in Aerospace Sciences, Volume 74, April 2015**);**

[7] Guido Manfredi, Yannick Jestin, *An Introduction to Fast Time Simulations for RPAS Collision Avoidance System Evaluation* **(**ICRAT 2018, International Conference for Research in Air Transportation, Jun 2018, Barcelone, Spain**) ;**

[8] Eduard Mihai, Oliver Ciuica, *The Influence of Organizational Culture on Flight Safety (*Science & Military Journal, 2015);

[9] Andrew Zeitlin and Andrew Lacher, James Kuchar and Ann Drumm, *Collision Avoidance for Unmanned Aircraft: Proving the Safety Case*, The MITRE Corporation and MIT Lincoln Laboratory, 2006;

[10] J. D. Boskovic, J. A. Jackson, and R. K. Mehra, *"Sensor and Tracker Requirements Development for Sense and Avoid Systems for Unmanned Aerial Vehicles,"* in AIAA Modeling and Simulation Technologies (MST) Conference, Boston, MA, Sep 2013. 7,9;

[11] R. H. Chen, A. Gevorkian, A. Fung, W. Chen, and V. Raska, "Multi-Sensor DataIntegration for Autonomous Sense and Avoid," in *Proceedings of the AIAA Infotech atAerospace*, 2011. 9, 16;

[12] J. Mackie, J. Spencer, and K. F. Warnick, "*Compact FMCW Radar for GPS-Denied Navigation and Sense and Avoid*," in IEEE Antennas and Propagation Society, AP-S International Symposium, 2014, pp. 989–990. 9;

[13] D. Dey, C. Geyer, S. Singh, and M. Digioia, "Passive, Long-range Detection of Aircraft: Towards a Field Deployable Sense and Avoid System," in *Field & Service Robotics*, 2009.10. https://substance.etsmtl.ca/en/software-defined-radio-support-aviation-efficiency, accesed at 12.05.2019

[14] F. Martel, M. Mullins, N. Kaabouch, and W. Semke, "Flight Testing of an ADSB-based Miniature 4D Sense and Avoid System for Small UAS," in *AIAA Infotech@Aerospace Conference, pages 1–7, 2011*;

[15] C. Moody and R. Strain, "Implementation Consideration for Automatic Dependent Surveillance - Broadcast on Unmanned Aircraft Systems," in *AIAA Infotech@Aerospace Conference*, Reston, Virigina, Apr. 2009, pp. 1–8. 10, 11, 110;

[16] V. M. Contarino and M. R. Contarino, "Using ADS-B to Avoid Collisions Between UAS," in *Association for Unmanned Vehicle Systems International*, 2013. 11.

THEORETICAL CONSIDERATIONS IN THE SELECTION OF THE OPTIMAL TECHNOLOGY FOR THE DEPOLLUTION OF A CONTAMINATED SOIL WITH LIQUID PETROLEUM PRODUCTS

Mirela COMAN*, Bogdan CIORUȚA**

*Technical University of Cluj-Napoca - North University Centre of Baia Mare, Faculty of Engineering, Romania (comanmirela2000@yahoo.com)
**Technical University of Cluj-Napoca - North University Centre of Baia Mare, Office of Informatics & Communications, Romania (bogdan.cioruta@staff.utcluj.ro)

DOI: 10.19062/2247-3173.2019.21.16

Abstract: *Soil pollution with liquid petroleum products is a category of frequently encountered incidents with significant environmental and economic consequences. In most cases of soil pollution, negative effects extend shortly from production to both the subsoil and the atmosphere by evaporation of high volatility pollutant compounds. The problem of soil depollution is, in these circumstances, one of the most complex activities in the field of environmental protection, both theoretically, economically and organizationally.*

Through this paper we aim to show that the correct choice of an efficient depollution technology for a contaminated soil with liquid petroleum products is a very difficult decision especially because of the very large number of variables and interactions on which the final results depend. Soil structure in correlation with the physico-chemical characteristics of the pollutant form specific systems that require specific approaches in the choice of appropriate depollution technologies.

Keywords: *contaminated soil, depollution technologies, liquid petroleum products.*

1. INTRODUCTION

Problems of environmental pollution by oil products has recently become more and more relevant, due to the high cost of work during the use of mechanical, physical, chemical and thermal methods of depollution, as well as their limited capabilities [3, 8]. Soil pollution with liquid petroleum products is a category of frequently encountered incidents with significant environmental and economic consequences. In most cases of pollution of soils with liquid petroleum products, the negative effects expand, shortly after production, both on the subsoil, to the groundwater, through infiltration, and on the atmosphere by evaporation of highly volatile pollutant compounds.

The polluted surface with oil products, as an expression of anthropogenic pressure [2, 3], is like a mosaic in the perimeter of the wells extraction and sometimes outside of them, near oil and gas production refineries or facilities, along the transport pipelines, in the warehouses and refineries, in the car maintenance and washing workshops etc.

The large number of factors influencing the pollution and depollution processes, and the inappropriate way they are addressed, lead to situations where the expected results from the depollution are not achieved. The systematic and organized approach to optimal depollution technology is a prerequisite for achieving favorable results [3].

Through this paper we aim to show that the correct choice of an efficient depollution technology for a contaminated soil with liquid petroleum products is a very important and difficult decision, the equivalent of an engineering challenge, especially because of the very large number of variables and interactions depend on the final results. The composition and structure of the soil in relation to the physico-chemical characteristics of the pollutant form specific systems that require certain approaches in the choice of depollution technologies [3], approaches that will be discussed in detail during the work.

2. SOIL POLLUTION WITH PETROLEUM PRODUCTS: SHORT CHARACTERIZATION OF THE PHENOMENON

The harmful effects of petroleum hydrocarbons on the environment and on the community may be among the most diverse; we can only mention the following:

- some compounds may affect taste and smell, so that their presence in surface water and groundwater, even in small quantities, makes them no longer suitable for consumption;
- volatile compounds can form explosive mixtures with oxygen in the air;
- some polyaromatic compounds have a carcinogenic effect and may be toxic;
- inhalation of vapors may lead to nausea, acute toxic reactions, liver problems.

In the Order of the Minister of Waters, Forests and Environmental Protection no. 756/1997 for the approval of the Regulation on the assessment of environmental pollution are presented as guidelines for the total oil content in soils the following: normal values: less than 100 mg/kg, alert values for susceptible polluted soils - 200 mg/kg, alert values for less sensitive soils - 1,000 mg/kg, intervention values for susceptible soils - 500 mg/kg and intervention values for less sensitive soils - 2,000 mg/kg.

Sensitive soils include all types of soils in residential and recreational areas, soils used for agricultural purposes and soils in underdeveloped areas. Less sensitive soils include all commercial and industrial types of soils and land areas that will be in use in the near future. Less polluting sources of pollution, including those generating oil pollution, are encountered at the level of less sensitive soils (see Fig. 1).

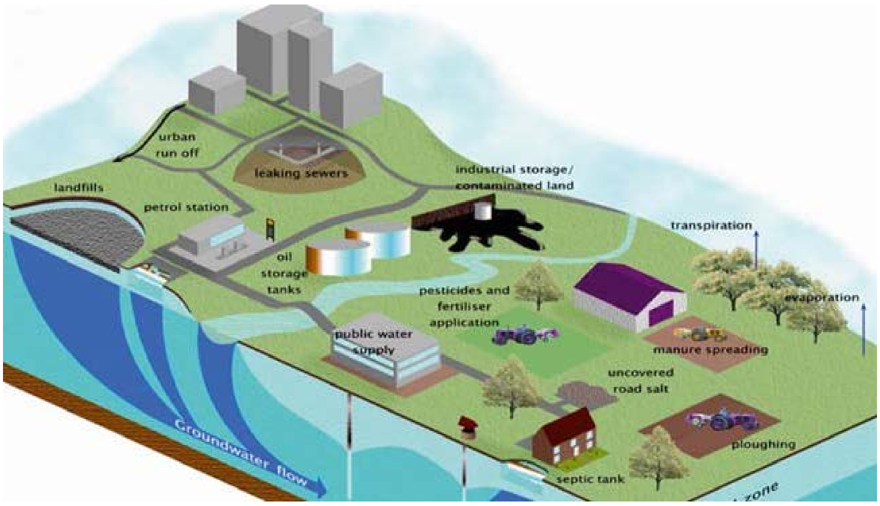

FIG. 1. The distribution of the main sources of pollution in soils with less sensitive use [2]

The toxicity of petroleum products is divided into two categories: immediate and long-term. Immediate is caused by saturated hydrocarbons which in high concentrations cause the death of organisms.

Aromatic hydrocarbons are the most toxic and olefinic hydrocarbons, in comparison with heavy metals [4], for example, have an intermediate toxicity between saturated and aromatic hydrocarbons. A method of classification which takes into account the nature of chemical pollutants is shown in Table 1.

Table 1. Classification of environmental pollutants (adapted by [4])

The nature of pollutants	Compartment / ecosystem affected			
	atmospheric	continental	limnos	marine
physical pollutants				
ionizing radiation	+	+	+	+
thermal pollution	+	+	+	+
chemical pollutants				
hydrocarbs	+	+	+	+
plastic materials		+	+	+
pesticides	+	+	+	+
detergents		+	+	+
…				
mineral particles	+	+		
heavy metals	+	+	+	+
other compounds of synthesis	+	+	+	+
biological pollutants				
dead organic matter	+	+	+	+

Long-term toxicity is due to the interference between hydrocarbons and soil components dissolved in water, interference with numerous chemical messengers, with the role of nutrition and reproduction of many aquatic organisms, for example, leading to ecological imbalances.

The profile distribution of the pollutant is dependent, in the vast majority of cases, on the quantity and characteristics of the pollutant, the configuration and characteristics of the soil and the residence time of the pollutant. In soils with poorly permeable or waterproof horizons, a pollutant concentration zone appears above (see Fig. 2), because by its polydisperse body properties, the soil acts as a chromatographic column.

FIG. 2. An example of an unwanted accident causing soil pollution with petroleum products

Petroleum components are retained especially in the higher horizons, and the film water accompanying the oil in varying proportions, with higher and less viscous density, penetrates faster in the lower horizons (see Fig. 3).

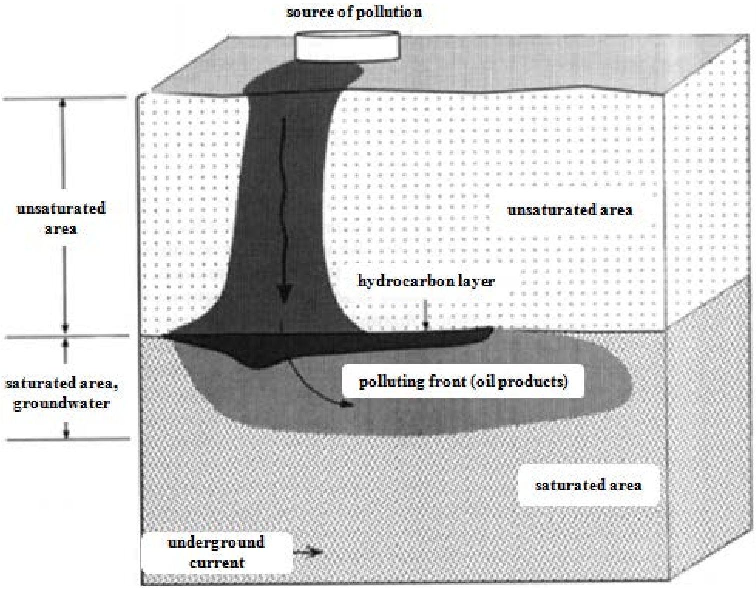

FIG. 3. Distribution and migration of a liquid petroleum product within a soil profile [8]

Petroleum volatile fractions containing 6-7 carbon atoms in the molecule are volatilized and non-volatile hydrocarbons tend to concentrate and solidify. As time passes, the process of redistribution of oil components on the soil profile is accentuated, with tars and asphaltenes being retained.

3. REMEDIATING OPPORTUNITIES FOR A SOIL CONTAMINATED WITH LIQUID PETROLEUM PRODUCTS

The phenomenon itself, the pollution of the environment with the fluids produced from the wells (crude oil, gas, condensation, salt water, sludges, sand), occurred with the start of the exploitation of crude oil and its use as an energy source.

Crude oil extraction and transport affect the environment both through the development of technological processes as well as by some undesirable accidents, such as tank discharges, overpasses or underground pipelines etc. The general technological flow specific to the crude oil - gas extraction and separation activity comprises the following important steps:

- the mixture of hydrocarbons in liquid and gaseous form with water and mechanical impurities is extracted through wells;
- the extracted fluids (crude oil, emulsified or free water, gas) are transported by pipeline to the separation / collection parks;
- separating the liquid phase (impurities - water from the deposit) from the gas phase is done in the separators of the scaffolding parks;
- the oil mixed with the sewage water, after gas separation, is provisionally stored in the park's tanks for disposal to the treatment and storage stations;
- rich gases are directed to the degazolination plant and the poor are directed to the internal consumption of the scaffolding or the gas distribution stations;
- the oil is treated thermo-chemically in the treatment tanks;
- wastewater is collected and reinjected through the injection wells.

The industrial objectives of oil exploration and separation are, according to [8, 10]: *oil and gas wells*, *separator parks*, *compressor stations*, *boiler batteries*, *storage facilities*, *wastewater collection plants*, *treatment plants*, *transport pipelines* and so on.

Pollution sources for environmental factors are the machines in which the basic activities of the scaffolding are carried out [2, 10]: *extraction*, *collection*, *separation*, *treatment*, *storage*, *transport* and machinery in which related activities are carried out: *production*, *steam distribution*, *wastewater treatment*, *water injection*, *sludge storage* etc.

Soil pollutants characterized by drilling, exploitation, separation, storage and transport of crude oil and gas can be: oil - which produces chemical pollution of the soil through radical changes (forming a waterproof film to prevent the exchange of gas), reservoir water - can cause changes in saturation, humus quality and microfauna degradation, detritus - has harmful action on crops due to the content of toxic metals: Cr, Ba and Cd, and drilling mud - has harmful action on crops due to heavy metals and salt contents.

Soil pollution with hydrocarbons from oil products directly hinders the processes of water infiltration into the soil, water circulation in the soil, and the exchange of gaseous substances with the atmosphere [5]. Indirectly, the activity of the entire edaphon being disrupted, vegetation on polluted soils develops with difficulty, and on the heavily polluted soils vegetation does not grow at all [5]. According to that, we must say that the type and composition of a particular petroleum fraction, through its specific properties, influences the mobility and retention of these fractions in the soil. Among the most important properties that can influence the soil-polluting behavior are density, dynamic viscosity, solubility and vapor pressure.

The density of petroleum products is lower than that of water, which may have an important effect on the flow and retention of oil products in wet and saturated soils; an increase in temperature tends to decrease density and viscosity and may increase the mobility of petroleum products in the soil.

Vapor pressure can be used to express the volatilization tendency of a liquid component; the degree of volatilization of a liquid gasoline depends on the vapor pressure of its components, the higher the vapor pressure, the volatility is stronger.

Adsorption refers to the binding of a component to the surface of an existing solid in the soil; when the components of the gasoline are present in a soil containing water, they will be distributed between the liquid phase and the dissolved phase, in proportion to the adsorption constants. In the layer near the soil surface, rich in organic matter, the adsorption increases directly in proportion to the organic matter content of the soil.

The main soil properties that influence the behavior of the soil-pollutant assembly and which we must take into account in the choice of depollution technologies are: *density and porosity*, *granulometry and capillary*, *moisture and suction*, *permeability and retention capacity*. Also, the state of the underground water, that can be affected, is characterized by *temporary hardness and pH*, *dissolved suspensions and gases*, *anion and metals content*, *radioactivity and corrosivity*, respectively by *electrical conductivity*, *microbiological content* and *organoleptic characteristics*.

We further consider as a case study an accidental pollution (breaking an overhead oil pipeline) into a chernozem. In these conditions, the determinants in the choice and application of a depollution technology are summarized in:

- the final degree of depollution, desired or imposed;
- duration of depollution actions;
- the total cost needed to carry out the depollution;
- the side effects produced during the application of depollution technologies and the effects arising after the application of the depollution process.

Knowing that the depollution technologies for soil contaminated with liquid petroleum products do not respond optimally, at the same time, to the four listed factors, we present and propose a number of possibilities for soil depollution according to our engineering knowledge so far.

Our proposals are summarized, as is natural, in the need to prioritize the choice of depollution technologies (starting with the minimal technology, continuing with the complex technology and ending with the one that we consider the best) depending on the concrete conditions in the field (we have to deal with a chernozem polluted with petroleum products) without considering a certain financial or technological capital.

For each of the 3 proposed (minimal, complex and optimal) depollution technologies to remedy the chernozem polluted with liquid petroleum products, we have decided to continue to expose a series of 3 sub-technologies (if we can call them in that way).

The minimal depollution technology with 3 possible variants includes, as simple as possible, minimal financial and, human and technological resources, removal of excess pollutants, excavation and sealing, and shows that:

- removal of excess pollutant is necessary as a first intervention in the case of accidental oil pollution and consists in removing hydrocarbons from the surface of the soil as quickly as possible to reduce the depth of penetration into the soil [1]. Collection pitches and small pits for concentration of the pollutant will be carried out in order to be collected by means of sorption systems in a tank and then transported to a treatment plant.
- excavation is applied in the case of accidental and point soil pollution [1] (as is the case with the pollution of a chernozem with liquid petroleum products), when the pollutant can shortly reach groundwater.
- sealing involves the physical closure of the contaminated environment by the use of a waterproofing system consisting of walls, quilt and bottom [1]; the objective is to stop the migration of pollutants by using physical barriers that counteract the effects of dispersion.

In addition to the technology of removing excess pollutants (see Fig. 4), it is necessary for the soil-removal technology, which is considered to be complex, as a result of financial and technological investments, the application of pumping depollution technology. This is used for the decontamination of soils contaminated with hydrocarbons floating at the interface between the saturated area and the unsaturated zone. It is also possible to call for hydraulic blocking, which involves stopping the migration of pollutants by installing water wells or wells, below the contaminated area and exhausting the water outdoors. If the depolar has consistent resources, we also consider the excavation to be auspicious.

FIG. 4. An example of technology involving the removal of excess pollutant (petroleum)

At the same time, we also welcome the application of absorbents, which has several main objectives, extremely well-defined, considering that we are talking about a polluted chernozem - sensitive soil (the alert value - 200 mg/kg) from our point of view:

- absorption of oil and its retention at the soil surface in order to be collected and sent to a recovery and treatment plant;
- retention of oil to prevent entry into the soil profile and thus hindering the remediation process;
- preventing the formation of waterproof film on the surface of the soil;
- stimulate multiplication of microorganisms involved in bioremediation.

An ultimate approach to be taken into consideration is also the enrichment of the oil-chernozem contaminated with selected microorganisms, which intensifies the triggering and development of biodegradation [6, 9]. Numerous biorem-technologies have been developed, including knowledge of biodegradation optimization pathways and the selection and use of microorganisms with superior degradation abilities [6, 7, 9].

The optimal environmental conditions required for the degradation of existing oil in a chernozem, according to numerous studies for the scientific literature, are: soil pH 6.5-8.0, humidity 30-90%, oxygen content 10-40% temperature 20-30°C and nutrient ratio C:N:P = 100:10:1. If the soil, whether it is a chernozem, is polluted with both oil and salt water, the bioremediation measures are combined with appropriate desalination measures, respectively, for washing the salts on the soil profile and capturing the water washing in a drainage system to be treated before discharge into the emissary.

4. ECO-TECHNOLOGY RECOMMENDATIONS

Taking into account the previously mentioned statements regarding the ways of polluting soils with liquid petroleum products, we should synthetically present a series of eco-technological recommendations, unconditionally applied on polluted soil, as follows:

- ✓ digging ditches for the rapid collection of petroleum hydrocarbon spread on land and transporting it to a treatment and recovery facility;
- ✓ application of 16 t/ha of peat to absorb the remaining oil and to limit its penetration into the soil, to soil the soil and to stimulate the development of hydrocarbon degrading microorganisms;
- ✓ loosen the soil by repeatedly tapping with the cutter and the disc at a depth of 25 cm to ensure aeration;
- ✓ if the soil is acidic or basic it is recommended to apply the amendments and incorporate them into the soil;
- ✓ fertilization with 150 t/ha of fermented or compost manure by applying it as homogeneous to the polluted land;
- ✓ fertilize with mineral fertilizers, especially humate-based liquids at 650 l/ha, which differ according to soil characteristics;
- ✓ the field is recommended to be cultivated with corn, lucerne, barley, oats and other mixtures of grasses, which are suitable for the specifics of the area.

CONCLUSIONS

Pollution of soils and aquifers with petroleum products is a category of frequently encountered incidents with significant environmental and economic consequences. In most cases of soil pollution, the negative effects extend shortly from production to both the subsoil, groundwater, infiltration and the atmosphere by evaporation of highly volatile pollutant compounds.

The problem of depolluting soils contaminated with oil products is one of the most complex activities in the field of environmental protection, both theoretically, economically and organizationally. The large number of factors that influence the processes and the inappropriate way in which they are addressed, leading to situations where the results expected from the depollution are not obtained.

If we are talking about optimal depollution technologies, optimizing the activity in this area involves compromising the results obtained by applying a depollution technology and the financial, material and human efforts that have made these results. The decision-maker or the depollution technology manager, is the person or organizational structure over which the ultimate responsibility is most often focused. The comparative analysis of the advantages and disadvantages of each category of depollution technologies should be done in relation to a list of priority objectives set according to the specific pollution conditions. The results of such analysis must guide the final solution to variant that corresponds in a given context.

REFERENCES

[1] M. Călinoiu, *Techniques for extracting pollutants from the soil by applying physical methods for depollution*, Analele Universităţii "C. Brâncuşi" din Târgu Jiu, seria Inginerie, 3: 387-396, 2011;

[2] B. Cioruța, *Considerations regarding the systematic analysis and management of the sites polluted with oil products from the Maramureș County*, Proceedings of the International Scientific Conference for Young Scientists "Current state and quality of environment for particular regions", 1-3 June 2016, Ukraine, pg. 3-8, 2016;

[3] M. Coman, *Tehnologii de depoluare a solurilor (îndrumar de laborator)*, Ed. Risoprint, ISBN: 973-751-292-8, Cluj-Napoca, 2006;

[4] M. Coman, L. Muntean, B. Cioruța, *Regarding the eco-models in the characterization of soil pollution with heavy metals*, The 40th International Conference on Mechanics of Solids, Acoustics and Vibrations & The 6th International Conference on "Advanced Composite Materials Engineering", 24-25 nov., Transilvania University, Brașov, pg. 65-69, 2016;

[5] M. Coman, B. Cioruța, R. Pop, *Regarding the evolution of soils polluted with oil products in Săcel oilfield (Romania)*, AgroLife Scientific Journal, vol. 5., no. 2, pg. 44-49, 2016;

[6] L. Doboș, C. Puia, *Poluarea cu petrol, bioremedierea și microorganismele implicate în acest proces*, USAMV, Cluj-Napoca, 2015;

[7] M. Dumitru, C. Simota, M. Toti, N. Marin, *Reabilitarea solurilor poluate cu hidrocarburi petroliere*, Ed. Terra Nostra, Iași, 2016;

[8] M. Hreniuc, M. Coman, B. Cioruța, *Considerations regarding the soil pollution with oil products in Săcel - Maramureș*, International Conference "Scientific Research and Education in the Air Force" (AFASES®), 28-30 mai 2015, Brașov, pg. 557-562, 2015;

[9] ***, www.ecoterra-online.ro/files/1355165635.pdf;

[10] ***, http://erpisa.utcb.ro/files/Download/pdf/Poluarea solului cu titei si produse petroliere.pdf.

CANARD UAV IMPROVEMENT USING VECTORED THRUST

Liviu DINCA, Jenica-Ileana CORCAU, Dionis CUMPAN

University of Craiova, Romania (ldinca@elth.ucv.ro)

DOI: 10.19062/2247-3173.2019.21.17

Abstract: *This paper presents a study concerning a canard UAV improvement using vectored thrust. There are taken into account the take-off and landing behavior. Vectored thrust can extent the attack angle range for a canard UAV, and so, one can decrease the take-off and landing speeds and also the take-off and landing distances.*

Keywords: *canard airplane, vectored thrust*

1. ADVANTAGES AND DISADVANTAGES FOR CANARD UAV CONFIGURATION

It is well known in literature the fact that canard airplane has some important advantages, but also some disadvantages which limit this application in some situations. The main advantage of canard configuration is both wing and horizontal empennage produce positive lift, so their lift forces add to obtain the global lift of the airplane. A classical configuration airplane has horizontal tail with negative lift, in order to maintain the entire plane balance, so the horizontal tail lift is subtracted from the wing lift in order to obtain the global lift of the airplane. At the same lift, the canard airplane will have a lower drag due to the lower attack angle of the wing, so the lift to drag ratio is improved for this airplane in cruise configuration.

Another advantage for canard airplane is that in static stable configuration the horizontal empennage has a higher attack angle than the wing, so for an airplane attack angle increase, the horizontal empennage reach first at the critical attack angle and does not permit anymore attack angle increase for the wing. The wing will never reach the critical attack angle, so this airplane will never stall. This is an important advantage from the pilot point of view.

As a disadvantage, one can mention the horizontal empennage is in front of the wing and its down-wash will decrease the wing attack angle and the wing lift. Down-wash is stronger as attack angle is higher. So, for small attack angle (cruise regime), horizontal empennage will have a small influence on the wing and prevails the advantage of both wing and empennage lift. But at high attack angle, as in take-off and landing regimes, horizontal empennage down-wash will produce an important attack angle decrease on the wing, so the global lift for the airplane is possible to decrease, not to increase comparing to a classical configuration.

Further, the fact that horizontal empennage produce an attack angle decrease on the wing, that means the wing has an important growth reserve until it reach the critical attack angle, so it exist an important possibility to decrease the take-off and landing speeds. But the problem is to obtain a pitch moment to bring the airplane closer to the wing critical angle and to obtain a higher global lift which means lower take off and landing speeds.

One solution is to use both a canard and a classical empennage as Piaggio-Avanti airplane – Fig. 1).

FIG. 1 Piaggio P 180 Avanti with two horizontal empennages

FIG. 2 Corte UAV, canard configuration with vectored thrust

This method permits to improve the airplane behavior at take-off and landing, but also the airplane handling qualities. This method can be applied only at jet thrust airplane as jet engine or electric ducted fans (EDF).

2. METHODS TO OBTAIN VECTORED THRUST

One have to mention at the beginning that vectored thrust appeared first on jet thrust airplanes. In order to obtain vectored thrust some methods were developed and used such: steering nozzle (Fig. 3) [3], deflection shutters placed in the thrust jet (Fig. 4) [3], Coanda effect deflection (Fig. 5) [4].

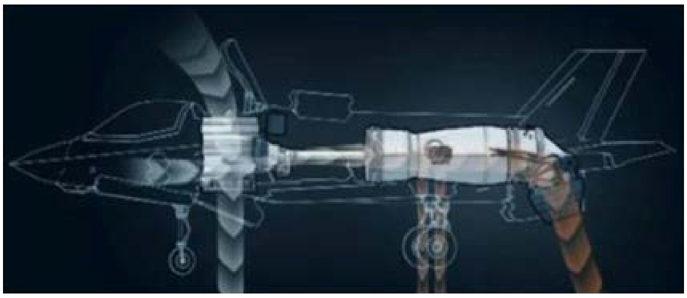

FIG. 3 Vectored thrust obtained by steering nozzle

FIG. 4 Vectored thrust obtained with deflection shutter

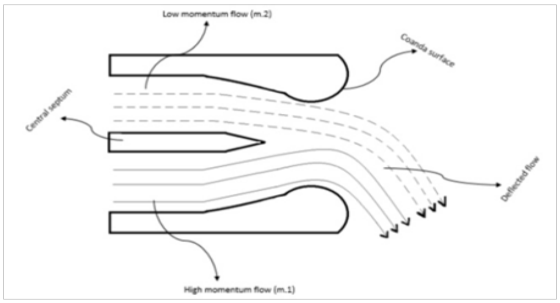

FIG. 5 Vectored thrust obtained by Coanda effect

FIG. 6 Tilt rotor vectored thrust

Tilt-rotor is also a vectored thrust, used on propeller airplanes (Fig. 6).

Each method has advantages and disadvantages: steering nozzle is efficient but rise difficulties in steering nozzle construction, deflection shutters are very simple but produce thrust loss, Coanda effect is constructive simple but is difficult to control, tilt-rotor is efficient, uses the entire motor thrust, but rises construction difficulties and the airplane is hard to control at take-off and landing (automatic control systems are needed).

3. TAKE OFF AND LANDING MOVEMENT EQUATIONS

In this paper one considered a canard UAV with EDF and the vectored thrust is obtained by nozzle steering in vertical plane. As it is mentioned in many works, thrust deflections differs from the nozzle steering angle, but for simplicity, in this paper will consider thrust has the nozzle direction. Forces at take off run are presented in Fig. 7.

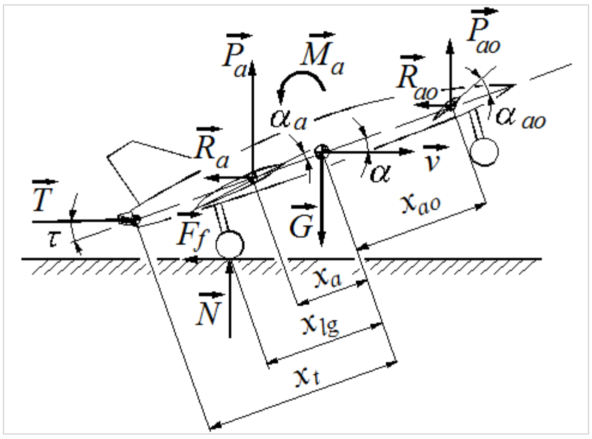

FIG. 7 Forces and moments in take off run

Following figure 7 one can write the airplane movement equations in take-off:

$$m\frac{\mathrm{d}v}{\mathrm{d}t} = T\cos(\alpha-\tau) - R_a - R_{ao} - F_f \tag{1}$$

$$0 = T\sin(\alpha-\tau) + P_a + P_{ao} + N + G \tag{2}$$

$$\begin{aligned} 0 = {} & M_a + P_{ao}\cdot x_{ao}\cos(\alpha+\alpha_{ao}) + R_{ao}\cdot x_{ao}\sin(\alpha+\alpha_{ao}) - \\ & - P_a\cdot x_a\cos(\alpha+\alpha_a) - R_a\cdot x_a\sin(\alpha+\alpha_a) \\ & - N(x_{\lg}\cos\alpha - h\sin\alpha) - F_f(x_{\lg}\cos\alpha + h\sin\alpha) + T\cdot x_t\sin\tau \end{aligned} \tag{3}$$

And one adds the link between friction and normal force

$$F_f = \mu N \tag{4}$$

In the take-off moment, normal force and friction disappear, so equation 3 becomes

$$\begin{aligned} 0 = {} & M_a + P_{ao}\cdot x_{ao}\cos(\alpha+\alpha_{ao}) + R_{ao}\cdot x_{ao}\sin(\alpha+\alpha_{ao}) - \\ & - P_a\cdot x_a\cos(\alpha+\alpha_a) - R_a\cdot x_a\sin(\alpha+\alpha_a) + T\cdot x_t\sin\tau \end{aligned} \tag{5}$$

At take off one prefer the wing has an attack angle as close as possible of critical attack angle (with a safety margin of course) in order to obtain a smaller take-off speed, but in this situation the horizontal empennage has already exceeded the critical angle, so the wing can't reach high attack angles only by elevator steering (considering the entire horizontal empennage is steering). A thrust deflection is needed to produce a supplementary pitching moment. One can consider the horizontal tail is at an over critic attack angle and has a lift coefficient less than maximum lift coefficient, but a drag coefficient considerably higher than for a under critic evolution.

One can determine the thrust nozzle steering angle in the take-off moment imposing the condition in this moment wing has critical attack angle minus 2-3 degrees. One can determine from the wing polar curves the corresponding lift and drag coefficients for this attack angle. Aircraft attack angle in the take off moment, neglecting the influence between wing and horizontal empennage is

$$\alpha = \alpha_{cra} - \alpha_a \tag{6}$$

where α_{cra} is the wing critical angle and α_a is the wing setting angle.

One obtain the nozzle steering angle

$$\sin\tau = \frac{P_a x_a \cos\alpha_{cra} + R_a x_a \sin\alpha_{cra}}{T \cdot x_t} - \frac{M_a + P_{ao} x_{ao} \cos(\alpha_{cra} - \alpha_a + \alpha_{ao}) + R_{ao} x_{ao} \cos(\alpha_{cra} - \alpha_a + \alpha_{ao})}{T \cdot x_t} \tag{7}$$

In the landing case, when the airplane descends on the γ slope, situation is presented in Fig. 8.

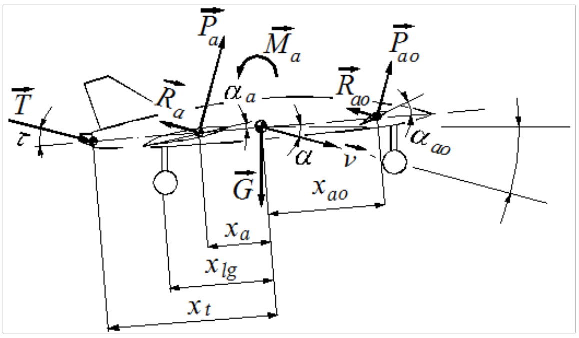

FIG. 8 Landing flight forces and moments

Translation equations (1) and (2) become

$$G\sin\gamma + T\cos(\alpha + \tau) - R_a - R_{ao} = 0 \tag{8}$$
$$P_a + P_{ao} + T\sin(\alpha - \tau) - G\cos\gamma = 0 \tag{9}$$

But thrust is not anymore at the maximum value as in take off situation. It has the necessary value to maintain the airplane on the landing slope γ.

Moment equations in this case is still (5). But the aerodynamic moment can differ substantially if the airplane has flaps set on the landing angle. In order to find the nozzle steering angle one can make the following considerations.

One prefers the wing has about two degrees less than critical attack angle. So one can find from polar curves the wing lift and drag coefficients. Elevator can be considered set on the maximum angle. Its attack angle can be found from geometrical considerations. This attack angle will be usually above its critical attack angle, but using horizontal empennage polar curves one can find the aerodynamic coefficients. Optimum landing slope is about 3 degrees. In this situation equations (8), (9) and (5) form a system with three variables v, T and τ which can be solved and find the nozzle steering angle. But it is interesting also to find the necessary thrust T for the landing flight. In landing flight pilot can modify two parameters - T and τ, considering the landing speed known.

Pilot will have to handle the thrust and nozzle steering angle avoiding exceeding the wing critical attack angle.

If the canard airplane has vectored thrust, it can lose the advantage it does not stall, especially in landing conditions. To limit this inconvenient one can design the air plane such that the nozzle steering angle in take off is equal to the landing one and to limit the nozzle steering angle at this value. By this way, if pilot will increases thrust over the landing thrust, the airplane will be accelerate and it will climb. If pilot decrease thrust under the landing one, pitching moment produced by the nozzle steering will be not enough to stall the airplane.

4. CONCLUSIONS

Using vectored thrust for a canard airplane one can improve the take-off and landing performances due to higher attack angles airplane can reach. One can bring by this way the wing closer to the critical attack angle and so one decrease the take-off and landing speeds comparing a canard without vectored thrust. It is determined the nozzle steering angle for take-off phase, considering in this situation thrust has the maximum value possible. A method to determine the thrust and nozzle steering angle in landing flight is identified. But one has to take care that the vectored thrust canard airplane looses the advantage it don't stall. If one try to land with a too big nozzle steering angle then it is a big danger to stall the plane in this critical flight phase. For this reason, automatic systems to limit the nozzle steering angle in this phase could be useful.

REFERENCES

[1] Nita, M.M., Sarbu, M., Patraulea, R., *Mecanica Zborului Avionului* – Reprografia UPB, Bucuresti, 1985;

[2] https://www.youtube.com/watch?v=f2F1hl8TOPA&list=PLBxIXzEjKcjjDk6qxq5o ZAYs_68N4QRft

[3] Schaefermeyer, M.R. – *Aerodynamic Thrust Vectoring for Attitude Control of a Vertically Thrusting Engine* - Master of Science thesis, Utah State University, Logan Utah, 2011;

[4] Bharathwaj, R. et. al. – Computational study of Coanda based Fluidic Thrust Vectoring System for Optimising Coanda Geometry ; *2016 IOP Conf. Ser.: Mater. Sci Eng. 149 012210;*

[5] https://www.ainonline.com/aviation-news/business-aviation/2018-04-06/long-road-tiltrotor;

[6] Dinca, L., Corcau, J.I. – *Mecanica si Dinamica Zborului Avionului* – Editura Universitaria, Craiova, 2018.

FLOW CONTROL INVESTIGATION USING THE COANDA EFFECT ON AIRFOILS

Alexandru DUMITRACHE*, Florin FRUNZULICA, Horia DUMITRESCU* Tudor IONESCU****

*Institute of Mathematical Statistics and Applied Mathematics, Romania
(alex_dumitrache@yahoo.com)
**Politehnica University of Bucharest, Romania

DOI: 10.19062/2247-3173.2019.21.18

Abstract: *Numerical investigations on the flow control around airfoils, in conjunction with Coandă effect, based on RANS equations are done. The circulation control uses the tangential blowing jet on the upper surface of the airfoil near the trailing edge with the rounded or modified flatback surface. Flow field spectra around such a configurations, involving the delayed of flow separation are obtained and analyzed by CFD methods. Thus can be identified the optimum domain of the geometric and jet flow parameters in which this flow control method should be used.*

Keywords: *Coandă effect, circulation control, high-lift system*

1. INTRODUCTION

One of the most important aerodynamic choices when designing an airplane wing or propeller blades is that of the appropriate airfoil, optimal first of all for the cruise flight phase or the nominal operating mode. However, for other operating phases (such as take-off, for example), it is necessary to obtain higher lift characteristics, or, more desirably, higher lift/drag- ratio.

There are currently several methods to achieve these performances. If the conventional methods, which involve slats or slotted flaps on trailing-edge or leading-edge of the wing, there are major drawback related to the complexity mechanics [1] and

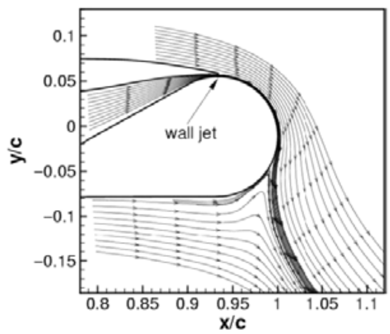

FIG. 1. Circulation control around a curved trailing edge of an airfoil.

thus of increasing the weight, the so-called gapless high-lift systems can be used, with the trailing-edge blowing [2] (Fig. 1), benefiting from the advantages of the Coandă effect to delay the flow separation [3].

This method is one of active flow control methods and even when using a small percentage of the cold engine flow, there is a good efficiency of obtaining the necessary high-lift coefficient for the take-off or landing flight phase.

The circulation control around an airfoil is obtained by tangentially blowing of a small thickness jet over the rounded trailing edge. As a result, the jet sheet remains attached and deflected on a longer portion of the curved surface, without separation of the flow.

That is why numerical investigations and analyses are needed using a CFD solver (in this case, Ansys Fluent [14]) to evaluate the advantages and limits of this circulation control technology for airfoils.

2. THEORETICAL ASPECTS

A passive or active circulation control based on blowing jet around a Coandă surface can augment the aerodynamic characteristics of an airfoil [4- 9]. The separation is delayed (Fig. 2a) and thus an improved lift coefficient is obtained, based on additional circulation (Fig. 2b).

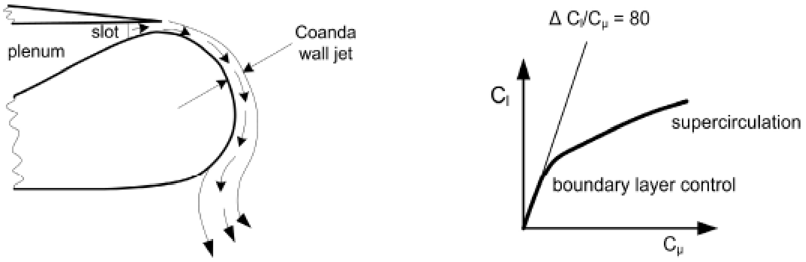

a) *Rounded trailing edge* b) *Schematic lift behaviour*

FIG. 2. Scheme of circulation control in conjunction with a Coandă surface.

By introducing an additional circulation term (Γ_{jet}) the reaction forces are increased:

$$P = \rho\, V_\infty \left(\Gamma_c + \Gamma_{jet}\right) \tag{1}$$

where ρ is the fluid density, V_∞ is the unperturbed fluid speed, Γ_c is circulation around the airfoil, and

$$\Gamma_{jet} = \frac{\dot{m} V_{jet}}{\rho\, V_\infty}\left(\alpha + \beta_{jet}\right) \tag{2}$$

where $\dot{m}$ is the mass flow rate, V_{jet} is the jet speed and β_{jet} is the jet deflection angle at the exit of the plenum chamber. Then aerodynamic coefficients in conjunction with Coandă jet are:

$$\begin{aligned} C_{L,jet} &= C_T \sin\left(\alpha + \beta_{jet}\right) \\ C_{D,jet} &= C_T \cos\left(\alpha + \beta_{jet}\right) \end{aligned} \tag{3}$$

where C_T is the thrust coefficient due to the Coandă jet. The enhanced total lift and drag coefficients are:

$$\begin{aligned} C_L &= C_{L,p+\tau} + C_{L,jet} \\ C_D &= C_{D,p+\tau} + C_{D,jet} \end{aligned} \tag{4}$$

where $C_{L,p+\tau}$ and $C_{D,p+\tau}$ are values of lift and drag coefficients, respectively, for the case without blowing jet.

The induced circulation is changed by the jet acting in the neighborhood of a Coandă type surface (Fig. 3), depending on the jet position [10, 11].

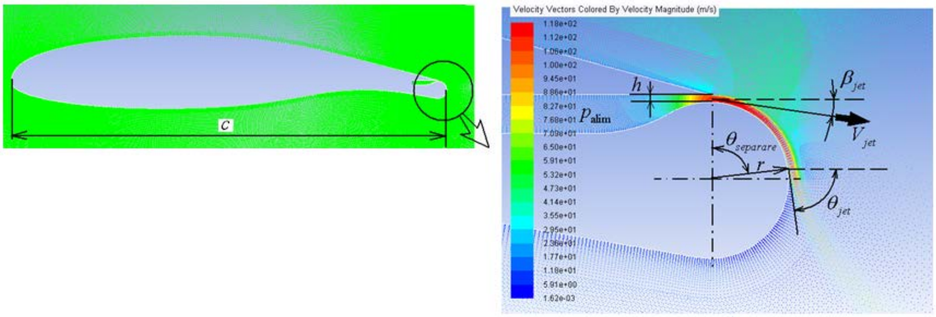

FIG. 3. Geometric data on the rounded trailing edge for the Coanda type flow

The momentum coefficient (C_μ) is one parameter in this investigation, based on thrust of the jet, obtained at the slot exit:

$$C_\mu = \frac{Thrust}{q\,S} = \frac{\dot{m} V_{jet}}{q\,S} = \frac{2\,h\,w}{b\,c}\,\frac{\rho_{jet}}{\rho_\infty}\,\frac{V_{jet}^2}{V_\infty^2} \qquad (5)$$

where $\dot{m}$ is mass flow rate

$$\dot{m} = \rho_{jet} V_{jet} h\, w\,, \qquad (6)$$

w = jet width, and $S = b \cdot c = 1 \cdot c$ is the reference surface.

An estimate of the total required power, P_f, can be made as the sum of required power to create the jet, P_{jet} and the lost power in the nozzle of the reservoir, P_{jet}:

$$P_f = P_{jet} + P_{rez} = \frac{1}{2}\rho V_{jet}^2 \frac{\dot{m}}{\rho} + \dot{m} V_\infty^2 = C_\mu \frac{V_{jet}}{2V_\infty}\left[1 + 2\frac{V_\infty^2}{V_{jet}^2}\right]\left(q_\infty V_\infty S\right) \qquad (7)$$

Then the dimensionless parameter, the fluid power coefficient is obtained:

$$C_{P_f} = \frac{P_f}{q_\infty V_\infty S} = C_\mu \left(\frac{V_{jet}}{2V_\infty} + \frac{V_\infty}{V_{jet}}\right) \qquad (8)$$

This ideal power coefficient can be expressed as a function only of the momentum coefficient C_μ and the dimensionless parameter, *h/c* ratio:

$$C_{P_f} = \frac{C_\mu^{3/2}}{2\sqrt{2(h/c)}}\left[1 + \frac{4(h/c)}{C_\mu}\right] \qquad (9)$$

In Fig. 4 the variation of the ideal fluid power coefficient, C_{P_f} as function of the momentum coefficient, C_μ, is represented, for various *h/c* ratios. Figure 5 shows the dependency results for the mass flow rate, $\dot{m} = f(C_\mu, h/c)$, under certain conditions given for external flow and also for geometry ($c = 0.5\,m;\ V_\infty = 30\,m/s; T_0 = 291K$).

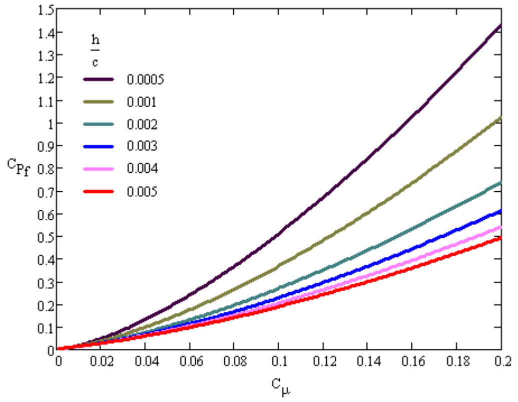

FIG.4. Required coefficient fluid power for ”Coandă” type jets, for various *h/c* ratios

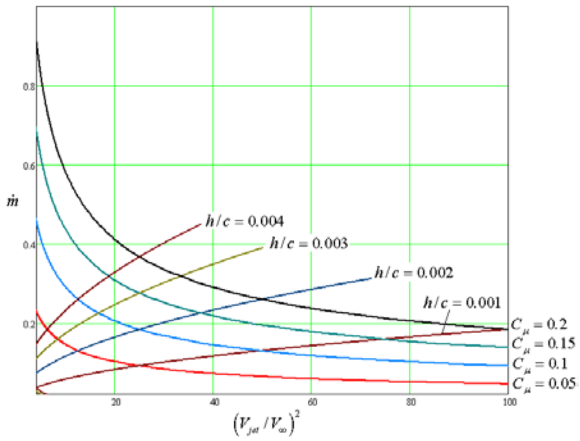

FIG. 5. Required mass flow rate for circulation control

3. NUMERICAL INVESTIGATIONS OF CIRCULATION CONTROL ON AIRFOILS WITH MODIFIED TRAILING EDGE

In recent years a lot of experiments and numerical simulations have been made to investigate and show that there are good premises for using the Coandă effect in controlling the flow around airplane wings or turbomachine blades [10 - 12].

For our numerical investigations the 17% Supercritical General Aviation Circulation Controlled Airfoil (GACC) with a round trailing edge as a Coandă surface was selected [11,12]. The geometric parameters are: *h/c* = 0.002, *h/r* =0.1, $\beta_{jet} = 0^0$ and *r/c*=2% (Fig. 6).

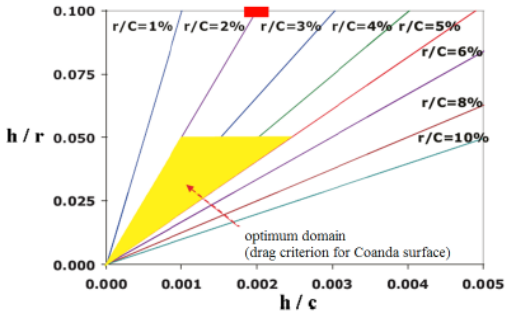

FIG. 6. Optimum geometry domain of the most effective circulation control

The momentum coefficient (C_μ) is obtained from the equation (7) and Reynolds number has a value of order of 10^6 for a fully turbulent flow.

With regard to CFD data it can be specified that a structured mesh is used (Fig. 7), where 0.4< y^+ < 1 and 25< Δx^+ <300, boundary conditions are given as usual for 2D aerodynamic analysis and to close and solve the RANS model, the $k-\omega$ SST turbulence model has been chosen [13].

Two configurations are numerically investigated based on the modified GACC airfoil and a third one is based on the DU97 airfoil with modified flat trailing edge.

Various momentum coefficients C_μ; for an undisturbed flow with velocity V_∞ = 30 m/s are basic parameters in these investigations.

3. 1 Flap with cylindrical trailing-edge. When the jet leaves tangentially the plenum chamber ($\beta_{jet} = 0^0$) it has the tendency to remain attached to the round surface on a certain length, depending on the jet momentum coefficient and on the external flow velocity (if the geometric parameters, *h/c* and *r/c*, are fixed).

For a low momentum jet the external flow on the upper side of airfoil will be quickly separate. When the jet momentum coefficient is increased, the separation occurred at an angle that exceeds 90 degrees to the direction of the initial jet, generating a virtual slat.

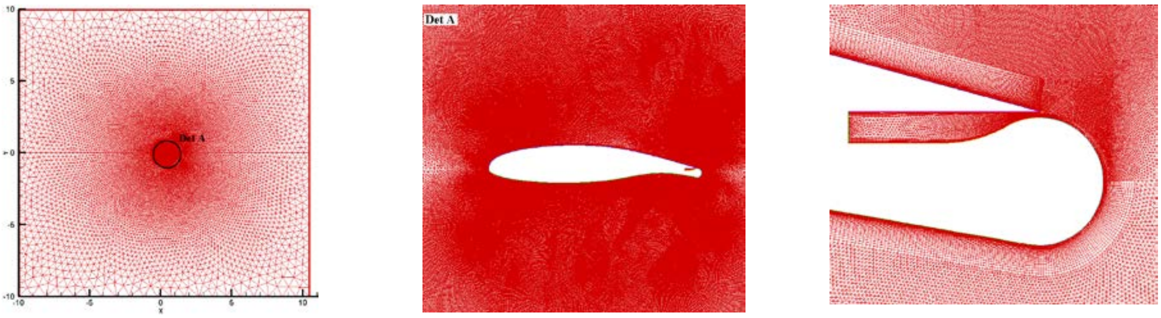

FIG. 7. Computational domain, meshing and trailing edge details

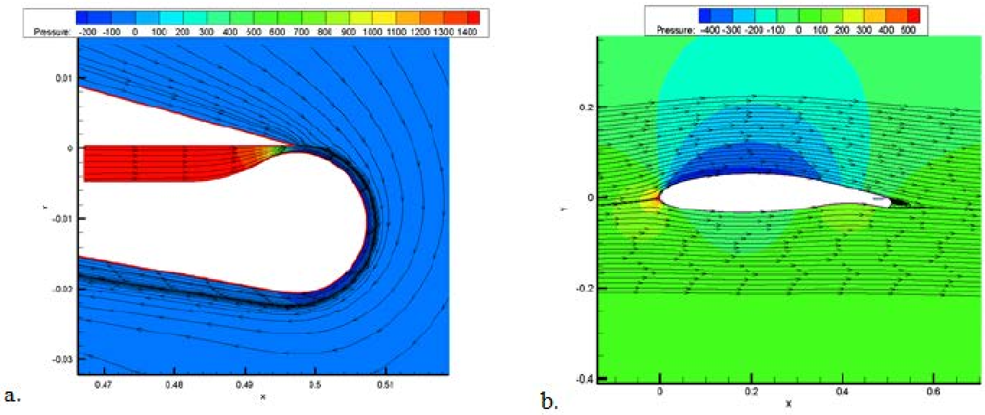

FIG. 8. Streamlines and pressures field: (a) without external flow ($V_{jet} = 9\ m/s,\ \ V_{\infty} = 0\ m/s$) and (b) external flow without jet ($V_{\infty} = 30\ m/s$)

Results of numerical simulations with $V_{jet} \geq 9\ m/s$ highlight that the jet is attached on the cylindrical trailing edge surface, with a value of θ_{jet} angle higher than 90^0 [10 - 12] (Fig. 8). This may have a reverse effect, that is, a decrease in the lift efficiency rate, due to the shortening of the suction portion on the lower side of the airfoil. Figures 9 and 10 show, the flow spectra (streamlines and pressure fields, with details around trailing edge (TE)), at various momentum coefficients.

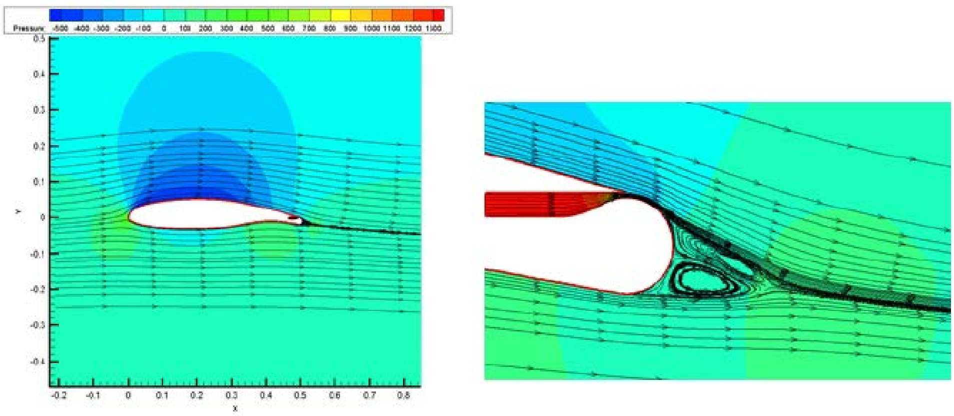

FIG. 9. Streamlines and pressures field with TE details; $V_{jet} = 9\ m/s,\ \ V_{\infty} = 30\ m/s$

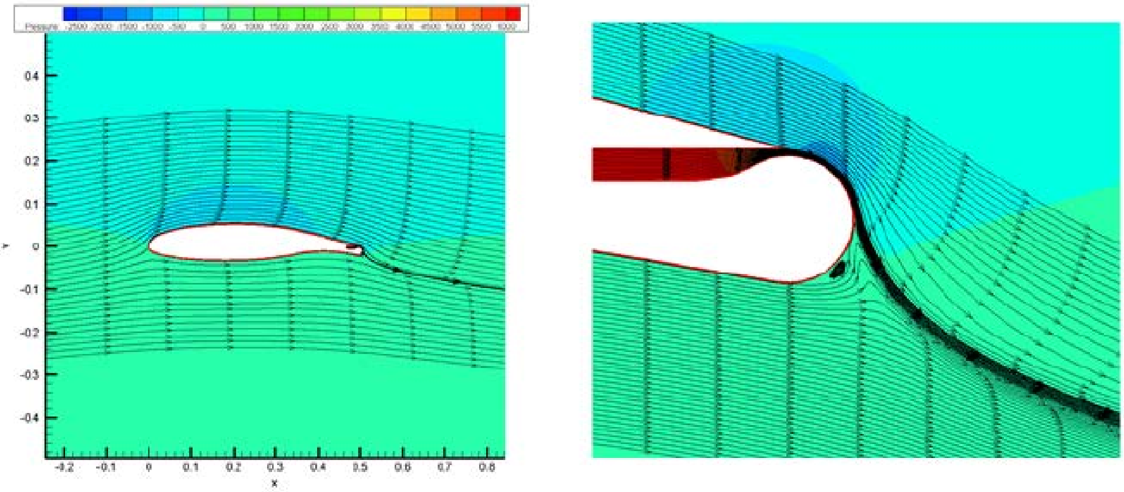

FIG. 10. Streamlines and pressures field with TE details; $V_{jet} = 20\ m/s,\ V_\infty = 30\ m/s$

3.2 Flap with double curvature. For this numerical simulations the configurations consists in an airfoil where the trailing edge with circular surface is replace with a flap that has a circular upper part with the same radius that in the previous test case, followed by another curved portion. For simulations, the flap is deflected with 55^0 angles.

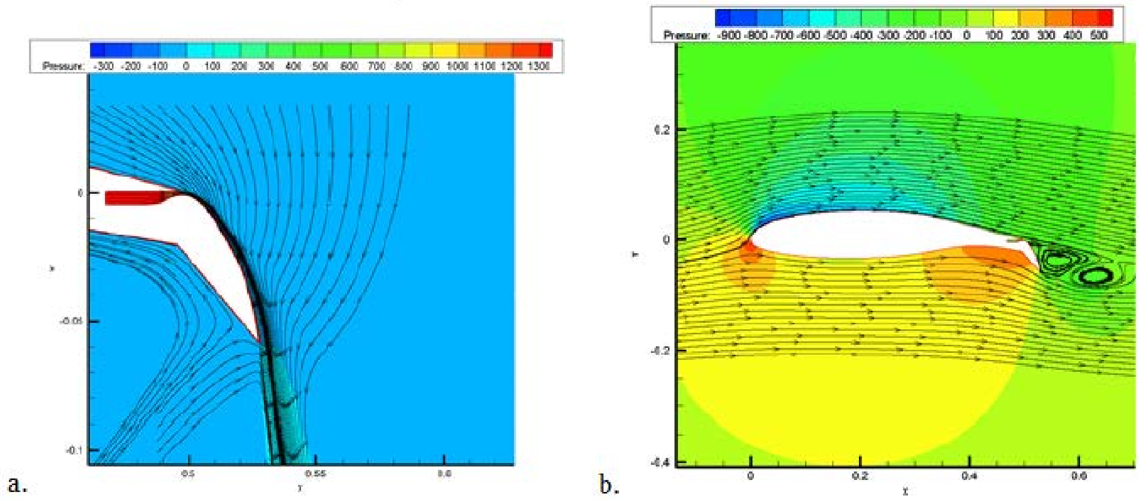

FIG. 11. Flowfield (streamlines and pressures):
(a) without external flow (V_{jet} = 9*m/s;* V_∞ = 0*m/s*) and (b) external flow without jet (V_∞ = 30*m/s*)

It is observed that for $V_{jet} \leq 10.549\ m/s$ and for a value of momentum coefficient $C_\mu = 0.0124$, the separation took place between 10^0-20^0 range on the circular zone.

For values of $V_{jet} \geq 10.55\ m/s$ the jet flow is reattached on the entire surface of the flap. In Fig. 11 and 12 these spectra of the flow can be seen. Comparing with the reference case (C_μ = 0:0) for this configuration, a double lift coefficient can be obtained, but must consider also and increasing drag.

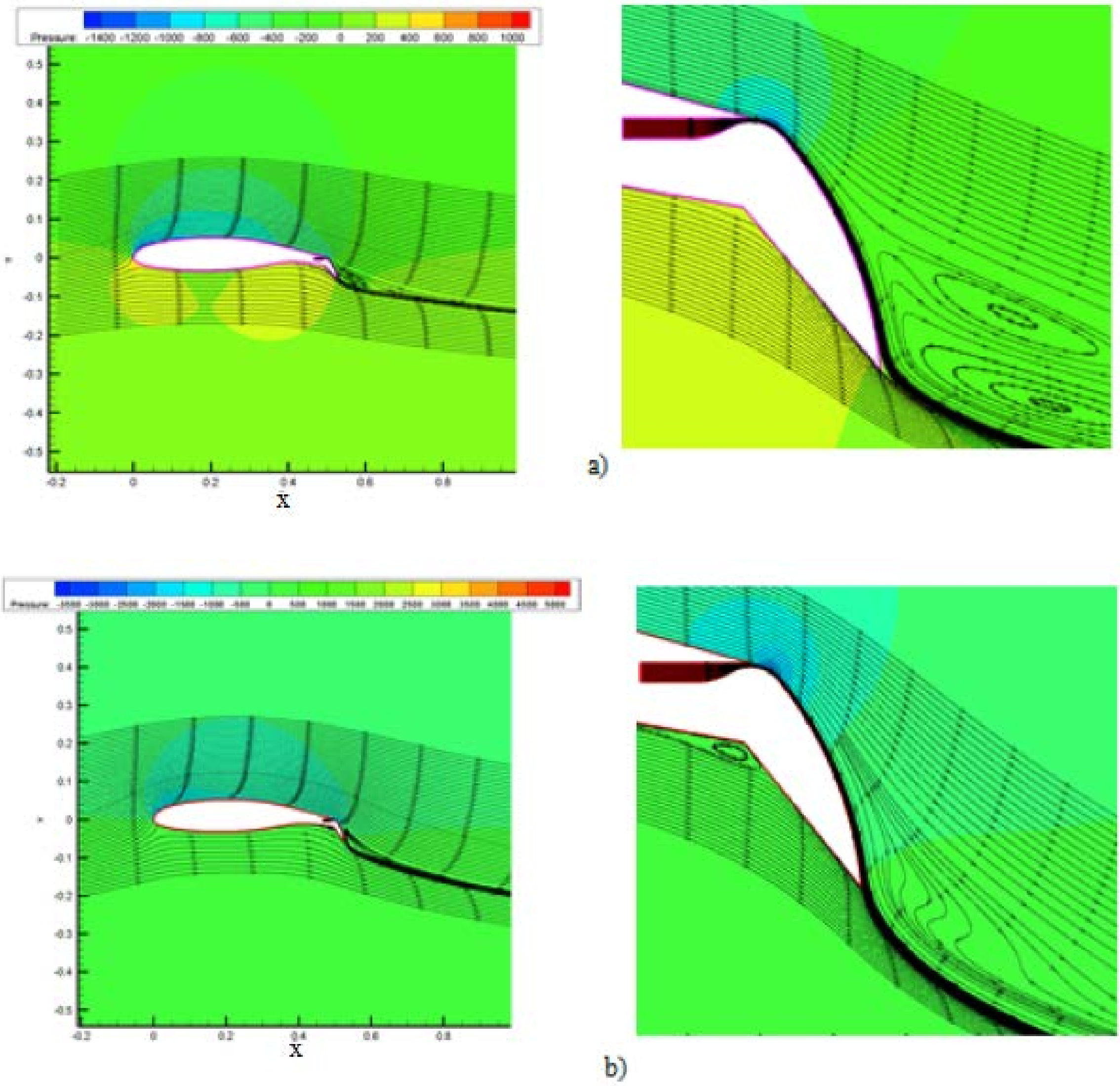

FIG. 12. Flowfield (streamlines and pressures) for two numerical simulations cases, with details: (a) V_{jet} = 10.55 *m/s;* V_{∞} =30 *m/s;* (b) V_{jet} = 20 *m/s;* V_{∞} =30 *m/s*

3.3 DU97 airfoil with modified flat trailing edge. With the development of wind turbines in last years, especially with the horizontal axis, it was necessary to use the airfoils with blunt trailing edge or called flatback airfoils, for rotor blades. Flatback airfoils provide several structural and aerodynamic performance advantages [15].

At the trailing edge, the upper side is prolonged by a cylindrical shape, up to half the thickness of the trailing edge and a linear lower portion is continued until it intersects the extension of the lower part of the airfoil (Fig. 13).

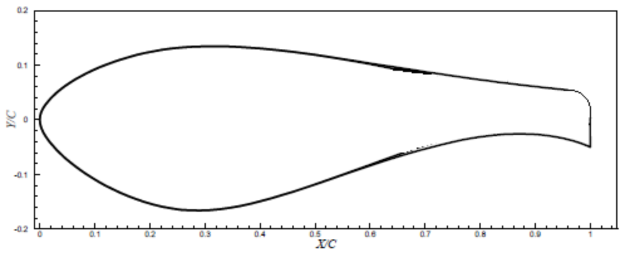

FIG. 13. Airfoil shape of DU97 with modified flatback TE.

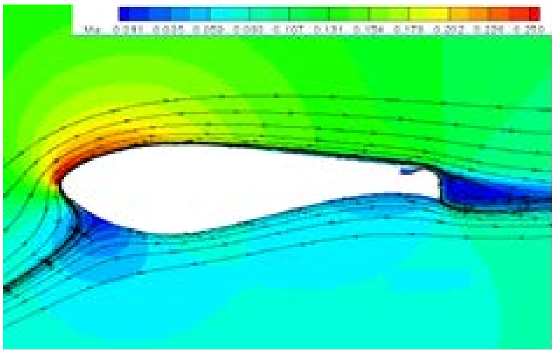

a.

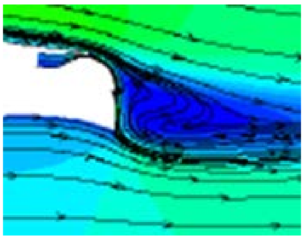

b.

FIG. 14. a) Flowfield around DU97 flatback airfoil (V_∞ = 30 *m/s*, incidence angle = 15^{0}, Re=3.0x10^6, C_μ=0.030); b) detail of TE flowfield

It was therefore necessary to analyze these modified airfoil shape and found optimal circulation control necessary for obtaining enhanced aerodynamic characteristics, and, finally, increasing the amount of harvested energy from the wind (Fig. 14).

The jet is attached on the Coandă surface for the value of momentum coefficient $C_\mu = 0.030$, but if this value is increased the jet can acting as a pneumatic flap. The enhancement in lift increases with increasing of jet momentum coefficient or decreasing of the slot height.

CONCLUSIONS

Three configurations in conjunction with the Coandă effect have been numerical investigated based on RANS solver. For all cases the blowing efficiency on a curved surface ("Coandă surface") is observed, compared with the reference cases without jet.

Based on this type of circulation control, equal or greater lift coefficients that than for classical high-lift systems are obtained. However, one must consider that this increase in lift is accompanied by an increase in drag.

It is obvious that this type of circulation control has to be used in addition to other flow control methods, in order to obtain the optimal parameters for all operating phases.

Future further investigations to be made on improving these methods, must be completed and compared with experimental investigations.

REFERENCES

[1] K. Pfingsten and C. Radespiel, *Use of upper surface blowing and circulation control for gapless high lift configurations*. In CEAS/KATnet Conference on Key Aerodynamic Technologies, Bremen, Germany, 2005;

[2] Y. G. Zhulev and S. I. Inshakov, On the possibility of enhancing the efficiency of tangential blowing of a slit jet from an airfoil surface, *Fluid Dynamics,* vol. 31, pp. 631-634, 1996;

[3] Y. Liu, L. N. Sankar, R. J. Englar, K. K. Ahuja and R. Gaeta, Computational Evaluation of the Steady and Pulsed Jet Effects on the Performance of a Circulation Control Wing Section, *AIAA Paper 2004-0056*;

[4] C.E. Lan and J.F. Campbell, Theoretical Aerodynamics of Upper-Surface Blowing Jet-Wing Interaction, *NASA TN D-7936*, 1975;

[5] R. J. Englar, M. J. Smith, S. M. Kelley and R. C. Rover, Application of Circulation Control to Advanced Subsonic Transport Aircraft, Part I: Airfoil Development, *Journal of Aircraft,* vol. 31, pp.1160-1168, 1994;

[6] R. J. Englar, M. J. Smith, S. M. Kelley and R. C. Rover, Application of Circulation Control to Advanced Subsonic Transport Aircraft, Part II: Transport Applications, *Journal of Aircraft*, vol. 31, pp. 1169-1177, 1994;

[7] Y. Liu, *Numerical simulations of the aerodynamic characteristics of circulation control wing sections*. Thesis, Georgia Institute of Technology, 2003;

[8] E.H. Gibbs, *Analysis of Circulation Controlled Airfoils*, Thesis, West Virginia University, Morgantown, WVa, 1975;

[9] R.A. Churchill, *Coandă Effect Jet Around a Cylinder with an Interacting Adjacent Surface*, Thesis. West Virginia University, Morgantown, WVa, 1992;

[10] G.S. Jones, *Pneumatic Flap Performance for a Two-Dimensional Circulation Control Airfoil*, In Applications of Circulation Control Technologies – Progress in Astronautics and Aeronautics, vol. 214, pp. 191-244, 2006;

[11] W.J. Baker and E.G. Paterson, *Simulation of Steady Circulation Control for the General Aviation Circulation (GACC) Wing*, In Applications of Circulation Control Technologies – Progress in Astronautics and Aeronautics, vol. 214, pp. 513–537, 2006;

[12] R.J. Englar, *Overview of Circulation Control Pneumatic Aerodynamics: Blown Force and Moment Augmentation and Modification as Applied Primarily to Fixed-Wing Aircraft*, In Applications of Circulation Control Technologies – Progress in Astronautics and Aeronautics, vol. 214. 2006;

[13] F.R. Menter, Eddy viscosity transport equations and their relation to the k-ε model, *ASME Journal of Fluids Engineering*, vol. 119, pp. 876-884, 1997;

[14] *** Ansys Fluent 13.0. User's Guide.

[15] H.Y. Xu, C.L. Qiao, H.Q. Yang and Z.Y. Ye, Active circulation control on the blunt trailing edge wind turbine airfoil, *AIAA J.* vol. 56, pp. 554–570, 2018,

A HYBRID PROPULSION SYSTEM FOR UAS

Dragoș Daniel ISVORANU, Petrișor-Valentin PÂRVU, Octavian GRIGORE

”Politehnica” University, Bucharest, Romania
(dragos.isvoranu@upb.ro, petrisor.parvu@upb.ro, octavian.grigore@upb.ro)

DOI: 10.19062/2247-3173.2019.21.19

Abstract: *Just like in the field of road vehicles, the tendency to increasingly electrify aeronautical systems is a topical trend triggered, first of all, by international legislation on pollutant emissions.*

The proposed subject is in line with this trend in civil aviation, investigating the use of a hybrid propulsion system (electric generator driven by a gas engine) for enhancing endurance of UAVs.

Electronically controlled ignition map for best performances of the generator is theoretically determined and then tested on an UAV testbed. Influences on the main performance features: payload and range are studied. Performances are calculated using classical civil aircraft methods (1). It is found that the better performances can be achieved with current approach.

Keywords*: Electric Aircraft, Pollution Reduction, UAV's Performance.*

1. INTRODUCTION

One of the critical requirements of UAVs in reconnaissance missions is the flight time without refueling. Duration varies considerably depending on the type of motor. Solar powered UAVs hold the long-term record (see Helios Prototype [1], the Solar Impulse 2016 project on a perpetual flight). On the other hand, this type of propulsion is recommended for those applications where the traction and payload needs are negligible.

In this study, several possibilities of UAV motorization were analyzed. For missions over 40 hours, fuel cells can be the most effective candidate for UAVs if power and payload are considerable. The same source of energy can also supply on-board electric power demand. Current technology explores the use of solid hydrogen (in the form of bars) instead of hydrogen gas in fuel cells [2]. For medium-term missions (20-40 hours), piston engines are best suited for UAV propulsion due to low fuel consumption compared to gas turbine engines of the same power [3].

It was found that for a VTOL (Vertical Take Off and Landing) UAV the best solution is a hybrid one: electric motor in quad configuration for takeoff and landing and thermal engine for fixed wing cruise flight. The main engine was fitted also with a generator to charge the batteries during cruise flight, which allows carrying smaller capacity batteries onboard.

The main engine options are either gas turbine engines (MTG) or piston engines (MP). From a theoretical point of view, the Brayton cycle at the base of the MTG operation offers an increased thermal efficiency compared to the Otto or Diesel cycle. However, with the reduction of the MTG sizes corresponding to the dimensions and load of the given UAV, a number of undesirable effects result in a reduction in the overall MTG performances [4].

With regard to MP, the two important variants to be taken into account are spark ignition engines (Otto) and compression-ignition (Diesel) engines. From a constructive point of view, both variants can be achieved in both 4-stroke and 2-stroke modes. From the point of view of thermodynamic efficiency the best results are provided by the Diesel engine due to the high compression ratio and the maximum cycle temperature close to the adiabatic flame temperature under poorly mixed conditions.

2. STATE OF THE ART

Analysis of the current state of the art is centered around correlations between power and weight as well as weight and size for various types of engine. Thus, Fig. 1 illustrates the power-to-weight relationship for piston engines, gas turbine and electric motors.

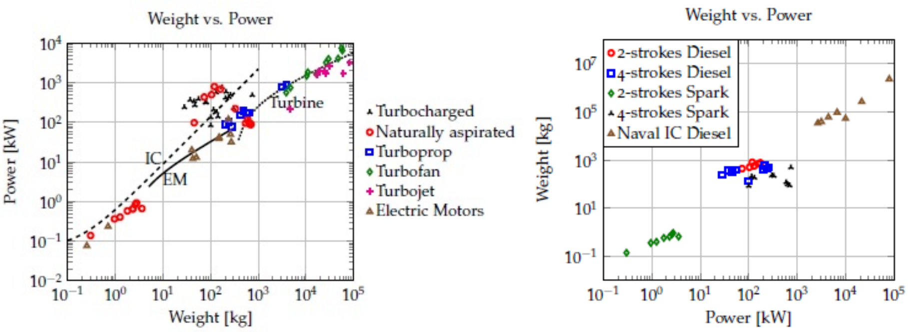

FIG. 1 Power-weight correlation for various engines. [5]

It is noted that in a logarithmic diagram, motors tend to be organized along a line, thus suggesting a $W = a + bP^c$ correlation, where W is the weight and P is the corresponding power.

For naturally aspirated piston engines, the specified correlation is especially fulfilled in the range of 0.1-30 kW and over 300 kW. In the intermediate field, there are deviations notably through the use of large bore to stroke ratio (usually > 1) as well as lightweight materials available from state-of-the-art technologies. However, these engines operate at very high speeds and are not extremely fuel efficient. At the same power, forced aspiration engines are generally heavier than those with natural aspiration due to turbocharger presence. Considering mass constraints (< 5kg), the range of power to be investigated is between 0.2 and 10 kW. For this power range, the only options are natural aspiration and electric engines. Consequently, the analysis of forced and gas turbine engines becomes useless.

Further, for this area of power, we are interested in the ignition mode correlated with the number of engine strokes (Fig. 1).

In the field of powers of interest, we find that we are at the limit between two-stroke or 4-stroke Diesel engines and two-stroke spark ignition engines. Moreover, the field of interest is somewhat devoid of more current information. As a result of the investigation of several manufacturers, air-cooled and fuel injection engines are the most commonly used in the power range of 2.5-6 kW and with a mass below 5 kg.

The previous analysis is concretized by the representation in the following graphs.

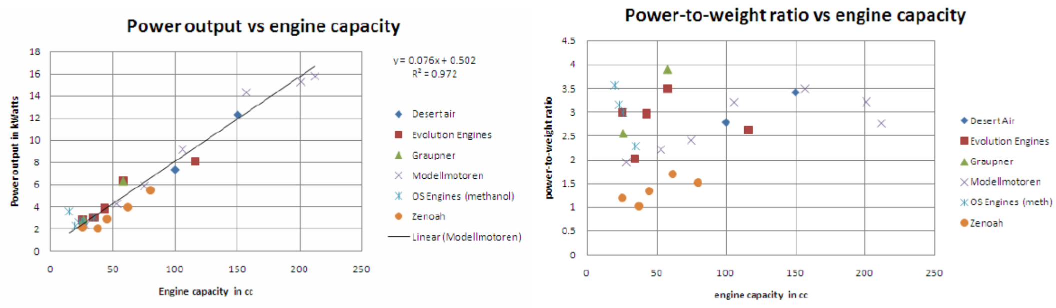

FIG. 2 Power-capacity correlation for various types of engines. [5]

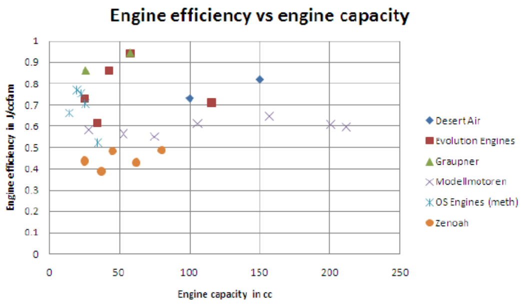

FIG. 3. The correlation between efficiency and capacity for the same engines. [5]

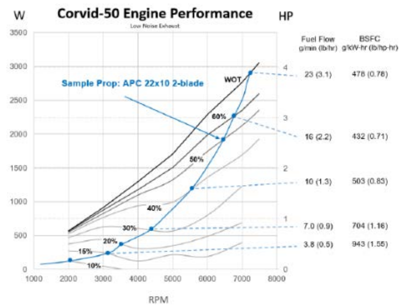

FIG. 4. Engine characteristic for corvid-50 (b50i)

The comparative analysis demonstrates, on the one hand, the linear power variation trend of 76 W/cc for the Modellmotor engines (Fig. 2). The small deviations from this trend are only characteristic of 2 and 4 cylinder variants (the last three in the upper right corner). Referring to Fig. 2, if we ignore Zenoah motors characterized by low power specific values, we conclude that for these applications the average specific power is around 2.9 kW/kg. From the last diagram (Fig. 3) results an average efficiency of 0.654 J/ccfam for the studied engines.

3. PROPULSION SYSTEM DESIGN

In view of the analysis presented in the previous paragraph, a 2-stroke, air-cooled and fuel-injected engine from the 3W-Modellmotoren 3W 55xi FI was chosen.

Unfortunately, the data provided is extremely brief and even incomplete. Thus, power, torque and specific power curves include data from both 100% and partial mode operation. Normally, for each regime it would have been necessary to specify the variation with the speed as shown in Fig. 4.

The fundamental purpose of any engine is to provide power to the shaft. Mechanical work is determined from:

$$W = \int p dV \tag{1}$$

$$W_{net\_ind} = W_{brut} - W_{pomp} \tag{2}$$

Mechanical work resulting from the integration of pressure along the paths of compression and expansion is defined as crude mechanical work. Pumping work is the mechanical work associated with gas exchange processes (inlet-evacuation). The mechanical work on the shaft is obtained after the frictional mechanical work is removed from the previous expression:

$$W_{arbore} = W_{net\_ind} - W_{frec} \tag{3}$$

The power generated is defined by:

$$P = \dot{W} = \int p \frac{dV}{dt} = \frac{i n_r W}{60 \frac{\tau}{2}} \tag{4}$$

where n_r is the revolution in revolutions per minute. Torque can be determined from power in the form:

$$T = \frac{60P}{2\pi n_r} \tag{5}$$

4. THERMODYNAMIC SIMULATION OF THE ENGINE CYCLE

The development and use of simulation of the thermodynamic cycles of internal combustion engines dates from the early 1960s with the increase of the calculation capacity. At first simulations were based on various simplifications and approximations. From the point of view of burning, the most common approaches used single-zone and two-zone formulations. One of the first simulations is that of Patterson and van Wylen [7]. Simulation of the base thermodynamic cycle does not have a spatial support. However, the accuracy of the simulation can be improved if empirical relations are considered to locate the flame front. Thus, this type of model receives the quasi one-dimensional attribute.

Generally, quasi one-dimensional models are capable of accurately estimating the performance of spark-ignition engines. Given the rather high level of empirical input data, simulations can be tuned to provide a sufficiently close approximation of experimental data.

Energy conservation equations for the two-zone model are given by:

$$\frac{d(mu)_b}{d\theta} = \dot{Q}_b - p\dot{V}_b + \dot{m}_b h_b \tag{6}$$

$$\frac{d(mu)_u}{d\theta} = \dot{Q}_u - p\dot{V}_u + \dot{m}_u h_u \tag{7}$$

where the index u refers to the unburned area and the index b to the burned area. Previous equations can be developed by explaining derivatives from left members to extract derived internal energy derivatives:

$$\dot{u}_b = \frac{\dot{Q}_b - p\dot{V}_b + \dot{m}_b(h_b - u_b)}{\dot{m}_b} \tag{8}$$

$$\dot{u}_u = \frac{\dot{Q}_u - p\dot{V}_u + \dot{m}_u(h_u - u_u)}{\dot{m}_u} \tag{9}$$

Because the thermodynamic properties depend on temperature, pressure and composition, the previous derivatives can be rewritten as:

$$\dot{u}_b = \frac{\partial u_b}{\partial T_b}\dot{T}_b + \frac{\partial u_b}{\partial p}\dot{p} + \frac{\partial u_b}{\partial \phi}\dot{\phi} \tag{10}$$

where ϕ is the concentration vector of the mixture. For the unburned area the derivatives by pressure and composition are null, so that temporal temperature derivates for the two areas can be written as:

$$\dot{T}_b = \frac{\dot{Q}_b - p\dot{V}_b + \dot{m}_b(h_b - u_b) - m_b\frac{\partial u_b}{\partial p}\dot{p} - m_b\frac{\partial u_b}{\partial \phi}\dot{\phi}}{m_b C_{v,b}} \tag{11}$$

$$\dot{T}_u = \frac{\dot{Q}_b - p\dot{V}_u + \dot{m}_u R_u T_u}{m_u C_{v,u}} \qquad (12)$$

Next we need temporal derivation of the mixture pressure $pV = (m_b R_b T_b + m_u R_u T_u)$. Taking into account the constraint $\dot{m}_b = -\dot{m}_u$ deduced from the mass conservation equation results:

$$\dot{p} = \frac{\left(m_b R_b \dot{T}_b + m_b \left(\frac{\partial R_b}{\partial T_b}\dot{T}_b + \frac{\partial R_b}{\partial \phi}\dot{\phi}\right) T_b + m_b (R_b T_b - R_u T_u) + m_u R_u \dot{T}_u - p\dot{V}\right)}{V\left(1 - \frac{m_b \frac{\partial R_b}{\partial p} T_b}{V}\right)} \qquad (13)$$

Continuity of volume allows us to write $\dot{V}_b = \dot{V} - \dot{V}_u$ from which it can be inferred that:

$$\dot{V}_u = \frac{(m_u R_u \dot{T}_u + \dot{m}_u R_u T_u - p\dot{V}_u)}{p} \qquad (14)$$

To conclude, the five ordinary differential equations are:

$$\begin{aligned}
\dot{T}_b &= \frac{\dot{Q}_b - p\dot{V}_b + \dot{m}_b(h_b - u_b) - m_b \frac{\partial u_b}{\partial p}\dot{p} - m_b \frac{\partial u_b}{\partial \phi}\dot{\phi}}{m_b C_{v,b}} \\
\dot{T}_u &= \frac{\dot{Q}_u - p\dot{V}_u + \dot{m}_u R_u T_u}{m_u C_{v,u}} \\
\dot{V}_b &= V_b\left(\frac{\dot{T}_b}{T_b} + \frac{\dot{m}_b}{m_b} + \frac{\dot{R}_b}{R_b} - \frac{\dot{p}}{p}\right) \\
\dot{V}_u &= \dot{V} - \dot{V}_b \\
\dot{p} &= \frac{\left(m_b R_b \dot{T}_b + m_b \left(\frac{\partial R_b}{\partial T_b}\dot{T}_b + \frac{\partial R_b}{\partial \phi}\dot{\phi}\right) T_b + m_b (R_b T_b - R_u T_u) + m_u R_u \dot{T}_u - p\dot{V}\right)}{V\left(1 - \frac{m_b \frac{\partial R_b}{\partial p} T_b}{V}\right)}
\end{aligned} \qquad (15)$$

A more complex approach takes into account the finite-speed heat transfer processes and mass losses through the segment area. In this context, it is defined by x the mass fraction that burned. The calculation procedure follows the simultaneous integration of the set of differential equations for P, T_u, T_b and subsidiary calculation of net mechanical work W, the lost heat Q_1 and thermal efficiency η.

The formulation of the first Law for the contents of the cylinder is:

$$\frac{dQ}{d\theta} - P\frac{dV}{d\theta} = \frac{dU}{d\theta} + \frac{\dot{m}_1 h_1}{\omega} = m\frac{du}{d\theta} + u\frac{dm}{d\theta} + \frac{\dot{m}_1 h_1}{\omega} \qquad (16)$$

The specific volume can be written according to the burnt fraction as:

$$v = \frac{V}{m} = x v_b + (1 - x) v_u \qquad (17)$$

Because $v = v(T, P)$ results:

$$\frac{dv_b}{d\theta} = \frac{dv_b}{dT_b}\frac{dT_b}{d\theta} + \frac{dv_b}{dP}\frac{dP}{d\theta} \qquad (18)$$

$$\frac{dv_u}{d\theta} = \frac{dv_u}{dT_u}\frac{dT_u}{d\theta} + \frac{dv_u}{dP}\frac{dP}{d\theta} \qquad (19)$$

Combining previous relationships leads to:

$$\frac{1}{m}\frac{dV}{d\theta}+\frac{VC}{m\omega}=x\frac{dv_b}{dT_b}\frac{dT_b}{d\theta}+(1-x)\frac{dv_u}{dT_u}\frac{dT_u}{d\theta}+ \left[x\frac{dv_b}{dP}+(1-x)\frac{dv_u}{dP}\right]\frac{dP}{d\theta}+\left(v_b-v_u\right)\frac{dx}{d\theta} \tag{20}$$

where C is the mass loss coefficient through the area of the segments. Given that the specific internal energy of the mixture can be written as $u=U/m=xu_b+(1-x)u_u$ and $u=u(T,P)$, then:

$$\frac{du_b}{d\theta}=\left(c_{p,b}-P\frac{\partial v_b}{\partial T_b}\right)\frac{dT_b}{d\theta}-\left(T_b\frac{\partial v_b}{\partial T_b}+P\frac{\partial v_b}{\partial P}\right)\frac{dP}{d\theta} \tag{21}$$

$$\frac{du_u}{d\theta}=\left(c_{p,u}-P\frac{\partial v_u}{\partial T_u}\right)\frac{dT_u}{d\theta}-\left(T_u\frac{\partial v_u}{\partial T_u}+P\frac{\partial v_u}{\partial P}\right)\frac{dP}{d\theta} \tag{22}$$

Partial derivatives $\frac{\partial v}{\partial T}$ and $\frac{\partial v}{\partial P}$ are calculated on the basis of variable properties with temperature and pressure, depending on the composition, properties expressed in polynomial form for the various states of the mixture specified by the mass fraction x. Component $mdu/d\theta$ from the equation of first Law becomes:

$$m\frac{du}{d\theta}=mx\left(c_{p,b}-P\frac{\partial v_b}{\partial T_b}\right)\frac{dT_b}{d\theta}+m(1-x)\left(c_{p,u}-P\frac{\partial v_u}{\partial T_u}\right)\frac{dT_u}{d\theta}- \left[mx\left(T_b\frac{\partial v_b}{\partial T_b}+P\frac{\partial v_b}{\partial P}\right)+m(1-x)\left(T_u\frac{\partial v_u}{\partial T_u}+P\frac{\partial v_u}{\partial P}\right)\right]\frac{dP}{d\theta}+m(u_b-u_u)\frac{dx}{d\theta} \tag{23}$$

The term that models the decrease of mass in the cylinder can be written as:

$$\frac{dm}{d\theta}=-\frac{\dot{m}_1}{\omega}=-\frac{Cm}{\omega} \tag{24}$$

So,

$$m(\theta)=m_1\,exp[-C(\theta-\theta_1)/\omega] \tag{25}$$

represents the mass of the cylinder at a given time point from the initial mass at the beginning of the compression m_1. The term related to the heat flow in the energy equation can be modeled in terms of heat transfer:

$$\frac{dQ}{d\theta}=-\frac{\dot{Q}_1}{\omega}=\frac{-\dot{Q}_b-\dot{Q}_u}{\omega} \tag{26}$$

$$\dot{Q}_b=hA_b(T_b-T_w);\quad \dot{Q}_u=hA_u(T_u-T_w) \tag{27}$$

in which h is the coefficient of heat transfer by convection A_u and A_b are areas of burned and non-combustion areas in contact with cylinder walls at temperature T_w. Area A_c the cylinder can be divided so:

$$A_c=\frac{\pi b^2}{2}+\frac{4V}{b};A_b=A_cx^{1/2};A_u=A_c(1-x^{1/2}) \tag{28}$$

The fraction of the area in contact with the flue gas is supposed to be proportional to the fraction of the mass fraction that burned to illustrate that, because of the density difference, the flue gases occupy a larger volume than that occupied by the non-fired gases. The enthalpy of the lost mixture through the area of the segments can be calculated from the relationship:

$$h_1 = (1 - x^2)h_u + x^2 h_b \tag{29}$$

The burned mass fraction can be either Wiebe's function:

$$x = 1 - exp\left[-c\left(\frac{\theta - \theta_0}{\Delta\theta}\right)^{r+1}\right] \tag{30}$$

where θ_0 is the RAC angle of the beginning of burning, $\Delta\theta$ is the burning time and c and r are adjustable parameters, or the table function:

$$x = 0, \theta < \theta_0; x = \frac{1}{2}\left(1 - cos\left(\frac{x(\theta - \theta_0)}{\Delta\theta}\right)\right);\ x = 1, \theta > \theta_0 + \Delta\theta \tag{31}$$

Considering unbound gas as an open chemical reagent that loses mass, it can be shown that:

$$-\dot{Q}_u = \omega m(1 - x)T_u \frac{ds_u}{d\theta} \tag{32}$$

Since $s_u = s_u(T_u, P)$, results

$$c_{p,u}\frac{dT_u}{d\theta} - T_u \frac{dv_u}{dT_u}\frac{dP}{d\theta} = \frac{-hA_u}{\omega m\,(1-x)}(T_u - T_w) \tag{33}$$

Taking into account all the equations mentioned so far, the following variables can be defined:

$$\begin{aligned}
A &= \frac{1}{m}\left(\frac{dV}{d\theta} + \frac{VC}{\omega}\right)\\
B &= \frac{hA_c}{\omega m}\left[\frac{1}{c_{p,b}}x^{1/2}(T_b - T_w)\frac{\partial v_b}{\partial T_b} + \frac{1}{c_{p,b}}(1 - x^{1/2})(T_u - T_w)\right]\\
C &= -(v_b - v_u)\frac{dx}{d\theta} - \frac{\partial v_b}{\partial T_b}\frac{h_u - h_b}{c_{p,b}}\left[\frac{dx}{d\theta} - \frac{(x - x^2)C}{\omega}\right]\\
D &= x\left[\frac{T_b}{c_{p,b}}\left(\frac{\partial v_b}{\partial T_b}\right)^2 + \frac{\partial v_b}{\partial P}\right]\\
E &= (1 - x)\left[\frac{T_u}{c_{p,u}}\left(\frac{\partial v_u}{\partial T_u}\right)^2 + \frac{\partial v_u}{\partial P}\right]
\end{aligned} \tag{34}$$

The equations to be integrated are:

$$\begin{aligned}
\frac{dP}{d\theta} &= \frac{A+B+C}{D+E}\\
\frac{dT_b}{d\theta} &= \frac{-hA_c(T_b - T_w)}{\omega m c_{p,b} x^{1/2}} + \frac{T_b}{c_{p,b}}\frac{\partial v_b}{\partial T_b}\frac{A + B + C}{D + E} + \frac{h_u - h_b}{x c_{p,b}}\left[\frac{dx}{d\theta} - \frac{(x - x^2)C}{\omega}\right]\\
\frac{dT_u}{d\theta} &= \frac{-hA_c(1 - x^{1/2})(T_b - T_w)}{\omega m c_{p,b}(1 - x)} + \frac{T_u}{c_{p,u}}\frac{\partial v_u}{\partial T_u}\frac{A + B + C}{D + E}
\end{aligned} \tag{35}$$

$$\frac{dW}{d\theta} = P\frac{dV}{d\theta}$$
$$\frac{dQ_1}{d\theta} = \frac{hA_c}{\omega}\left[x^{1/2}(T_b - T_w) + (1 - x^{1/2})(T_u - T_w)\right]$$
$$\frac{dH_1}{d\theta} = \frac{Cm}{\omega}[(1 - x^2)h_u + x^2 h_b]$$

The above equations are numerically integrated in Matlab. Input data are bore, stroke, speed, compression ratio, mass loss coefficient, heat transfer coefficient, cylinder temperature, initial pressure and temperature. The initial temperature for the burnt area is estimated from the calculation of the adiabatic temperature of the flame based on the enthalpy at the moment of initiation of the spark. If $x < 0.001$, the system is considered to be composed only of non-fired gases and if $x > 0.999$, we only deal with flue gases. The program contains a routine for the expression of the thermodynamic properties depending on the residual fraction (flue gas from the previous cycle) and another routine for calculating the composition and the equilibrium properties for a chemical reactive mixture.

As the compression ratio is completely unknown, we had to try several sets of values for the input data and compare the power obtained with the manufacturer's data. For this, it is necessary to estimate the power lost by friction and pumping (2), (3). The power lost through friction inside the cylinder depends on the cylinder and the speed can be estimated from the relationship:

$$P_f = (100000 + 20n_r)V_s n_r/60 \quad (36)$$

The power lost due to the pumping process depends to a large extent on the inlet pressure P_1 and the exhaust pressure in the environment P_e

$$P_p = (P_e - P_1)V_s n_r/60 \quad (37)$$

With this data the following results were obtained:

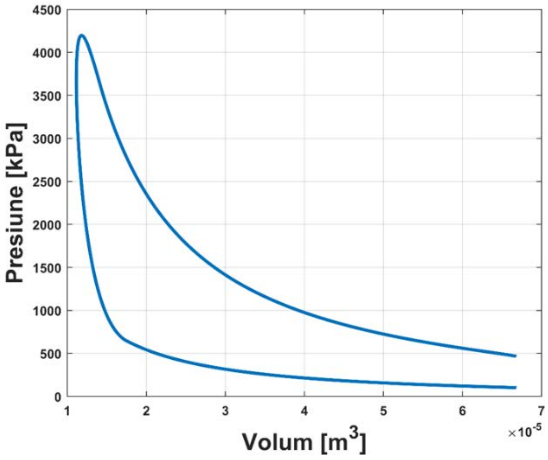

FIG. 5 Variation of cylinder pressure for no mass exchange evolutions.

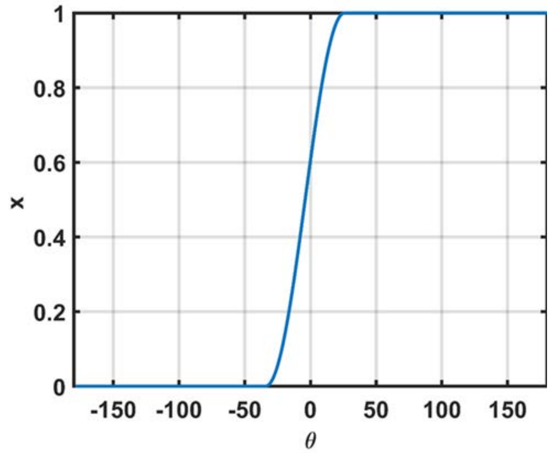

FIG. 6 The variation of the burning mass fraction burned with the crankshaft angle.

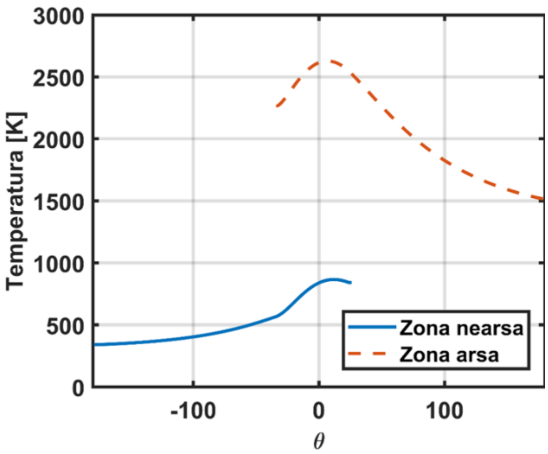

FIG. 7. Temperature variation in the burned and unburned area with the crank angle.

Since the engine test was carried out with the attached generator, the power to the shaft must be penalized by taking into account the power absorbed by the generator. The variation of this generator power is specified in Fig. 8. The results of the simulation are compared with the experimental results in Fig. 9.

FIG. 8 Power absorbed by the generator.

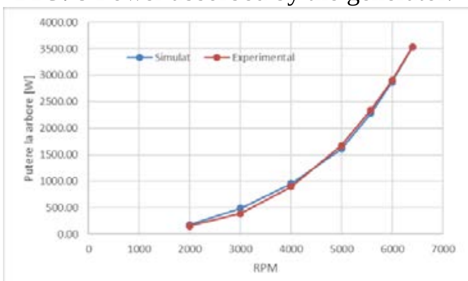

FIG. 9 Simulation comparison and SLS experiment for engine 3w 55xi fi.

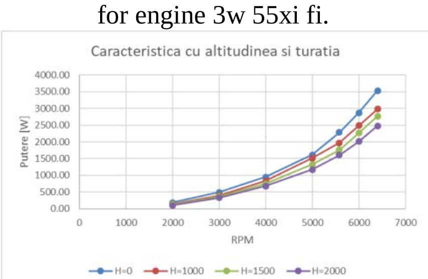

FIG. 10 Characteristics with turning and altitude.

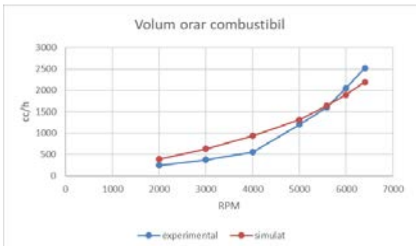

FIG. 11 Comparison of fuel consumption between simulation and SLS experiment for the engine 3w 55xi fi.

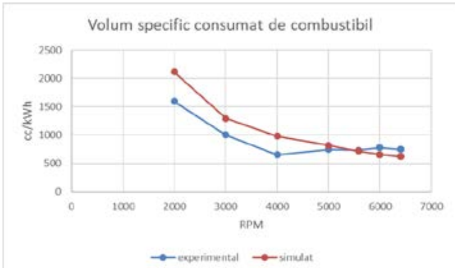

FIG. 12 Specific fuel consumption comparison between simulation and SLS experiment for the engine 3w 55xi fi.

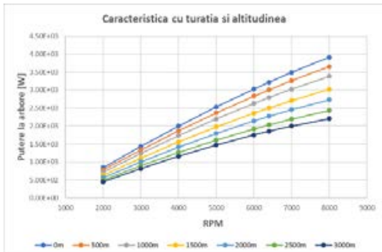

FIG. 13 Shaft power.

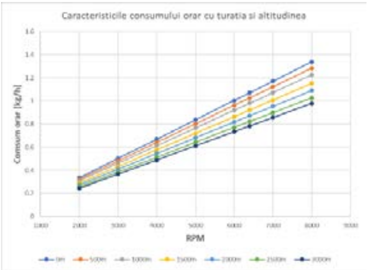

FIG. 14 Hourly consumption

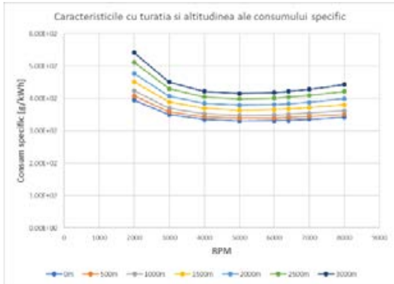

FIG. 15 Specific consumption

The results are quite promising, especially in terms of sea level power variation. Hourly and specific consumption are somewhat affected by less accurate engine yield estimation, so errors that fall within the 10% margin of uncertainty about data used in the simulation.

5. PERFOMANCES OF THE HYBRID PORPULSION FIXED WING VTOL UAV

The geometric reference data taken into account for the performance calculations are shown in Fig. 16, considering a reference origin at the nose of the fuselage, the Ox axis along the fuselage, the Oy axis along the wing span, and the Oz axis perpendicular to the Oxy plane pointing downwards.

The mass of the structural components was estimated by statistical methods and their weight centers were determined by considering the average density introduced in the 3D CAD model shown in Fig. 17.

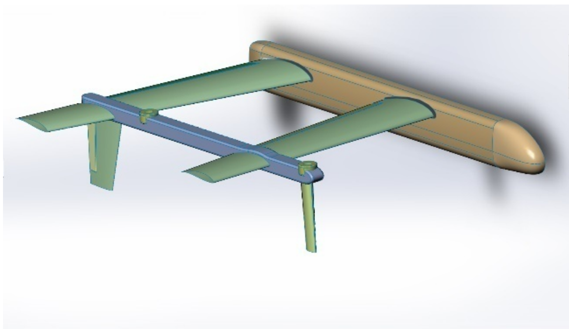

FIG. 16 Reference geometry

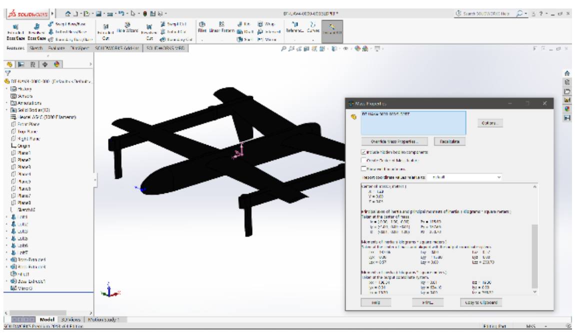

FIG. 17 Aircraft balance

The aerodynamic characteristics of the aircraft were determined by a method developed by the authors, based on the work [8]. The results were compared with those obtained from specialized software systems:

- XFLR5, [9], which uses the Vortex Lattice Method for small Re numbers;
- AVL, [10], a program for aerodynamics and flight dynamics analysis of rigid aircraft of arbitrary configuration. It uses a model of Extended Vortex Lattice for lifting surfaces, along with a thin body model for fuselage and nacelles. General nonlinear flight states can be specified. Dynamic Flight Analysis combines a complete aerodynamic alignment for any flight state with the specified mass properties;
- Advanced Aircraft Analysis, [11], produced by DARcorporation, is a comprehensive airplane design program that gives users full authority over the entire preliminary design process. From weight and performance to aerodynamic analysis and stability and control, all aspects of design at every step of the road can be monitored.

• RDSwin allows engineers to take up an aircraft project from the first conceptual point of view through functional analysis, resulting in performance, endurance, weight and cost. RDSwin integrates design (CAD), aerodynamic calculation, mass estimate, propulsion, stability and control, sizing, performance and cost analysis.

Most performance calculations and flight dynamics have gone from defining a basic, stationary movement, usually straight cruise flight uniform. The aerodynamic characteristics of the airplane will be equilibrium. Therefore, the equilibrium polar determined by calculation or experiment is used.

Starting from the expression of the moment of pitch according to the flight incidence and the elevator deflection, we can determine for each angle of attack the equilibrium by solving the equation:

$$C_m(\alpha, \delta_e) = 0 \tag{38}$$

6. PROPELLER DESIGN, AVAILABLE POWER

The next step to determine the performance in uniform motion of the aircraft requires the determination of available power depending on speed and fuel consumption; it is necessary to obtain:

- Power supplied by the engine to the propeller shaft (Fig. 13)
- Propeller characteristics: coefficients of traction C_T, moment of drag C_Q, used power C_P and propeller efficiency η (Fig. 18)
- Specific fuel consumption (Fig. 15)

Calculation of the propeller characteristics was done with the propCalc program [12]. The calculated propeller geometry is given in Fig. 18 and its features are shown in Fig. 19.

FIG. 18 Geometry of the propeller

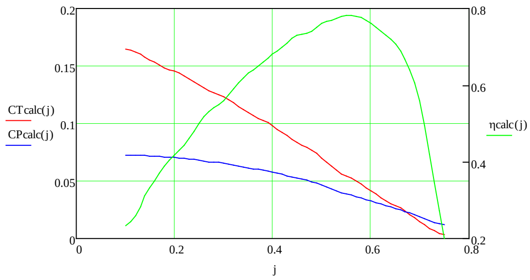

FIG. 19 Propeller features

The algorithm for determining the power available by the speed implies the determination of the propeller speed from the balance between the power consumed by the propeller and the power supplied to the shaft.

At a given altitude the $P_a(\Omega)$ function is extracted (Ω = propeller speed in rad/s), then, from the propeller characteristics, the power consumed by the propeller is calculated with:

$$J = \frac{60V}{\Omega D_{prop}}; \quad P_e(\Omega, \mathrm{V}) = \rho(H)\left(\frac{\Omega}{60}\right)^3 D_{prop}^4 \, CP_{calc}(J) \tag{39}$$

where $D_{prop} = 21" = 0.533m$ is propeller diameter, and $P_{prop} = 11" = 0.279m$ is propeller pitch.

The steady speed is found by solving the equation below for a selected flight speed:

$$P_e(\Omega, \mathrm{V}) - P_a(\Omega) = 0 \quad \rightarrow \quad \Omega(\mathrm{V}) \tag{40}$$

Finally, the available power is given by (Fig. 20):

$$P_d(\mathrm{V}) = \eta(J(\Omega(\mathrm{v}),\mathrm{V}))P_e(\Omega(\mathrm{V}),\mathrm{V}) \tag{41}$$

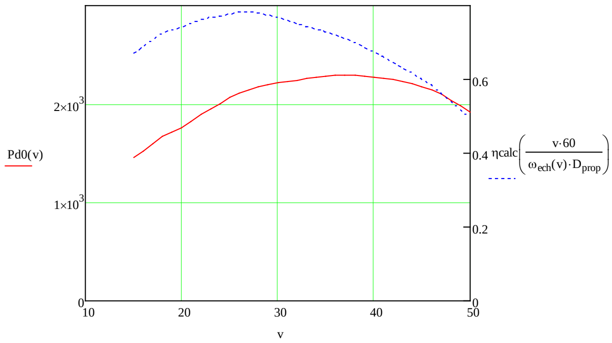

FIG. 20 Available power

7. FLIGHT PERFORMANCES IN SIMETRIC MOVEMENTS IN THE VERTICAL PLANE, FLIGHT ENVELOPE

The limits of the rectilinear flight velocity are determined at each altitude of calculation by the intersection of available and necessary power for maximum speed and by determining the speed corresponding to the minimum required power. The minimum required power is determined with the relations:

$$C_L = \frac{2Wg}{\rho(H)SV^2}; \quad P_n(\mathrm{V}) = 0.5\rho(H)SV^3C_D(C_L) \tag{42}$$

and the intersection $P_d = P_n$ gives us the speed of balance $V2$. The minimum power point allows us to find the minimum speed $V1$:

$$V2_0 = root(P_n(V) - Pd_0(V), V) = 43.41\, m/s$$
$$V1_0 = root\left(\frac{d}{dV}P_n(V), V\right) = 19.94\, m/s \tag{43}$$

This algorithm was shown graphically in Fig. 21, where the equilibrium flight incident was also represented at each speed. Note that the steady-state incidence is negative $\alpha_{ech} = -1.4$ deg., but it has a small value, so it is acceptable.

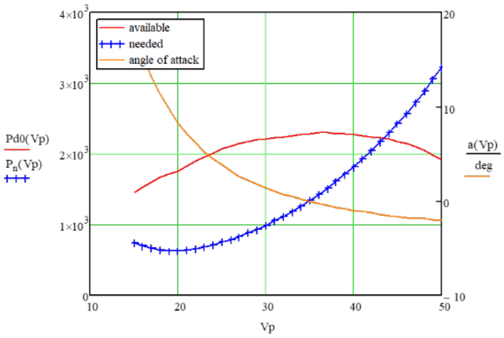

FIG. 21 Method of power available and required (H = 0m)

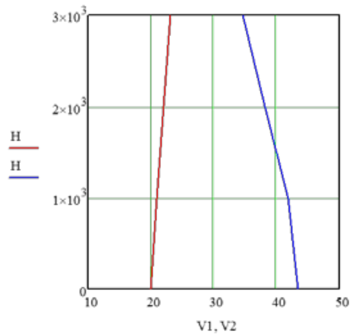

FIG. 22 Flight envelope

Doing the same for all altitudes for which the outputs for the shaft power supplied by the engine are calculated: 1000, 2000 and 3000m, it can be obtained $V2(H)$ and $V1(H)$, which are graphically represented in the flight envelope of Fig. 22.

For the study of the uniform rectilinear climb, also the necessary and available power method is applied starting from the stationary motion equations:

$$C_L = \frac{2Wg\cos(\gamma)}{\rho(H)SV^2}; \quad P_n(\mathrm{V}) = 0.5\rho(H)SV^3C_D(C_L) + Wg * \sin(\gamma) \tag{44}$$

where through γ the trajectory slope was noted. For a given altitude and a flight slope we determine the necessary C_L as a function of velocity. From the equilibrium polar is determined C_D and the $P_n(\mathrm{V})$.

Intersect the required power with the available power and determine the speed. The pairs (γ, V) such obtained are used to plot the climbing characteristic (Fig. 23), in coordinates $(Vcos(\gamma), Vsin(\gamma))$.

Based on the climbing characteristic, it can be concluded that:

- The maximum ascending speed, in steady state, is 3.8m/s, at a flight speed of 25.9m/s, and
- The maximum climb slope is 9deg. At a flight speed of 22.6m/s

Gliding flight is treated similarly, with the difference that we have no available power and the slope is negative. The gliding flight characteristic is shown in Fig. 24.

The conclusion of the gliding flight study is that:

- The minimum descent speed in stationary mode is 2m/s at a flight speed of 23m/s due to limitation given by the maximum speed, and
- The minimum gliding slope is 5 degrees, at a flight speed of 21m/s

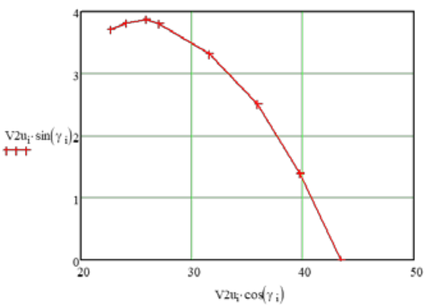

FIG. 23 The climbing characteristic

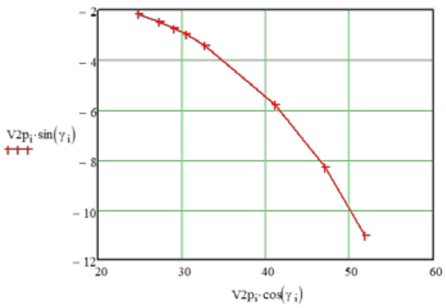

FIG. 24 The gliding characteristic

8. ELECTRO-ENERGETIC SYSTEM

According to the ISO 1540: 2006-Electric Power System [6], the Power System is the set of power sources and converters, their control and protection equipment, as well as electrical consumers connected through the distribution network. Figure 25 shows the power system of the UAV. From this it can be noticed that the electric energy is obtained with the generator and the on-board battery. This is used to provide UAV propulsion in VTOL mode, to power the equipment required for control and navigation as well as payload.

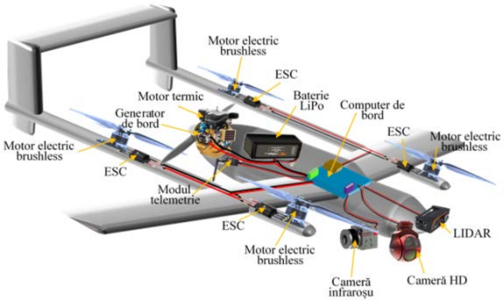

FIG. 25 The power system of the uav - biplane-quad-copter hybrid

9. ANALYSIS OF VTOL FLIGHT

To determine the engine power needed during VTOL flight, it is necessary to determine the traction force of the fixed wing vector in the takeoff and landing phase for different scenarios. Studying the type of missions of this type of UAV, 3 flight ceilings were established: 100m, 1000m and 2500m. Entering the specific data in the eCalc program [13] for the three flight ceilings we obtain:

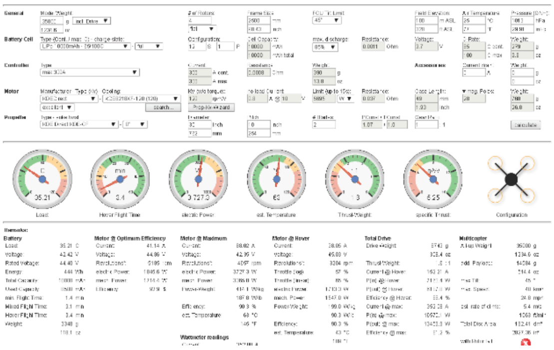

FIG. 26 The simulation data at la 100m

FIG. 27 The simulation data at 1000 m

FIG. 28 The simulation data at 2500 m

Corroborating the results of the three scenarios, the following maximum engine power and hover power dependence on the altitude (Fig. 29) results:

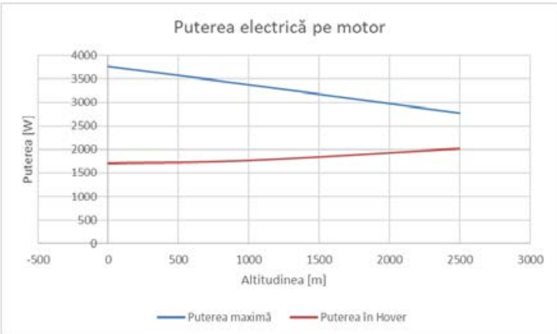

FIG. 29 Maximum and hover power

For designing the battery required to power the four KDE8218XF-120 motors, as well as the internal systems we propose the following scenarios:

1. The battery is used to secure the lifting of the fixed wing to ceiling 2500 m, 1000 m and 100 m, respectively, powering only the four KDE8218XF-120 motors without powering the onboard electronics;
2. Hover to the ceiling 2 min. required for the transition to and from the horizontal flight, and power the onboard electronics during the flight until the generator starts;
3. The battery is used both to ensure that the fixed wing vector is lifted to the flight ceiling, 2 min to hover for transition and to power the onboard electronics (if the generator failure is signaled).

From Flight Simulations we extract the following data:

Altitude [m]	Rate of climb [m/s]	Rate of descent [m/s]
100	5.4	3
1000	4.5	3
2500	1.3	3

with which the following durations are calculated:

Ceiling [m]	Climb time [s]	Descent time [s]
2500	670	833
1000	202	333
100	19	33

where an average descent speed of 3 m/s was assumed, regardless of altitude.

From the maximum power and hover:

Altitude [m]	Max Power [W]	Hover Power [W]
0	16762	7138
100	16570	7163
1000	14840	7391
2500	11985	8524

calculate an average power up to the flight ceiling, with which, for a battery 12S ($U = 44{,}4V$), the energy requirement is calculated for the three scenarios:

Altitude [m]	Battery capacity [Ah]			Flight time [min.]		
	Scenario 1	Scenario 2	Scenario 3	Scenario 1	Scenario 2	Scenario 3
100	63	70	96	11	13	27
1000	20	26	37	3.4	5.4	10.9
2500	2	7.4	8.6	0.3	2.3	2.9

The following characteristics are obtained:

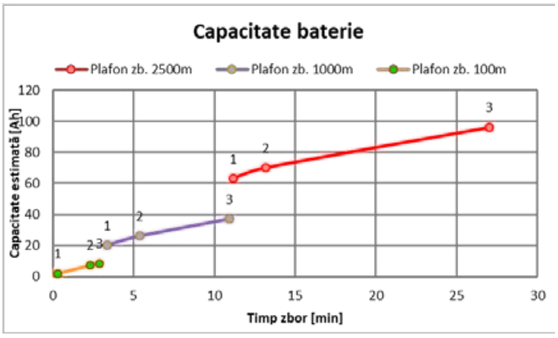

FIG. 30 Battery capacity

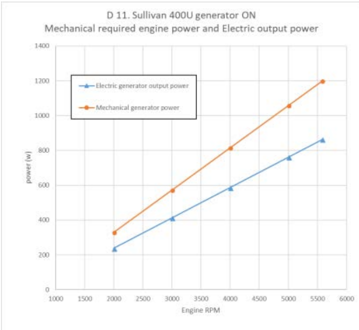

FIG. 31 Generated and required generator power

The following conclusions can be drawn:

• For Scenario 3 that requires the most battery, a capacity of about 100Ah is required, which requires a too heavy battery;

• For a capacity of 30Ah, the ceiling of approximately 1500m in Scenario 1, 1200m in Scenario 2, and 800m in Scenario 3 (generator failure and landing of the aircraft) can be reached.

• For a 30Ah capacity, the combined flight time would be about 8 minutes.

In conclusion we choose a 30Ah 12S3P battery with an approximate weight of 4kg.

For the onboard generator from the electrical characteristics of the generator it follows that the electric generated power at 4000rpm is 587W.

As the battery is 12S3P, with a voltage at 44.4 V, the voltage at the generator terminals, for the battery to charge, can be 50V, meaning a nominal current of 10A.

The time required to charge the battery in the most favorable condition (reaching the highest flight ceiling), Scenario 1, at approximately 1500 m is:

$$t_{încărcare,1} = \frac{C}{I_N} = \frac{33\,Ah}{10\,A} = 3{,}3\,h \tag{45}$$

But as the engine power during vertical descent is 1/3 of the maximum climb power, it turns out that only 1/3 of the battery capacity is required for safe landing, which means:

$$t_{încărcare,2} = \frac{C/3}{I_N} = \frac{33\,Ah/3}{10\,A} = 1{,}1\,h \tag{46}$$

an acceptable time for most flight missions.

10. CONCLUSIONS

A hybrid propulsion system for a fixed wing VTOL UAV was designed and tested. Shaft Power of the main engine was determined for a whole range of operating conditions were computed using an in-house developed mathematical model.

Propeller characteristics were determined and an original method to determine available power was used. With this, cruise, climb and descent performances of the aircraft were determined with in-house methodology and compared with result from commercial available software, result showing good agreement.

Takeoff and landing electric motors characteristics and hoover time were determined from the power provided from the batteries. Also the time to recharge during cruise flight was assessed. Results shows good performances for the mission required.

REFERENCES

[1] *** The UAVs. A brief introduction to the UAV Endurance. May 22, 2016. [Interactive] [Quoted: 30 October 2018] http://www.theuav.com;

[2] Button, K., Powering Airlines with hydrogen, Aerospace America, Vol. 54, p. 5, 2016;

[3] Daidzic, N. E., Piancastelli, L. și Cattini, A., Diesel engines for light-to-medium helicopters and airplanes, International Journal of Aviation, Aeronautics, and Aerospace, Vol. 1, 2014;

[4] Frisch, A. M., Scaling Effects on the Performance and Efficiency of Gas Turbine Engines, Master of Science Project, University of California. Irvine, 2017;

[5] Cirigliano, D., Engine-type and propulsion configuration selections for long-duration UAV flights, M.Sc. Thesis, Department of Aerospace Science and Technology, School of Industrial and Information Engineering, Politecnico di Milano, 2017;

[6] ***. ISO 1540. 2006;

[7] Patterson, D. J. și van Wylen, G., A digital computer simulation for spark-ignited engine cycles, in Digital Calculations of Engine Cycles, SAE Progress in Technology, Society of Automotive Engineers, Vol. 7, 1964;

[8] M., M. Niță, F., V. Moraru și R., N. Patraulea, Aeronave și rachete. concepte de proiectare, Editura Militară, 1985;

[9] A. Deperrois, et. al., XFLR5, [Interactive] [Quoted: 22 11 2018.], http://www.xflr5.com/xflr5.html;

[10] Mark Drela, Harold Youngren, AVL, [Interactive] [Quoted: 22 11 2018], http://web.mit.edu/drela/Public/web/avl/;

[11] Dr. Jan Roskam, DAR Corporation, Advanced Aircraft Analysis, [Interactive] [Quoted: 22 11 2018], http://darcorp.com/Software/AAA/;

[12] Schenk, Helmut, Propeller Calculator, [Interactive] [Quoted: 22 11 2018], http://www.drivecalc.de/PropCalc/.

[13] M., Muller, e-Calc the most reliable RC Calculator on the Web, [Interactiv] [Quoted: 22 01 2019] https://www.ecalc.ch/.

ASPECT REGARDING THE CHOICE OF AN AIR OR GROUND AMBULANCE FOR THE PROVISION OF EMERGENCY MEDICAL CARE ON THE TERRITORY OF THE REPUBLIC OF BULGARIA

Ivan IVANOV, Yulian STANCHEV

”Vasil Levski” National Military University, Aviation Faculty, Dolna Mitropolia, Bulgaria (ikivanov@nvu.bg, jstanchev@aff.nvu.bg)

DOI: 10.19062/2247-3173.2019.21.20

Abstract: *An algorithm and a program instrument for making a decision on the use of a helicopter or a specialized car for emergency medical care in the Republic of Bulgaria is proposed. A Matlab program implementation is developed. As a result, helicopter or ambulance from the nearest centre is activated.*

Keywords: *helicopter, ambulance, emergency medical care, air rescue center, algorithm*

1. INTRODUCTION

The report proposes one possible algorithm for decision making on the use of a helicopter or a specialized car for emergency medical care in the Republic of Bulgaria. The basic criterion of the presented algorithm is the time of one hour “golden hour” to help an injured person.

2. DECISION-MAKING ALGORITHM FOR THE USE OF EMERGENCY MEDICAL ASSISTANCE BY AIR OR A SPECIALIZED CAR IN THE REPUBLIC OF BULGARIA

The report presents the main centers for emergency medical care in Bulgaria. Their exact coordinates are determined in Google Earth in degrees [1]. There are hospitals capable of providing the necessary help to a injured person close to these centers for emergency medical care.

There is also a minimum number of air rescue centers on Bulgaria's territory, where helicopters for emergency medical care are located. Their coordinates are determined also [1]. In practice, such centers do not exist in Bulgaria in this way. The following factors have been taken into account to determine their location:

✓ the most complete coverage on the territory of the country, places difficult to reach for road vehicles (areas with hilly-mountain and mountainous relief), main roads and railways, sea and river areas;

✓ possible disaster threats analyzed for the territory of Bulgaria;

✓ availability of centers for emergency medical care and hospitals, disposable helicopters and airport infrastructure;

✓ dislocation of formations by the Bulgarian Army to help the population in disasters Fig. 1.

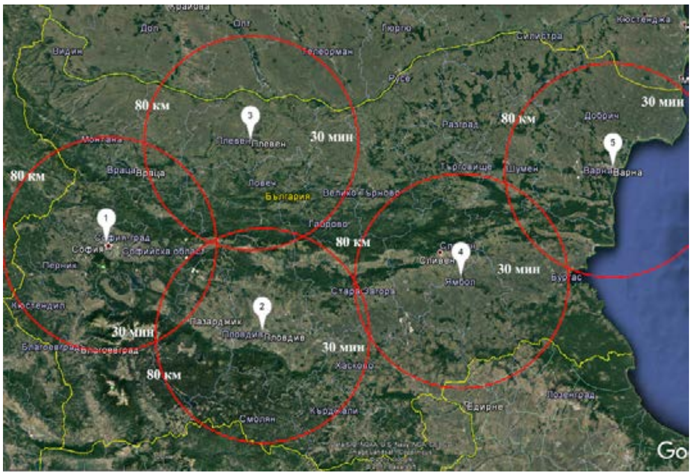

FIG. 1. Location of possible air rescue centers on the territory of the Republic of Bulgaria

The purpose of the algorithm is to allow the selection of an emergency medical center or an air rescue center from which an ambulance or helicopter can be dispatched. The selection criterion is the time for transporting an injured person to a hospital from reporting a case, which should not exceed one hour.

The possible areas of helicopter and ambulance action from the respective centers are determined, depending on their average speeds and the reaction time of the centers. The response time of the centers is 10 minutes. The speed of an ambulance is estimated at 70 km/h, for a helicopter - 230 km/h. The algorithm drawn is the type shown in Fig. 2.

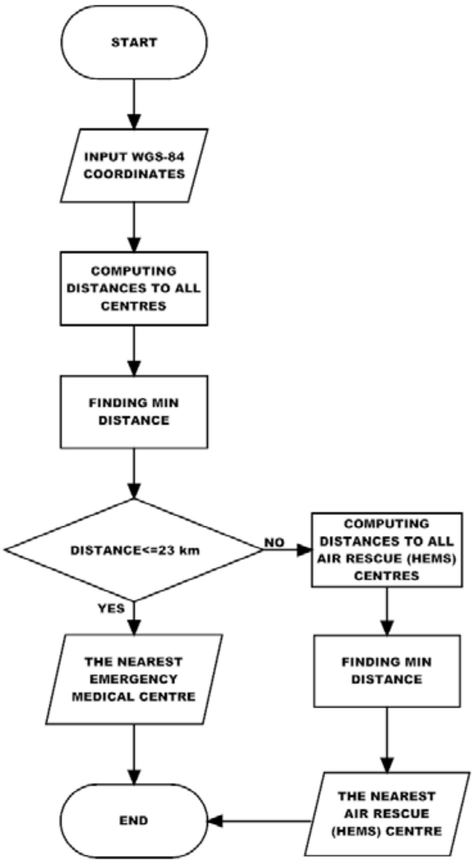

FIG. 2. Algorithm for selecting an ambulance or helicopter from the nearest center to help an injured person

3. PROGRAM IMPLEMENTATION

This algorithm is used to compile a program that allows you to select and activate a specific emergency medical center or air rescue center from the territory of Bulgaria. If there is a possibility an injured person to be transported to a hospital within 1 hour from reporting a case by ground ambulance, it is not necessary to use a helicopter. When entering the coordinates of an injured person, the program provides the option of choosing a particular center to be activated.

Fig. 3 and Fig. 4 represents results after program calculation.

Command Window

```
>> emergency_medical_care
 Input WGS-84 coordinates of injured person
 Longitude (degrees):  24.53
 Latitude (degrees):  43.24
 The nearest emergency medical care centre is in
Lovech
 on distance 18.5971 km
 Use ambulance from emergency medical care centre. The distance is less than 23 km.
```

Fig. 3. Decision to use an ambulance to provide emergency medical care

```
>> emergency_medical_care
 Input WGS-84 coordinates of injured person
 Longitude (degrees):  23.51
 Latitude (degrees):  42.23
 The nearest emergency medical care centre is in
Blagoevgrad
 on distance 41.4855 km
The nearest air rescue (HEMS) centre is in
Sofia
 on distance 54.536 km
 Use helicopter from air rescue centre.
```

Fig. 4. Decision to use a helicopter for emergency medical care

CONCLUSIONS

The program implemented on the presented algorithm is to be improved by introducing a detailed digital map of Bulgaria. This will increase the accuracy of choosing a particular center and better illustrate the specific situation of the emergency.

REFERENCES

[1] *** Google Inc. *Google Earth*

CALCULATING TOOL FOR THE SPRING CONSTANT OF A SERPENTINE FLEXURE USED IN INERTIAL MEMS DEVICES

Petre NEGREA, Vlad Aurelian VĂDUVESCU

University of Craiova, Romania (pnegrea@elth.ucv.ro, vlad93v@yahoo.com)

DOI: 10.19062/2247-3173.2019.21.21

Abstract: *A Matlab/Simulink tool for calculating the constant of elasticity of a serpentine flexure is here presented. The tool is developed for four different equations, in terms of two axis, and even or odd number of meanders. Here are shown four types of microsuspension used in the MEMS devices, the component elements and structure of a serpentine flexure and the Matlab/Simulink models resulted from the mathematical equations. The simulations results, compared with those in the literature, confirms that the developed tool is correctly implemented.*

Keywords: *MEMS, microsuspension, serpentine flexure.*

1. INTRODUCTION

The tendency of systems miniaturization has led to the revolution of any product, but also brought with it some major problems, mainly from the manufacturing point of view.

Miniaturization of the systems led to new technologies such as MEMS (micro-electro-mechanical-systems) and NEMS (nano-electro-mechanical-systems). In the field of inertial navigation, from the point of view of aerospace, transport and naval engineering, miniaturized devices occupy an important place due to accelerometers and gyros, sensors that are used to detect and measure movements. MEMS actuators and sensors, due to their small size, brought the advantages of a low mass and volume, low energy consumption, greatly reducing the mass and size of a vehicle without sacrificing functionality. The major disadvantages are that they are susceptible to parasitic vibrations, mechanical and thermal shocks, and require a considerable amount of optimization calculation [1, 2, 3].

An important component in the study of inertial sensors, and in general of MEMS devices, is the elastic element. The microsuspensions (elastic element) used in the MEMS field can vary, both in shape and as the material of which they are composed, depending on their use [4].

2. COMMONLY USED ELASTIC STRUCTURES FOR THE INERTIAL SENSORS

The most commonly used elastic structures for inertial sensors are shown in Fig. 1 [4, 5]. Thus, four flexion patterns can be observed: a) fixed-fixed flexure; b) crab leg flexure; c) folded flexure; d) serpentine flexure. The four configurations present a seismic mass attached at the ends with different elastic elements.

The calculation for the elasticity constant of each configuration is rigorous and can be found in [4, 5].

According to the Fig. 1, can be observed an increase in structural complexity in terms of the number of components and their design, thus, the architecture of the model d) can provide a higher sensitivity from the input measurement point of view. Also, the rigidity of the serpentine flexure can be greatly adjusted, in the design phase, by changing the number of items, depending on the utility.

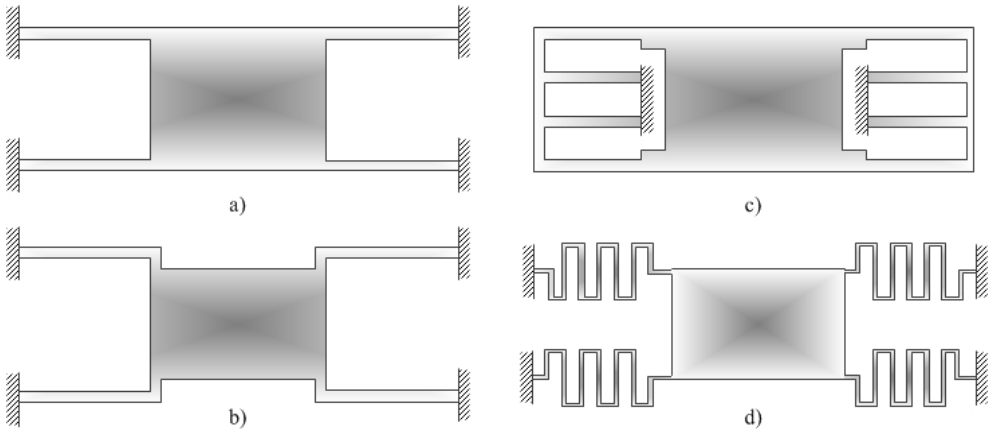

FIG. 1. Elastic structures for inertial sensors: a) fixed-fixed flexure; b) crab leg flexure; c) folded flexure; d) serpentine flexure

3. MATLAB/SIMULINK MODEL

In the calculus of the acceleration for an inertial accelerometer, an important role has the elasticity constant of the sensing element, this being directly related to the movement of the seismic mass [3]. The elastic force acting on the seismic mass is:

$$F_e = k \cdot x \tag{1}$$

where, F_e is the elastic force, k is the constant spring and x is the displacement of the proof mass.

If an acceleration acts on the seismic mass, for the simple configuration [seismic mass → elastic element], due to the Newton's 2nd law, in eqilibrum can be written:

$$m \cdot a = k \cdot x \tag{2}$$

So, it can be observed that in the determination of acceleration, spring constant plays an important role.

For this purpose, the paper presents a Matlab/Simulink calculation tool for the spring constant of the serpentine flexure. A schematic representation of the serpentine is shown in Fig. 2, where in a) is illustrated the overall configuration with four springs attached to the proof mass, that intuitively hints the fact that they can be adjusted in number of its elements, and in b) is detailed one typical spring [4, 5, 6, 7, 8].

The model is composed of several meanders, each meander has the same length *a* and width *b*, more precisely each meander is composed of 2 segments of different lengths, vertically *b*, horizontal *a*. Each segment of the meanders, according to right picture from the fig. b) is of width w_a for the horizontal segment and w_b for the vertical segment, and thickness *h* [4].

The coordinate system for which the calculation was performed was considered as the *x*-axis along the segment *b*, positive upwards, the *y*-axis along segment *a*, positive from the fixed end to the seismic mass, and the *z*-axis along the thickness *h*, perpendicular to the two axis.

The spring constants for which the Matlab/Simulink model has been created are only those in the *x* and *y* directions.

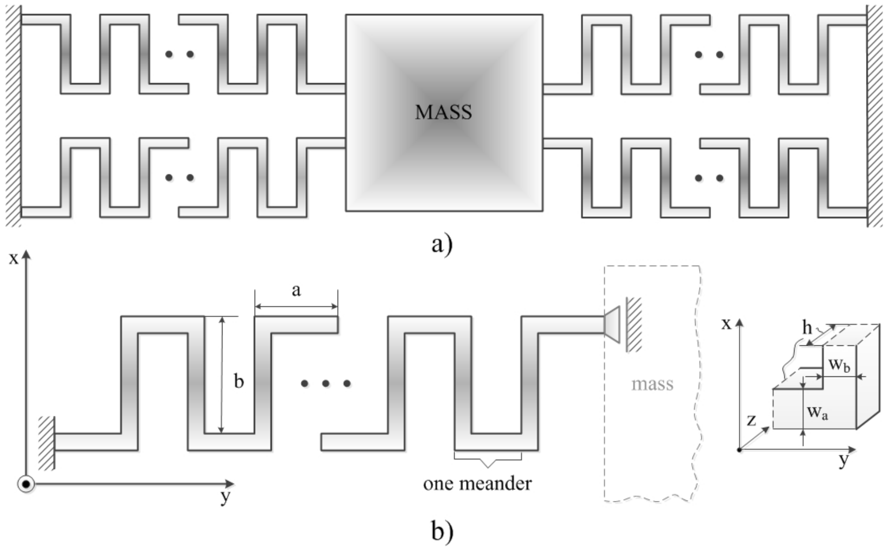

FIG. 2 Serpentine schematic representation: a) overall configuration with four springs; b) one typical spring

The general equation of the spring constant changes according to the parity of the number of meanders. Thus, according to [4], for even *n*:

$$k_x = \frac{48EI_{z,b}\left[(3\overline{a}+b)n-b\right]}{a^2n\left[(3\overline{a}^2+4\overline{a}b+b^2)n^3-2b(5\overline{a}+2b)n^2+(5b^2+6\overline{a}b-9\overline{a}^2)n-2b^2\right]}, \tag{3}$$

$$k_y = \frac{48EI_{z,b}\left[(\overline{a}+b)n^2-3bn+2b\right]}{b^2\left[(3\overline{a}^2+4\overline{a}b+b^2)n^3-2b(5\overline{a}+2b)n^2+(5b^2+6\overline{a}b-9\overline{a}^2)n-2b^2\right]} \tag{4}$$

where, k_x, k_y are the spring constants in the *x* and *y* directions, *n* is the number of meanders, *E* is the Young modulus and,

$$\overline{a} = \frac{I_{z,b}\cdot a}{I_{z,a}}; \tag{5}$$

$$I_{z,b} = \frac{h\cdot w_b^3}{12}; \tag{6}$$

$$I_{z,a} = \frac{h\cdot w_a^3}{12}; \tag{7}$$

with $I_{z,a}$, $I_{z,b}$ the moment of inertia.

For odd *n*:

$$k_x = \frac{48EI_{z,b}}{a^2n\left[(\overline{a}+b)n^2-2bn+2b\right]}, \tag{8}$$

$$k_y = \frac{48EI_{z,b}\left[(\bar{a}+b)n - b\right]}{b^2(n-1)\left[(3\bar{a}^2 + 4\bar{a}b)n + 3\bar{a}^2 - b^2\right]}. \tag{9}$$

Using the equations (3-9) a Matlab/Simulink model was created and calculates the spring constant on two axes, x and y. Given that the equations differ according to the parity of the number of meanders and the fact that there are two axes, 4 distinct blocks were created (Fig. 3). For the respective blocks, grouped into one (Fig. 4) that represents the final calculation tool, a mask was implemented (Fig. 5) to introduce the constructive parameters of the analyzed structure. The user can easily enter these parameters manually, without having to introduce the equations.

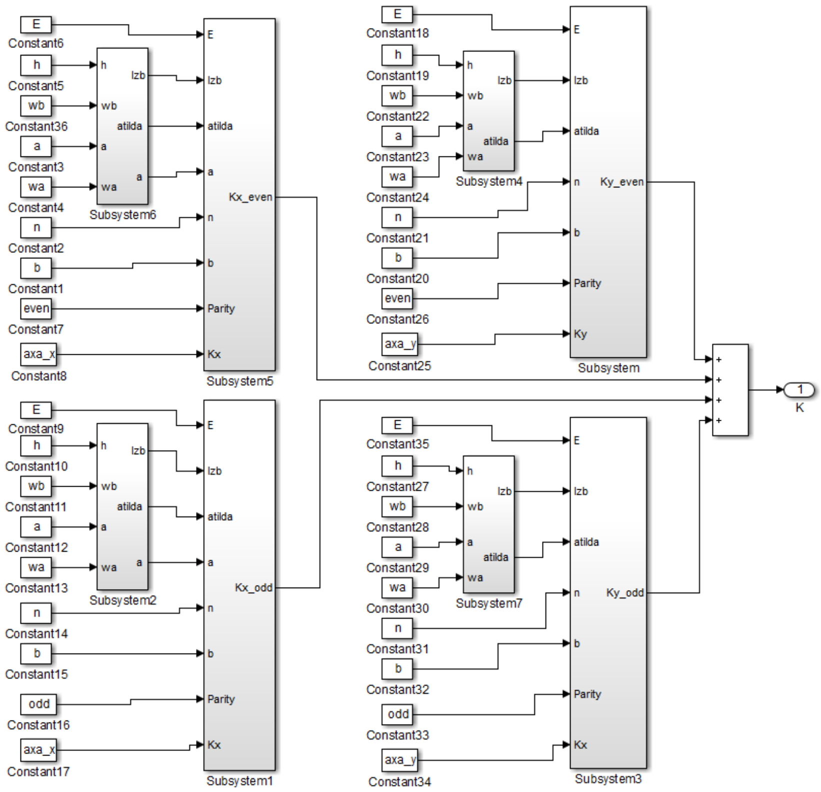

FIG. 3 Matlab/Simulink model for the serpentine flexure

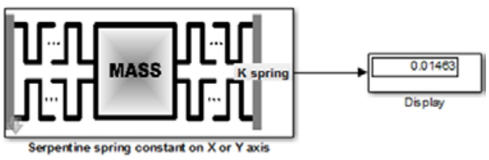

FIG. 4 Serpentine flexure Matlab/Simulink block

Also, with the number of meanders entered, the block automatically selects, for even or odd, the computing equation. The tool has a background process that allows this switch, from odd to even and vice versa. In Fig. 6 is shown a block diagram for the k_x equation.

The model was simulated using a set of parameters given in other specialized works [4, 6, 7]. After the simulations, identical results were obtained, which confirms that the developed calculation tool is correctly implemented.

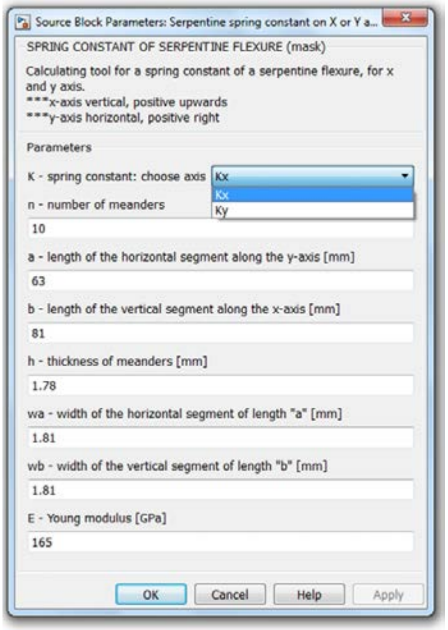

FIG. 5 Parameters settings

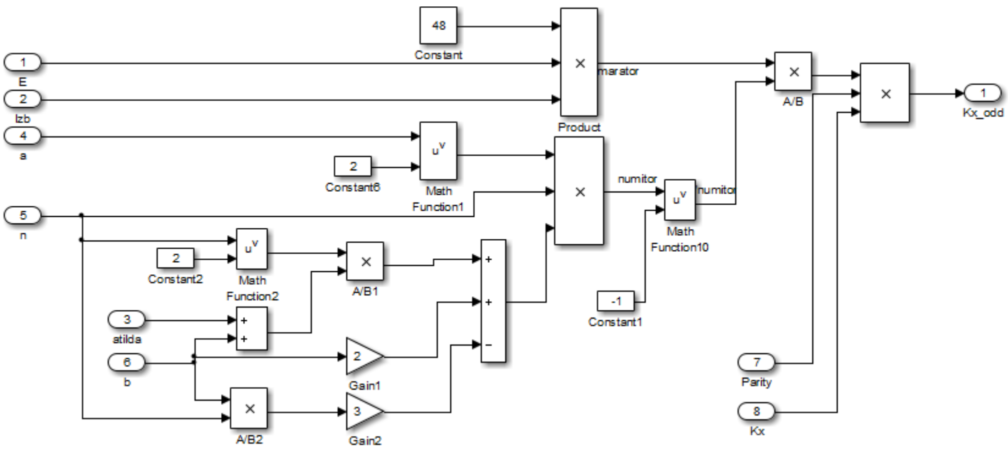

FIG. 6 K_x Matlab/Simulink block diagram

CONCLUSIONS

In the field of microsuspensions, different architectures are used, but a particular attention is focused on the serpentine configuration. This paper presents a calculating tool for the spring constant on two axis of a serpentine flexure, commonly used in inertial MEMS devices. Given the equations, a Matlab/Simulink model was created, which allows the user to manually introduce the constructive parameters and showing the final results and which can be used in other block diagrams. Because the equations differ, if the meanders number is odd or even and the computing is on two axes, 4 blocks were initial created, eventually included in one, which, due to a software written in Matlab, switches automatically, depending on the number of meanders and the selected axis. For a set a parameters given by the specialized literature, the simulation confirms that the implemented tool works correctly.

REFERENCES

[1] Sunil Kumar, *Design and Fabrication of Micromachined Silicon Suspensions*, Ph.D. Thesis, University of California, Irvine 2000;
[2] Wong Wai Chi, *Analysis of the Suspension Beam in Accelerometer for stiffness constant and resonant frequency by using Analytical and Numerical Investigation*, Master Science Dissertation, University Sains Malaysia, 2007;
[3] T.L. Grigorie, S*isteme de navigatie inertiala strap-down*, SITECH, Craiova, Romania, 2007
[4] G.K. Fedder, *Simulation of Microelectromechanical Systems*, Ph.D. Thesis, University of California at Berkeley, 1994;
[5] Nicolae Lobontiu and Ephrahim Garcia, *Mechanics of Microelectromechanical Systems*, 2005 Springer Science + Business Media, Inc., Print ©2005 Kluwer Academic Publishers
[6] Giuseppe Barillaro, Antonio Molfese, Andrea Nannini, and Francesco Pieri, *Analysis, Simulation and Relative Performances of two kinds of Serpentine Springs*, Journal of Micromechanics and Microengineering, February 2005;
[7] Winne Jerry, P.Anitha Saraswathi, *A novel design of serpentine structure for enhanced performance of MEMS based pressure sensors*, International Journal of Instrumentation, Control and Automation (IJICA), ISSN: 2231-1890, Volume-2, Issue-1, 2013;
[8] Dimitrios Peroulis, Sergio P. Pacheco, Kamal Sarabandi and Linda P.B. Katehi, *Electromechanical considerations in developing low-voltage RF MEMS Switches*, IEEE Transactions on microwave theory and techniques, VOL. 51, NO. 1, JANUARY 2003.

ON THE USE OF SUPER CAPACITORS FOR ELECTRIC MOTORS POWER SUPPLY

Constantin Daniel OANCEA*, Sabin CODREA, Adrian-Mihai ALEXEI**, Marin DUMITRU**, Daniel ŞUTEU****

*Politehnica University, Bucharest, Romania (oancea@ieee.org)
**Military Equipment and Technologies Research Agency, Romania (codrea_d@yahoo.com)

DOI: 10.19062/2247-3173.2019.21.22

Abstract: *Finding more efficient solutions for storing electricity is an objective of present research. The sources for powering the electric motors are characterized by the need to provide from time to time high peaks of power. Thus, the power supply is overloaded, with implications for its lifetime and performances. The solution analyzed in this article for power supply is to use super-capacitors instead of chemical batteries especially for high power density demands . The experiments are done with current components on the market. Super-capacitor technology is under development, it is not excluded that in the future it will become a viable alternative to the power supply along with classical chemical batteries.*

Keywords: *super-capacitor, UAV, propulsion, battery*

1. INTRODUCTION

Current trends in the field of electrical mobility, whether on land, on air, or on naval (especially for drones) - are close related to the storage capacity of batteries even as a systemic - integrative approach. The hybrid car or drone can be considered in the full-electric approach of the on board power storage and management capability. The technological development of the last decades has generated new opportunities in terms of the possibility of extending the energy of the batteries. These include photovoltaic cells and super-capacitors.

The super capacitor (also called, ultra-capacitor or double layer capacitor) is an electric capacitor type with much greater capacity than a conventional electrical capacitor. This double layer configuration creates the ability to store a higher amount of electro-static energy, more than conventional capacitors. This seems to be the best concept to replace the classical batteries, including lithium-ion or lithium-polymer based, as there are no chemical reactions, the charge-discharge time is very short, and the efficiency is close to 100%. The charge-discharge cycles of this device can reach up to 1 million, which allows the use of it for decades. Additionally, another advantage of the super-capacitor is that it does not destroy if the discharge is complete. For now, the only restriction that is required is that the nominal voltage on the element is not exceeded. It is usually 2.7 V and is due to the technology to achieve them, [1].

The super capacitor differs fundamentally in its internal structure from a normal capacitor. Instead of having two electrodes separated by an insulating layer, an ultra-capacitor uses a porous medium that produces the effect of a pair of gigantic surface plates separated by only a few nanometers gap.

As a result, the ultra-capacitor has a much higher capacity than any conventional high-capacity component (such as an electrolytic capacitor). The main constituent element is carbon (in the graphite structure), [1].

2. TECHNICAL DESCRIPTIONS

Super capacitors store electrical energy by physically separating positive and negative charges, different from classic batteries that make this chemically. The electric charge they have is much higher due to the extremely large surface of the interior materials, [2].

An advantage of the super capacitor is the very high charging and discharging speed; it is determined exclusively by physical properties. A classic battery is based on a slower chemical reaction to store and release energy, [2].

The super capacitor is unbeatable at the power density (W/kg) compared to the batteries, but the energy density is, commercially, still behind the batteries, but increasing.

A super capacitor can be seen as a device consisting of two non-reactive plates or collectors suspended inside an electrolyte with a voltage potential applied over the collectors. In an individual super capacitor cell, the potential applied to the positive electrode attracts negative ions from the electrolyte, while the potential on the negative electrode attracts positive ions, [2]. A dielectric separator between the two electrodes prevents discharge between the two electrodes, Fig. 1.

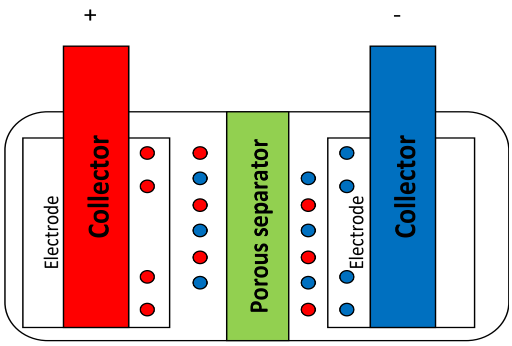

FIG. 1. The internal structure of a super capacitor

Power storage devices, such as capacitors, store electrical charge on an electrode. Other devices, such as electrochemical cells or batteries, use the electrode to create an electrical charge on the electrodes through the chemical reaction. In both cases, the ability to store or create electrical charge is a function of the surface of the electrode. For example, in capacitors, a larger surface of the electrode surface increases the storage capacity of the energy.

As a storage device, the super-capacitor is based on the microscopic separation of the electric charge. Because the capacity of these devices is proportional to the active surface of the electrode, increasing the surface of the electrode will increase the capacity, thus increasing the amount of energy that can be stored. This large surface design uses materials such as activated carbon or sintered metal powders.

However, in both situations, there is an intrinsic limit to the porosity of these materials, that is, there is an upper limit of the amount of surface that can be achieved simply by making particles smaller and smaller. An alternative method should be developed to increase the active surface of the electrode without increasing the size of the device, [2].

3. SPECIFIC ISSUES

One of the disadvantages of super-capacitors is the very low voltage at which they work (2.7V).

To remedy this situation, several such super-capacitors can be connected in series. It is obvious that if there are small differences between the values of the super-capacitors connected in series, this will be reflected on the voltage distribution at their terminals, Fig 2. To estimate the voltage difference at the capacitor terminals, let us suppose we have three super-capacitor connected in series. The individual nominal value is 400F with a working voltage of 2.7V. Suppose real values are: C1 = 390F, C2 = 400F and C3 = 410F. Supply voltage U = 7.5V. Relationships (1) - (6) describe the calculation of the voltage distribution. Cs represents the equivalent capacity of the series and Q is the electrical charge accumulated on the armatures.

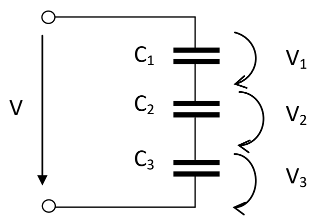

FIG. 2. Distribution of voltage in a series group

$$\frac{1}{C_s} = \frac{1}{C_1} + \frac{1}{C_2} + \frac{1}{C_3} \tag{1}$$

$$C_s = 133.27\ [F] \tag{2}$$

$$\mathrm{Q} = \mathrm{C_s} \cdot \mathrm{V} = 133.27 \cdot 7.5 = 999.58\ [C] \tag{3}$$

$$V_1 = \frac{Q}{C_1} = \frac{999.58}{390} = 2.56\ [V] \tag{4}$$

$$V_2 = \frac{Q}{C_2} = \frac{999.58}{400} = 2.49\ [V] \tag{5}$$

$$V_3 = \frac{Q}{C_3} = \frac{999.58}{410} = 2.43\ [V] \tag{6}$$

Thus, a variation in the capacity of 2.5% of the nominal value, will be reflected as a variation of 2.8% of the voltage at the terminals. There are several voltage equalization methods, from passive balancing networks with resistive dividers to active circuits, with integrated devices that act at 2.7V at the super-capacitor terminals.

Another problem is measuring the actual value of the super-capacitor. The easiest method is to measure the charging time with a constant current between two preset voltage limits followed by a simple calculation according to the formula (7).

$$C = \frac{Q}{\Delta V} = \frac{I \cdot \Delta t}{\Delta V} \tag{7}$$

4. TESTING THE POWER SUPPLY PERFORMANCE OF SUPER-CAPACITOR BATTERIES

For the experimental setup Fig. 3 two super-capacitors batteries were set. Their parameters are summarized in Table 2. The first battery consists of 10 super capacitor Heter 400F each.

Their bonding is mixed to achieve required voltage (~ 13V) but also a higher capacity. The second battery consists of 6 super-capacitor GreenCap connected in series but equipped with protection/balancing circuits for individual voltage limit.

Table 2. Super-cap battery parameters used

Super-cap battery type	Rated voltage [V]	Rated capacity [F]	Measured capacity [F]	Notes
Heter (2x400/5 [F])	2.7x5 = 13,5 [V]	160	~133	It has no surge protection circuit
GreenCap (1x500/6 [F])	2.7x6 = 16,2 [V]	83.3	~120	It has surge protection circuit on each element

As external load, an scale-model wood propeller driven by an out-runner brushless motor has been used. The two blade propeller has 12 x 8 inch characteristics. Tests have been carried out for an absorbed current of about 1 A. The engine speed-controller has been designed for electrochemical accumulators (Li-Po or Ni-MH). Therefore, it stops the motor supply when the voltage at the input terminals drops below a certain voltage threshold in order to avoid deep discharge phenomena.

FIG. 3. Super Capacitor Batteries (Heter, left, Umax = 13.5 V; GreenCap, right, Umax = 16.2 V)

In the present case, the threshold was somewhere between 8 and 10 volts. Figures 4 and 5 shows the evolution of the current and the voltage at the terminals of the super-capacitor battery until the power supply was automatically cut-off.

Figure 5 shows the start-up time of the engine (the characteristic suddenly starts at the beginning) and the final moment when the speed-controller disconnects the motor. The voltage value increases slightly due to the phenomenon of voltage return as a result of dielectric absorption.

Data was collected through a National Instruments, USB 6008 acquisition board, the application being developed in LabVIEW, Fig. 6.

A calibration phase was required before experiments started. This procedure is required because voltage and current are not harvested directly. The voltage, since it exceeds 10 V (maximum limit for the input data acquisition card), was taken over by a resistive divider. For voltage there was no need to correct the offset, except find the calibration constant for voltage.

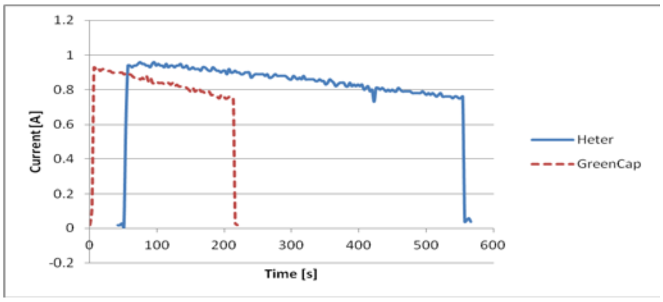

FIG. 4. Evolution of current absorbed from super capacitor batteries

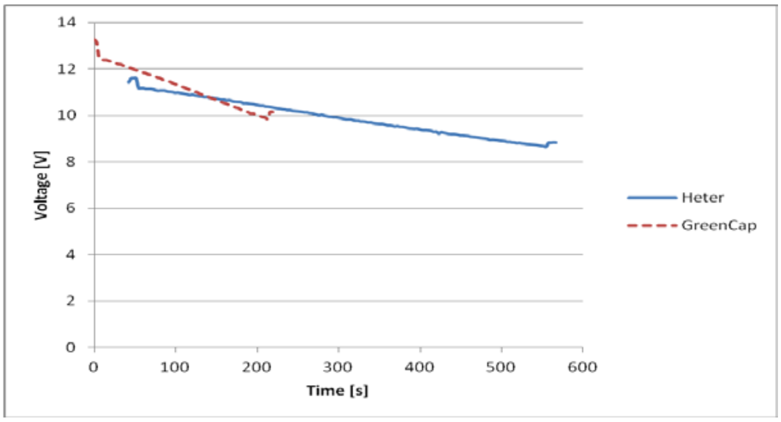

FIG. 5. Voltage evolution at super-capacitor battery terminals

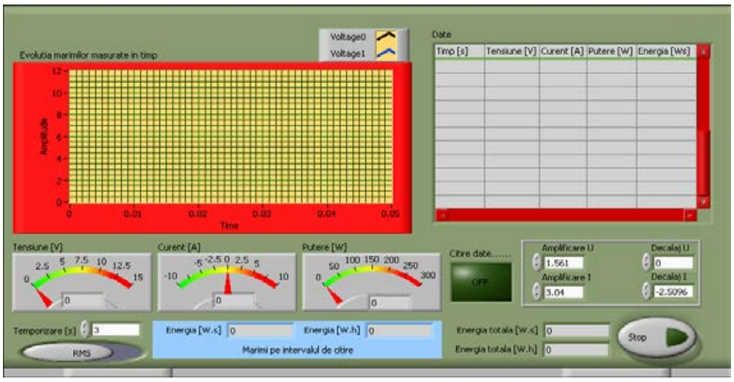

FIG. 6. Front panel of the data acquisition application

A LEM LTS 6-NP type transducer, was used for the current harvest. It supplies at 2.5V output for a null current. Thus, in order to obtain the real value of the current, an offset correction was needed, and then the result was multiplied by a calibration constant. Primary quantities are the voltage of the super-capacitor battery and the current transferred by it. The calculated quantities are power and energy consumed.

CONCLUSIONS

The use of super-capacitors as power supply, has gone from simple back-up applications for safety devices to primary storage means, used to replace electrochemical battery. Already there are vehicles, which by their nature have an intermittent operating mode, which can be loaded after a few minutes of operation (urban transport).

Charging can be done for any super capacitor batteries used in these experiments from any power source or voltage, and the charging time depends only on the charging source parameters.

Super capacitors used in experiments are currently commercialized, with no special preference (preferably from the same manufacturing batch). A source with a current limit of ~ 29A was also used in the experiments, and the super-capacitors charged without problems in less than a minute. The only precaution is related to not exceeding the maximum allowable voltage on the super capacitor. Any overshoot leads to rapid heating, followed by damage of the super-capacitor. It has also been observed during the experiments that the speed-controller for the brushless motor is also sensitive to the variation in voltage from (voltage gradient) charged from the super-capacitor battery terminals.

If the power of the super-capacitor battery is higher and the discharge slower, it can go below 9 V. When voltage decreased quickly (high gradient), the speed-controller protection engaged at 10V.

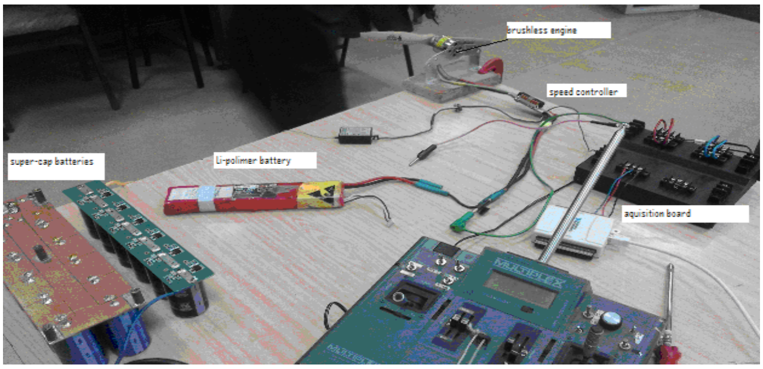

FIG. 7. Experimental setup

Experiments have demonstrated the feasibility of using super-capacitor batteries for situations where it is necessary to provide a high power in a relatively short time. Hybrid power solutions (electrochemical battery + super-capacitor battery) can be imagined to dedicated applications. One of them could be the power supply for electric driven fixed wing UAV's with classical flight pattern – in which the supper-capacitor battery is used on first stage of ascension, while the chemical battery could be used for cruise at lower currents characteristics for optimum use.

In order to be able to use a reasonable time, it is necessary for the variable power supply to be designed so that it can supply the constant demand parameters (voltage, current) even if the voltage supplied by the super-capacitor battery has an important variation. One solution would be to use a buck-boost converter. In the future, larger capacities will be developed, preliminary tests indicating the possibility of supplying over 40 amperes to the electric propulsion of an electric fixed-wing UAV.

REFERENCES

[1] C.T. Goh, A. Cruden, *Automated High Current Cycling Test System for Supercapacitor Characterisation*, International Symposium on Power Electronics, Electrical Drives, Automation and Motion, 20-22 Iunie, 2012, Sorrento, Italy;

[2] C. D. Oancea, *Supercapacitor, a battery replacement*, „Scientific Research and Education in the Air Force", AFASES 2012, The 14th International Conference, "HENRI COANDA" Air Force Academy Romania, "GENERAL M.R. STEFANIK" Armed Forces Academy Slovak Republic, May 24-26, 2012, Brasov, Romania, ISSN-L 2247-3173.

DESIGN FOR ADDITIVE MANUFACTURING WITH CASE STUDIES ON AIRCRAFTS AND PROPULSION SYSTEMS

Özgür POYRAZ*, Melih Cemal KUŞHAN**

*TEI, Tusaş Engine Industries, Eskişehir, Turkey (ozgur.poyraz@tei.com.tr)
**Eskişehir Osmangazi University, Eskişehir, Turkey (erzesk@gmail.com)

DOI: 10.19062/2247-3173.2019.21.23

Abstract: *In order to fulfill the demands of civil and military aviation, aircraft industry needs to deal with various challenges. The major reasons of these challenges are the reduction of cost for aircraft and airline operations, minimizing the downtime for maintenance, decreasing the fuel consumption and thus the emissions, and fast delivery of newly developed products to market. As a result of these decades-long efforts of the aviation industry, there have been significant developments to overcome the abovementioned challenges. However, for this sector to approach the development limits as time passes, it is only possible to advance in the competition with the methods that present a significant innovation. Additive manufacturing, aka 3d printing, is such a method to bring many advantages for aircraft and propulsion industry being applicable for diverse material groups, allowing to production of complex geometries without tools and dies, and thus making possible lightweight and functionally improved designs. Additive manufacturing is also beneficial for low volume production which is common for aviation industry and provides decreased buy-to-fly ratios, eliminating material waste for precious alloys and cut down long machining times. However, it is important to apply this method properly and there is lack of knowledge for this emerging method. This paper presents essential principles for additive manufacturing and design issues to utilize the method properly for aviation industry. Furthermore, it benchmarks and analyze designs made for aircraft and propulsion components. Finally, the advantages and limitations utilized during design for additive manufacturing were highlighted, and research needs were emphasized*

Keywords: *Additive manufacturing, design for additive manufacturing, metals and alloys, aircraft components, propulsion system components.*

1. INTRODUCTION

The utilization of military and commercial aviation is continuously expanding, and together with this, the demand for aircrafts is also increasing. Compared to previous decades, there are many types of aircraft such as next-generation fighters, unmanned aerial vehicles (UAV), high-capacity passenger planes and giant cargo carriers. In addition to the ones that are currently in service, it is forecasted that new ones will be needed in the following years. An example can be provided from a forecast report based on commercial aircrafts. According to that, the need for new aircrafts will be double in the next 20 years and a total of more than 37500 commercial aircrafts will be delivered as the total of growing demands and also the replacement of old aircrafts [1]. Although the aircraft industry is promising when considering the number of deliveries and product sales prices, it has to meet the demands of airlines, airforces and other users to be competitive.

These demands include reduction of cost for aircraft and airline operations, minimizing the downtime for maintenance, decreasing the fuel consumption and thus the emissions, and fast delivery of newly developed products to market.

As a result of these decades-long efforts of the aviation industry, there have been significant developments to satisfy the abovementioned demands. These developments took place under different disciplines such as design, material, manufacturing and test technologies. It is well known that developments in aviation and space are the leaders of today's technology and rapidly extend to other industries. For example, some tecnologies are developed for aerospace industry and today they are utilized in different sectors such as automotive and marine [2].

Additive manufacturing (AM) is such a technology which was developed in the beginning of 1980s under the name 3d printing, and did not draw attention until it's utilization for aircraft and aircraft propulsion systems in the beginning of 2010s. At the present time, this emerging technology is the main subject of many industrial and academic research projects and is of high interest to various industries in addition to aviation. The 2017 Wohlers Report showed that AM represented a more than $6 billion global industry in 2016, including products and services to have a aerospace utilization ratio of 18% [3].

Although the promising AM technology provides many benefits in terms of design freedom, manufacturing flexibility and material diversity, it is mostly utilized in aircraft industry as a replacement of conventional manufacturing. There are a lot of subjects that need to be researched and known in order to take full advantage of this technology and to advance the products in which it is used.

In order to cover the knowledge gaps for the related technology, this paper presents essential principles for additive manufacturing and design issues to utilize the method properly for aviation industry. Furthermore, it benchmarks and analyze designs and case studies made for aircraft and propulsion components. The rest of the paper is organized as follows: In the next section principles for additive manufacturing are presented together with different technologies. Following section explains the advantages and drawbacks of design for additive manufacturing covering the limitations and considerations of issues related to materials and manufacturing. Case studies from aircraft and propulsion system components are benchmarked in the subsequent section. The last section summarizes the paper and emphasizes prospective research.

2. ADDITIVE MANUFACTURING

Additive manufacturing (AM), also known with different names such as 3d printing, solid free-form fabrication (SFF), rapid prototyping (RP), is defined as a manufacturing process of joining materials to make objects from 3D model data usually layer upon layer, as opposed to subtractive manufacturing methodologies, such as traditional machining [4]. Although the processing methods may vary according to applied technology, a generic AM process consists of 7 basics steps [5]. It starts with the creation of 3d product model in a computer aided design (CAD) software and it is exported in a AM compatible file format such as stereolithography (STL). Later on the exported file is transferred to the machine after editing in a customized job preparation software. With the loading of job file and consumables, the additive manufacturing machine is set-up. By this way the build is started and the part is manufactured layer by layer. The last steps of the process include part removal from machine and post-processing such as cleaning, polishing, machining, etc.

Today AM is capable of manufacturing diverse material groups such as metal, ceramics and polymers with the development of sub technologies. American Society for Testing and Materials (ASTM) categorizes these sub technologies under 7 families of vat photopolymerization, powder bed fusion, binder jetting, material jetting, sheet lamination, material extrusion and directed energy deposition. All these families have also commercial names and each can be applied to specific materials. Table 1 summarizes these families with the common commercial names and applicable materials [6].

Table 1 – 7 families of additive manufacturing [6]

Vat photo polymerization	Powder bed fusion (PBF)	Binder jetting	Material jetting	Sheet lamination	Material extrusion	Directed energy deposition (DED)
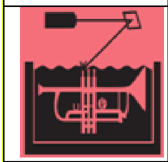	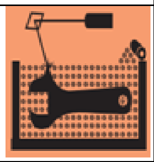	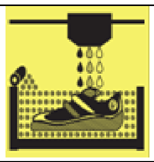	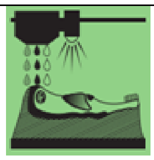	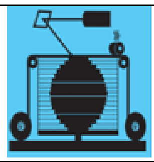	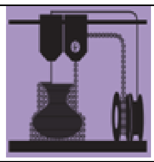	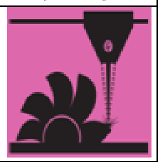
A vat of liquid photopolymer is cured through selective exposure to light and converts exposed areas to solid part.	Powdered material is selectively consolidated and/or melted using a heat source such as laser or electron beam	Liquid bonding agents are selectively applied onto thin layers of powder material to build up parts.	Droplets of material are deposited layer by layer to build up the parts.	Sheets of material are stacked and laminated to form an object using adhesive, chemicals, ultrasound, etc.	Material is extruded through a nozzle or orifice in tracks or beads, and combined into a model.	Powder or wire is fed into a melt pool on the part build which is generated using and energy source such as laser.
Materials: Curable photopolymer resins	Materials: Metals, ceramics, plastics	Materials: Metals, ceramics, plastics, glass	Materials: Photopolymers, waxes	Materials: Metal foils, plastic sheets	Materials: Thermoplastic filaments	Materials: Metal powder and wire
Commercial Names: SLA, DLP, 3SP	Commercial Names: SLS, DMLS, SLM, EBM	Commercial Names: 3DP, ExOnei Voxeljet	Commercial Names: Polyjet, Projet, MJM.	Commercial Names: LOM, UAM	Commercial Names: FDM, FFF	Commercial Names: LMD, DMD, LENS

Although AM offers 7 families of technologies and each technology offers different method and materials, it is important to consider advantages and drawbacks of AM [7] and conduct necessary activities, such as part screening, before transforming the AM technologies within the relevant companies and/or other establishments, see FIG. 1 [8].

FIG. 1. Strategic considerations and benefits for AM adoption across value chain elements [8]

3. DESIGN FOR ADDITIVE MANUFACTURING

As in other industries, design for additive manufacturing (DfAM) activities should be conducted carefully in aircraft and propulsion system components production and all the above mentioned technologies, advantages and drawbacks should be consider to make the most benefit of this technology.

The very first and important step for the DfAM is the selection of the parts. Since assessment of appropriate part candidates could be time consuming, the part selection step is conducted in three phases as information, assessment and decision [9]. In the initial information phase, advantages and current product spectrum of the technology is shown and detailed technical information gathered in and provided to designers for discussing the potential parts. In the second assessment phase, the number of potential parts is reduced using systematical benchmark methodologies. In this regard considered aspects may include material availability of AM for already used parts in aerospace, size limitations of the reachable machines, part specifications and the geometric conditions as well as economical aspects of material consumption and processing time. At this phase, added values that can be obtained are taken into account, opportunities such as part simplification, weight reduction and function improvement are also considered. For the last phase decisions are made for the AM parts and redesign can be conducted when necessary [9].

With the ongoing technological developments, the types of AM compatible materials are increasing day by day. Together with the 3d printing culture in the background, polymers and their composites are already in use for many years and materials with low density, good mechanical properties and dimensional accuracy such as CarbonMide, PA 3200 GF, ULTEM [10]. Technological developments added a wide range of metal alloys such as titanium, nickel, aluminum and stainless steel to the polymers [9]. Size limitation issues are also being solved by machine manufacturers and the processing time for the so called large machines is also reduced by utilization of high power and/or multiple energy inputs to the process [11]. Today even metal AM systems can manufacture parts as large as 1 m in closed chamber systems and that can be extended using robotic arms [12].

The assessment of geometric conditions is not straightforward like material types and part sizes. It is necessary to conduct technical studies on geometric conditions and it is subject to both scientific and industrial research. Design for Additive Manufacturing (DfAM) can be used to break down a product and to make sure that AM is used to its fullest. Many times this process is used as Adaptation for Additive Manufacturing (AfAM), where AM is employed to redesign an existing product or geometry [13]. A similar classification can also be made as manufacturing driven strategy and function driven strategy [14]. Among five design complexity group, three group of simple tools/components, optimized parts and the parts with embedded features can be designed with AfAM or manufacturing driven strategy, whereas bionic or lattice parts need utilizing of DfAM or function driven strategy [15]. In all of these approaches, the assessment of geometric conditions require several investigations such as dimensional limits of geometrical features [16], support structure studies [17] for overhanging face and surface quality issues [18].

Although it is not easy to generalize the guidelines of design for additive manufacturing through hundreds of combinations considering manufacturing families, machine sizes, available materials, dimensional limits of geometrical features and other affecting factors, a summary is provided for an overview of considerations, FIG. 2 [19].

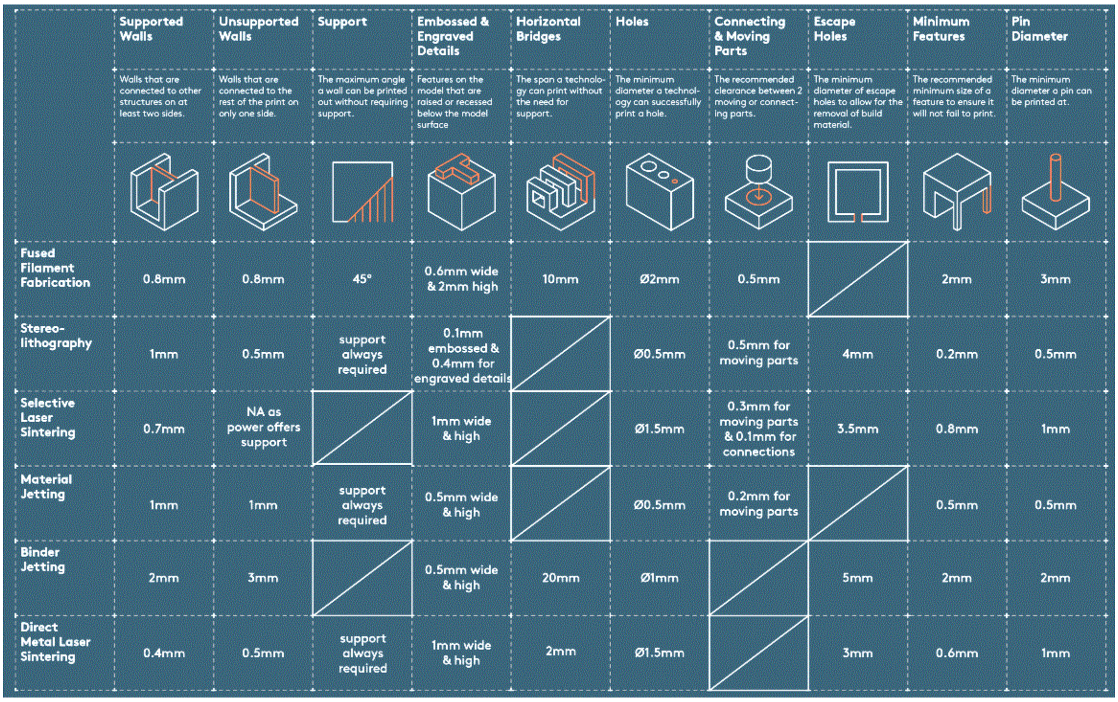

FIG. 2. Key design considerations for 3D Printing [19]

4. CASE STUDIES IN AIRCRAFT AND PROPULSION SYSTEM COMPONENTS

The aviation sector takes into account all of the listed issues such as design for additive manufacturing and increases the use of additive manufacturing in its products day by day to benefit from the emerging technology. As a result aviation industry currently utilizes different families of AM such as powder bed fusion, directed energy deposition, binder jetting and material extrusion. The extend of this utilization reaches to airframe, cabin and engine components including metal, polymer and ceramic materials [20]. It is also worth to emphasize that the technology is not only applied for new component production but also actively used for repair purposes [21]. Today all major original equipment manufacturers (OEM) such as Airbus, Boeing, General Electric, Pratt & Whitney, Rolls-Royce and Safran are currently investigating and developing AM capabilities, with >70% of OEMs having experience with AM [22].

Today example parts of additive manufacturing in airframes, interiors, jet engines, rotorcrafts and other vehicles such as satellites include forward fuselage parts [23], stringer clips [24], cabin brackets, bleed pipes [25], fuel nozzles [26], low pressure turbine blades [27], UAV wings [28], satellite brackets [29] and toroid housings [28]. Following section presents design considerations of diverse applications of AM of different materials and processing technologies, and for various types of target products.

4. CASE STUDIES ON AIRCRAFT AND PROPULSION COMPONENTS

This section provides AM case studies on aircraft, aerospace and propulsion system components in a tabulated manner for a better understanding and benchmarking of different situations. The tables on the case studies includes various information such as description of the component and its function, component geometry before and after design for AM (where available), design features, special requirements, replaced manufacturing technology, achievements through the utilization of AM and areas of further improvements.

Table 2 – Aileron hinge fitting [30]

<table>
<tr><td colspan="2">Description of the component: This case study belongs to a aileron hinge baseline fitting of a regional aircraft demonstrator. Its main function is connecting the aileron to the wing while carrying it and also allowing its movements.</td></tr>
<tr><td>Original design
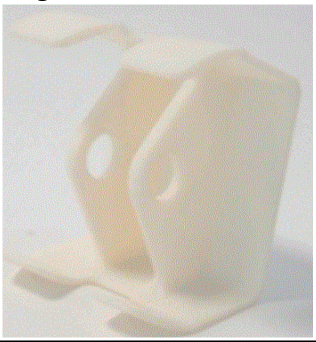</td><td>Design for AM
</td></tr>
<tr><td colspan="2">Design features: Original design features include mechanical assembly function from holes and it also centers the hinge. The main focus of design intent is on structural integrity.</td></tr>
<tr><td colspan="2">Special requirements: Special requirements of the design is to maintain reductions in weight and also in raw material usage. A consideration was also given for minimizing the use of support structures.</td></tr>
<tr><td colspan="2">Replaced manufacturing technology: Original aileron hinge features a set of manufacturing technologies including raw material manufacturing, milling and drilling. Used AM technology is powder bed fusion (electron beam melting) and part material is Ti-6Al-4V.</td></tr>
<tr><td colspan="2">Achievements: Achievements through AM includes reduction in weight and decrease in raw material waste comparing to traditional manufacturing technologies by utilizing novel topology optimization techniques.</td></tr>
<tr><td colspan="2">Further improvements: Further improvements may be to disseminate the use of the technology for serial production.</td></tr>
</table>

Table 3 – Galley fitting [31]

<table>
<tr><td>Description of the component: This case study belongs to an interior cabin galley fitting of a Boeing 787 commercial aircraft. Its main function is connecting the galley to the aircraft.</td></tr>
<tr><td>Design for AM
</td></tr>
<tr><td>Design features: Original design features include mechanical assembly function from side flange holes and back slots.</td></tr>
<tr><td>Special requirements: Special requirements of the design is to maintain minimum use of support structures all over the part and give access to tools for post processes such as machining.</td></tr>
<tr><td>Replaced manufacturing technology: Original galley fitting features a set of manufacturing technologies including raw material manufacturing, milling and drilling. Used AM technology is directed energy deposition (rapid plasma deposition) and part material is titanium alloy. Following to AM, machining was conducted.</td></tr>
<tr><td>Achievements: Achievements through AM includes reduction in weight and decrease in raw material waste comparing to traditional manufacturing technologies.</td></tr>
<tr><td>Further improvements: Flight certification of the component has been completed and the component received orders for serial production. Further improvements may be done by expanding the product portfolio for the related technology by part screening.</td></tr>
</table>

Table 4 – Turbine frame [32]

<table>
<tr><td colspan="2">Description of the component: This case study belongs to a turbine frame (assembly) of a commercial turbo-prop engine of General Electric. Its main function is to route the flow of hot gases exiting the high-pressure turbine past structural components and tubes toward the low-pressure turbine, keeping aerodynamic losses at a minimum.</td></tr>
<tr><td>Original design
</td><td>Design for AM
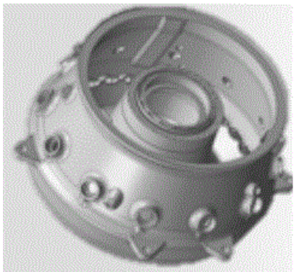</td></tr>
<tr><td colspan="2">Design features: Original design features include mechanical assembly function from circumferential holes and bosses as well as flanges in aft and forward sides. The design intent comprises of structural integrity at elevated temperatures.</td></tr>
<tr><td colspan="2">Special requirements: Special requirements of the design is to maintain minimum use of support structures all over the part. A significant consideration should also be given for inner faces, where the removal of support structures is not easy.</td></tr>
<tr><td colspan="2">Replaced manufacturing technology: Original turbine frame features a set of manufacturing technologies including forging, turning, milling, drilling, fastening and welding. Used AM technology is powder bed fusion (selective laser melting) and part material is nickel base alloy.</td></tr>
<tr><td colspan="2">Achievements: Achievements through AM includes the simplification of design, reducing the number of sub parts, and reducing the weight through elimination of fasteners. It is also important to highlight that the manufacturing resources and number of engineers were also reduced.</td></tr>
<tr><td colspan="2">Further improvements: Further improvements may be to disseminate the use of the technology for larger parts.</td></tr>
</table>

Table 5 – Cabin ventilation distributor [33]

<table>
<tr><td>Description of the component: This case study belongs to a cabin ventilation distributor of Airbus Helicopters. Its main function is to pressurize cabin air and ventilate it.</td></tr>
<tr><td>Design for AM
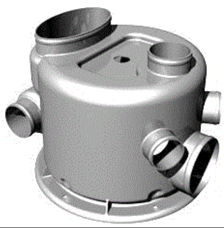</td></tr>
<tr><td>Design features: Original design features include mechanical assembly function from flanges in top and bottom sides. The design intent comprises of ventilation function as well as structural carrying.</td></tr>
<tr><td>Special requirements: Special requirements of the design is to maintain geometrical feature sizes for the used AM technology.</td></tr>
<tr><td>Replaced manufacturing technology: Original cabin ventilation distributor features a set of manufacturing technologies including draped composite manufacturing and joining. Used AM technology is powder bed fusion (selective laser sintering) and the part material is polyamide powder PA12.</td></tr>
<tr><td>Achievements: Achievements through AM includes the simplification of design, reducing the number of sub parts, decrease in manufacturing time and financial savings.</td></tr>
<tr><td>Further improvements: Further improvements may be to disseminate the use of the technology for other cabin interior parts.</td></tr>
</table>

Table 6 – Satellite antenna bracket [34]

<table>
<tr><td colspan="2">Description of the component: This case study belongs to a satellite antenna support bracket of SENTINEL-1 satellite developed by RUAG Space. Its main function is connecting the necessary antenna to the satellite platform and carrying it.</td></tr>
<tr><td>Original design
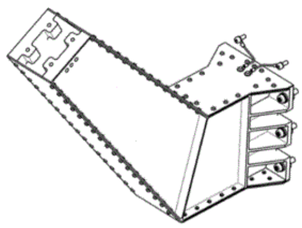</td><td>Design for AM
</td></tr>
<tr><td colspan="2">Design features: Original design features include mechanical assembly function from two sides of the bracket and has a dimensional envelope of approximately 385 X 345 X 115 mm. The design intent also comprises of total weight, stiffness and eigen frequency.</td></tr>
<tr><td colspan="2">Special requirements: Special requirements of the design is to maintain a special surface angle under the overhanging struts after optimization to minimize the use of support structures.</td></tr>
<tr><td colspan="2">Replaced manufacturing technology: Original bracket features a set of manufacturing technologies including hole drilling, riveting, fastening and welding. Used AM technology is powder bed fusion (direct metal laser sintering) and part material is AlSi10Mg aluminum alloy.</td></tr>
<tr><td colspan="2">Achievements: Achievements through AM includes the simplification of design, reducing the number of sub parts, and reducing the weight while maintaining the stresses and eigen frequency values inside the limits.</td></tr>
<tr><td colspan="2">Further improvements: Further improvements may be to disseminate the use of the technology for larger parts.</td></tr>
</table>

5. CONCLUSIONS

This paper has focused on the design for additive manufacturing with case studies on aircrafts and propulsion system components. Paper presents essential principles for additive manufacturing and design issues to utilize the method properly for aviation industry.

In this regard, it benchmarked five different case studies of aircraft, aircraft interior, aircraft engine, helicopter cabin interior part and aerospace satellite part. Benchmarked case studies includes both metal and plastic components. For the manufacturing of the metal and plastic components, various AM methods were utilized but mostly the methods under powder bed fusion group was used. The reason for this is the wide range of available materials and favored dimensional and surface quality of the powder bed technology group [7]. On the other hand, diverse methods of directed energy deposition could also be seen but with a post machining need [31].

Although there are different requirements of each component according to the used technology and material, common achievements include simplification of design, reducing the number of sub parts and decrease in manufacturing times. It can be seen that in all cases, AM also provided benefits in terms of decreasing the type and number of manufacturing operations and ease of resource planning. Furthermore, other major impact of design for AM is the ability to manufacture topology optimized parts and examples of this application can also be seen among case studies.

However, the dissemination of the application of AM to aircraft and propulsion system parts should be carried out. One of the common barriers for the dissemination is the part sizes. Other barriers which are subject to different studies and not emphasized in this paper include certification procedures for aviation.

REFERENCES

[1] Airbus. *Global Market Forecast 2018-2037*, 2018. Available at https://www.airbus.com/content/dam/corporate-topics/publications/media-day/GMF-2018-2037.pdf, accessed on 1 Apr. 2019;

[2] M. C. Kuşhan, *Aircraft Technology*, Intechopen, London, 2018;

[3] T. Wohlers, *Wohlers report*, Wohlers Associates Inc., 2017;

[4] American Society for Testing and Materials, *ISO / ASTM52900 – 15 Standard Terminology for Additive Manufacturing – General Principles – Terminology*, West Conshohocken, PA, 2015;

[5] I. Gibson, D.W. Rosen, and B. Stucker, *Additive manufacturing technologies (Vol. 17)*, Springer, New York, 2014;

[6] Hybridmanutech, *7 Families of additive manufacturing*, http://www.hybridmanutech.com/uploads/2/3/6/9/23690678/7_families_of_3d_printing_by_hybrid_v9_2pps.pdf, accessed on 10 Apr. 2019;

[7] O. Poyraz and M. C. Kushan, *Investigation of the effect of different process parameters for laser additive manufacturing of metals*, Journal of the Faculty of Engineering and Architecture of Gazi University, 33(2), 699-711, 2018;

[8] J. Coykendall, M. Cotteleer, J. Holdowsky and M. Mahto, *3D opportunity in aerospace and defense: Additive manufacturing takes flight*, A Deloitte series on additive manufacturing, 1, 2014;

[9] C. Lindemann, Y. Reiher, U. Jahnke and R. Koch, *Towards a sustainable and economic selection of part candidates for additive manufacturing*, Rapid Prototyping Journal, 21(2), 216-227, 2015;

[10] S.C. Joshi and A.A. Sheikh, *3D printing in aerospace and its long-term sustainability*, Virtual and Physical Prototyping, 10(4), 175-185, 2015;

[11] W.T. Carter, *Systems and methods for additive manufacturing in-build assessment and correction of laser pointing accuracy for multiple-laser systems*, US Patent, 2017;

[12] 3dprinting Media Network, *10 top hybrid manufacturing companies*, https://www.3dprintingmedia.network/ the-top-ten-hybrid-manufacturing-companies/, accessed on 22 Apr. 2019;

[13] J. Sönegard and M. Warholm, *Industrialization of Additive Manufacturing Development of an Additive Manufacturing Design Guide for Metal Laser Powder Bed Fusion*, Chalmers University of Technology, 2017;

[14] B. Leutenecker, C. Klahn and M. Meboldt, *Indicators and design strategies for direct part production by additive manufacturing*, In Proceedings of the 20 th International Conference on Engineering Design ICED (pp. 27-31), 2015;

[15] E. Todorov, R. Spencer, S. Gleeson, M. Jamshidinia and S.M. Kelly, *Project 1: Nondestructive Evaluation (Nde) Of Complex Metallic Additive Manufactured (Am) Structures (No. 55028GTH)*, America Makes: National Additive Manufacturing Innovation Institute (Namii), 2014;

[16] G.A. Adam and D. Zimmer, On *design for additive manufacturing: evaluating geometrical limitations*, Rapid Prototyping Journal, 21(6), 662-670, 2015;

[17] Ö. Poyraz, E. Yasa, G. Akbulut, A. Orhangul and S. Pilatin, *Investigation of support structures for direct metal laser sintering (DMLS) of IN625 parts*, In Proceedings of the solid freeform fabrication symposium, Austin, Texas, USA (pp. 560-574), 2015;

[18] G. Strano, L. Hao, R.M. Everson and K.E. Evans, *Surface roughness analysis, modelling and prediction in selective laser melting*, Journal of Materials Processing Technology, 213(4), 589-597, 2013;

[19] R. Brockotter, *Key design considerations for 3D Printing*, https://www.3dhubs.com/knowledge-base/key-design-considerations-3d-printing, accessed on 22 Apr. 2019;

[20] Special Interest Group for the Technology Strategy Board UK, *Shaping Our National Competency In Additive Manufacturing*, 2012.

[21] Ö. Poyraz and M.C. Kuşhan, *Havacılık Komponentlerinin Bakım Uygulamalarında Katmanlı İmalat Teknolojilerinin Kullanımı (The Use of Additive Manufacturing Technologies in Maintenance Applications of Aviation Components)*, Engineer & the Machinery Magazine, 59(691), 2018;

[22] Roland Berger Study, *Additive Manufacturing in Aerospace and Defense.* Available at https://www.rolandberger.com/publications/publication_pdf/roland_berger_additive_manufacturing.pdf accessed on 30 Apr. 2019;

[23] Additive News, *Aerospace Industry is one of the best investors in Additive Manufacturing*, https://additivenews.com/aerospace-industry-one-best-investors-additive-manufacturing/, accessed on 30 Apr. 2019;

[24]Additive 3d, *Applications of Additive Manufacturing: Transportation – Aerospace*, https://additive3d.com/ applications-additive-manufacturing-transportation-aerospace/, accessed on 30 Apr. 2019;
[25]P. Caracciolo, *Improving metal 3D printing processes for aircraft parts,* https://www.theengineer.co.uk/ metal-printing-processes-aircraft-parts/, accessed on 1 May. 2019;
[26]General Electric, *New manufacturing milestone: 30,000 additive fuel nozzles* https://www.ge.com/additive/blog/new-manufacturing-milestone-30000-additive-fuel-nozzles, accessed on 1 May. 2019;
[27] Avio Aero, *Turbomachinery,* https://www.avioaero.com/What/Turbomachinery, accessed on 1 May. 2019;
[28]J. Hiemenz, *Additive Manufacturing Trends In Aerospace*, https://www.additiveflightsolutions.com/wp-content/uploads/2018/08/Additive-Manufacturing-Trends-in-Aerospace-Leading-the-Way-EN-A4-Whi....pdf, accessed on 2 May. 2019;
[29]EOS, *Aerospace: RUAG - Additive Manufacturing of Satellite Components*, https://www.eos.info/ case_studies/ additive-manufacturing-of-antenna-bracket-for-satellite, accessed on 2 May. 2019;
[30]Acitturi, *First prototypes of Additive Manufacturing technologies in EWIRA Project*, https://www.aciturri.com/en/press-media/news/aciturri-ewira, accessed on 3 May;
[31]Norsk Titanium, *Norsk Titanium to Deliver the World's First FAA-Approved, 3D-Printed, Structural Titanium Components to Boeing,* https://www.norsktitanium.com/media/press/norsk-titanium-to-deliver-the-worlds-first-faa-approved-3d-printed-structural-titanium-components-to-boeing, accessed on 3 May; 2019;
[32]General Electric, *Arcam and SLM Solutions acquisition,* https://www.ge.com/sites/default/files/ ge_webcast_presentation_009062016_0.pdf, accessed on 3 May; 2019;
[33]Prodways, *The New Premium alternative in Laser Sintering*, http://focus3d.pl/catalog-sls.pdf, accessed on 4 May. 2019;
[34]F. Mouriaux, *Motivations, Opportunities and Challenges of Additive Manufacturing for Space Application,* http://morf3d.com/wp-content/uploads/2015/05/RUAG-AATC-2015.pdf, accessed on 4 May. 2019.

AERODINAMIC ANALYSIS OF HELICOPTER FENESTRON VERTICAL TAIL

Vasile PRISACARIU, Alexandru CHIRILĂ

"Henri Coandă" Air Force Academy of Braşov (aerosavelli73@yahoo.com, chirila.alexandru91@yahoo.com)

DOI: 10.19062/2247-3173.2019.21.24

Abstract: *The Eurocopter EC135 (now Airbus Helicopters H135) is a twin-engine civil light utility helicopter produced by Airbus Helicopters (formerly known as Eurocopter). It is mainly used for helicopter emergency medical services then for corporate transport, law enforcement, offshore wind and military flight training. This publication contains the theoretical aspects and analyzes aerodynamically the performance of fenestron vertical tail with XFLR5 freeware.*

Keywords: *Airbus H135, fenestron tail, XFLR5 6.06, aerodynamic analysis.*

Simbols and acronyms

OEI	One Engine Inoperative	AEO	All Engines Operative
MTOW	Maximum Takeoff Weight	HMI	Human Machine Interface
FADEC	Full-Authority Digital Engine Controls	TOP	Takeoff-Power
LLT	Lifting Line Theory	VLM	Vortex Lattice Method
AoA	Angle of Attack	C_l, C_m, C_n,	Moments coefficients (pitch, roll, yaw)

1. INTRODUCTION

The H135 is light twin-engine multi-purpose helicopter in the 3 ton class, with up to 8 seats for pilots and passengers. The H135 delivers exceptional power reserves including full class 1 & class 2 performances, enhanced safety margins, best-in-class payload and the industry benchmark for control response and precision flying thanks to the hinge and bearing less main rotor system. All composite main rotor blades, with an advanced tip geometry design, in combination with the fenestron anti-torque system make the H135 the quietest helicopter in its class, with certified sound levels well below the ultra-stringent ICAO limit, (see figure 1). The H135 can be powered by either Safran Helicopter Engines Arrius 2B2 or Pratt & Whitney Canada PW206B3 engines - both are FADEC controlled and provide efficient fuel burn characteristics. These powerful and reliable engines, combined with the improved dynamic lifting system components, provide outstanding performance and vital power reserves especially in One Engine Inoperative (OEI) scenarios and in all flight regimes including demanding High & Hot conditions, [1, and 2].

FIG. 1 Airbus H 135 helicopter

Airbus developed new, optimized aerodynamic elements for H135 granting optimal mission capability. More in detail: the vertical fin is extended in its upper section to extend the envelope of the autopilot.

Table1 Airbus H135 features, [1, 2]

Features	Value	Features	Value
Fuselage geometry	10,2x2,0x3,50 m	Ceiling (TOP)	4570 m
Rotor diameter	10,4 m	(MTOW)	2,900 kg
Max speed (2200 kg)	287 km/h	Takeoff-Power (TOP)	528 KW

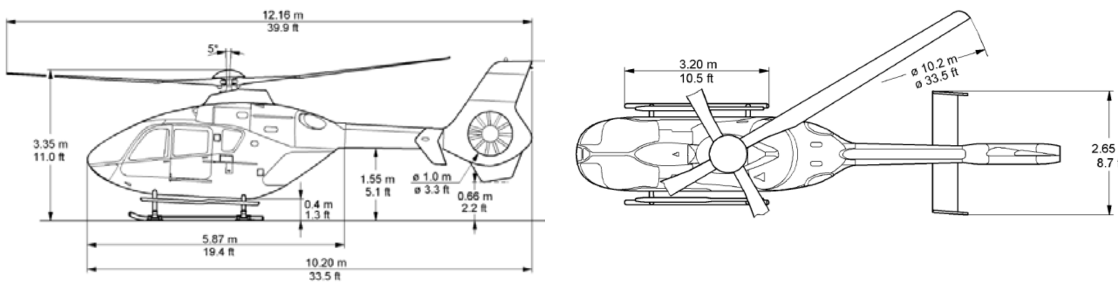

FIG. 2 H 135 external dimensions, [1]

2. HELICOPTER VERTICAL STABILIZER

The primary role is providing stability in yaw, while the stability in yaw is provided by the tail rotor, the vertical stabilizer can: alleviate the rotor thrust therefore reducing the power; replace the tail rotor in case of failure. The counter clockwise sense of rotation of the main rotor results in a clockwise torque acting on the main gear box and the fuselage.

Thus in hover or in flight with low forward speed the H/C nose tends to turn to the right. To counteract this movement the tail rotor thrust has to keep the H/C nose straight by creating a force on the tail boom to the right with the airflow from right to left.

With higher forward speeds flying straight and level, the power demand to the tail rotor decreases significantly due to the aerodynamic shape of the vertical fin and the angle between endplates and the flight direction. The rear structure is the aft section of the fuselage. It stabilizes the helicopter in flight by means of the vertical fin with the integrated Fenestron tail rotor and provides the lever arm on which the thrust of the tail rotor counteracts the torque of the main rotor system. The rear structure of the H135 consists of the following assemblies: tail boom, horizontal stabilizer, vertical fin with fenestron structure, see figure 3 and 4, [3].

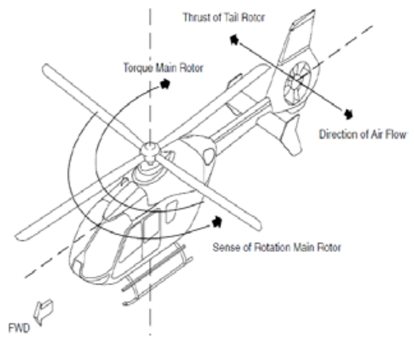

FIG.3 Fenestron concept

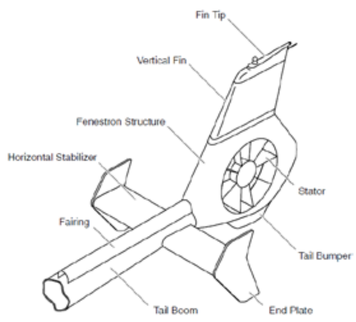

FIG.4 Tail Unit

Fenestron Vertical Fin

The vertical fin together with the integral Fenestron structure forms a unit. The upper region of the vertical fin has an aerodynamic function, while the Fenestron structure below it encloses the tail rotor system. The yaw control of the helicopter is made possible by the Fenestron, see Fig. 4.

3. AERODYNAMIC ANALYSIS

3.1. Freeware XFLR5

Aerodynamic analyzes were performed with the XFLR5 freeware tool. XFLR5 is an analysis tool for airfoils, wings and planes operating at low Reynolds Numbers. It includes: XFoil's direct and inverse analysis capabilities; wing design and analysis capabilities based on the Lifting Line Theory (LLT), on the Vortex Lattice Method (VLM), and on 3D Panel Method, [4, 5, 6 and 8].

3.2. Helicopter design H135

2D geometry.

For helicopter design I used tree airfoils: NACA 0012, NACA 0021 and NACA 2411, (see Fig.5), [4, 5 and 7].

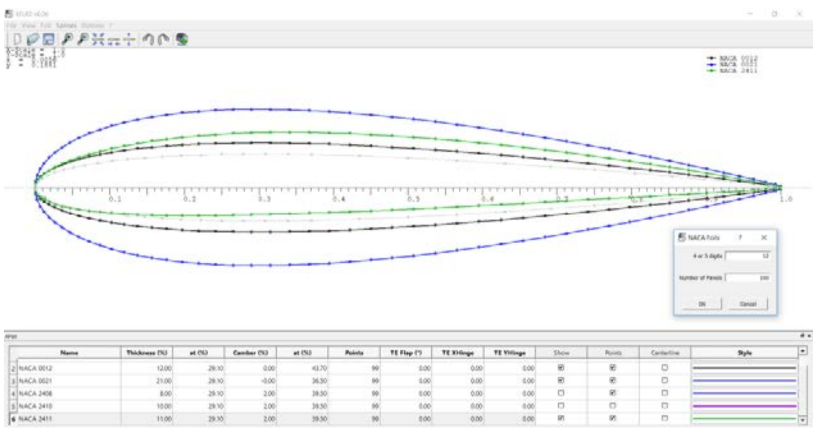

FIG.5 Direct Foil Design

The case study includes a comparative analysis of the aerodynamic aspects of the H135 fuselage without the influence of the lifting rotors. We have travelled a series of stages with XFLR5, as follows: a similar geometric configuration of the H135 helicopter in a 1:10 scale was considered, (see Fig. 6).

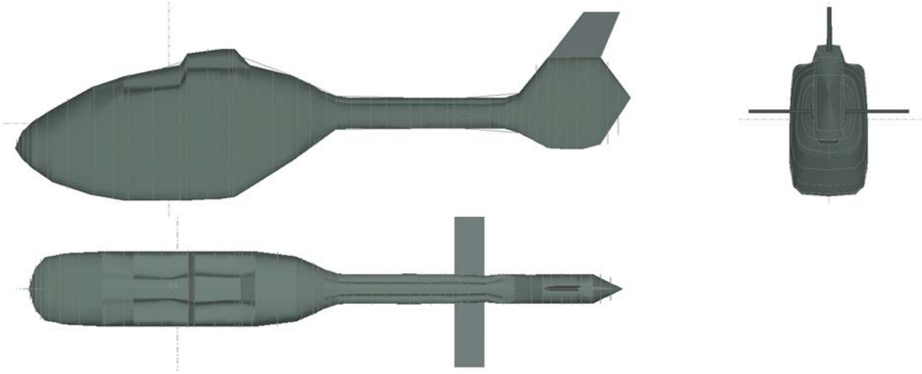

FIG.6 Airbus H135 XFLR5 design

For the design of the fuselage we have activated *Wing and Plane Design*, in *Body* and then in *Define a New Body*, from which we entered the spatial coordinates for each *Frame Positions* on the OX axis. Each *Frame Positions* has as spatial coordinates the OY and OZ axes from where we changed their positions through the *Current Frame Definition* window, see figure 7. On the OX axis we have defined the length of the helicopter at a scale of 1:10. On the OY and OZ axis we define the helicopter's maximum width and height and shape.

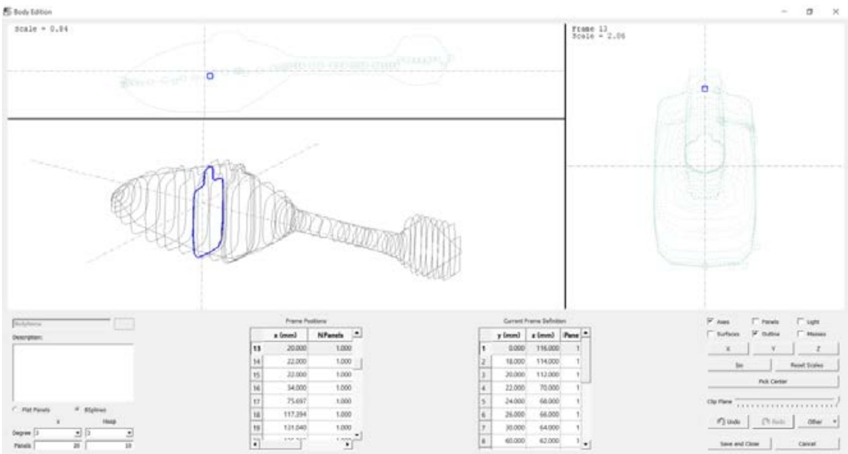

FIG.7 Body Design

Coupling the fuselage with the tail

We have introduced the elevator and fin where which we have modified by defining the desired dimensions (see figure 8) and positioning them by modifying values coordinate on axis, to could couple them with the fuselage. The working time for Airbus H135 design in xflr5 was 30 hours.

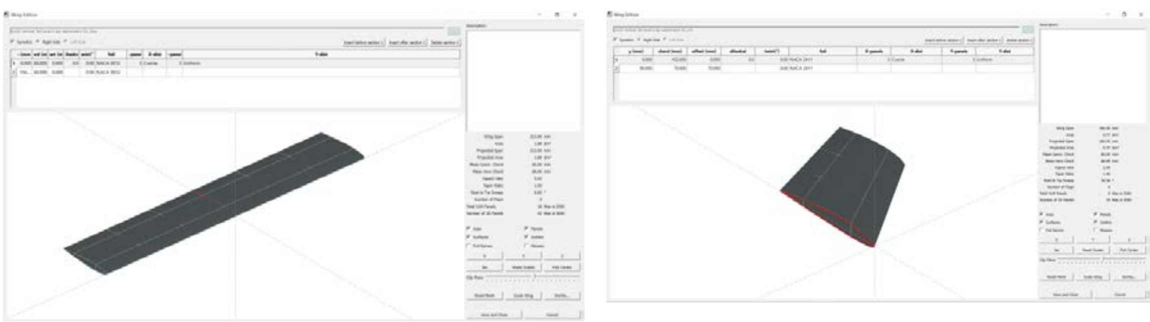

FIG. 8 Elevator and fin design

3.3. Aerodynamic analysis

Aerodynamic analyzes considered the initial conditions outlined in Table 6.

Table 6. Initial conditions

Parameter	Value	Parameter	Value
Speed	10 m/s	Inertial values	no
Air density	1.225 kg/cm^3	Viscosity	1.5e-05 m^2/s
Max. iterations	200	Method	3D/VLM
Alpha Precision	0.0100	Polar	constant speed
AoA interval	$-15^0 \div 15^0$, $\Delta=1^0$	Relax. factor	20

The analysis has two cases on two different geometries of different vertical tail and different twists, for the analysis conditions of the tables 6, the selected numerical data refer to C_l, C_m, C_n, and C_y, see Table 7.

Table7. Analysis cases

NACA0021 / NACA0012		NACA2411	
Twist 0^o	Twist 7^o	Twist 0^o	Twist 7^o

4. THE RESULTS

4.1. Vertical fin analysis with NACA2411.

According to figure 9 the pitch coefficient (C_m) variation for the two values of twist, has a similar slope is used for all incidence (see also Annex 1), the absolute difference for a zero incidence being 0.11 (-12.48 vs. -12.59), the twist of 7^o having an influence on the pitch coefficient, especially with the increase in speed. In figure 10, it is observed that an increase in the absolute value of the rolling coefficient (C_l) with the increase of the twist is expected, for a zero incidence (AoA) we have a difference of approximately 0.50.

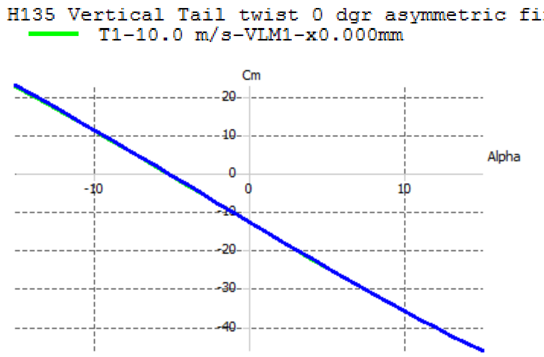

FIG.9 C_m vs AoA

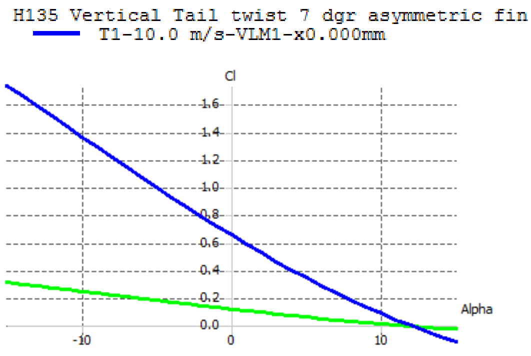

FIG.10 C_l vs AoA

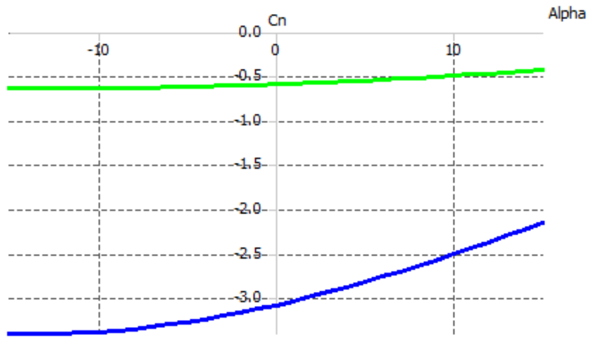

FIG.11 C_n vs AoA

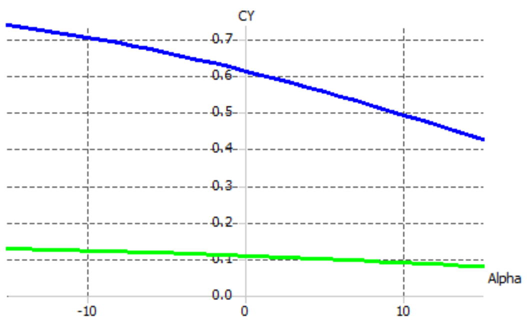

FIG.12 C_y vs AoA

The yaw coefficient (C_n) highlighted in Fig. 11 increases in absolute value with increasing speed indicating the great influence on lateral movement/yaw by a difference of 5 times greater (approximately 2.5) considered at zero incidence, coefficient of lateral force C_y see figure 12, with the same increase.

4.2.Vertical fin analysis with NACA 0021 and NACA 0012.

According to figure 13, the variation of the pitch coefficient (C_m) for the two twist values has a similar slope over the all incidence (see also Annex 2), the absolute difference for a zero incidence being 0.07 (-12.50 vs. -12.57), the twist of 7^o having an influence on the pitch coefficient, especially with the increase of the velocity.

In Fig.14, it is observed that an increase of the absolute value of the rolling coefficient (C_l) with the increase of the twist, for a zero incidence we have a difference of about 0.60

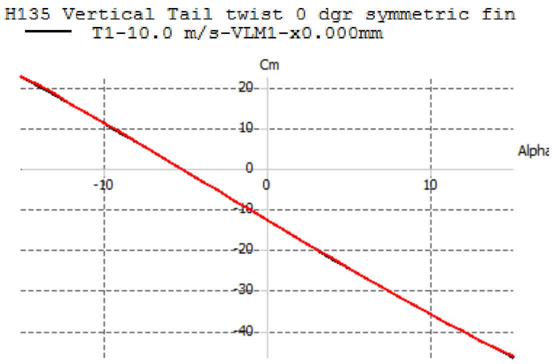

FIG.13 C_m vs AoA

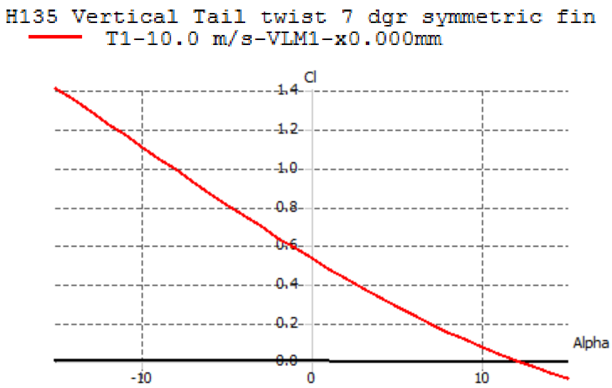

FIG.14 C_l vs AoA

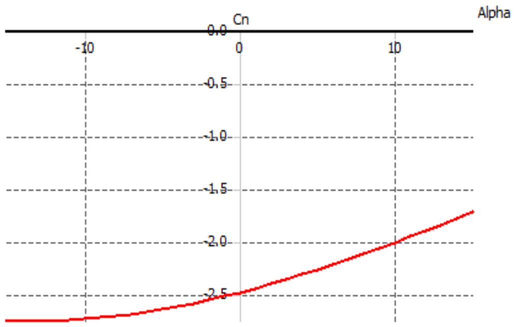

FIG.15 C_n vs AoA

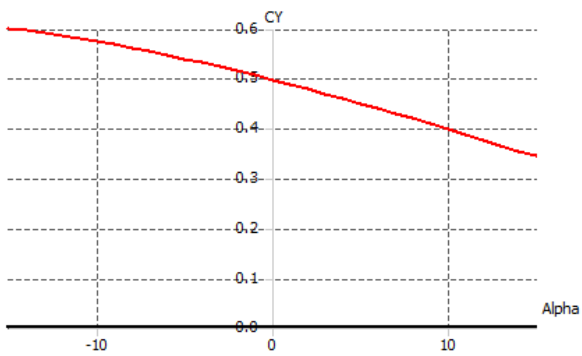

FIG.16 C_y vs AoA

The yaw coefficient (C_n) highlighted in figure 15 increases in absolute value with increasing speed, highlighting the great influence on lateral / yaw movement by a difference of 5 times greater (approximately 2.5) considered at zero incidence, influencing obviously the coefficient of the loop force C_y see figure 16, with the same sense of growth.

CONCLUSIONS

Design efforts to optimize the tails of modern helicopters have specific approaches based on the aerodynamic concept chosen to cancel the gyroscopic torque of the bearing rotor.

Although the analysis of the presented paper did not take into account the functioning of fenestron and was limited only to the influence of the geometrical characteristics of the vertical tail by using an open source aerodynamic analysis code (XFLR5), it was possible to highlight the degree of influence of the selected 2D geometries with a high degree to trust the results.

The results can be used successfully in the pre-dimensioning and general optimization steps and then be taken over in CFD commercial tools for refined optimizations.

The article can be used in the educational field to conceptualize the aerodynamic phenomena that arise due to geometrical changes.

REFERENCES

[1] Eurocopter, *EC 135 Technical data*, 135.02.101.01E, available at https://www.hdf.fr/public /PDF/EC_135_PDF.pdf;

[2] https://www.airbus.com/helicopters/civil-helicopters/light-twin/h135.html, accessed at 10.04.2019;

[3] Airbus, *General Description - Rear Structure Rear Structure*, SDS EC135 P1P2T1T2, https://keycopter.airbushelicopters.com /ORION/desktop/?cid=22447, accessed at 10.04.2019;

[4] Drela M., Yungren H., *Guidelines for XFLR5 v6.03 (Analysis of foils and wings operating at low Reynolds numbers)*, 2011, available at http://sourceforge.net/projects/xflr5/files, accessed at 14.04.2019;

[5] Guidelines for XFLR5 v6.03, 2011, 71 p. available at http://www.xflr5.com/xflr5.htm;

[6] Prisacariu V., *Analysis of UAVs flight characteristics*, vol. 38, nr. 3/2018, p.29-36, Review of the Air Force Academy, ISSN 1842-9238; e-ISSN 2069-4733, DOI: 10.19062/1842-9238.2018.16.3.4;

[7] http://airfoiltools.com, accessed at 24.04.2019;

[8] Prisacariu V., Simionescu L., *Flight performance analysis for UAVs. MFD NIMBUS*, Scientific research and education in the Air Force – AFASES 2018, ISSN, ISSN-L : 2247-3173, p.225-232, DOI : 10.19062/2247-3173.

ANNEXES

Annex 1. Vertical fin analysis with NACA2411

Wing name : H135 Vertical Tail twist 0 dgr asymmetric fin
Wing polar name : T1-10.0 m/s-VLM1-x0.000mm
Freestream speed : 10.000 m/s

alpha	CL	ICd	PCd	TCd	CY	Cm
-15.000	-3.577065	0.394408	0.000000	0.394408	0.127295	22.571976
-14.000	-3.378706	0.348491	0.000000	0.348491	0.126553	20.366787
-13.000	-3.174651	0.304949	0.000000	0.304949	0.125736	18.129532
-12.000	-2.965228	0.263913	0.000000	0.263913	0.124847	15.862936
-11.000	-2.750780	0.225507	0.000000	0.225507	0.123886	13.569760
-10.000	-2.531661	0.189848	0.000000	0.189848	0.122854	11.252800
-9.000	-2.308237	0.157042	0.000000	0.157042	0.121753	8.914877
-8.000	-2.080887	0.127188	0.000000	0.127188	0.120584	6.558839
-7.000	-1.849998	0.100375	0.000000	0.100375	0.119348	4.187558
-6.000	-1.615966	0.076683	0.000000	0.076683	0.118048	1.803921
-5.000	-1.379197	0.056183	0.000000	0.056183	0.116683	-0.589166
-4.000	-1.140102	0.038935	0.000000	0.038935	0.115257	-2.988787
-3.000	-0.899099	0.024990	0.000000	0.024990	0.113771	-5.392021
-2.000	-0.656610	0.014388	0.000000	0.014388	0.112227	-7.795938
-1.000	-0.413062	0.007161	0.000000	0.007161	0.110626	-10.197609
0.000	-0.168883	0.003326	0.000000	0.003326	0.108971	-12.594110
1.000	0.075496	0.002896	0.000000	0.002896	0.107263	-14.982518
2.000	0.319643	0.005868	0.000000	0.005868	0.105505	-17.359926
3.000	0.563129	0.012232	0.000000	0.012232	0.103699	-19.723436
4.000	0.805526	0.021967	0.000000	0.021967	0.101846	-22.070169
5.000	1.046406	0.035040	0.000000	0.035040	0.099950	-24.397268
6.000	1.285349	0.051411	0.000000	0.051411	0.098013	-26.701893
7.000	1.521937	0.071027	0.000000	0.071027	0.096036	-28.981239
8.000	1.755760	0.093826	0.000000	0.093826	0.094023	-31.232529
9.000	1.986415	0.119737	0.000000	0.119737	0.091976	-33.453022
10.000	2.213505	0.148679	0.000000	0.148679	0.089896	-35.640007
11.000	2.436646	0.180561	0.000000	0.180561	0.087788	-37.790825
12.000	2.655460	0.215283	0.000000	0.215283	0.085653	-39.902851
13.000	2.869583	0.252738	0.000000	0.252738	0.083494	-41.973518
14.000	3.078662	0.292809	0.000000	0.292809	0.081314	-44.000298
15.000	3.282358	0.335370	0.000000	0.335370	0.079115	-45.980724

Wing name : H135 Vertical Tail twist 7 dgr asymmetric fin
Wing polar name : T1-10.0 m/s-VLM1-x0.000mm
Freestream speed : 10.000 m/s

alpha	CL	ICd	PCd	TCd	CY	Cm
-15.000	-3.625169	0.446570	0.000000	0.446570	0.734481	22.687935
-14.000	-3.428159	0.400487	0.000000	0.400487	0.728967	20.483150
-13.000	-3.225427	0.356737	0.000000	0.356737	0.723029	18.246223
-12.000	-3.017298	0.315453	0.000000	0.315453	0.716674	15.979881
-11.000	-2.804112	0.276760	0.000000	0.276760	0.709910	13.686882
-10.000	-2.586219	0.240774	0.000000	0.240774	0.702745	11.370020
-9.000	-2.363985	0.207603	0.000000	0.207603	0.695187	9.032119
-8.000	-2.137782	0.177346	0.000000	0.177346	0.687247	6.676026
-7.000	-1.907998	0.150094	0.000000	0.150094	0.678933	4.304613
-6.000	-1.675025	0.125927	0.000000	0.125927	0.670256	1.920768
-5.000	-1.439267	0.104917	0.000000	0.104917	0.661226	-0.472604
-4.000	-1.201132	0.087124	0.000000	0.087124	0.651855	-2.872587
-3.000	-0.961036	0.072602	0.000000	0.072602	0.642153	-5.276257
-2.000	-0.719399	0.061390	0.000000	0.061390	0.632133	-7.680686
-1.000	-0.476645	0.053522	0.000000	0.053522	0.621807	-10.082944
0.000	-0.233202	0.049017	0.000000	0.049017	0.611187	-12.480104
1.000	0.010502	0.047888	0.000000	0.047888	0.600286	-14.869247
2.000	0.254037	0.050135	0.000000	0.050135	0.589118	-17.247461
3.000	0.496975	0.055748	0.000000	0.055748	0.577696	-19.611849
4.000	0.738889	0.064707	0.000000	0.064707	0.566035	-21.959528
5.000	0.979353	0.076982	0.000000	0.076982	0.554147	-24.287642
6.000	1.217948	0.092532	0.000000	0.092532	0.542049	-26.593351
7.000	1.454257	0.111308	0.000000	0.111308	0.529753	-28.873846
8.000	1.687870	0.133249	0.000000	0.133249	0.517277	-31.126352
9.000	1.918384	0.158285	0.000000	0.158285	0.504634	-33.348122
10.000	2.145406	0.186337	0.000000	0.186337	0.491840	-35.536446
11.000	2.368548	0.217314	0.000000	0.217314	0.478911	-37.688663
12.000	2.587435	0.251121	0.000000	0.251121	0.465863	-39.802151
13.000	2.801702	0.287650	0.000000	0.287650	0.452710	-41.874332
14.000	3.010996	0.326785	0.000000	0.326785	0.439471	-43.902683
15.000	3.214978	0.368403	0.000000	0.368403	0.426159	-45.884735

Annex 2. Vertical fin analysis with NACA 0021 and NACA 0012

```
Wing name :         H135 Vertical Tail twist 0 dgr symmetric fin
Wing polar name :  T1-10.0 m/s-VLM1-x0.000mm
Freestream speed :  10.000 m/s
```

alpha	CL	ICd	PCd	TCd	CY	Cm
-15.000	-3.576003	0.394141	0.000000	0.394141	0.000000	22.589949
-14.000	-3.377699	0.348133	0.000000	0.348133	0.000000	20.384899
-13.000	-3.173693	0.304499	0.000000	0.304499	0.000000	18.147772
-12.000	-2.964313	0.263371	0.000000	0.263371	0.000000	15.881289
-11.000	-2.749900	0.224874	0.000000	0.224874	0.000000	13.588217
-10.000	-2.530810	0.189124	0.000000	0.189124	0.000000	11.271345
-9.000	-2.307410	0.156228	0.000000	0.156228	0.000000	8.933499
-8.000	-2.080076	0.126284	0.000000	0.126284	0.000000	6.577527
-7.000	-1.849197	0.099383	0.000000	0.099383	0.000000	4.206297
-6.000	-1.615169	0.075605	0.000000	0.075605	0.000000	1.822700
-5.000	-1.378397	0.055019	0.000000	0.055019	0.000000	-0.570360
-4.000	-1.139294	0.037688	0.000000	0.037688	0.000000	-2.969968
-3.000	-0.898277	0.023661	0.000000	0.023661	0.000000	-5.373201
-2.000	-0.655768	0.012980	0.000000	0.012980	0.000000	-7.777130
-1.000	-0.412194	0.005675	0.000000	0.005675	0.000000	-10.178825
0.000	-0.167984	0.001766	0.000000	0.001766	0.000000	-12.575363
1.000	0.076431	0.001264	0.000000	0.001264	0.000000	-14.963822
2.000	0.320619	0.004166	0.000000	0.004166	0.000000	-17.341293
3.000	0.564150	0.010464	0.000000	0.010464	0.000000	-19.704880
4.000	0.806596	0.020135	0.000000	0.020135	0.000000	-22.051701
5.000	1.047530	0.033149	0.000000	0.033149	0.000000	-24.378899
6.000	1.286530	0.049462	0.000000	0.049462	0.000000	-26.683636
7.000	1.523179	0.069025	0.000000	0.069025	0.000000	-28.963108
8.000	1.757066	0.091774	0.000000	0.091774	0.000000	-31.214535
9.000	1.987788	0.117639	0.000000	0.117639	0.000000	-33.435173
10.000	2.214947	0.146538	0.000000	0.146538	0.000000	-35.622318
11.000	2.438159	0.178382	0.000000	0.178382	0.000000	-37.773308
12.000	2.657045	0.213070	0.000000	0.213070	0.000000	-39.885521
13.000	2.871243	0.250494	0.000000	0.250494	0.000000	-41.956379
14.000	3.080397	0.290538	0.000000	0.290538	0.000000	-43.983364
15.000	3.284168	0.333077	0.000000	0.333077	0.000000	-45.964005

```
Wing name :         H135 Vertical Tail twist 7 dgr symmetric fin
Wing polar name :  T1-10.0 m/s-VLM1-x0.000mm
Freestream speed :  10.000 m/s
```

alpha	CL	ICd	PCd	TCd	CY	Cm
-15.000	-3.612519	0.427772	0.000000	0.427772	0.600512	22.659481
-14.000	-3.414994	0.381791	0.000000	0.381791	0.595821	20.454559
-13.000	-3.211759	0.338160	0.000000	0.338160	0.590784	18.217512
-12.000	-3.003138	0.297011	0.000000	0.297011	0.585405	15.951067
-11.000	-2.789474	0.258466	0.000000	0.258466	0.579692	13.657985
-10.000	-2.571117	0.222644	0.000000	0.222644	0.573651	11.341059
-9.000	-2.348435	0.189651	0.000000	0.189651	0.567291	9.003113
-8.000	-2.121802	0.159585	0.000000	0.159585	0.560618	6.646995
-7.000	-1.891604	0.132538	0.000000	0.132538	0.553641	4.275576
-6.000	-1.658236	0.108589	0.000000	0.108589	0.546368	1.891744
-5.000	-1.422103	0.087809	0.000000	0.087809	0.538809	-0.501596
-4.000	-1.183613	0.070259	0.000000	0.070259	0.530972	-2.901528
-3.000	-0.943183	0.055991	0.000000	0.055991	0.522867	-5.305128
-2.000	-0.701234	0.045045	0.000000	0.045045	0.514504	-7.709467
-1.000	-0.458192	0.037453	0.000000	0.037453	0.505893	-10.111617
0.000	-0.214483	0.033235	0.000000	0.033235	0.497045	-12.508651
1.000	0.029462	0.032401	0.000000	0.032401	0.487970	-14.897648
2.000	0.273215	0.034953	0.000000	0.034953	0.478679	-17.275698
3.000	0.516345	0.040879	0.000000	0.040879	0.469184	-19.639902
4.000	0.758425	0.050159	0.000000	0.050159	0.459496	-21.987383
5.000	0.999030	0.062762	0.000000	0.062762	0.449628	-24.315277
6.000	1.237740	0.078647	0.000000	0.078647	0.439590	-26.620752
7.000	1.474137	0.097764	0.000000	0.097764	0.429396	-28.900995
8.000	1.707812	0.120050	0.000000	0.120050	0.419057	-31.153231
9.000	1.938362	0.145437	0.000000	0.145437	0.408587	-33.374714
10.000	2.165392	0.173843	0.000000	0.173843	0.397998	-35.562737
11.000	2.388516	0.205179	0.000000	0.205179	0.387303	-37.714638
12.000	2.607359	0.239346	0.000000	0.239346	0.376515	-39.827789
13.000	2.821555	0.276237	0.000000	0.276237	0.365647	-41.899624
14.000	3.030752	0.315736	0.000000	0.315736	0.354713	-43.927612
15.000	3.234611	0.357719	0.000000	0.357719	0.343725	-45.909283

NUMERICAL SOLUTIONS FOR COMBUSTION WAVE VELOCITY

Constantin ROTARU

”Henri Coandă” Air Force Academy, Braşov, Romania (rotaru.constantin@afahc.ro)

DOI: 10.19062/2247-3173.2019.21.25

Abstract: *Starting from the basic equations of mass, momentum and energy, in this paper are presented some aspects regarding the gas-dynamic model of the detonation wave, where the combustion wave speed was obtained from a given initial conditions. The compatibility, the existence and the unicity of the solution with the dynamics of the combustion behind the wave depend on the singularities of dimensionless forms of momentum and species conservation equations. This combustion model can be extended to others propulsion systems which are designed for a high thrust and velocity.*

Keywords: *propulsion systems, combustion, shock waves, detonation, deflagration*

1. INTRODUCTION

In a combustion process can appear two types of self-propagating waves: deflagration which propagates at subsonic velocities and depend not only on the initial state of the combustion mixture but also, on the boundary conditions behind the waves and detonation which has a transient three-dimensional structure a supersonic velocity and it can be considered as a reacting shock wave where the reactants (which are situated ahead of it) are not disturbed prior to the arrival of the detonation, remaining at their initial state. Deflagration has a velocity, proportional to the square root of the reaction rate and in stationary conditions it is defined as a flame, while behind a strong detonation wave the flow is subsonic and the wave penetrates the reaction zone attenuating the detonation, so, a freely propagating detonation has a sonic or supersonic condition behind it.

The deflagration and detonation can be distinguished from each other: by the expansion (deflagration) versus compression (detonation) nature of the wave; by their propagation speed; a deflagration wave propagates via the diffusion of heat and mass from the flame zone to effect ignition in the reactants ahead; deflagration requires fractions of the millijoule of energy for ignition, whereas a detonation requires joules (or kilojoules) for ignition; a detonation wave is a supersonic compression shock wave that ignites the mixture by heating across the leading shock front. The transition from deflagration to detonation in a long smooth tube, occurs when the velocity is about half the Chapman-Jouguet (CJ) detonation speed and from gas-dynamic considerations, deflagration solutions are represented on the lower branch of the Hugoniot curve and the maximum deflagration speed (for a given initial state ahead of the flame) corresponds to the point where the Rayleigh line and the Hugoniot curve are tangent, therefore, for detonations, the solution is represented on the upper branch of this curve and the minimum velocity detonation solution corresponds to the tangency of the Rayleigh line to the Hugoniot curve on the on the upper branch.

For a propagating deflagration wave, a precursor shock is usually generated ahead of the flame and this precursor shock changes the initial state ahead of the flame and depending on its strengths, will result different deflagration solutions.

The rate of mass burnt gas increase inside a spherical flame of radius r is $4\pi r^2 \rho_0 v_0$ and since the mass of burnt gas is $\frac{4}{3}\pi r^3 \rho_\infty$ it follows that the flame speed is $v_0 = \frac{\rho_\infty}{\rho_0}\frac{dr}{dt}$ and it depends on the pressure, temperature and composition of the initial combustible mixture, where ρ_0 is the density of the unburnt mixture and ρ_∞ is the density of burnt gas. The burning velocity v_0 can be related to the wave thickness δ considering a stationary plane deflagration with q-the heat of reaction, w-the reaction rate and $q \cdot \delta \cdot w$ the energy released per unit area of the wave, per second. For an adiabatic process no energy is lost from the sides of the wave, then $q = c_p\left(T_\infty - T_0\right)$, where c_p is the average specific heat of the mixture and T_∞ is the burnt gas temperature and the rate of which heat is conducted upstream is $\lambda dT / dx \cong \lambda\left(T_\infty - T_0\right)/\delta$, where T is the temperature, λ is the mean thermal conductivity of the gas and x is the distance normal to the wave. From the equation $c_p\left(T_\infty - T_0\right)w \cdot \delta = \lambda\left(T_\infty - T_0\right)/\delta$ it follows that $\delta = \sqrt{\lambda/\left(c_p \cdot w\right)}$, the combustible material mass flow rate following into the wave is $\rho_0 v_0$ and the deflagration wave consumes these reactants at the rate $w \cdot \delta$ (mass per unit area per second), therefore $\rho_0 \cdot v_0 = w \cdot \delta$ which yields to $v_0 = \sqrt{\lambda w / c_p} / \rho_0$. In these expressions, w is the factor with the strongest temperature dependence, which varies as $e^{-\frac{E}{R^0 T}}$, where E is the activation energy and R^0 is the universal gas constant.

2. COMBUSTION WAVES

Under some assumptions (one step first order reaction in a binary mixture with a Lewis number of unity and an effective Prandtl number of ¾; the effective coefficient of viscosity equals the ratio of the thermal conductivity to the average specific heat, λ / c_P; all chemical species may be considered to have constant and equal average specific heats at constant pressure, c_p), the structure of a combustion wave can be analyzed, based on the following system of equations

$$\begin{cases} \dfrac{d\varphi}{d\tau} = \dfrac{\varphi - 1 + \dfrac{1}{\gamma M_0^2}\left\{\dfrac{1}{\varphi}\left[1 + \alpha'\tau - \dfrac{\gamma - 1}{2} M_0^2\left(\varphi^2 - 1\right)\right] - 1\right\}}{\tau - \varepsilon} \\ \dfrac{d\varepsilon}{d\tau} = \dfrac{\dfrac{\lambda \rho B_1 T^{\alpha_1}}{m^2 c_p}\left(1 - \tau\right) e^{-\frac{E_1}{R^0 T}}}{\tau - \varepsilon} \end{cases} \tag{1}$$

where $\varphi = \frac{v}{v_0}$; ε is the reaction progress variable ; q – the total heat release per unit mass of mixture; q – the total heat release per unit mass of mixture;

M_0 is the Mach number, γ is the specific heats ratio; B_1 is a constant of reaction; T is the temperature; $\tau = \dfrac{\left(c_p T + \dfrac{v^2}{2}\right) - \left(c_p T_0 + \dfrac{v_0^2}{2}\right)}{q}$; $\alpha' = \dfrac{q}{c_p T_0}$; ε is the reaction progress variable.

These differential equations have the boundary conditions:

$$\text{at } \tau = 0 \;\Rightarrow\; \begin{cases} \varepsilon = 0 \\ \varphi = 1 \end{cases} \text{ and at } \tau = 1 \;\Rightarrow\; \begin{cases} \varepsilon = 1 \\ \varphi = \varphi_\infty \end{cases} \qquad (2)$$

In the three dimensional $(\varepsilon, \varphi, \tau)$ space, the solutions of the system (1) are lines, beginning at the point $(0, 1, 0)$ and ending at the point $(1, \varphi_\infty, 1)$ and they must lie within a region of semi-infinite beam of unit square cross section (fig. 1), with the singularities of equations (1) located at the points where both the numerator and the denominator vanish. When $\varepsilon = \tau$ the denominators vanish (which defines a plane containing the φ axis), and the numerators of equations vanish when

$$\begin{cases} \varphi - 1 + \dfrac{1}{\gamma M_0^2}\left\{\dfrac{1}{\varphi}\left[1 + \alpha'\tau - \dfrac{\gamma - 1}{2} M_0^2 \left(\varphi^2 - 1\right)\right] - 1\right\} = 0 \\ \dfrac{\lambda \rho B_1 T^{\alpha_1}}{m^2 c_p} (1 - \tau) e^{-\frac{E_1}{R^0 T}} = 0 \end{cases} \qquad (3)$$

The solutions of the above equations define cylindrical surfaces with the generatrices parallel to the ε axis.

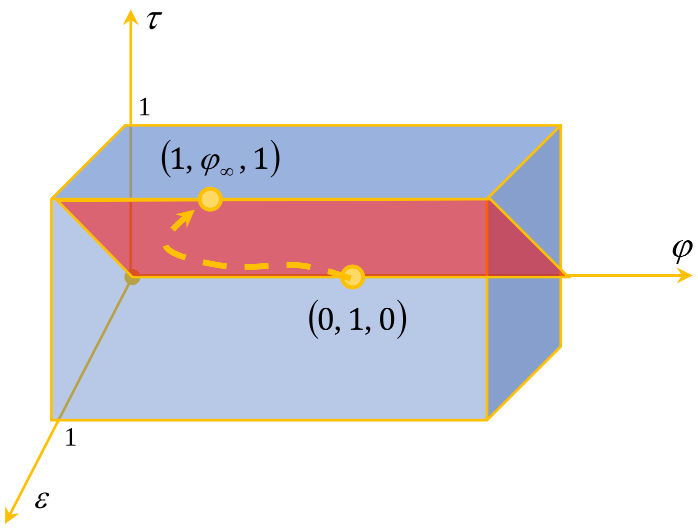

FIG.1 The boundary conditions for equations (1)

3. DETONATION WAVE STRUCTURE

For a perfect gas with a constant specific heat ratio, γ, the one-dimensional gas-dynamic equations are given as

$$\begin{cases} \dfrac{\partial \rho}{\partial t} + \rho \dfrac{\partial u}{\partial r} + u \dfrac{\partial \rho}{\partial r} + \dfrac{j \rho u}{r} = 0 \\ \dfrac{\partial u}{\partial t} + u \dfrac{\partial u}{\partial r} + \dfrac{1}{\rho} \dfrac{\partial p}{\partial r} = 0 \\ \left(\dfrac{\partial}{\partial t} + u \dfrac{\partial}{\partial r} \right) \dfrac{p}{\rho^{\gamma}} = 0 \end{cases} \tag{4}$$

where j denotes the cylindrical ($j = 1$), planar ($j = 0$) and spherical symmetry ($j = 2$). In the case of a steady detonation wave at constant velocity, D, the entropy increase is the same, being valid the following isentropic relationship:

$$\frac{T}{p^{\frac{\gamma-1}{\gamma}}} = const.; \quad \frac{T}{\rho^{\gamma-1}} = const. \tag{5}$$

The temperature T can be replaced, starting from the sound speed expression, $c^2 = \gamma R T$, with the sound speed,

$$\frac{c}{p^{\frac{\gamma-1}{2\gamma}}} = const.; \quad \frac{c}{\rho^{\frac{\gamma-1}{2}}} = const. \tag{6}$$

Replacing the pressure p and the density ρ, by the sound speed c and the velocity u (which are the dependent variable), equations (1) can be written as

$$\begin{cases} \dfrac{\partial c}{\partial t} + c \dfrac{\gamma - 1}{2} \dfrac{\partial u}{\partial r} + u \dfrac{\partial c}{\partial r} + \dfrac{\gamma - 1}{2} \dfrac{jcu}{r} = 0 \\ \dfrac{\partial u}{\partial t} + u \dfrac{\partial u}{\partial r} + c \dfrac{2}{\gamma - 1} \dfrac{\partial c}{\partial r} = 0 \end{cases} \tag{7}$$

With the following nondimensional transformation of dependent and independent variables, simple progressive wave solution for the flow behind the detonation can be obtained

$$\begin{cases} \varphi(\xi) = \dfrac{u}{D} \\ \eta(\xi) = \dfrac{c}{D} \end{cases} \tag{8}$$

where $\xi = \dfrac{r}{D \cdot t}$.

Replacing the derivatives for c and u in the equations (7) we can obtain the expressions for $\varphi'(\xi)$ and $\eta'(\xi)$,

$$\begin{cases} \varphi'(\xi) = \dfrac{j\varphi(\xi)}{\xi} \dfrac{\eta^2(\xi)}{[\varphi(\xi)-\xi]^2 - \eta^2(\xi)} \\ \eta'(\xi) = -\dfrac{\gamma-1}{2} \dfrac{j\eta(\xi)\varphi(\xi)}{\xi} \dfrac{\varphi(\xi)-\xi}{[\varphi(\xi)-\xi]^2 - \eta^2(\xi)} \end{cases} \tag{9}$$

For the planar case we get the trivial solutions, $\varphi'(\xi)=0$ and $\eta'(\xi)=0$, or else $\varphi'(\xi)$ and $\eta'(\xi)$ are nonzero but the denominator of the above equations is zero, $[\varphi(\xi)-\xi]^2 - \eta^2(\xi)=0$. The solutions $\varphi(\xi)=0$ and $\eta(\xi)=0$, correspond to an uniform flow behind the planar detonation and from equation $[\varphi(\xi)-\xi]^2 - \eta^2(\xi)=0$, it follows that

$$\begin{cases} \varphi(\xi) = \dfrac{2}{\gamma+1}(\xi-1)+\varphi_1 \\ \eta(\xi) = \dfrac{\gamma-1}{\gamma+1}(\xi-1)+\eta_1 \end{cases} \tag{10}$$

where φ_1 and η_1 are the constants, evaluated from the boundary conditions (the front, $\xi=1$). The particle velocity decreases to zero at about half the distance that the detonation has propagated from the closed end of the tube, because the value of ξ for which $\varphi(\xi)=0$ is $\xi = 1-\dfrac{\gamma+1}{2}\varphi_1$ and for a strong detonation, where the particle velocity can be approximated by $\varphi_1 = \dfrac{1}{\gamma+1}$ it follows that $\xi=0.5$, therefore, the Chapman-Jouguet condition at the detonation front gives $\varphi\big|_{\xi=1} + \eta\big|_{\xi=1} = 1$, and $u\big|_{\xi=1} + c\big|_{\xi=1} = D$.

In the stagnant region of the detonation product, the pressure can be calculated as

$$\frac{p}{p_1} = \left(\frac{\eta\big|_{\varphi=0}}{\eta_1} \right)^{\frac{2\gamma}{\gamma-1}} \tag{11}$$

and for the regions where $\xi=0.5$ and $\xi=1$, it follows that

$$\frac{p\big|_{\xi=0.5}}{p\big|_{\xi=1}} == \left(\frac{\frac{1}{2}}{\frac{\gamma}{\gamma+1}} \right)^{\frac{2\gamma}{\gamma-1}} \tag{12}$$

This ratio becomes $p\big|_{\xi=0.5} / p\big|_{\xi=1} = 0.34$, for the case when $\gamma = 1.4$ and at the open end of the tube, where $x = 0$ (and $\xi = 0$), the flow reverses and propagates away from the detonation, toward the tube exit, and the velocity can be obtained from the equations (10), $\varphi(0) = -1/(\gamma+1)$ and $\eta(0) = 1/(\gamma+1)$that means the pressure at the open end is

$$\frac{p\big|_{\xi=0}}{p\big|_{\xi=1}} == \left(\frac{\frac{1}{\gamma+1}}{\frac{\gamma}{\gamma+1}} \right)^{\frac{2\gamma}{\gamma-1}} = 0.1 \tag{13}$$

The detonation velocity is linear dependent on the tube diameter (fig. 2), and it permits an interpolation of the straight line to infinite tube diameter, in order to get a value of the detonation velocity, D_∞, which can be considered independent of the tube diameter. The behavior of the detonation velocity for the large-diameter tubes, may not follow the inverse tube diameter dependence, when the boundary layer thickness become negligible compared to the tube diameter and the flow in the reaction zone can be approximated as quasi-one-dimensional. The Mach number at the CJ plane is equal to unity, an expression for M_1 is given by

$$M_1 = \left[\frac{Q}{c_1^2}(\gamma_1 - 1) - \frac{\gamma_1 - \gamma_2}{\gamma_1(\gamma_2 - 1)} \right] \sqrt{\left(\frac{\gamma_2^2 - 1}{\gamma_1 - 1} \right) \frac{1}{1 + \gamma_2^2 \psi}} \tag{14}$$

where

$$\psi = \left(\frac{1}{1-\nu} \right)^2 - 1; \ \nu = \frac{\varepsilon\xi}{(\gamma_2+1)(1+\xi)}; \ \ \xi = \frac{A_2}{A_1} - 1 \tag{15}$$

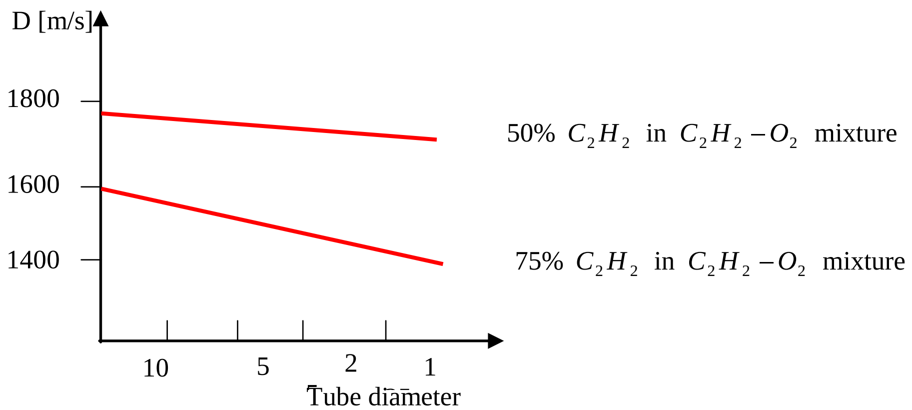

FIG. 2 The dependency of the detonation velocity on the tube diameter

The velocity deficit may be written as a function of the thickness, δ^*, of the boundary layer, where $\xi = 4\delta^* / d$, in the followings form

$$\frac{\Delta V_1}{V_1} = \frac{4\gamma_2^2}{\gamma_2 + 1}\frac{\delta^*}{d} \tag{16}$$

It was found, experimentally that the reaction zone thickness is a function of the detonation velocity and the critical tube diameter, d_c (which represents the minimum diameter through which a planar detonation can be developed in a spherical detonation), therefore, the detonation induction distance (the distance travelled by the flame before detonation onset) can be increased by more three times when the wall of the detonation tube is lined with an acoustically attenuating material such as porous sintered bronze. For high pressure behind the wave front, the ratio of densities approaches a certain finite value, being equal to

$$\frac{\rho_1}{\rho_0} = \frac{\gamma + 1}{\gamma - 1} \tag{17}$$

which leads to the following limiting values: for monoatomic gas with $\gamma = 5/3$ the density ratio is equal to 4, for diatomic gas with $\gamma = 7/5$, it is equal to 6 and for the full vibrational excitation case, $\gamma = 9/7$ and the density ratio is equal to 8. The density increases very slowly at high pressure p_1,. in the limit of a strong shock, the following expressions being valid

$$\frac{T_1}{T_0} = \frac{\gamma - 1}{\gamma + 1}\frac{p_1}{p_0}; \quad u_0 = \sqrt{\frac{\gamma + 1}{2}\frac{p_1}{\rho_0}}; \quad u_1 = \sqrt{\frac{(\gamma - 1)^2}{2(\gamma + 1)}\frac{p_1}{\rho_0}} \tag{18}$$

With respect to the discontinuity, the gas velocities divided by the speed of sound are given by

$$\left(\frac{u_0}{c_0}\right)^2 = \frac{(\gamma - 1) + (\gamma + 1)\frac{p_1}{p_0}}{2\gamma}; \quad \left(\frac{u_1}{c_1}\right)^2 = \frac{(\gamma - 1) + (\gamma + 1)\frac{p_0}{p_1}}{2\gamma} \tag{19}$$

For the weak shock wave $p_1 \approx p_0$ and $\rho_1 \approx \rho_0$, (the pressures on both sides of the discontinuity are close to each other), therefore the sound speeds are almost equal, $c_1 \approx c_0$, that means, a weak shock wave travels through the gas with a velocity which is very close to the speed of sound, while for a shock wave, across which the gas is compressed $(\rho_0 < \rho_1)$ and $(p_1 > p_0)$ the gas flows into the discontinuity with a supersonic velocity $(u_0 > c_0)$ and it flows out with a subsonic velocity $(u_1 < c_1)$In terms of the viscosity and thermal conductivity coefficients, the gas-dynamic equations are

$$\begin{cases} \rho u = \rho_0 u_0 \\ p + \rho u^2 - \frac{4}{3}\mu \frac{du}{dx} = p_0 + \rho_0 u_0^2 \\ \rho u\left(h + \frac{u^2}{2}\right) - \frac{4}{3}\mu u \frac{du}{dx} - k\frac{dT}{dx} = \rho_0 u_0 \left(h_0 + \frac{u_0^2}{2}\right) \end{cases} \tag{20}$$

where the constants of integration are considered as functions of the x coordinate, expressed in terms of the initial values of the variables p, ρ, T and velocity u, so, in order to describe the adiabatic motion of a fluid it is necessary to specify either the entropy or the specific internal energy as a function of density and pressure.

The presence of dissipative processes such as viscosity and heat conduction indicate the irreversibility of a shock compression, which lead to the increase in the entropy, so, the time it takes the fluid in a shock wave to go from the initial to the final state is very short, much shorter than the characteristic times over which the flow variables change in the continuous flow region behind the shock front. The front thickness is much less than the characteristic length scale over which the state of the gas behind the front changes significantly, therefore, the kinetics of the internal processes which take place within a shock front propagating through a gas with given initial conditions depend only on the wave strength. In a coordinate system moving with the wave front the one-dimensional flow equations for viscous and heat conducting gas flow, are

$$\begin{cases} \frac{d}{dx}\rho u = 0 \\ \rho u \frac{du}{dx} + \frac{dp}{dx} - \frac{d}{dx}\frac{4}{3}\mu \frac{du}{dx} = 0 \\ \rho u T \frac{d\sum}{dx} = \frac{4}{3}\mu\left(\frac{du}{dx}\right)^2 - \frac{dS}{dx} \end{cases} \tag{21}$$

where μ is the coefficient of viscosity, k represents the coefficient of thermal conductivity, $\sum$ is the specific entropy and S is a nonhydrodynamic energy flux, $S = -k\frac{dT}{dx}$. The constants of integration are expressed in terms of the initial values of the flow variables, distinguished by the subscript "0" and by the front velocity $D = u_0$. The dimensionless velocity $\eta = u / D = \rho_0 / \rho$ satisfies the equations

$$\frac{1-\eta(x)}{[\eta(x)-\eta_1]^{\eta_1}} = \frac{1-\sqrt{\eta_1}}{\left[\sqrt{\eta_1}-\eta_1\right]^{\eta_1}} \exp\left(1.1\frac{M^2-1}{M}\cdot\frac{x}{l_0}\right) \tag{22}$$

where η_1 refers to the final state behind the shock front

$$\eta_1 = \frac{\gamma-1}{\gamma+1} + \frac{2}{\gamma+1}\frac{1}{M^2} \tag{23}$$

and M is the Mach number, $M = D / c_0$ and c_0 is the speed of sound in the initial state.

The contribution of each of these coefficients to the formation of a shock are not equal, despite the fact that the values of the transport coefficients for kinematic viscosity and thermal diffusivity are close to each other. The equations for one-dimensional steady flow (by neglecting viscosity) take the form

$$\begin{cases} \rho u = \rho_0 u_0 \\ p + \rho u^2 = p_0 + \rho_0 u_0^2 \\ h + \dfrac{u^2}{2} + \dfrac{S}{\rho_0 D} = h_0 + \dfrac{D^2}{2} \end{cases} \quad (24)$$

In the absence of viscosity, it follows that in the process of shock compression, the state of a gas particle changes along a straight line in the pressure-density diagram

$$p = p_0 + \rho_0 D^2 (1-\eta) \quad (25)$$

The ratio of temperatures, T/T_0 and the energy flux, S can be calculated starting from the expression of the enthalpy, $h = \frac{\gamma}{\gamma-1}\frac{p}{\rho}$, as it follows

$$\frac{T}{T_0} = 1 + \gamma M^2 (1-\eta)\left(\eta - \frac{1}{\gamma M^2}\right) \quad (26)$$

$$S = -\frac{\rho_0 D^3}{2}\frac{\gamma+1}{\gamma-1}(1-\eta)(\eta-\eta_1) \quad (27)$$

Here the dimensionless velocity in the final state, η_1 has the expression

$$\eta_1 = \frac{\gamma-1}{\gamma+1} + \frac{2}{\gamma+1}\frac{1}{M^2} \quad (28)$$

In Fig. 3 are resented the T/T_0 and S diagrams for the case of heat conduction.

The temperatures ratio has a maximum at the point $\eta = \frac{1}{2} + \frac{1}{2\gamma M^2}$, and if the shock is sufficiently weak, then η_1 is greater than this value. A monotonic increase in the temperature from the initial value T_0 to the final value T_1 (for a monotonic compression of the gas from the initial to the final volume) results and has the expression

$$\frac{T_1}{T_0} = 1 + \frac{2\gamma(\gamma-1)}{(\gamma+1)^2}(M^2-1)\left(1 + \frac{1}{\gamma M^2}\right) \quad (29)$$

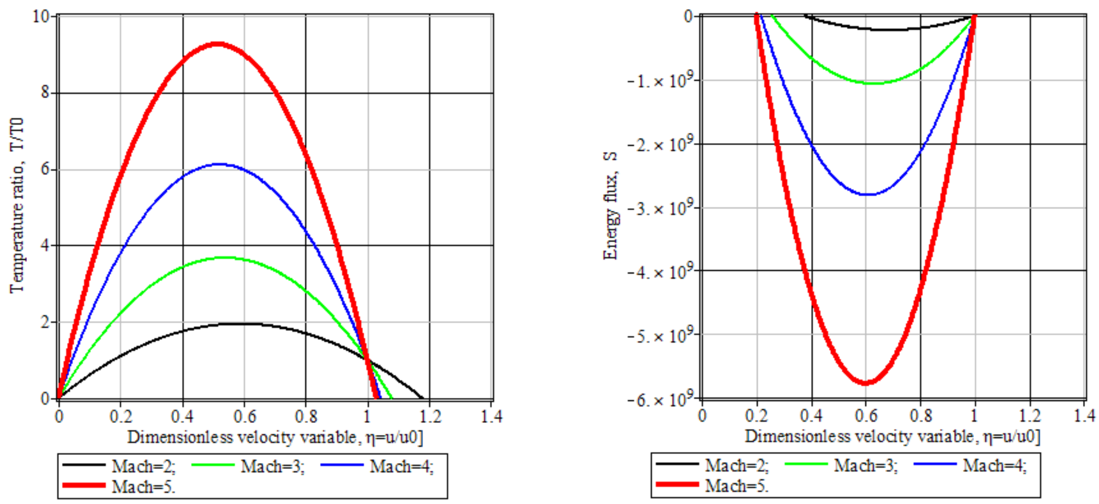

(a) (b)

FIG. 3. Temperature ratio (a) and energy flux (b)

CONCLUSIONS

The detonation velocity is independent of initial and boundary conditions but, due to the thickness of the reaction zone, the initial and boundary conditions can have a strong influence on the propagation of the detonation wave and on the instability of the detonation front, the effect of the boundary consisting in a velocity propagation reduction, a generating of traverse waves which have various positive and negative roles. The detonation velocity depends almost linearly on the inverse tube diameter and flames propagating upward, downward and horizontally in combustion chambers behave differently due to the buoyant effects. Combustion chamber walls have a great influence upon the flame motion and approximate values of flame speeds can be obtained by monitoring the pressure histories with data reduction performed on the basis of an assumed flame spherical shape with negligible thickness.

AKNOWLEDGMENT

This work was supported by a grant of the Ministry of National Education and Romanian Space Agency, RDI Program for Space Technology and Advanced Research - STAR, project number 174/20.07.2017.

REFERENCES

[1] C. Rotaru, G. Răducanu, *Analytical Approaches of Detonation Waves*, in Review of the Air Force Academy, DOI: 10.19062/1842-9238.2017.15.3.6, (2017), pp.57-64.

[2] F. A. Williams, *Combustion Theory*, Princeton University, USA, (1985)

[3] J. H. S. Lee, *The Detonation Phenomenon*, ISBN 978-0-521-89723-5, Cambridge University Press, New York, USA, (2008).

[4] Y. B. Zeldovich and Y. P. Raizer, *Physics of Shock Waves and High Temperature Hydrodynamic Phenomena*, Academic Press, New York, (2002).

[5] C. Rotaru, M. Mihăilă-Andres, P. G. Matei, *An Extended Combustion Model for the Aircraft Turbojet Engine*, in International Journal of Turbo & Jet Engines, ISSN 0334-0082, Vol. 31, Issue 3, Pages 229-237, doi:10.1515/tjj-2013-0048, WOS: 000341513200004, (2014), pp. 229-237.

THE IMPORTANCE OF LIFE-CYCLE ANALYSIS IN ECONOMIC ANALYSIS OF ENVIRONMENTAL IMPACT OF ALTERNATIVE AIRCRAFT FUEL

Jozsef TOTH, Bertold BEKESI

National University of Public Service, Budapest, Hungary (toth.jozsef@uni-nke.hu, bekesi.bertold@uni-nke.hu)

DOI: 10.19062/2247-3173.2019.21.26

Abstract: *In the coming years, the projected increase in air passenger and freight transport will put the climate and the environment at greater risk. In the aviation sector, greenhouse gases and air pollutants such as carbon dioxide (CO_2), nitrogen oxides (NO_X) and sulfur dioxide (SO_X) are expected to increase. The aviation sector intends to address some of these problems by improving fuel efficiency through improved engine and aircraft design, air traffic management and the use of alternative fuels. The ICAO sample is the main organization that sees the ways to solve the problem in these tools. One type of alternative fuels is biofuels, which have a key role to play, as their use ensures the smallest air pollution, taking into account the entire supply chain. The article analyzed the issues and the importance of Life-Cycle analysis (LCA) of alternative jet fuels can be used in the future with regard to these issues and some aspects of Hungary.*

Keywords: *alternative jet fuel, biofuel, life cycle analysis, modelling*

1. INTRODUCTION

Reducing emissions of greenhouse gases (GHG) from the transport sector is an important challenge in the fight against climate change. Emissions from the sector have temporarily decreased as a result of the economic crisis of 2008, but the rebound in production has brought about an increase in demand for goods and travel. The ICAO recently agreed to develop a Global Market-based Measure (GMBM) to achieve carbon neutral growth after 2020 [1]. In this scheme, aircraft operators should offset any annual increase in the GHG emissions beyond 2020 from international aviation between participating states using the Carbon Offsetting and Reduction Scheme for International Aviation (CORSIA). The scheme is currently approved until 2035. Consumption of alternative jet fuels may also be included as part of a basket of measures [2].

The Aircraft emissions will give the impact surface to air quality through the formation of ozone and Particulate Matter (PM) (Fig. 1).

A lot of study has shown the changes in the fuel efficiency are analyzed and the potential reasons for those changes are investigated [1].The aviation biojet fuel was solely depending on its feasibility studies to compare with the rail and road transport, where electric propulsion systems do not offer an alternative way to reduce the emissions. While batteries remain too weak and too heavy for aircraft. The possibility of using renewable wind, hydro, and solar power in commercial aviation, unfortunately, is ruled out for the foreseeable future. So, the capability to offer climate-friendly mobility from renewable energies in aviation is the only mode of transport that has to rely on the use of biofuel [1].

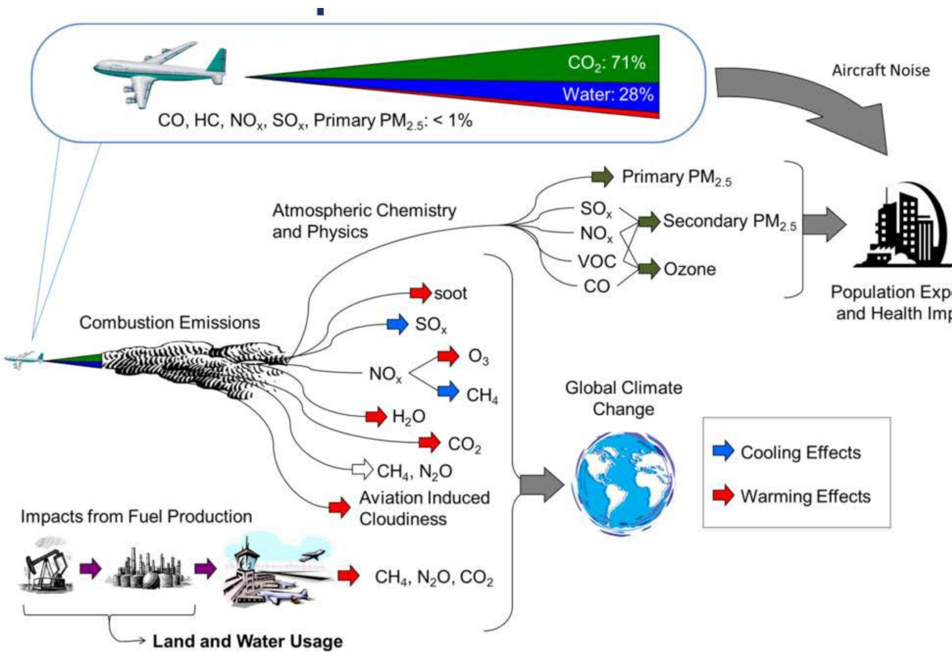

FIG. 1. Environmental impact of Aviation [2]

At decisions related hereby the distinguished importance economic viewpoint analysis and valuation of the application. The decision at the public aviation means choosing between alternatives, in contradistinction to the profit maximization at the commercial aviation.

2. LIFE-CYCLE ANALYSIS

Safety is paramount to aviation authority, hence there will be no requirement of any changes to aircraft engine fuel systems, distribution methods, or storage facilities. Therefore, aviation biofuel can be a “drop-in” fuelthat meets or exceeds internationally recognized as biojet fuel. As ASTM D4054 is where the approval for biojet fuel specification with unchanged operating. [2]

In our time the entire life-cycle approach is the basis for investment decisions on alternative fuels. The Life-cycle analysis (LCA) includes all stages in a product’s life — from the extraction of law materials through the materials’ processing, manufacture, distribution, use, and disposal or recycling. For this analysis, we have to account for all the stages in the life cycle of aviation fuels, including feedstock recovery and transportation, fuel production and transportation, and fuel consumption in an aircraft.

The exploration and recovery activities from the well to fuel production and the subsequent transportation to the pump constitute the well-to-pump (WTP) stage. The combustion of fuel during aircraft operation constitutes the pump-to-wake (PTWa) stage. These two stages combined comprise the well-to-wake (WTWa) fuel cycle [4].

As shown in Fig. 2, the WTWa analysis system boundary includes feedstock recovery and extraction of mineral oil (e.g., crude recovery, corn farming and harvesting, and corn stover harvesting), feedstock transport, fuel production (e.g., petroleum refining to jet, ethanol production, ETJ production), fuel transportation and distribution, and aircraft fuel combustion.

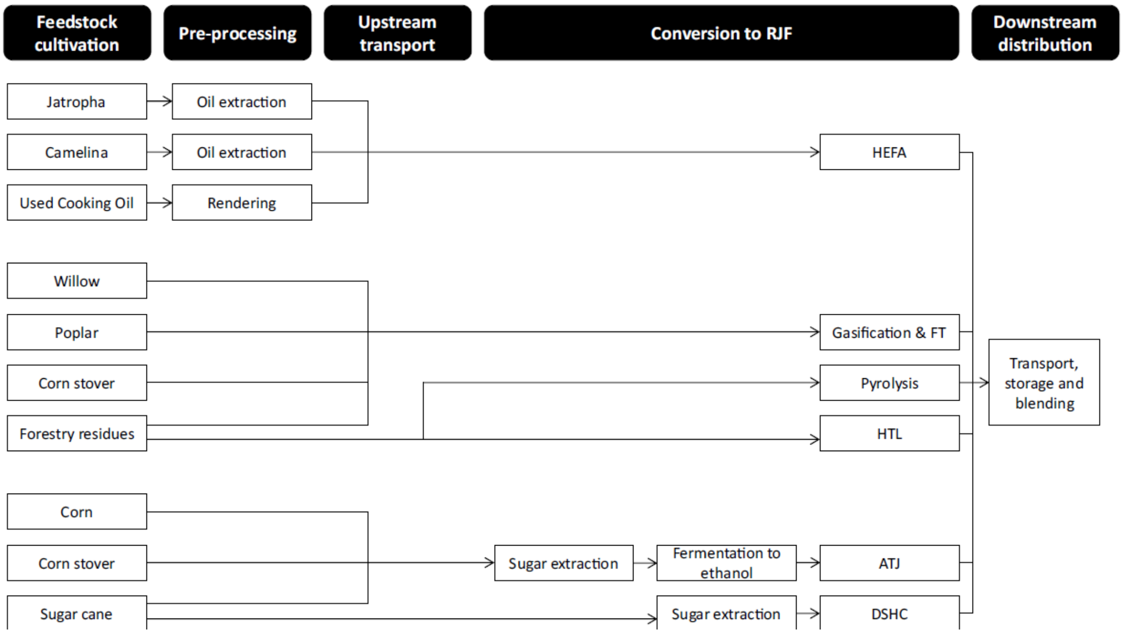

FIG. 2. A schematic overview of the renewable jet fuel supply chain [3]

With the alternative renewable fuels refer in Fig. 2. we present as example the „Well to Wake" model of ethanol-to-jet fuel.

Among alternative fuels one solution can be the use of biofuels, which can be produced from various kinds of biomass, like photosynthetic microorganisms, that is, algae. Oil produced by them may be the appropriate source material for producing biodiesel, moreover, for this process the carbon dioxide from the atmosphere is used [4]. Nowdays the biodiesel is keeping his spread within limits more factor, featured high cost of his production. It can be told , that more and more research are in this topic on large part of the world , and increases the number of the companies, what consider with fuel analysis, development of the biodiesel, or with its establishment [5].

Nowadays a lots of study compares the well-to-wake (WtWa) GHG emission performance of various RJF conversion pathways and shows the impact of different co-product allocation procedures [3][4][5].

Conversion pathways based on residues or lignocelluloses crops yield low WtWa GHG emissions, irrespective of allocation method. The FT pathway shows the highest GHG emission savings (86–104%) of the pathways considered, followed by HTL (77–80%), pyrolysis (54–75%), UCO-based HEFA (68%), and sugarcane- (71–75%) and corn stover-based ATJ (60–75%) [4].

3. BIOFUEL PRODUCTION POTENTIAL IN HUNGARY

The European Parliament and Council Directive (Renewable Energy Directive, hereinafter referred to as "RED") sets a binding target for all Member States to represent at least 10% of the total energy used by 2020 in the transport sector, including biofuels. There are a number of alternatives to reduce CO_2 emissions in the transport sector, with biofuels playing a key role in the European Union. Biofuels are liquid or gaseous transport fuels produced from biomass, ie. biodegradable agricultural, forestry or fishery products, waste, residues or biodegradable industrial and household waste [4].

The use of biofuels can bring many benefits:

- reduces GHG emissions as a function of raw material and production technology;
- reduces the release of certain harmful substances (carbon monoxide, solids) that do not directly affect climate change but cause local air pollution and present serious health risks;
- reduces energy dependency, increases security of supply;
- contribute to the development of agriculture and related industries

A basic factor is that biofuels have lower GHG emissions than fossil fuels if their production does not result in additional emissions from land use change [6].

The importance of sustainability has also become an important requirement. The main elements of the sustainability criteria system are:

- From 2017, GHG savings from the use of biofuels should be at least 50% compared to fossil fuels. In 2018, the minimum value for new production facilities will increase to 60 percent. GHG savings are needed to calculate the full life cycle of biofuels.
- Biofuels should not be made from raw materials of high biodiversity value or land with significant carbon stocks. It belongs to the former category eg. the primary forest or the high diversity grassland, for example the latter. wetlands and intermittent forest areas [4].

In Hungary, the possible ethanol raw materials are wheat and maize, sugar beet, sugar currants, potatoes and Jerusalem artichokes. With regard to raw materials, there is no doubt that maize with higher yields than wheat in Hungary and available in bulk can be the main source of bioethanol production, at least in the medium term.

Most bioethanol can be extracted from the Jerusalem artichoke (4,200 l / ha), sugar beet (4000 l / ha) and sugar circus (3500 l / ha), but this requires a crop of between 50 and 35 tonnes. In addition, these products can be poorly stored, which is detrimental to the continuity of bioethanol production. The value of the main product per unit area is very high in the case of potatoes, but due to the high price of the raw material and the relatively small amount of alcohol that can be extracted from it, only an exceptional situation can justify the use of potatoes as raw material for bioethanol. Sugar beet is still outstanding in terms of the main product value of the area. The economical position of sugar beet is significantly improved by the production of agricultural by-products of 180-240 Euro (60-80 thousand HUF) per hectare. However, this latter use must be accompanied by an appropriate livestock sector. As a usable agricultural by-product, straw is still the corn stalk in the corn. They are currently used mainly as feed and litter [7].

Among the examined raw materials, sugar circus, Jerusalem artichoke and maize are the most favorable for the cost of producing bioethanol.

To be able to produce one liter of bioethanol economically, taking into account all the conditions, the price per tons of maize should be "normal" for 100-120 Euro, for 25-30 thousand HUF, but not more than 35-37 thousand HUF. It can only exceed 10-20 percent in exceptional and exceptional years, so that bioethanol production can be profitable under current technological conditions [7].

CONCLUSIONS

Depending on the feedstock source, fuel conversion technology, and allocation or displacement credit methodology applied to co-products, preliminary WTWa results show that alternative bio-jet fuel pathways can reduce life-cycle GHG emissions by 55–85 percent compared with petroleum-based jet fuel [7].

At modelling of the life-cycle analysis on beyond the estimation of the individual cash flows serious difficulty appears the setting of recourse of dates.

According to the source material it can also be concluded that the production of biofuels, in addition to investment decisions related natural resources of a country depends to a large extent on the state market regulation.

Hungary is one of the poor countries in energy-producing raw materials, but it has the right potential for agricultural to produce agricultural raw materials for biofuels.

ACKNOWLEDGMENT

This work was supported by the European Regional Development Fund (GINOP 2.3.2-15-2016-00007, “Increasing and integrating the interdisciplinary scientific potential relating to aviation safety into the international research network at the National University of Public Service - VOLARE”). The project was realised through the assistance of the European Union, and co-financed by the European Regional Development Fund.

REFERENCES

[1] ***ICAO A39-WP/56 Assembly – 39th Session Sustainable Alternative Fuels For Aviation, 17/06/16, Available at www.icao.int/Meetings/a39/Pages/WP_Num.aspx, accessed on 14 Apr. 2017;

[2] B. Varga, J. Tóth: *A széndioxid, mint a legfőbb ellenség, avagy mi az ICAO által létrehozott CORSIA szerepe ebben a harcban* REPÜLÉSTUDOMÁNYI KÖZLEMÉNYEK (1997-TŐL) XXIX : 3 pp. 243-252. , 9 p. (2017) accessed on 12. Dec. 2018;

[3] de Jong et al.: *Life-cycle analysis of greenhouse gas emissions from renewable jet fuel production*, Biotechnology for Biofuels (2017) 10:64; DOI 10.1186/s13068-017-0739-7;

[4] *** United Nations Environment Programme: *Global Guidance for Life Cycle Impact Assessment Indicators*, Volume 1. Available at https://www.lifecycleinitiative.org/about/about-lci;

[5] A. Elgowainy, J. Han, M. Wang, N. Carter, R. Stratton, J. Hileman, A. Malwitz, S. Balasubramanian, *Life Cycle Analysis of Alternative Aviation Fuels in GREET*, Available at https://greet.es.anl.gov/publication-aviation-lca; accessed on 14 Apr 2017;

[6] M.D. Staples et al.: *Aviation CO2 emissions reductions from the use of alternative jet fuels* https://doi.org/10.1016/j.enpol.2017.12.007. Energy Policy 114 (2018) 342–354;

[7] F. Laczó: *Bioüzemanyagok előállításnak lehetőségei Magyarországon*, Környezettudományi Központ, Budapest, 2008, Available at: http://www.ktk-ces.hu/biouzemanyag.pdf, accessed on 12 Febr. 2019.

CONTROL LAW FOR AN AIRCRAFT SUPERSONIC AIR INLET WITH INTERNAL COMPRESSION

Alexandru-Nicolae TUDOSIE[*], Emanuel DUMITRU[*], Marius-Alin ASPRA[**]

[*]University of Craiova, Craiova, Romania (atudosie@elth.ucv.ro, antudosie@yahoo.com, edumitru49@yahoo.com)
[**] S.C. Eneria S.R.L. Craiova, Romania (alin_aspra@yahoo.ro)

DOI: 10.19062/2247-3173.2019.21.27

Abstract: *This paper deals with a supersonic air inlet Laval-type. Based on thermo- and gas-dynamic phenomena, the authors have determined the possibilities of Laval-type intake starting process; the starting envelope of the intake was also defined and graphically depicted. Some operating regimes of the intake, correlated to engine's operation were studied and intake's adjusting possibilities were described, as intake's work-lines; these lines were depicted on intake's operational envelope and some control law(s) were determined with respect to the work-lines. Possible control architecture may be emphasized.*

Keywords: *intake, Laval, supersonic, starting, control, work line, Mach number.*

1. INTRODUCTION

The air inlet of an aircraft engine is of prime importance; in fact, for all airbreathing propulsion systems the inlet plays a major role. Its major function is to collect the atmospheric air at free stream Mach number, to slow it down (even if a change of flow direction might be involved) and so, to compress it efficiently.

In this matter of issue, aircraft engine's inlet is performing an essential part of its thermodynamic cycle; moreover, inlet's efficiency is connected to the engine's performance, being directly reflected in it. The inlet must supply engine's downstream components with air at suitable velocities and pressures, with an acceptable degree of uniformity, under any flight condition. Nevertheless, the air inlet has to achieve all these tasks with minimum external drag and to assure to the external flow (around aircraft's body and/or nacelle) a minimum disturbance.

Air inlets (or simply intakes) play important roles in the stability and performance of the installed propulsion systems and, as a result, in overall flying vehicle operation. Moreover, supersonic air inlets (for supersonic aircraft) have a crucial importance, since they must satisfy, for all flight conditions, the needs of the engine for sufficient air, obviously with specific properties and requests, such as low pressure-loss (high recovery coefficient) and low value of distortion, running from ground test operation to supersonic flights [8]. Withal, supersonic inlets have complex flow-field; it might occur shock waves and/or expansion waves, shock waves-boundary layer interactions, flow separation, buzz/stall instability etc. That is the reason why inlets' studying involves both experimental and numerical analysis, in order to better understand their internal and external flow-field, as well as to better predict their operational characteristics and behavior during flights at subsonic and at supersonic velocities.

There are several classifications for supersonic intakes based on their characteristics, like geometry or compression mechanism.

The two-dimensional (2D) and axisymmetric CFD analysis of air inlets are conventional respectively for rectangular and axisymmetric/semi-axisymmetric intake, which neglect the 3D effects of flow-field. However, 3D effects, for example due to sidewall and cross flows, particularly in separation and shock-boundary layer interaction regions for all air intake types, are considerable [5, 8, 10, 11, 17].

Supersonic inlets with internal compression are devices that perform dynamic air compression only inside the flow channel, the air velocity in the forward inlet section being supersonic. Some of them uses internal shock-waves for slow down the flow stream (as presented in [2, 12, 13]), but other uses their specific geometry. These inlets have their flow passage of the inward compression intake devices of the form of a Laval nozzle, so they are also called just intakes, or Laval intakes.

This paper intends to study such a Laval intake and to establish possible control law(s), as well as a possible control architecture(s).

2. ABOUT SUPERSONIC LAVAL INTAKES

As presented in Fig.1, the Laval intake operates like a reversed Laval nozzle; from the input inlet section $1^{/}$ to its throat (its minimum section, noted as *"min"*), the channel is convergent, while from the throat to the output section 1 (which is, in fact, the compressor's input section) the channel is divergent.

Under ideal conditions, when the air flow deceleration is rendered isentropically (hence the name of the device) and the boundary layer is absent, in the convergent zone of the flow channel of the device the compression of the supersonic air stream occurs in the form of a system of low intensity pressure waves (as seen in Fig.1). In the minimum section of the channel, the air velocity becomes sonic (equal to the sound speed). Further compressed air, which already has a subsonic speed, takes place in the divergent zone of the flow channel. Therefore, the ideal device with internal compression operates as an inverted Laval nozzle.

Thus, the breathed air tube in front of the device is cylindrical, the cross area of its section being the same in the inlet's input section $1^{/}$ as in any undisturbed upstream sections, generically denoted by *H*. Inside the air intake, in its convergent zone, the air flow decreases continuously its speed, but it still remains supersonic, between the sections $1^{/}$ and *min* where it reaches the sonic speed (which is also the critical section; after it, the air flow converts to a subsonic flow and continuously decelerates as a result of the divergence between the sections *min* and 1. If the air were an inviscid fluid, its evolution would be realized under ideal conditions, without total pressure loss, thus $\sigma^{*}_{DA} = 1$.

Obviously, in the real operation mode, the boundary layer appears on the walls of the channel and its thickness increases spectacularly in the direction of the air flow, inside the flow channel of the Laval intake.

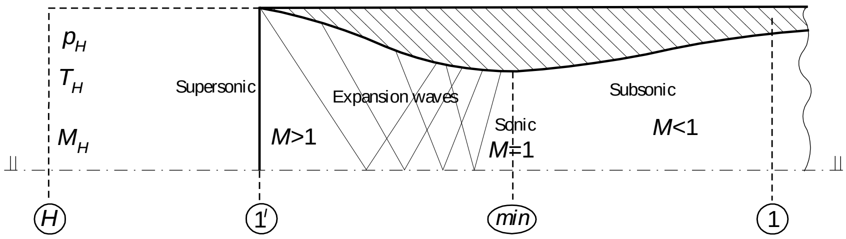

FIG. 1 Supersonic inlet with internal compression of inverted Laval type

If the profiling of the internal flow channel would thus be realized as its walls are generators of oblique shock waves, then, due to the interaction between these waves and the boundary layer, wall flow separations may occur, as well as changes of the flow spectrum compared to the calculation regime situation.

Therefore, in order to maintain the flow pattern corresponding to the compression mode of the internal compression inlets, it is necessary to profile their flow channel so that the flow section area succession to be smooth, without any sudden changes in the geometry of the walls; furthermore, the walls might be provided with holes for the boundary layer sucction, which, overall, is difficult to achieve.

Apart from the difficulties coming from the profiling of the inlet's channel and from the substantial influence of the boundary layer on the flow regime, the practical use of supersonic intakes with internal compression is also difficult because of the difficulty of bringing and stabilizing their operation at a nominal regime, operation generally known as "Starting the inlet". In order to reveal the peculiarities of the starting process, it is necessary to determine the mathematical relations for the calculation of the functional sections areas of the Laval intake.

3. SUPERSONIC INLET'S INTERNAL COMPRESSION STARTING

The mechanism of the internal dynamic compression's starting inside the inversed Laval inlet device must be explained after the classical Laval nozzle starting is studied and explained; this kind of nozzle assures the output of a supersonic flow starting from a subsonic flow input, using only its geometry (its internal flow channel shape).

3.1. Laval nozzle's starting. The starting of the subsonic-supersonic Laval-type nozzle, described in [7,8], calls for the assumption of continuous flow, without friction or heat exchange. It is supposed to be known: the nozzle geometry (A_{cr} and A_e , as well as the cross section area variation along the length of the nozzle $A = A(x)$), the air flow rate $\dot{m}_a$ passing through the nozzle, as well as the parameters of the upstream air (p^* and T^* or i^*), as presented in Fig. 2. Depending on the downward pressure values, there are several flow-related situations, which means several nozzle pressure variation curves.

If the flow rate $\dot{m}_a$ through the nozzle is less than the maximum (critical) flow rate, then the flow velocity is maintained subsonic across the Laval nozzle (curves 1 and 2, Fig. 2).

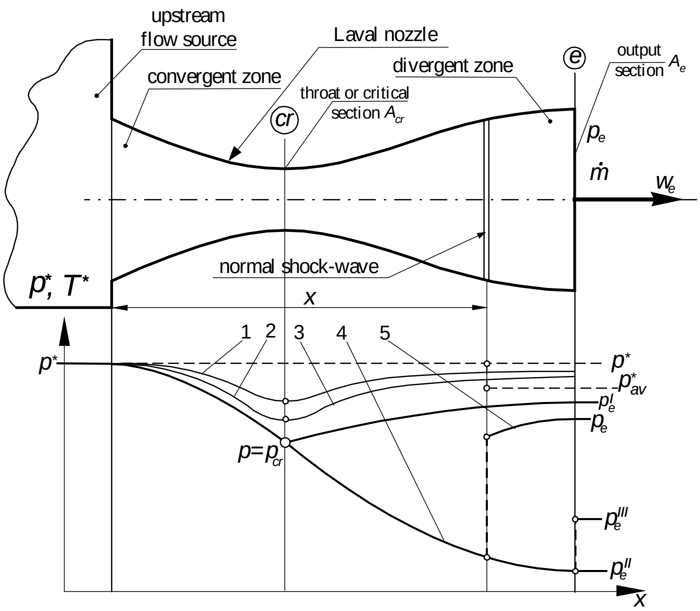

FIG. 2 Laval-type exhaust nozzle starting process [8]

When the maximum flow rate is reached, critical conditions are obtained in the throat, so the convergent portion is considered as primed, but the flow in the divergent zone may be subsonic (curve 3, Fig. 2), or supersonic (curve 4), depending on the downstream effective conditions (that means the static pressure at the nozzle exit p_e).

From the Saint-Venant equation [7], written for both throat and exit section, one obtains

$$\beta_e^{\frac{2}{\chi}}\left(1-\beta_e^{\frac{\chi-1}{\chi}}\right)=\frac{\chi-1}{2}\left(\frac{2}{\chi+1}\right)^{\frac{\chi+1}{\chi-1}}\left(\frac{A_{cr}}{A_e}\right)^2, \tag{1}$$

where $\beta_e = \dfrac{p_e}{p^*}$ is a value which may be calculated, knowing p_e and p^*. This equation has two roots, one for the subsonic regime $\beta_e^{/} > \beta_{cr}$, the other for the supersonic regime $\beta_e^{/} < \beta_{cr}$, where $\beta_{cr} = \left(\dfrac{2}{\chi+1}\right)^{\frac{\chi}{\chi-1}}$; they correspond to the pressures in the exit section $p_e^{/}$, respectively $p_e^{//}$.

If the pressure downstream of the nozzle is $p_e \geq p_e^{/}$, then the flow regime is completely subsonic (curves 1, 2, 3). Curve 3 of Fig. 2 corresponds to the pressure value $p_e^{/}$ and represents the limit curve of the subsonic flow range across the nozzle. If $p_e < p_e^{//}$, then, the flow regime is supersonic in the divergent zone (curve 4), and the Laval nozzle is completely started.

The situation when $p_e^{//} < p_e < p_e^{/}$ corresponds to the establishment of a mixed flow regime in the divergent zone, characterized by the occurrence of a normal shock wave within this area. The pressure range may be even more limited if it is considered that the starting of the nozzle is complete when the normal shock-wave occurs in the output section; the velocity coefficient $\lambda_e^{///}$ before the shock-wave, can be determined from the flow rate equation, choosing the supraunit solution $\left(\lambda_e^{///} > 1\right)$,

$$q\left(\lambda_e^{///}\right)=\frac{\dot{m}\sqrt{T^*}}{KA_e p^*}, \tag{2}$$

while, behind the shock-wave, the velocity coefficient is $\dfrac{1}{\lambda_e^{///}}$. The flow rate function is

$$q(\lambda)=\lambda\left[\frac{\chi+1}{2}\left(1-\frac{\chi-1}{\chi+1}\lambda^2\right)\right]^{\frac{1}{\chi-1}}. \tag{3}$$

By the shock-wave the total pressure suffers a loss, so, behind the wave, the pressure will be calculated starting from the same flow conservation equation,

$$p_{av}^* = \frac{\dot{m}\sqrt{T^*}}{KA_e q\left(\dfrac{1}{\lambda_e^{///}}\right)}, \tag{4}$$

One can also calculate the limit of the external pressure $p_e^{///}$ (the value of the outside pressure below which the Laval nozzle is fully started)

$$p_e^{///} = p_{av}^* \Pi\left(\frac{1}{\lambda_e^{///}}\right) = \left[\dot{m}\sqrt{T^*}\,\Pi\left(\frac{1}{\lambda_e^{///}}\right)\right] / \left[KA_e q\left(\frac{1}{\lambda_e^{///}}\right)\right], \tag{5}$$

where $\Pi(\lambda) = 1 - \frac{\chi - 1}{\chi + 1}\lambda^2$ is the thermodynamic funcion of the pressure.

Consequently, it can be concluded that the following situations may occur during the Laval nozzle starting, depending on the value p_e of the static pressure downstream of the nozzle:

a) if $p_e \geq p_e^/$ the nozzle is totally under subsonic flow;

b) if $p_e^/ > p_e > p_e^{///}$ the nozzle shows a mixed flow in its divergent zone, being triggered a shock-wave; the upstream flow is supersonic, re-becoming subsonic downstream (curve 5, in Fig. 2);

c) if $p_e < p_e^{///}$, the shock-wave is completely discharged from the nozzle, and this one is fully primed (started).

One of the most importnt problems to be studied in the case of the emergence of a shock-wave in the nozzle's divergent zone is the determination of its position, with respect to the critical section or to the nozzle entry section, under the conditions of knowledge of the upstream (p^*, T^*) and downstream (p_e)parameters and of the nozzle geometry (nozzle section with respect to the longitudinal coordinate, $A = A(x)$). This situation corresponds to curve 5 in Fig. 2; the pressure will drop in the first part of the nozzle after curve 4, the flow being supersonic up to the shock-wave. Through the normal shock-wave the pressure undergoes a jump, then following the 5-curve till the pressure p_e in the exit section.

3.2. Laval intake's starting. The Laval air intake with internal compression must realize the pressure variation after the same curve as shown in Fig. 2, but obviously in the opposite direction. In order to achieve a better correlation with the phenomena presented in the previous paragraph, but reversed as a direction of realization, it is assumed that, in the case of the studied convergent-divergent air intake, there is another Laval nozzle, which performs the supersonic velocity *V* and the air flow $\dot{m}_a$ necessary to operate the air intake at the nominal calculation mode. Therefore, one considers two succesive Laval nozzles (see Fig. 3), the first-one has constant geometry, while the second-one (which is the studied variable air intake) has variable geometry.

The critical section (the throat) of the first nozzle has the cross-section A_{cr1} determined by the condition that the nozzle must be able to drive the imposed air flow rate. The second air nozzle has variable throat cross-section A_{cr2} and will take up the air supplied by the first nozzle at the speed and at the flow rate imposed by this one.

Initially, it is considered that the air intake has the critical section "closed" (position 1), at its minimum value $(A_{cr2} < A_{cr1})$, which is the value which corresponds to the critical flow regime in this section. The pressure distribution corresponds to the curve 1 in Fig. 3.

Further, the critical section of the variable nozzle is increased to a new position, denoted by *"cr"* when the equality $A_{cr2} = A_{cr1}$ is obtained. The airflow through the air intake has increased, compared to the previously described case; in addition, in both critical sections the sound speed is obtained.

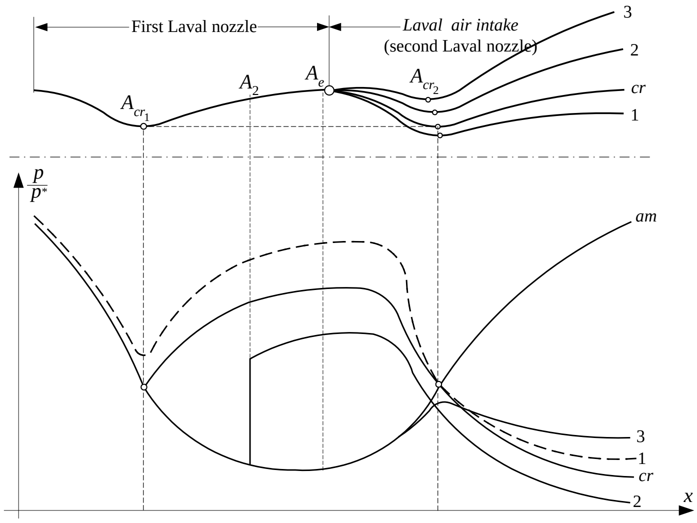

FIG. 3. Laval-type air intake starting process [8]

As in the first nozzle, in the divergent zone, the flow velocity is subsonic, in the second nozzle the air accelerates in its convergent zone (the curve denoted by *"cr"*).

If the critical area of the air intake opens even more, so that $A_{cr2} > A_{cr1}$, then a sudden depression wave occurs behind the first nozzle, which implies the occurrence of a normal shock-wave point in its divergent portion (in position A_2); behind the wave, the flow rebecomes subsonic and is compressed isentropically in the first nozzle's diffuser, then it accelerates to the sound speed in the throat (critical section) of the Laval intake, then accelerates further (curve 2 in Fig. 3).

From the written flow conservation equation for the two nozzles, it results:

$$\dot{m}_a = A_{cr1}\frac{p^*_{am}}{i^*_{am}} = A_{cr2}\frac{p^*_{av}}{i^*_{av}}, \tag{6}$$

and taking into account the fact that the total enthalpy does not change, it is obtained:

$$\frac{A_{cr2}}{A_{cr1}} = \frac{p^*_{am}}{p^*_{av}} = \frac{1}{\frac{p^*_{av}}{p^*_{am}}} = \frac{1}{\sigma^*_{us}}. \tag{7}$$

Therefore, since the shock-wave of the first nozzle diffuser moves outwardly, its greater the intensity and the total pressure loss coefficient σ^*_{us} decreases; consequently, the ratio $\frac{A_{cr2}}{A_{cr1}}$ increases, so the section A_{cr2} is growing. On the magnitude of the increasing opening of the variable section A_{cr2}, the shock-wave of the first nozzle diffuser is getting closer and closer to the exit from it, where the area of the section is A_{e1}; at a time, a small additional opening of A_{cr2}, the shock-wave is discharged from the first nozzle and "sent" to the terminal area of the second nozzle (the air intake) at the section A_{e2}, whose mode corresponds to curve 3 in Fig. 3. As a consequence, it can be stated that the critical area of the air intake varies between extreme values A_{cr1} and A_{e2}.

If a current section $A_x \left(A_x \in \left[A_{cr1}, A_{e2}\right]\right)$ is considered, from the equation of air's evolution, assumed to be isentropic, it is obtained

$$\frac{A_{cr1}}{A_x} = q(\lambda_x). \tag{8}$$

From the moment when the shock-wave was discharged from both nozzles, the reduction of the throat of the air intake would lead to the return of the shock-wave to the minimum section of the intake, in its divergent zone. When reating the value $A_{cr2} = A_{cr1}$, it is obtained the starting of the air intake (curve "am" in Fig. 3). Therefore, the starting of the air intake assumes a complex maneuver, initially complete opening (up to $A_{cr} = A_{1'}$), then closing, to the section A_{cr} that can support the air flow rate required for the engine. However, a small variation of the throat section or of the downstream pressure leads to the disengagement of the air intakes, which means the return on the *"cr"* curve, which produces an imbalance between the flow rate required by the engine and the flow provided by the air intake, sometimes resulting the engine unexpected shutting down.

4. INTAKE'S CONTROL LAW DESIGN

From the previously presented, it results that the starting of the Laval air inlet with internal compression is an extensive process, requiring a variation of its minimum section (throat) in both directions, initially increasing, then returning. In fact, the process resides in the repositioning, in the divergent zone of the air intake channel, of the normal shock wave, which initially was formed in front of the air intake.

4.1. Control law's limits establishing. For a certain but known flight regime, characterized by Mach flight number M_H (or velocity ratio λ_H), according to (8), it results

$$\frac{A_{cr}}{A_{1'}} = \frac{A_{cr}}{A_H} = q(\lambda_H), \tag{9}$$

where A_H is the area of the cross section of the current tube upstream of the intake, equal to $A_{1'}$ the area of the intake's input section. The size of this area is given by the required air flow rate, according to that flight regime.

To start the internal compression, in the first phase the shock wave must be "transferred" to the exit area of the divergent zone of the intake, so it is necessary to enlarge the critical section. This must be done in accordance with (8), to conserve the flow even behind the shock wave (already reached in the channel), where, according to Prandtl's law, the velocity coefficient is the inverse of the velocity coefficient before the shock wave

$$\frac{A_{cr}}{A_{1'}} = q\left(\frac{1}{\lambda_H}\right). \tag{9}$$

After the shock wave evacuation, the throat section must be reduced so that it reaches the initial value.

Taking into account the formulas (8) and (9), for each flight regime (for each M_H or λ_H), it is possible to identify the range of values for A_{cr} with respect to $A_{1'}$.

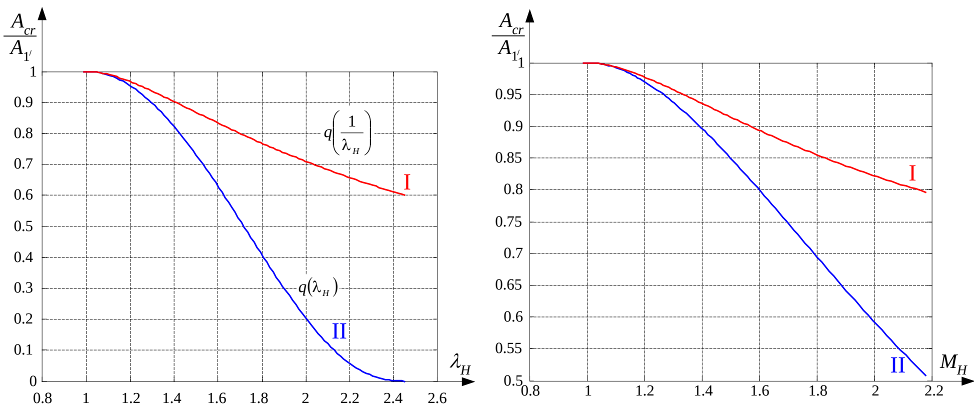

a) b)

FIG. 4. Laval-type air intake starting limits

For a sequence of flight regimes, two curves (I and II in Fig. 4) are obtained, which determine the air intake with internal compression starting envelope. Inside this envelope the sarting is stable, varying only the intensity of the prerssure losses $\left(\sigma_{us}^{*}\right)$; the losses are even less as the operating mode of the intake approaches the curve I (where the losses are, under ideal conditions, null). Consequently, all adjustment and control laws must be within this envelope area. Curves in Fig. 4.a) are traced with respect to the velocity coefficient, while in Fig. 4.b) is the same envelope with respect to the Mach number, based on the connection between M_H and λ_H:

$$M_H = \sqrt{\frac{2\lambda_H^2}{\chi + 1 - (\chi - 1)\lambda_H^2}}\,. \tag{10}$$

It is precisely because once with the return to the I curve, when the isentropic compression is started, the air intake becomes very sensitive to the accidental variations of either the throat cross section, or the flight regime, losing its stabile operation; it is preferred to reduce the throat of the intake (to return to curve I) and to maintain a reserve with respect to the lower limit curve I $\left(\left(A_{cr}\right)_{real} > \left(A_{cr}\right)_{nec}\right)$. In this way, the shock wave is fastened in the area of the throat, but in intake's divergent zone, with the consequence of the keeping the intake started, even under conditions of disturbance; it assures low total pressure losses, acceptable under conditions of stability to the action of the various disturbances.

4.2. Intake's work line. Based on the above considerations, it is possible to determine the air intake work line, to be drawn on the starting envelope; the complete work line is very complex, but some possible aspects of it are drawn on the starting envelope in Fig. 5.

The following important zones of the intake work line can be identified, depending on the flight speed (more precisely, depending on the Mach number):

a) starting the engine, corresponding to point A. Engine's start is facilitated by the presence of a significant dynamic compression component, if the aircraft whics uses tis device is already in flight. The intake must be fully open, so the critical area (the throat) is equal to the intake area;

b) acceleration to the sound speed, section A-B, when the air intake must hold the same aperture. At the end of accelerating, when the sound speed is reached, a normal shock wave occurs in front of the air intake;

c) acceleration in the supersonic mode, section B-C, until the shock wave is attached to the intake's lip. In this zone, the intake's throat must be gradually reduced (on curve I), following the increase of the speed.

To stabilize the shock-wave's position, once the Mach limit is reached, the throat section must close to point D, near the limit curve II. Point D is not on curve II, but there is a certain reserve, in order not to „destart" the intake;

d) the further acceleration on section D-E is done with the same throat cross-section value, on a horizontal line in the diagram in Fig. 5, to the restraint in the proximity of the curve I, with the evacuation of the shock-wave from the intake;

e) accelerating on the EF line, graduated with the throat's section drop, on a parallel curve to curve I and very close to it. When reaching the maximum speed (maximum Mach number), the throat section can be reduced to curve II (vertical FG) to start the isentropic flow in the intake. However, the G point is not on the curve II, in order to keep a reserve and avoid disruption in the event of disturbances occurance. One may affirm that the G point represents the starting regime of the isentropic flow through the Laval air intake.

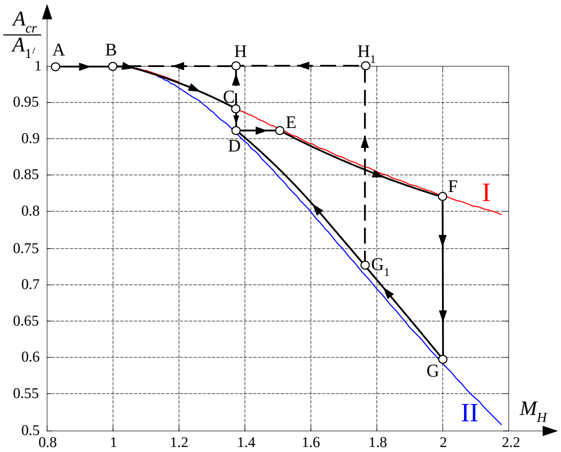

FIG. 5 Laval-type air intake work lines used as control law(s)

In the situation where the deceleration of the airplane is desired, then the operating point of the Laval Intake must be maintained within the starting envelope, as far as possible on the curve II. For the same reasons as mentioned above, a reserve is kept against the curve II towards the inside of the envelope, therefore any deceleration operation, which can not be safely performed on the curve II, must be made on a close curve, respectively, on the GD path, the current point G_1 being displaceable between the two limits. Further, if the subsonic regime is to be regained, then the reverse path might be followed, such as the curve D-C-B-A, or the point A might be moved to the left; in fact, in transonic or subsonic mode, the air inlet is completely open. If the deceleration occurs suddenly, commanded or accidentally, then the air intake must be open to restore the starting on one of the routes in Fig. 5 (either on the G_1-H_1-H-B route, where G_1 can have any position between G and D or on the alternative route D-C-H-B, if the deceleration is made from low supersonic regime).

CONCLUSIONS

It can be argued that a Laval-type air intake with fixed geometry can only provide a single flight regime and operating mode of the engine, so it is imperative to use variable-geometry air intakes, with their minimum section (throat) of variable dimensions. Two possible forms of the intake are: axisymmetric, or plane-parallel.

However, if a throat adjustment method is possible, the Laval-type inlet control becomes possible; the work-line(s) for such an intake was (were) determined, correlated to the flight regime, which made possible a control law issuing, as well as an appropriate control architecture design; anyway, the starting problem must always be overcome and the control laws must follow the work lines inside the starting (operational) envelope, in order to keep always correlated the engine's air needs and the intake's air offer with an appropriate structure.

It is very difficult (virtually impossible) to construct an axisymmetric air inlet whose throat can be adjusted to be able to adapt to various flight regimes. The planar parallel intakes can be manufactured with much simpler geometry, since they have the frontal section of a rectangular shape of constant depth, and the scaling of their throat requires only the scaling of the other rectangle dimension (the height). However, when the internal compression is combined with the external compression (in the mixed compression inlets), one can imagine a special form of its centerbody, which, together with the shape of the air intake and the channel, generates a Laval-type nozzle, with variable minimum section (both in size and axial position) by the favorable repositioning of the central body [13, 14, 16]. Starting problems are also issuing both for internal and mixed compression inlets.

REFERENCES

[1] R. H. Abraham, *Complex dynamical systems*, Aerial Press, Santa Cruz, California, 1986.

[2] I. Aron and A. N. Tudosie, Hydro-mechanical system for the supersonic air inlet's channel's section control, *Proceedings of the International Conference on Applied and Theoretical Electricity*, ISBN-973-657-005-3, pp 266-269, Craiova, 2000.

[3] C. Berbente and N. V. Constantinescu, *Gases Dynamics*, vol. I, II. Politehnica University in Bucharest Inprint, 1985.

[4] E. Carafoli and V. N. Constantinescu, *Compresible Fluids Dynamics*. RSR Academy Publishing House, Bucharest, 1984.

[5] Y. P. Goonko and E. Alexandrov, Aerodynamic design of a supersonic three-dimensional inlet, *Thermophysics and Aeromechanics*, Vol. 1, Nr. 17, pp. 57-68, 2010.

[6] P. G. Hill and C. Peterson, *Mechanics and Thermodinamics of Propulsion*, Addison - Wesley Publications, New York, 1993.

[7] R. Lungu, A. N. Tudosie, L. Dinca, *Fluid mechanics and technical thermodynamics*, Craiova, SITECH Publisher, 2004.

[8] V. Pimsner, *Air-breathing Jet Engines. Processes and Characteristics*, Bucharest, Didactic and Pedagogic Publishing, 1983.

[9] V. Pimsner, C. Berbente, et al. *Flows in turbomachinery*, ISBN 973-165-4-17, Tehnica Publishing Bucharest, 1996.

[10]H. Ran and D. Mavris, Preliminary Design of a 2D Supersonic Inlet to Maximize Total Pressure Recovery, *Proceedings of AIAA 5th Aviation, Technology, Integration and Operations Conference (ATIO)* , pp. 1-11, 26-28 Sept., Arlington, Virginia, 2005.

[11] J. J. Seddon and E. L. Goldsmith, *Intake Aerodynamics*, 2nd edition, AIAA Education Series, 1999.

[12] A. N. Tudosie, Axis-symmetrical supersonic inlet with inner compression, *Proceedings of the XVI-th Teaching Staff Scientific Papers Session*, pp.185-190, "Mircea cel Batran" Naval Academy, Constantza, 3-5 of June, 1999.

[13] A. N. Tudosie, Supersonic Air Inlet's Control System Based On The Inner Normal Shock Wave's Position Stabilisation, *Proceedings of the International Conference on Military Technologies ICMT 07* (ISBN: 978-80-7231-238-2) , pp 342-349, University of Defense, Brno, 2-4 May 2007.

[14] A. N. Tudosie, Supersonic Air Inlet Control System Based On The Inner Channel Minimum Cross Section Position Control, *Proceedings of the International Conference on Military Technologies ICMT'09* (ISBN: 978-80-7231-648-9) , pp 350-359, University of Defense, Brno, 5-7 May 2009.

[15] A. N. Tudosie, Control laws for an aircraft supersonic inlet with mobile panel, *Proceedings of International Conference Scientific Research And Education In The Air Force –AFASES 2017*, pp. 231-242, Brasov, 22-24 May 2017.

[16] A. N. Tudosie, Pneumo-hydro-mechanical control system for an aircraft supersonic inlet with mobile ramp, *Review of Air Force Academy*, pp. 123-130, no.1 (33), 2017.

[17] K. Venkat-Ramana, and S. Gokhale, Numerical computation of supersonic inlet flow, *International Journal for Numerical Methods in Fluids,* no. 36, pp. 597-617, 2001.

METHOD OF CONTROL OF AIRCRAFT CENTER OF GRAVITY BASED ON THE FUEL CONSUMPTION ORDER

Alexandru-Nicolae TUDOSIE*, Petre NEGREA, Vlad Aurelian VĂDUVESCU*****

*Univeristy of Craiova, Craiova, Romania (atudosie@elth.ucv.ro)
** Univeristy of Craiova, Craiova, Romania (pnegrea@elth.ucv.ro)
*** Master Student, Univeristy of Craiova, Craiova, Romania (vlad93v@yahoo.com)

DOI: 10.19062/2247-3173.2019.21.28

Abstract: *The paper deals with an architecture of fuel tanks onboard an aircraft. The fuel consumption mode has a great influence above the position of aircraft's center of gravity; the authors have determined the position of each fuel tank center of gravity and have also determined its space trajectory during the fuel consumption. When a malfunction of the fuel consumption occurs, aircraft's center of gravity might be displaced outside the safety envelope, which might badly influence the stability of the aircraft and, because of the autopilot intervention, it might also increase aircraft attitude, its total drag, as well as the specific fuel consumption of aircraft engines. The authors have designed a subroutine for restore the stability, by reordering the fuel consumption to rebalance the aircraft, to restore aircraft attitude and to reduce the engine's specific fuel consumption initially increased by the drag.*

Keywords: *Center of gravity, fuel tank, position vector, balance, control;*

1. INTRODUCTION

One of the most important parameters of the aircraft is its center of gravity position. This is determined beforehand in the design phase, but from the moment it is given to operation, it changes its position according to several factors (on-board crew, embarked passengers and their luggage, unequal fuel distribution or consumption etc.). Over time, monitoring and maintaining the center of gravity during the flight was a major challenge for flight safety and efficiency. Therefore, the problem of positioning the center of gravity on the aircraft must be approximated from the design phase, determining a safe volume within which it can move.[1,2]

One of the parameters that can be changed during the flight is the fuel mass on a particular tank or in a group of tanks; it might be generated by several causes, such as the damage or the malfunction of an engine, the uneven fuel consumption of aircraft's engines during the flight, or mechanical/electrical disruption of some fuel system parts. If a major imbalance occurs, caused by the lack of fuel consumption from one of the tanks, aircraft's autopilot must react and restore aircraft's attitude; however, it involves aircraft's aerodynamic commands architecture reconfiguration, in order to suppress the moment which has occurred because of the unsymmetrical distribution of the fuel. Consequently, the global drag of the aircraft might increase, which, obviously, increase the engines' fuel consumption; in the mean time, passengers' comfort might be affected, due to repeated autopilot's small maneuvers to restore airplane's flight attitude.

This work has as goal to determine a control method of the on-board fuel's center of gravity, to keep it inside the safe volume, even when it occurs an important fuel consumption difference between the symmetrically arranged tanks (especially between the wing fuel tanks).

2. FUEL DISTRIBUTION CENTER OF GRAVITY

On the aircraft, the fuel consumption is made in a certain order, so that the center of gravity (noted in the paper with C_g) must be found in the safety envelope [1,3].

It is considered the placement of the fuel tanks according to Fig. 1, where it can be observed a number of five fuel tanks (which shapes are considered as random) left wing tank, right wing tank (symmetrically arranged with respect to the aircraft body), front fuselage tank, rear fuselage tank and the center tank (main fuel tank, usually meant to supply the engines). OXYZ is the aircraft frame, with the origin in the theoretical C_g, Y-axis on the left side, X-axis in front, following the flight direction, Z-axis upward, perpendicular to the other two. With $\vec{r}_L, \vec{r}_R, \vec{r}_F, \vec{r}_B,$ were noted the C_g tanks position vectors for the left, right, front and rear respectively. The C_g of the main tank is assumed to be imposed, from the design phase, inside of the envelope [4].

Starting from the hypothesis that any fuel tank is not symmetrical by any axis, it results that its inside fuel center of gravity varies during its consumption after a three-dimensional curve, presumed and illustrated in red on the figure.

The position vectors of C_g's relative to the aircraft frame for each tank must be calculated using a vector description, as in [5,6,7]:

$$\begin{cases} \vec{r}_L = \vec{r}_{L1} + \vec{r}_{L2} \\ \vec{r}_R = \vec{r}_{R1} + \vec{r}_{R2} \\ \vec{r}_F = \vec{r}_{F1} + \vec{r}_{F2} \\ \vec{r}_B = \vec{r}_{B1} + \vec{r}_{B2} \\ \vec{r}_M = \vec{r}_{M1} + \vec{r}_{M2} \end{cases} \tag{1}$$

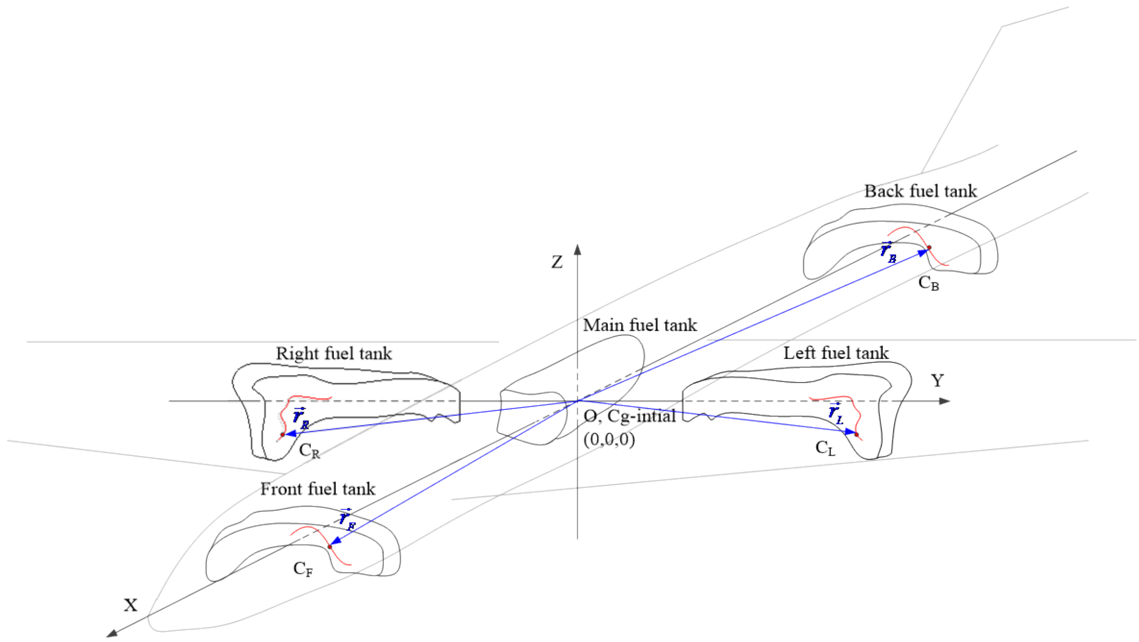

FIG. 1 Location of aircraft fuel tanks

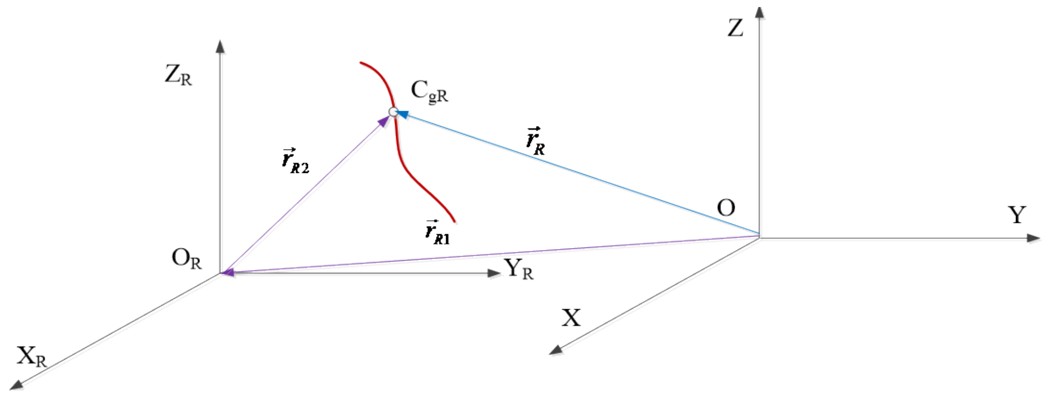

FIG. 2 Center of gravity's position vector for a fuel tank (the right wing tank)

where:

- $\vec{r}_{L1}, \vec{r}_{R1}, \vec{r}_{F1}, \vec{r}_{B1}, \vec{r}_{M1}$, are the position vectors of the five fuel tanks frames, relative to the aircraft frame.
- $\vec{r}_{L2}, \vec{r}_{R2}, \vec{r}_{F2}, \vec{r}_{B2}, \vec{r}_{M2}$, are the C_g's position vectors of the five fuel tanks relative to their own frames, as Fig. 2 shows.

3. FUEL TANK'S CENTER OF GRAVITY DETERMINING

For any of the aircraft's fuel tanks, its center of gravity is "moving" after a curve, as in Fig. 2, with respect to the fuel level inside. One has to determine this curve's equation and to emphasize its correlation to the fuel level (which is given by the fuel level sensor).

In order to determine the C_g for any tank fuel, a meshing method is used, with n volumes (samples) of known geometric shapes, as shown in Fig. 3. The tank level sensor is the one who gives information on the fuel volume, and also on its level by a vertical component h (fuel height in the tank). For k volumes (samples), the height of the fuel level in the tank is:

$$h_k = \sum_{j=1}^{k} z_j, \tag{2}$$

where z_j is the height of each item of fuel volume.

The C_g for each sample, depending on its geometry (the samples may differ from one sample to another) may be easy calculated, so that the coordinates of the fuel C_g result as a function of the height h (the fuel level, given by the sensor). Thus, for each fuel level, it corresponds a C_g (eg. for h_1 corresponds C_{g1}, for $\underline{h_2}$ corresponds C_{g2}, and so on).

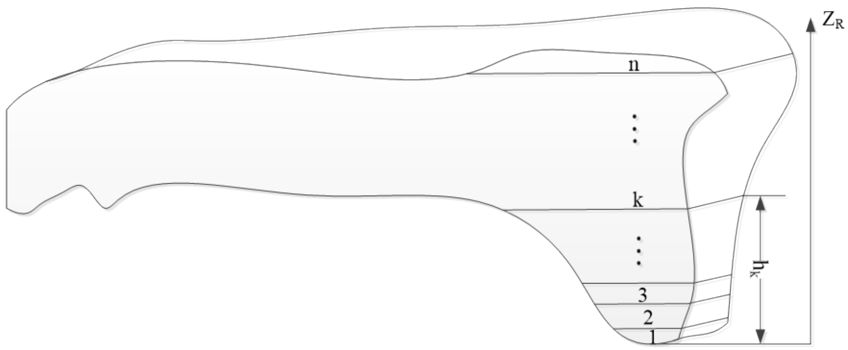

FIG. 3 Meshing method for center of gravity's position vector determining

The equation for the center of gravity's position vector for the geometric composed shape of the tank is, according to the equations in [5,6,7]:

$$\vec{r}_{Cgk}(x_{Cgk}, y_{Cgk}, z_{Cgk}) = \frac{\sum_{j=1}^{k} \vec{r}_j(x_{Cgj}, y_{Cgj}, z_{Cgj}) \cdot m_j(x_{Cgj}, y_{Cgj}, z_{Cgj})}{\sum_{j=1}^{k} m_j(x_{Cgj}, y_{Cgj}, z_{Cgj})}, \tag{3}$$

where $x_{Cgj}, y_{Cgj}, z_{Cgj}$, are the coordinates of the level *j*, and for the level *k* can be written as:

$$x_{Cgk} = \frac{\sum_{j=1}^{k} x_{Cgj} \cdot m_j(x_{Cgj}, y_{Cgj}, z_{Cgj})}{\sum_{j=1}^{k} m_j(x_{Cgj}, y_{Cgj}, z_{Cgj})}, \tag{4}$$

$$y_{Cgk} = \frac{\sum_{j=1}^{k} y_{Cgj} \cdot m_j(x_{Cgj}, y_{Cgj}, z_{Cgj})}{\sum_{j=1}^{k} m_j(x_{Cgj}, y_{Cgj}, z_{Cgj})}, \tag{5}$$

$$z_{Cgk} = \frac{\sum_{j=1}^{k} z_{Cgj} \cdot m_j(x_{Cgj}, y_{Cgj}, z_{Cgj})}{\sum_{j=1}^{k} m_j(x_{Cgj}, y_{Cgj}, z_{Cgj})}. \tag{6}$$

The equations (3) to (6) can be written [5,6,7] for each tank, and it results the position vectors relative to each fuel tank frame:

$$\vec{r}_L = \vec{r}_{L1}(x_{L1}, y_{L1}, z_{L1}) + \frac{\sum_{j=1}^{k_L} \vec{r}_{L_2 j}(x_{CgL_2 j}, y_{CgL_2 j}, z_{CgL_2 j}) \cdot m_{L_2 j}(x_{CgL_2 j}, y_{CgL_2 j}, z_{CgL_2 j})}{\sum_{j=1}^{k_L} m_{L_2 j}(x_{CgL_2 j}, y_{CgL_2 j}, z_{CgL_2 j})}, \tag{7}$$

$$\vec{r}_R = \vec{r}_{R1}(x_{R1}, y_{R1}, z_{R1}) + \frac{\sum_{j=1}^{k_R} \vec{r}_{R_2 j}(x_{CgR_2 j}, y_{CgR_2 j}, z_{CgR_2 j}) \cdot m_{R_2 j}(x_{CgR_2 j}, y_{CgR_2 j}, z_{CgR_2 j})}{\sum_{j=1}^{k_R} m_{R_2 j}(x_{CgR_2 j}, y_{CgR_2 j}, z_{CgR_2 j})}, \tag{8}$$

$$\vec{r}_F = \vec{r}_{F1}(x_{F1}, y_{F1}, z_{F1}) + \frac{\sum_{j=1}^{k_F} \vec{r}_{F_2 j}(x_{CgF_2 j}, y_{CgF_2 j}, z_{CgF_2 j}) \cdot m_{F_2 j}(x_{CgF_2 j}, y_{CgF_2 j}, z_{CgF_2 j})}{\sum_{j=1}^{k_F} m_{F_2 j}(x_{CgF_2 j}, y_{CgF_2 j}, z_{CgF_2 j})}, \tag{9}$$

$$\vec{r}_B = \vec{r}_{B1}(x_{B1}, y_{B1}, z_{B1}) + \frac{\sum_{j=1}^{k_B} \vec{r}_{B_2 j}(x_{CgB_2 j}, y_{CgB_2 j}, z_{CgB_2 j}) \cdot m_{B_2 j}(x_{CgB_2 j}, y_{CgB_2 j}, z_{CgB_2 j})}{\sum_{j=1}^{k_B} m_{B_2 j}(x_{CgB_2 j}, y_{CgB_2 j}, z_{CgB_2 j})}, \tag{10}$$

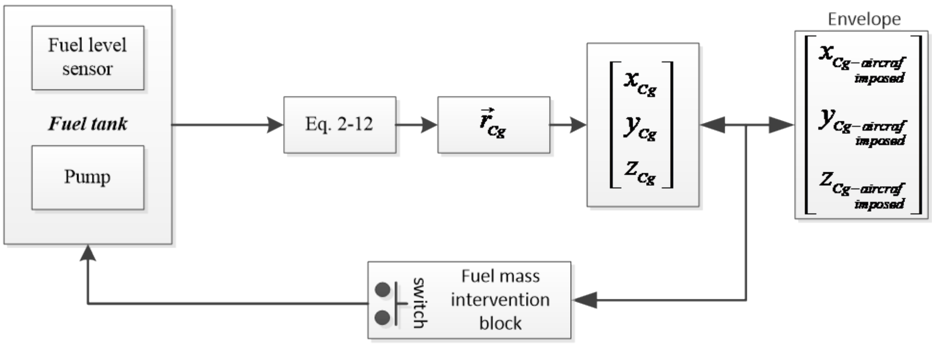

FIG. 4. Position vector calculation block-diagram (example for the right wing tank)

$$\vec{r}_M = \vec{r}_{M1}(x_{M1}, y_{M1}, z_{M1}) + \frac{\sum_{j=1}^{k_M} \vec{r}_{M_2 j}(x_{CgM_2 j}, y_{CgM_2 j}, z_{CgM_2 j}) \cdot m_{M_2 j}(x_{CgM_2 j}, y_{CgM_2 j}, z_{CgM_2 j})}{\sum_{j=1}^{k_M} m_{M_2 j}(x_{CgM_2 j}, y_{CgM_2 j}, z_{CgM_2 j})}. \tag{11}$$

The final equation of the center of gravity for the fuel system that encompasses all the tanks is:

$$\vec{r}_{Cg}(x_{Cg}, y_{Cg}, z_{Cg}) = \frac{\vec{r}_L \cdot m_L + \vec{r}_R \cdot m_R + \vec{r}_F \cdot m_F + \vec{r}_B \cdot m_B + \vec{r}_M \cdot m_M}{m_L + m_R + m_F + m_B + m_M}, \tag{12}$$

where m_L, m_R, m_F, m_B, m_M are also presented in the denominators of the equations (7) to (11) and represent the amount of fuel, determined for each tank.

According to the successive course of equations (2) to (12), it results the dependence between $\vec{r}_{Cg}$ and h.

4. FUEL MANAGEMENT CONTROL ALGORITHM

For a more complex system, following the calculation method, several tanks can be added to the system, thus obtaining other position (positions) of the center of gravity, depending on the case and on the specific design. Furthermore, the above determined mathematical equations can be later used in computer algorithms, which can further be used as part of the fuel management system and also part of the automatic flight control system [8].

A subroutine than runs as a background process, for the fuel management algorithm that is responsible for maintaining the fuel center of gravity inside the safety envelope, can be described as a simplified pseudocode (Table 1).

Table 1. Pseudocode model

```
if the coordinates of X_Cg can be found in the coordinate stack of X_CgImposed
      take no action
else if X_CgL 's modulus is greater than X_CgR's modulus
      turn on transfer pump_L until X_CgL modulus is equal to X_CgR modulus
      else
      turn on transfer pump_R until X_CgR modulus is equal to X_CgL modulus
if the coordinate of Y_CgCb can be found in the coordinate stack of Y_CgIMP
      take no action
```

else if Y_CgF 's modulus is greater than X_CgB's modulus
turn on transfer pump_F until X_CgF modulus is equal to X_CgB modulus
else
turn on transfer pump_B until X_CgB modulus is equal to X_CgF modulus

Supposing that, because of a malfunction of aircraft's engine 1 (left wing engine), the fuel consumption from the left wing tank is delayed (or even stopped); the left wing becomes more weighty and the center of gravity might left the safety envelope. Consequently, the autopilot reacts and compensates the bank of the aircraft, which means that ailerons and rudder control becomes active; however, if the fuel management system is active, it commands the cross-feed valve opening, the right wing tank valve closing and the consumption only from the left tank, until the balance is reestablished, that means that until the center of gravity rejoins the safety envelope. A similar situation might occur with the front and the rear fuel tanks, but the issue may be easier solved, in the same manner.

CONCLUSIONS

The fuel control system plays an important role in maintaining the center of gravity of the airplane. Thus, the estimation of the fuel weight center becomes part of the fuel management system and also the automatic flight control system. By determining the center of gravity of each fuel tank, it is possible to make a variable mass calculation system, that can estimate the center of gravity of the total fuel on board the aircraft. For future use, with these kind of methods, computer comparison algorithms may be used to analyze data, from the fuel system sensors (such as flowmeter, fuel pressure, fuel gauge), and compare it with the airplane's allowed tolerance of center of gravity.

The algorithm of fuel center of gravity calculation may be implemented as a subroutine of the flight control system, only after the safety envelope of the global center of gravity was specified and mathematically defined.

The study in this paper might be extended with an effective simulation for an existing airplane, with a complex fuel system (a complex distribution of the on-board fuel tanks).

REFERENCES

[1] H. Gavel, Linköping Studies in Science and Technology Dissertations, *On Aircraft Fuel Systems Conceptual Design and Modeling*, Linköping 2007, printed in Sweden by Liu-Tryck, ISBN 978-91-85643-04-2.

[2] Wildschek, A., F. Stroscher, T. Hanis, and T. Belschner. 2013. *Fuel management system for cruise performance optimization on a large blended wing body airliner*. In: Progress in §ight dynamics, guidance, navigation, control, fault detection, and avionics. Eds. Ch. Vallet, D. Choukroun, Ch. Philippe, G. Balas, A. Nebylov, and O. Yanova. EUCASS advances in aerospace sciences book ser. Moscow: Torus Press. 6:651 70;

[3] Z. Goraj, P. Zakrzewski, *Aircraft Fuel Systems and their influence on Stability Margin*, Transactions of the Institute of Aviation No. 183.

[4] *** Federal Aviation Administration Airframe Handbook, *Chapter 14: Aircraft Fuel System*, December 2017. Available at https://afoullous.com/2017/12/31/aircraft-fuel-system;

[5] R. Voinea, D. Voiculescu, V. Ceauşu, V. - *Mechanics*. Didactical and Pedagogical Publisher, Bucharest, 1983;

[6] F. L. Buzescu, C. Fetecau, *Elements of theoretical mechanics*, Performantica Publisher, Bucharest, 2009;

[7] J. L. Meriam, L. G. Kraige, *Engineering Mechanics – Statics – seventh edition*, John Wiley and Sons, Inc., 2006;

[8] R. Lungu, *Aircraft automation*, Universitaria Publisher, Craiova, 2000.